香港科技大學
THE HONG KONG UNIVERSITY OF SCIENCE AND TECHNOLOGY

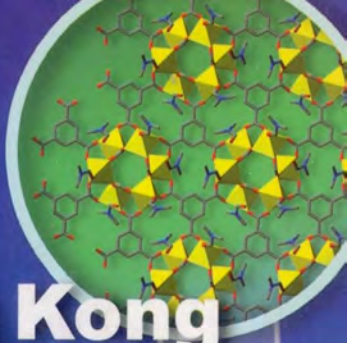

AsCA '04 Hong Kong

Programme & Abstracts

2004. 6

Se Won Suh

The Sixth Conference of the
Asian Crystallographic Association


The Sixth Conference of the
Asian Crystallographic
Association
AsCA'04
The Hong Kong University
of Science and Technology
27-30 June 2004
www.ust.hk/asca04

Order of Contents

Committees

Asian Crystallographic Association

President:	Prof. Yu WANG *National Taiwan University, Taiwan*
Vice-President:	Prof. M. VIJAYAN *Indian Institute of Science, India*
Secretary/Treasurer:	Dr. Brian W. SKELTON *University of Western Australia, Australia*

International Program Committee for AsCA'04

Chairman

Prof. Makoto SAKATA	*Nagoya University, Japan*
Prof. Kunio MIKI	*Kyoto University, Japan*
Dr. Chris HOWARD	*ANSTO, Australia*
Prof. Mitchell GUSS	*University of Sydney, Australia*
Prof. S.L.CHANG	*National Tsing Hua University, Taiwan*
Prof. Jing Tai ZHAO	*Chinese Academy of Sciences, China*
Prof. Y.J. PARK	*Sook Myung Womens University, Korea*
Prof. Nguyen VAN TRI	*Hanoi University of Technology, Vietnam*
Prof. M. VIJAYAN	*Indian Institute of Science, India*

International Organizing Committee for AsCA'04

Chairman

Prof. Ian D. WILLIAMS	*HKUST, Hong Kong*
Prof. Thomas C-W. MAK	*The Chinese University of Hong Kong*
Prof. Wing Tak WONG	*University of Hong Kong, Hong Kong*
Dr. Raymond W-Y. WONG	*Hong Kong Baptist University, Hong Kong*
Prof. Wa Hung LEUNG	*HKUST, Hong Kong*
Prof. Zhen Yang LIN	*HKUST, Hong Kong*
Prof. Yu Fong YEN	*HKUST, Hong Kong*
Prof. Ji Wen CAI	*Sun Yat-Sen (Zhongshan) University, China*
Prof. Zhong Yuan ZHOU	*Hong Kong Polytechnic University*

AsCA04 Secretariat:

Mr. Alvin W-H. SIU	*HKUST, Hong Kong*
Dr. Eiji NISHIBORI	*U. Nagoya, Japan*

IUCr Scientific Freedom Policy Statement

The organizing committee of the AsCA'04 conference observes the basic policy of non-discrimination. We affirm the rights of scientists throughout the world to adhere to, or to associate with, international scientific activity. There will be no restrictions based on nationality, race, color, age, religion, political philosophy, ethnic origin, citizenship, language or sex, in accordance with the statutes on the International Council of Scientific Unions. At this meeting no barriers will exist which would prevent the participation of *bona fide* scientists.

Scientific Program

Plenary Lectures:

Prof Jun AKIMITSU
Department of Physics, Aoyama Gakuin University, Japan
Superconductivity and Magnetism of Borides

Prof Tej. P. SINGH
Department of Biophysics, All India Institute of Medical Sciences, India
Structures of Novel Signaling Proteins Secreted During Involution and Involved in Apoptosis

Prof Shie Ming PENG
Department of Chemistry, National Taiwan University, Taiwan
From Metal String Complexes to Molecular Metal Wires

Prof Isao TANAKA
Division of Biological Sciences, Hokkaido University Japan
High-throughput Protein Crystallography

Dr Jian Wei MIAO
Stanford Linear Accelerator Center, Stanford University, USA
Crystallography without Crystals

Prof Mike HURSTHOUSE
University of Southampton, UK
A Grid-enabled High Throughput Chemical Crystallography - New Opportunity for Structural Chemistry

Microsymposia

Monday, June 28 10:15-12:15

MS-1 Molecular Recognition and Catalysis

MS-2 Synchrotron-related Science and Applications

MS-3 Structural Chemistry

Monday, June 28 16:00-18:00

MS-4 Macromolecular Assemblies

MS-5 Neutron Scattering Science

MS-6 Supramolecular Chemistry & Crystal Engineering

Tuesday, June 29 10:15-12:15

MS-7 Receptors, Signaling & receptor-drug Interactions

MS-8 Materials Science I

MS-9 Electron Diffraction and Microscopy

Tuesday, June 29 16:00-18:00

MS-10 Structural Genomics

MS-11 Structural Nanoscience

MS-12 Bio-informatics and Computational Analysis I

Wednesday, June 30 10:15-12:15

MS-13 Bio-informatics and Computational Analysis II

MS-14 Advanced Applications of Powder Diffraction

MS-15 Materials Science II

Sponsors and Exhibitors

International Union of Crystallography

Asian Crystallographic Association

Crystallographic Society of Japan

Society of Crystallographers in Australia and New Zealand

Hong Kong University of Science and Technology

Rigaku Corporation

Bruker Nonius

PANalytical

marresearch

Oxford Cryosystems

Oxford Diffraction

CCP4

Fluidigm

Universal Analytical - Discovery Partners

Crystal Impact Xenocs

RCSB Protein Data Bank

Stoe & CIE

Hitachi	Fujifilm
Ishikawajima	LAS
Ricoh	Ryoka Systems

Gloria-Tourist, Japan

Hong Kong Tourist Association

Evening Social Functions:

Sunday June 27

PANalytical Welcome Mixer

A reception and social mixer will be organized for all AscA04 registrants and accompanying persons in the University Bistro, University Center, HKUST. Free drinks and light buffet meal will be provided. Time 18:30-21:00. We are grateful to PANalytical for their sponsorship of this event.

Monday June 28

Bruker Nonius Harbor Cruise and Dinner Buffet

The Hong Kong harbor at night is a spectacular sight not to be missed. Space is limited to 200 persons. Available to all full conference registrants and accompanying persons. Some space available for students, enquire at conference desk to sign up ! Buses will depart HKUST at 18:45 and return 21:45. We are grateful to Bruker/Nonius for their sponsorship of this event.

Tuesday June 29

Rigaku Traditional Chinese Seafood Banquet

The Star Seafood Floating restaurant in Shatin is famous for its seafood banquet. This event is open to all conference registrants and accompanying persons. Buses will depart HKUST at 18:45 and return at 21:45. Residents of Nikko Hotel please contact conference secretariat for arrangements. We are grateful to Rigaku Corporation for their sponsorship of this event.

Wednesday June30

marresearch Farewell Party

Say good-bye with a farewell party featuring drinks and snack buffet at the conclusion of the final academic session in the afternoon. Open for all participants and held in the academic concourse, HKUST. We are grateful to marresearch for their sponsorship of this event.

General Information:

Meeting Dates and Venue:

The meeting is being held on the campus of the Hong Kong University of Science and Technology, June 27- 30 2004. Registration will commence on the afternoon of Sunday June 27 (12:00 - 21:00) and may be continued on Monday June 28 (08:00). In case of early check in on Saturday 26 June or late arrival on Sunday evening, please call (9777-4149), (9276-7717) or (6112-0829).

Conference Office:

The conference office is located in the academic concourse, opposite Lecture Theatre B. It will be open on Sunday June 27 for registration from 14:00 until 21:00. Delegates arriving after this time should register on Monday morning before 10:00. Messages and communications for delegates may be posted on notice boards next to the conference desk. During the conference period FAXes may be sent to +(852)-3106-3446 and clearly marked to the attention of the delegate in question. For phone contact please call +(852)-2358-7359, or +(852)-9777-4149. The time zone for Hong Kong in June is +7 GMT.

Phone, Fax and Post:

If you wish to make an overseas call or FAX please contact the conference secretariat at the conference desk. In general only local calls can be made from the public phones on campus. Local calls within Hong Kong are normally 8-digits. For directory enquiries in English dial 1081. Phone cards with discount IDD rates may be purchased at the airport or down-town. When phoning overseas, for example on mobile phones, note that the international dialing code should be preceded with 001. Due to the relatively short duration of the conference and variability of post we do not recommend sending regular mail. If you wish to send mail there is a mailing desk inside the University Souvenir Shop on the Entrance Plaza near Lift 2.

In case of need speed-post items may be sent to: AsCA Secretariat, c/o Prof. Ian Williams, Department of Chemistry, HKUST, Clear Water Bay, Kowloon Hong Kong.

E-mail and Internet:

The university has over 20 workstations for free E-mail and internet access around the campus and we have arranged computing facilities to be available in Computer Barn A, Lift 17-18. For further details or assistance please contact Prof. Zhenyang Lin at the conference help desk.

Banking and Currency Exchange:

Currency in Hong Kong is the Hong Kong dollar, which is pegged at a rate of 7.78 per US$. It is advisable that you change to local currency before you depart, since exchange rates at the Hong Kong airport may not be favorable. The campus of HKUST has two bank branches, the Hang Seng Bank (Ph: 2198-0441) and the Bank of China (Ph: 2358-2345) located near Lift 1 across from the sun-dial. Opening hours Mon-Fri 09:00 to 17:00. They can provide exchange to HK dollars for limited foreign currencies such as US dollars, Japanese Yen or Renminbi. There are numerous money exchanges in the tourist areas of Tsim Sha Tsui, Kowloon or Hong Kong Island, but these are located far from the university campus.

The most convenient access to local cash may be from four ATM machines on campus, two at the bank branches and two at the entrance to the academic concourse. These are open 24 hours and should accept most international credit cards, or bank cards on the Plus or Cirrus systems.

Name Badges:

Name badges are required for entry to all scientific sessions, lunches and evening functions. Different colors for name badges of participants is as below;

Conference organizers	**Red**
Exhibitors	**Yellow**
Full registrants	**Green**
Students	**Blue**
Accompanying persons	**White**

For inquiries when the conference desk is closed, please contact member of organizing committee or one of the assistants. Students must show proof of a current valid student identity upon registration. Accompanying persons are allowed access to all meals and social functions but not the academic sessions

Medical and Emergency Contacts:

The phone number for emergency in Hong Kong is **999**. This will connect you to POLICE, FIRE and AMBULANCE (MEDICAL) services. State your problem and location clearly and assistance will be sent as soon as possible. Help should be available in English, Cantonese or Mandarin. *If you are on the university campus* either dial extension **8999** or **6565** from a campus internal phone (otherwise 2358-8999 or 2358-6565). The 8999 number is the line for all main emergency services. The campus security center will contact 999 on your behalf and send more immediate assistance. For difficulties such as report of stolen property, locked out of room, please use the 6565 number.

Accommodation:

Many delegates have elected to stay on campus in faculty apartments, visitor center or student dormitory rooms. An information sheet on guest facilities and procedures for check-in/out will be provided to you upon registration.

Special conference room rates had been negotiated with the Nikko Hotel, Mody Road, East Tsim Sha Tsui. Please contact Ms. Pat Chan (Ph: 2313-4508) for details. A conference bus to the HKUST campus will be provided at 08:00 on Monday, Tuesday and Wednesday from outside the lobby of Nikko Hotel.

Meals and Catering Arrangements:

Delegates staying on campus accommodation will be given breakfast vouchers and all delegates will receive lunch vouchers. Details of time and locations for these will be given at registration. The campus is relatively remote from the urban area and so there are few off-site restaurants within walking distance. A list of restaurants, bars and tourist attractions are listed on the pages that follow.

On-campus there are a number of dining choices:

Maxim's Chinese Restaurant: Ground Floor (Lift 14-16)
Chinese food - meals for ca HK$50 (US$7.50)

Dim sum and Sun Roast Chinese Tea room: Level LG1 (Lift 14-16)
Also operated by the Maxims group, set meals for ca HK$25 (US$3.00)

Student Canteens and Eateries: Levels LG7 and LG5 (Lift 11/12)
variety of meals, noodles and rice dishes ca HK$20 (US$2.50)
there is also a MacDonald's franchise on LG5 if you crave a 'happy meal'

University Bistro: University Center
mostly Western meals for ca HK$50 (US$7.50) Venue for the welcome mixer.

Coffee Shop: Academic concourse (Lift 25-26)
This has snacks, sandwiches and light meals. Starbuck's coffee in the cart outside with espresso and cappuccino. Conveniently located near to the conference desk and lecture theatres.

Transport:

Buses will be provided to campus on Sunday 27 June from HK International airport. Please sign up at conference desk if you need assistance with a return trip to the airport on Wednesday 30 June or Thursday 1 July. The nearest shops and restaurants to HKUST campus are in the newly developed Tseung Kwan O, which can be accessed in 10-15 mins. by shuttle mini-bus from outside the university main gate. There are large shopping centers based around the Hang Hau and Po Lam MTR stations in Tseung Kwan O.

Transportation to Down Town:

Kowloon:
Taxis to the Nikko Hotel or Star Ferry terminal in Tsim Sha Tsui should cost about HK$100 (US$12) and take 25-30 minutes. Alternatively take public mini bus to Choi Hung MTR station and then the MTR subway to stations in Mongkok, Yau Ma Tei, Jordan or Tsim Sha Tsui.

Hong Kong Island:
Taxis to Causeway Bay, Wanchai, Admiralty or Central districts of Hong Kong Island will cost ca HK$140-160 (about US$20) and take about 30-35 minutes. Alternatively take a mini-bus to Hang Hau MTR station in Tseung Kwan O and then MTR subway to Hong Kong Island.

Tours and Attractions:

Hong Kong is a world famous travel destination and city. It is a center for international commerce and trade. Most visitors are familiar with the high rise skyscrapers of Hong Kong island and the views of Victoria Harbor. The conference venue is outside of the urban area with a beautiful vista overlooking Clear Water Bay. However there is relatively easy access to the down-town areas of Kowloon and Hong Kong Island by variety of public transportation.
A number of attractions are listed on the next few pages. For further details it is suggested that you purchase one of the many guide books available in different languages. Some information leaflets from the Hong Kong Tourist Association are available at the conference desk.

Things to Do/See:

Kowloon:

Victoria Harbor
The Star ferry terminal is a good place to begin a visit to the down town area. From near the old KCR clock tower there is an excellent view of the harbor, and a pleasant walk along the water front. Star ferry is also a convenient starting place for shopping in the nearby Star House (computers) or the Ocean Center shopping mall. The Star Ferries are the famous green and white boats that traverse the Hong Kong harbor. They offer a cheap mode of transport (ca HK$2) for a crossing between Kowloon (Star Ferry terminal) and Hong Kong Island (either Central or Wanchai piers) and at least one trip is recommended!

Tsim Sha Tsui (TST)
Near to Star Ferry is the main tourist area of Kowloon, called Tsim Sha Tsui. The main shopping strip is along Nathan Road, which is referred to as the Golden Mile, due to the lights at night-time. Be cautious when buying gold, jewelry, 'copy' watches and electronic goods. In stores look for HK tourist association signs in the window. TST also houses many of the museums in Hong Kong near the Star Ferry or along Chatham Road.

Jordan, Yau Ma Tei and Mongkok
These areas north of TST along Nathan Road are also served by MTR stations and offer a glimpse of a more authentic Hong Kong. Highlights in Yau Ma Tei include the Jade Market open 10:00-15:30 and the Temple Street night market.

Wong Tai Sin Temple
To get good karma or a glimpse of your future, a visit to Wong Tai Sin temple and its fortune tellers may be worthwhile. It is open from 07:00 - 17:30. Relatively close to HKUST, take MTR from Choi Hung to Wong Tai Sin station.

Hong Kong Island:

Victoria Peak via the Peak Tram
The highest overlook of the city and Hong Kong harbor, has lookout with telescope. Sadly these days pollution has reduced the beauty of this vista however the weather in late June predominates from the sea so the air is clear, even though hot and humid. The Peak can be accessed via the Peak Tram, which is a funicular cable railway ride, some sections have steep ascent descent and are not for the faint hearted!

Hong Kong Island Tram
Hong Kong island is famous for its modern skyscraper landscape, whilst few older buildings survive one tradition is the Hong Kong island tram, which runs between North Point and Kennedy Town and costs about HK$2. Though rather slow a ride provides an interesting and way of sightseeing through the main business and shopping districts at a leisurely pace.

Ocean Park
In the hot weather of June, some like to cool down with a visit to this water theme-park, located on Hong Kong island between Stanley and Aberdeen. It is open daily 10:00-18:00, admission ca. HK$150. To get there we suggest take MTR to Admiralty station and then taxi.

Causeway Bay
One of the busiest parts of downtown Hong Kong, this is an experience for those who are comfortable with crowds. Causeway Bay is accessible from the MTR system and has a host of shopping options from expensive to bargain. There is a large Japanese department store, Sogo, and variety of outlets in air-conditioned Times Square shopping mall.

Stanley
An alternative to down town bustle is to take a trip to Stanley on the far south side of Hong Kong island. This has a recently developed water-front with modern shops and eateries as well as retaining the old tourist bazaar, which is the place to get presents, silk fashions, chops, tee-shirts, local art and souvenirs.

Shopping malls can be found based around most of the subway (MTR) stations. Hong Kong's past reputation for shopping bargains is rather jaded these days, the city has become one of the most expensive in the world so high overhead costs mean bargains are usually a thing of the past. Regarding electronic goods people from the West are often amazed by the range of modern items, but shoppers from Taiwan or Japan are less likely to be impressed.

Outlying Islands and Beyond:

If you have 1 or 2 free days the following may be interesting side trips:

Lantau Island

A visit to the world's largest seated golden Buddha statue on Lantau Island (the other side of the airport) is a popular trip. Take MTR/taxi to Central to the Pier for the Outlying Islands and the ferry (1hr) to Silver-mine Bay. Bus or taxi to the buddha then takes about another 30 mins. There are excellent hiking trails on Lantau, though the weather in late June is hot and humid so take plenty of water.

Macau

This former Portugese colony is readily reached from the Hong Kong-Macau Ferry Terminal, Shum Tak Center, Central district Hong Kong Island. (Sheung Wan MTR station) The trip takes 1 hr by jetfoil which leave every 30 minutes, or more frequently at weekends. Macau is a separate Special Administrative Region within China from Hong Kong, so please check on your entry and visa requirements beforehand. If you intend to stay overnight you can book a hotel room at one of the travel agents near to the ferry terminal entrance. The room rates for Macau in mid-week are quite favorable, since Macau relies heavily on visitors from Hong Kong at the weekends. Note that July 1 is a public holiday in Hong Kong so discount rates may not apply. Macau is famous for its nightlife, casinos (we advise you not to take too much money with you!) restored colonial buildings and some excellent Macanese and Portuguese cuisine. Macau has a quite different atmosphere from Hong Kong and despite the higher population density, it actually can seem less crowded. Sites worth visiting include St. Paul's Edifice, the Guia Lighthouse and its surrounding park, a casino such as the famous Hotel Lisboa and the new observation tower, which is one of the tallest in Asia.

Guangzhou, Shenzhen and China

Trips across the border to China can be arranged through most travel agents in Hong Kong, or visit an office of the China Travel Service (CTS). Trains leave Kowloon main railway station to Guangzhou about every hour. For a more simple trip across the border to the adjacent city of Shenzhen a Special Economic Zone of China, you can take the KCR railway to the last station (Lo Wu) and cross over the foot-bridge. Make sure you have appropriate paper work and visa before you travel. Whilst the economic prosperity of Shenzhen has dramatically improved, we do advise that you be aware that security is more of a concern than in Hong Kong and be especially careful with valuables and cash. That having been said a trip to China can offer much to the first time visitor and, like Macau, provides an interesting contrast to Hong Kong.

Restaurants and Night-life:

Although we hope to cater for registrants through the course of the conference Hong Kong has some of the widest range and best food in Asia-Pacific region. Excellent restaurant information can be the Guide 2004, published by bc magazine or visit the website *www.hongkongrestaurantguide.com*.

A variety of restaurants are selected here, naturally there are many more Chinese than listed, but these are not difficult to find. One suggestion is to visit the food 'tower' Times Square, Causeway Bay, which has a number of regional Chinese restaurants including Shanghai and Yunnan.

Chinese:

Serenade Ph: 2722-0932 *Cantonese*
HK Cultural Center, Tsim Sha Tsui
Fine local cuisine, located near to Star Ferry terminal.

The Red Pepper Ph: 2577-3811 *Szechuan*
7 Lan Fong Rd., Causeway Bay
A good choice for those who wish to try fiery Chinese food.

Pasha Ph: 3162-3544 *Xinjiang*
G/F Cleveland Mansions, Cleveland St, Causeway Bay
One of the latest trends in Hong Kong is Xinjiang cuisine from the uighur region of Western China. Lamb shank is recommended.

Asian:

Wasabisabi Ph: 2506-0009 *Japanese*
13/F Times Square, Causeway Bay Fashionable Japanese fusion cuisine.

Unkai Ph: 2369-1111 ext 3087 *Japanese*
Sheraton Hotel, Tsim Sha Tsui
Popular Japanese restaurant - one of the best in Hong Kong.

Gaylord Ph: 2376-1001 *Indian Food*
1F Ashley Center 23-5 Ashley Road Tsim Sha Tsui

Woodlands Ph: 2369-3718 *Vegetarian Indian*
Rm5/6 G/F Mirror Tower 61 Mody Road Tsim Sha Tsui
Long established south indian vegetarian food, try the *thali*.

Nepal Restaurant Ph: 2869-6212 *Nepalese*
SoHo, Central
Pioneer restaurant in SoHo area. Small so reservations recommended.

Indochine 1929 Ph: 2869-7399 *Vietnamese*
2F California Tower, Lan Kwai Fong
Fine vietnamese dining, hard to beat, try soft shell crabs.

Western:

The Verandah Ph: 2812-2722 *European*
109 Repulse Bay Rd, Repulse Bay
Upmarket and expensive for an elegant, romantic candlelight dinner.

Ivan the Kozak Ph: 2851-1193 *Ukrainian/Russian*
LG 46-8 Cochrane St, SoHo, Central
Unusual cuisine from eastern europe along with wide selection of vodkas!

The Swiss Chalet Ph: 2191-9197 *Swiss*
12-14 Hart Avenue Tsim Sha Tsui
Quality european cuisine including veal, fondue, cheese and fine wine.

Le Tire Bouchon Ph: 2523-5459 *French*
45 Graham St, SoHo, Central
High quality bistro home style French cuisine.

Dan Ryan's Chicago Grill Ph: 2735-6111 *American*
Ocean Centre, Tsim Sha Tsui
Popular American restaurant chain, with three outlets. The one in Tsim Sha Tsui may be the most accessible. Ideal for US steaks, burgers, crab cakes or try a Philly cheese steak or Reuben - surprisingly authentic.

King Ludwig Beer Hall Ph: 2899-0122 *German*
202 Murray House, Stanley
If you like german beer and wurst (sausages) this is the place, overlooking the sea in Stanley in refurbished Murray House. Recommended stop after shopping for tourist bargains in Stanley market.

Entertainment:

Hong Kong is a lively city at night with several active centers for night-life. Late night shopping can also be found in some of the tourist areas like Tsim Sha Tsui in Kowloon. For restaurants, bars and clubs the main areas include in Kowloon, Mongkok, Jordan to Tsim Sha Tsui and on Hong Kong island SoHo, Lan Kwai Fong and Wanchai through to Causeway Bay.

Recommended bars include Dixieland jazz at **Ned Kelly's**, Ashley Rd, TST. **Bit Point and Schnurrbart,** two german bars next door to each other in Lan Kwai Fong entertainment district offer good draft beer and food. The **Dublin Jack**, SoHo off Mid-levels Escalator is an Irish bar with vast selection of whiskies from around the world. For the young at heart discos include the upmarket **JJ's** in the Grand Hyatt Hotel, North Wanchai and popular **Joe Banana's** in Wanchai. For those enjoying karaoke Hong Kong has number of chains with many outlets around Hong Kong, especially in TST and Causeway Bay.

For any other specific inquiries and assistance with bookings please ask us at the conference desk.

Program Timetable

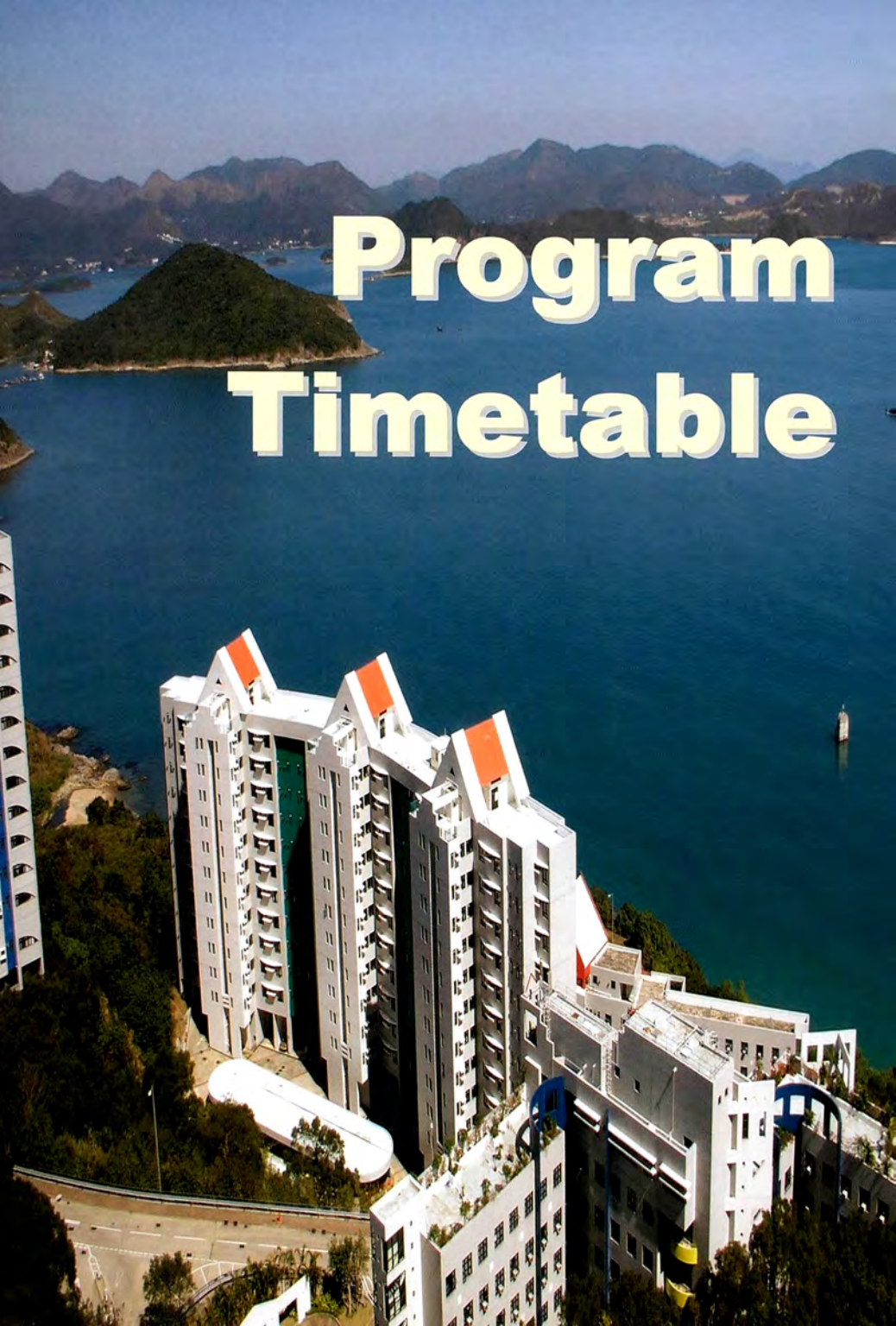

AsCA'04 Program Timetable

June	27 Sunday	28 Monday	29 Tuesday	30 Friday
08:00		**Registration**		
08:30		from 08:00		
09:00		**Opening Ceremony**	**Plenary 1 / 2**	**Plenary 3 / 4**
09:30		LT B 09:00-09:45	LT B /C 09:00-09:45	LT B / C 09:00-09:45
10:00		**MS - 1, 2 & 3**	**MS - 7, 8 & 9**	**MS -13, 14 & 15**
10:30		LT B, C & E 10:15-12:15	LT B, C & E 10:15-12:15	LT B, C & E 10:15-12:15
11:00				
11:30				
12:00		**Lunch**	**Lunch**	**Lunch**
12:30				
13:00				
13:30		**Posters - 1**	**Posters - 2**	**Plenary 5** LT B 13:30 -14:15
14:00	**Registration**	(odd numbers)	(even numbers)	**Plenary 6** LT B 14:15 -15:00
14:30		Concourse 13:30 -16:00	Concourse 13:30 -16:00	
15:00	12:00-21:00			
15:30	Academic			**marresearch** **Farewell Party** Concourse
16:00	Concourse	**MS - 4, 5 & 6**	**MS -10, 11 & 12**	
16:30		LT B, C & E 16:00 - 18:00	LT B, C & E 16:00 - 18:00	
17:00				
17:30				
18:00				
18:30	**PANalytical** **Welcome**			
19:00	**Mixer**	**Bruker-Nonius**	**Rigaku**	
19:30	UC Bistro	**Harbor Cruise**	**Chinese**	
20:00		**and Buffet**	**Banquet**	
20:30		Tsim Sha Tsui	Shatin	
21:00				
21:30				

Notes: Morning coffee and Afternoon tea will be served in the concourse during am and pm sessions, snacks will be provided at 9:45 and 15:30.

The original MS-12 and 13 are now merged under the topic 'Bio-informatics and Computational Analysis'.

June 28 Monday

09:00 **Welcoming Ceremony** *Lecture Theatre B*

Morning Microsymposia

MS01: *Molecular recognition and catalysis* *Lecture Theatre B*

Chair/Co-Chair: S. Suh/ K. Miki

10:15 MS01-1 **CRYSTAL STRUCTURE OF A HEMOLYTIC LECTIN CEL-III FROM MARINE INVERTEBRATE CUCUMARIA ECHINATA AT 1.7 Å RESOLUTION**
Tatsuya Uchida, Tomomitsu Hatakeyama, Takayuki Yamasaki, Seiichiro Eto, Hajime Sugawara, Kurisu Genji, Atsushi Nakagawa and Masami Kusunoki

10:40 MS01-2 **CRYSTAL STRUCTURES OF ARTOCARPIN-SUGAR COMPLEXES: VARIATION IN THE LENGTH OF A LOOP AS A STRATEGY FOR GENERATING LIGAND SPECIFICITY**
M. Vijayan, Anand Srivastav, A. Surolia and A. Arockia Jeyaprakash

11:05 MS01-3 **CRYSTAL STRUCTURE OF ZINC CONTAINING MONOFERRIC C-LOBE OF BOVINE LACTOFERRIN AT 1.9 Å RESOLUTION**
Sujata Sharma, Talat Jabeen, Jayashankar Jasti, Janesh Kumar, Ashok K. Mohanty and Tej P. Singh

11:25 MS01-4 **STRUCTURAL BASIS OF BACTERIAL LIPOPROTEIN TRANSPORT**
Kazuki Takeda, Hideyuki Miyatake, Naoko Yokota, Shin-ichi Matsuyama, Hajime Tokuda and Kunio Miki

11:50 MS01-5 **CRYSTAL STRUCTURE OF LEUA, AN ESSENTIAL BIOSYNTHETIC ENZYME FROM MYCOBACTERIUM TUBERCULOSIS**
Edward N. Baker, Nayden Koon and Christopher J. Squire

MS02: *Synchrotron related science and applications* *Lecture Theatre C*

Chair/Co-Chair: S.L.Chang/ S.Sasaki

10:15 MS02-1 **SYCHROTRON RADIATION AND SAD PHASING IN PROTEIN CRYSTALLOGRAPHY**
Hai-fu Fan and Yuan-xin Gu

10:45 MS02-2 **HIGH- RESOLUTION XRD AND IMAGING POLYCRYSTALLINE MICROSTRUCTURES BY MOVING AREA DETECTOR METHOD WITH HIGH-ENERGY SYNCHROTRON RADIATION**
L. Wcislak, H.J. Bunge, H. Klein, U. Garbe and J.R. Schneider

11:15 MS02-3 **X-RAY SCATTERING STUDY OF SELF-ASSEMBLED QUANTUM DOTS**
C.-H. Hsu, Yuri P. Stetsko, Mau-Tsu Tang, Hsin-Yi Lee, Yung-Wei Hsieh, Chih-Mon Huang, W. -S Liu, N.T. Yeh, J.-I. Chyi and K.S. Liang

11:35 MS02-4 **NOVEL TECHNIQUE OF NON-RESONANT X-RAY MAGNETIC SCATTERING**
Hiroyuki Ohsumi, Masaki Takata and Hiroyoshi Suematsu

11:55 MS02-5 **OBSERVATION OF TRANSIENT ROTATOR PHASE OF N-HEXADECANE IN EMULSIFIED DROPLETS BY SMALL- AND WIDE-ANGLE X-RAY SCATTERING**
Y. Shinohara, N. Kawasaki, S. Ueno, I. Kobayashi, M. Nakajima and Y. Amemiya

June 28 Monday

MS03: *Structural chemistry*

Lecture Theatre E

Chair/Co-Chair: H. Uekusa/ D. E. Hibbs

10:15 MS03-1 **VERY SHORT OACID-H···OWATER HYDROGEN BOND STUDY BY VARIABLE TEMPERATURE NEUTRON DIFFRACTION**
Ashwini Nangia, P. Vishweshwar, John A. Cowan, Sax A. Mason, Horst Puschmann, and Judith A. K. Howard

10:40 MS03-2 **TOPOLOGY AND SUBMOLECULAR PARTITIONING OF BIOLOGICALLY ACTIVE MOLECULES BASED ON EXPERIMENTAL CHARGE DENSITY DETERMINATIONS AT 100 K AND AT 20 K**
Peter Luger, Marc Messerschmidt, Stephan Scheins and Birger Dittrich

11:05 MS03-3 **STUDIES ON THE VARIANT COORDINATION MODES OF ARENESULFONATE**
Jiwen Cai and Jin-Sen Zhou

11:30 MS03-4 **NTHU-2: A HIGHLY POROUS ORGANO-METALLOPHOSPHATE STRUCTURE DETERMINED FROM A NON-MEROHEDRAL TWIN**
Yueh-Chun Liao, Fen-Ling Liao and Sue-Lein Wang

11:55 MS03-5 **REACTION CAVITY GEOMETRY DEPENDENT CONFORMATIONAL TRANSFORAMTION ON MIXED CRYSTAL FORMATION**
Champika Vithana, Hidehiro Uekusa, Akiko Sekine and Yuji Ohashi

Afternoon Microsymposia

MS04: *Macromolecular assemblies*

Lecture Theatre B

Chair/Co-Chair: K. Fukuyama/ S. H. Eom

16:00 MS04-1 **CRYSTAL STRUCTURE OF BACTERIAL MULTIDRUG EFFLUX TRANSPORTER AcrB**
Satoshi Murakami, Takashi Matsumoto, Ryosuke Nakashima, Eiki Yamashita and Akihito Yamaguchi

16:25 MS04-2 **CRYSTAL STRUCTURE OF CYTOCHROME B_6F COMPLEX OF OXYGENIC PHOTOSYNTHESIS**
Genji Kurisu, Huamin Zhang, Janet L. Smith and William A. Cramer

16:50 MS04-3 **THE ATOMIC STRUCTURE OF RICE DWARF VIRUS REVELAS THE SELF-ASSEMBLY MECHANISM OF COMPONENT PROTEINS**
Atsushi Nakagawa, Naoyuki Miyazaki, Junichiro Taka, Hisashi Naitow, Akira Ogawa, Zui Fujimoto, Hiroshi Mizuno, Kyoji Hagiwara, Takahiko Higashi, Yasuo Watanabe, Toshihiro Omura, R. Holland Cheng and Tomitake Tsukihara

17:10 MS04-4 **STRUCTURAL BASIS OF MEMBRANE-INDUCED CARDIOTOXIN A3 OLIGOMERIZATION**
C.-D. Hsiao, F. Forouhar, We.N. Huang, J.-H. Liu, K.-Y. Chien, and W.-G. Wu

17:35 MS04-5 **VESICLE TRANSPORT MACHINERY: X-RAY STRUCTURES OF HUMAN GGA PROTEINS AND THEIR PARTNERS IN THE TRANS GOLGI NETWORK**
Soichi Wakatsuki, T. Shiba, T. Nogi, M. Kawasaki, R. Kato, Y. Yamada, M. Inoue, S. Kametaka, M. Shibata, S. Waguri, Y. Uchiyama, Y. Shiba and K. Nakayama

June 28 Monday

MS05: *Neutron scattering science* — *Lecture Theatre C*

Chair/Co-Chair: R. A. Robinson/ K. Kakurai

16:00 MS05-1 **A NEW OPPORTUNITY OF NEUTRON SCIENCE - J-PARC PROJECT IN JAPAN**
Yasuhiko Fujii

16:30 MS05-2 **ON STRUCTURAL PHASE TRANSITIONS IN PEROVSKITES**
Christopher J. Howard, Michael A. Carpenter, and Kevin S. Knight

16:55 MS05-3 **STRUCTURAL DISTORTION, CHARGE AND SPIN ORDERINGS IN $Pr_{0.65}Ca_{0.25}Sr_{0.1}MnO_3$**
W.-H. Li, C. C. Yang, F. C. Tsao, P. J. Huang, J. W. Lynn and H. D. Yang

17:20 MS05-4 **IN SITU NEUTRON DIFFRACTION DURING DEUTERIUM ABSORPTION OF Pd PARTICLES EMBEDDED IN ZrO_2 MATRIX**
Stefanus Harjo, Takashi Kamiyama, Toshimitsu Yamazaki, Wataru Higemoto, Akinori Hoshikawa, Shin-ichi Yamaura, Hisamichi Kimura, Akihisa Inoue and Yoshiaki Arata

17:40 MS05-5 **THE NEW QUASI-LAUE DIFFRACTOMETER AT THE REPLACEMENT RESEARCH REACTOR**
Wim T. Klooster

MS06: *Supramolecular chemistry and crystal engineering* — *Lecture Theatre E*

Chair/Co-Chair: A. Nangia/ S. R. Batten

16:00 MS06-1 **RECENT ADVANCE IN CONSTRUCTION OF NEW TOPOLOGICAL COORDINATION POLYMER NETS**
Xiao-Ming Chen, Ming-Liang Tong, Jie-Peng Zhang and Xiao-Chun Huang

16:25 MS06-2 **CRYSTAL STRUCTURE OF 2D GRID-LIKE POLYMER BASED ON 3d-4d MIXED METALS**
Peng Cheng and Bin Zhao

16:50 MS06-3 **THE ROLE OF DOUBLE C-H...N WEAK HYDROGEN BONDING MOTIFS IN N-HETEROAROMATIC INCLUSION CHEMISTRY**
Roger Bishop, Solhe F. Alshahateet, Donald C. Craig, A. Noman, M.M. Rahman and Marcia L. Scudder

17:15 MS06-4 **HYDROGEN-BONDED POLYROTOXANE STRUCTURE CONTAININT CYCLIC $(H_2O)_4$ in $[Zn(OAc)_2(\mu\text{-bpe})]\cdot 2H_2O$: X-RAY AND NEUTRON DIFFRACTION STUDIES**
Jagadese J. Vittal, Ng Meng Tack, Wim T. Kloooster and Garry J. McIntyre

17:40 MS06-5 **FROM HEXANUCLEAR TO DODECANUCLEAR AZAMETALLACROWNS**
Shi-Xiong Liu, Shen Lin, Wen-Shi Wu, Chi-Chang Lina and Jian-Quan Huang

June 29 Tuesday

Plenary Lectures

Lecture Theatres B & C

9:00 PL1 **SUPERCONDUCTIVITY OF BORIDE AND CARBIDE SYSTEMS**
Jun Akimitsu

9:00 PL2 **STRUCTURES OF NOVEL SIGNALING PROTEINS SECRETED DURING INVOLUTION AND INVOLVED IN APOPTOSIS**
T.P. Singh

Morning Micro-symposia

MS07: *Receptors, signaling and receptor – drug interactions* *Lecture Theatre B*
Chair/Co-Chair: P. M. Colman/ T. P. Singh

10:15 MS07-1 **DRUG-RECEPTOR INTERACTIONS : CRYSTAL STRUCTURE OF A COMPLEX FORMED BETWEEN PHOSPHOLIPASE A2 AND ASPIRIN AT 1.9 Å RESOLUTION**
Rajendra Kumar Singh, A. S. Ethayathulla, Talat Jabeen, Sujata Sharma, Punit Kaur, A. Srinivasan and Tej P. Singh

10:45 MS07-2 **CRYSTAL STRUCTURE OF AN INHIBITORY ANTI-FACTOR IX FAB IN COMPLEX WITH FACTOR IX GLA DOMAIN**
Mingdong Huang, Barbara Furie and Bruce Furie

11:15 MS07-3 **STRUCTURE OF THE N1 DOMAIN OF XpsE PROTEIN FROM XANTHOMONAS CAMPESTRIS**
Nei-Li Chan, Yeh Chen, Jiun-Li Chang, and Nien-Tai Hu

11:45 MS07-4 **CRYSTAL STRUCTURE OF A SECRETORY ANTIAPOPTOTIC GLYCO -PROTEIN FROM SHEEP (SPS-40)**
Devendra B. Srivastava, Janesh Kumar, K. Sarvanan, Nagendra Singh, Sujata Sharma, A. Srinivasan and Tej P. Singh

MS-08: *Materials Science I* *Lecture Theatre C*
Chair/Co-Chair: M. Takata/ B. Kennedy

10:15 MS08-1 **3D POROUS MAGNETS OF $M_3(HCOO)_6$ (M=Mn and Co)**
Zheming Wang, Bin Zhang, Hideki Fujiwara, Takeo Otsuka, Hayao Kobayashi and Mohamedally Kurmoo

10:45 MS08-2 **CUBIC PEROVSKITE-RELATED PHASES IN THE TERNARY SrO-CuO-Nb_2O_5 SYSTEM**
Y. Liu, R. L. Withers, F. Brink, L. Noren andV. Ting

11:15 MS08-3 **NON-AMBIENT X-RAY DIFFRACTION ANALYSIS OF PHARMACEUTICAL SOLIDS**
A. Stefanovic

11:45 MS08-4 **CRYSTAL STRUCTURE OF POLY (3-HYDROXYBUTYRATE-CO-3-HYDROXYHEXANOATE) CLOSE TO MELTING POINT**
Katsuhito Mori, Masayuki Nakamura, Harumi Sato, Isao Takahashi, Hikaru Terauchi, Yukihiro Ozaki, Fuminobu Hirose, Kenichi Senda, and Isao Noda

June 29 Tuesday

MS-09: *Electron diffraction and microscopy*

Lecture Theatre E

Chair/Co-Chair: J. Etheridge/ K. Saitoh

10:15 MS09-1 **BLOCH WAVE DEGENERACIES IN NON-SYSTEMATIC CRITICAL VOLTAGE EFFECT OBSERVED IN ELECTRON DIFFRACTION**
Hirfumi Matsuhata and Jon Gjønnes

10:45 MS09-2 **DIRECT IMAGING OF A LOCAL DEBYE-WALLER FACTOR ANOMALY IN QUASICRYSTALS THROUGH ADF-STEM OBSERVATIONS**
Eiji Abe

11:15 MS09-3 **STRUCTURAL STUDIES OF THE A2LnNbO6 1:1 AND A3CoNb2O9 1:2 ORDERED PEROVSKITES (A= Ca^{2+}, Sr^{2+}, Ba^{2+})**
V.Ting, Y. Liu, R. L Withers and L. Noren

11:35 MS09-4 **UNUSUAL MAGNETIC BEHAVIOR IN $Pr_{1-x}Sr_xCoO_3$: A LORENTZ MICROSCOPE STUDY**
Masaya Uchida, Ramanathan Mahendiran, Yasuhide Tomioka, Yoshinori Tokura and Yoshio Matsui

11:55 MS09-5 **ICOSAHEDRAL QUASICRYSTAL MISSING ICOSAHEDRAL SYMMETRY**
Koh Saitoh, Tadahiro Yokosawa, Michiyoshi Tanaka and An Pang Tsai

Afternoon Micro-symposia

MS-10: *Structural genomics*

Lecture Theatre B

Chair/Co-Chair: Z. Rao/ I. Tanaka

16:00 MS10-1 **STRUCTURAL GENOMICS STUDY OF THE SARS CORONAVIRUS - THE CRYSTAL STRUCTURES OF SARS VIRUS MAIN PROTEASE (Mpro) AND ITS COMPLEX WITH AN INHIBITOR**
Zihe Rao

16:30 MS10-2 **A HIGH-THROUGHPUT APPROACH TO LINK THE BIOCHEMICAL AND CELLULAR FUNCTIONS OF MACROPHAGE PROTEINS**
Bostjan Kobe, Pawel Listwan, Nathan Cowieson, Anna Aagard, Thomas Huber, Timothy Ravasi, Christine Wells, David A. Hume and Jennifer L. Martin

17:00 MS10-3 **STRUCTURAL GENOMICS OF C. ELEGANS**
Ming Luo

17:30 MS10-4 **AN INTEGRATED APPROACH FOR SYNCHROTRON BASED STRUCTURAL PROTEOMICS ON PROTEIN GLYCOSYLATION AND TRANSPORT**
Soichi Wakatsuki, M. Kawasaki, R. Kato, M. Hiraki, N. Matsugaki, N. Igarashi and M. Suzuki

June 29 Tuesday

MS-11: *Structural nanoscience* — *Lecture Theatre C*

Chair/Co-Chair: D. Y. Noh/ C. -H. Hsu

16:00 MS11-1 **MAGNETIC STRUCTURE ANALYSIS OF ANTIFERROMAGNETIC AND FERROELECTRIC COMPOUND $ErMn_2O_5$ and YMn_2O_5**
Y. Noda, S. Kobayashi, T. Osawa, Y. Fukuda, H. Kimura, I. Kagomiya and K. Kohn

16:25 MS11-2 **RESONANT X-RAY SCATTERING FROM Fe_3O_4 SINGLE CRYSTAL: A SCENARIO OF ELECTRONIC PHASE SEPARATION BELOW THE VERWEY TRANSITION**
Hsueh-Hsing Hung

16:50 MS11-3 **CORRELATIONSHIP BETWEEN CRYSTAL STRUCTURE AND PIEZOELECTRICITY IN LANGASITE WITH FOUR CATIONS**
H. Ohsato, T. Iwataki, N. Araki, H. Morikoshi and K. Kakimoto

17:15 MS11-4 **CRYSTAL STRUCTURES AND PHASE TRANSITIONS IN THE SYSTEM $SrTiO_3$-$La_{2/3}TiO_3$**
Christopher J. Howard, A. Gregory R. Lumpkin, Ronald I. Smith and Zhaoming Zhang

17:40 MS11-5 **ANTIPHASE DOMAINS AND B-SITE ORDERING IN $Pb(Mg_{1/3}Nb_{2/3-\delta})O_3/SrTiO_3$ THIN FILMS**
Seon Hee Seo, Suraj Yadav, Do Young Noh and Kiyotaka Wasa

MS-12&13: *Bioinformatics and Computational Analysis I* — *Lecture Theatre E*

Chair/Co-Chair: S. Hall/ M. Bansal

16:00 MS12&13-1 **MULTIPLE OPEN READING FRAMES, CODON BIOS AND AMINO ACID USE AND THE EVOLUTION OF THE GENETIC CODE.**
W. L. Duax, R. Huether, L. Habegger, S. Connare, V. Pletnev and J. Schaber

16:30 MS12&13-2 **STRUCTURE BASED 'PUNCTUTATION MARKS' IN GENOMIC DNA**
Manju Bansal and Aditi Kanhere

17:00 MS12&13-3 **BIOINFORMATICS IN STRUCTURAL GENOMICS OF C. ELEGANS**
Jun Tsao, David H. Johnson and Mike Carson

17:30 MS12&13-4 **SSEP: SECONDARY STRUCTURAL ELEMENTS OF PROTEINS**
K. Sekar, V. Shanthi, P. Selvarani, Ch. Kiran Kumar and C.S.Mohire

June 30 Wednesday

Plenary Lectures

Lecture Theatres B & C

9:00 PL3 **FROM METAL STRING COMPLEXES TO METAL WIRES**
Chih-Chieh Wang and Shie-Ming Peng

9:00 PL4 **HIGH-THROUGHPUT PROTEIN CRYSTALLOGRAPY**
Isao Tanaka

Morning Micro-symposia

MS-12&13: ***Bioinformatics and Computational Analysis II*** *Lecture Theatre B*
Chair/Co-Chair: M. Bansal/ N. Niimura

10:15 MS12&13-5 **THE ROLE OF DATA DICTIONARIES IN KNOWLEDGE RETENTION**
Sydney R. Hall and Nick Spadaccini

10:45 MS12&13-6 **3D STRUCTURAL ANALYSIS OF PROSITE PATTERNS**
Sukanta Mondal, Vasanthakumar B., S. P. Jaishankar and S. Ramakumar

11:15 MS12&13-7 **MATCHING STRUCTURE TO CELL DISTORTION IN TWINNED CRYSTALS.**
A. David Rae

11:45 MS12&13-8 **DATA BASE OF HYDROGEN AND HYDRATION IN PROTEINS.**
N. Niimura, I.Tanaka, K.Kurihara,T.Chatake and M.Maeda

MS-14: ***Advanced Applications of Powder Diffraction*** *Lecture Theatre C*
Chair/Co-Chair: C. Howard/T. Kamiyama

10:15 MS14-1 **AB INITIO STRUCTURE DETERMINATION OF $Co(dt)_2$ BY GENETIC ALGORITHM**
Makoto Sakata, Yuichi Fujishiro, Eiji Nishibori, Masaki Takata, Akiko Kobayashi and Hayao Kobayashi

10:45 MS14-2 **APPLICATIONS OF LARGE 2D DETECTORS FOR NEUTRON POWDER DIFFRACTION.**
Alan W. Hewat

11:15 MS14-3 **SCREENING STABILIZING POLYMERS FOR DRUG DEVELOPMENT USING VARIABLE TEMPERATURE X-RAY DIFFRACTION**
Z. Ping Wu, R. Hart, and D. Stirling

11:35 MS14-4 **STUDY OF CRYSTAL STRUCTURE IN $LaMn_{1-x}Cu_xO_3$ COMPOUNDS**
S. Ravi and Manoranjan Kar

11:55 MS14-5 **POWDER DIFFRACTION STUDIES OF BISMUTH DOUBLE PEROVSKITE $Ba_2A^{3+}B^{5+}O_6$**
Qingdi Zhou and Brendan J. Kennedy

June 30 Wednesday

MS-15: *Materials Science II*

Lecture Theatre E

Chair/Co-Chair: J. Lin/X.-M. Chen

10:15 MS15-1 **MOLTEN SALT SYNTHESIS AND CRYSTAL STRUCTURES OF PALLADIUM PHOSPHATES AND ARSENATES**
Kwang-Hwa Lii, Ling-I Hung and Sue-Lein Wang

10:40 MS15-2 **SPIN DENSITY AND CHARGE DENSITY STUDIES ON AN ORGANIC MAGNET**
Jey-Jau Lee and Yu Wang

11:05 MS15-3 **A NOVEL ALUMINOBORATE MOLECULAR SIEVERS CONTAINING OCTAHEDRAL FRAMEWORKS OF 3D TUNNEL STRUCTURE**
Jianhua Lin and Jing Ju

11:30 MS15-4 **MODULATED STRUCTURES IN THE Ta_2O_5-WO_3 SYSTEM FROM X-RAY AND NEUTRON POWDER DIFFRACTION DATA**
Siegbert Schmid and Anja Binder

11:55 MS15-5 **A CHIRAL METAL ZINCOBOROPHOSPHATE TEMPLATED BY ACHIRAL TRIAMINE: SYNTHESIS AND CHARACTERIZATION OF $(C_4N_3H_{16})[Zn_3B_3P_6O_{24}]\cdot H_2O$**
Wei Liu, Hao-Hong Chen, Xin-Xin Yang, Man-Rong Li, Ming-Hui Ge and Jing-Tai Zhao

Plenary Lectures

Lecture Theatre B

13:30 PL5 **CRYSTALLOGRAPHY WITHOUT CRYSTALS**
Jianwei Miao, Keith O. Hodgson, Tetsuya Ishikawa, Bart Johnson Yoshiki Kohmura and Yoshinori Nishino

14:15 PL6 **GRID-ENABLED HIGH THROUGHPUT CHEMICAL CRYSTALLOGRAPHY: A NEW OPPORTUNITY FOR STRUCTURAL CHEMISTRY.**
Michael B. Hursthouse

15:00 **Concluding Remarks** *Lecture Theatre B*

June 28 Monday and June 29 Tuesday

Poster sessions

PO1 **ANALYSES OF HYDROGEN BONDS IN AMINO ACID - INORGANIC ACID 2:1 COMPLEXES**
B.Sridhar, K.Anitha and R.K.Rajaram

PO2 **BONDING AND AGGREGATIONS OF SOME AMINO ACID - INORGANIC ACID COMPLEXES**
B.Sridhar, K.Anitha and R.K.Rajaram

PO3 **ELECTRONIC STRUCTURES OF La1-xSrxCoO3 EXAMINED BY XMCD MEASUREMENS AT THE Co K ABSORPTION EDGE**
Takayasu Hanashima, Satoshi Sasaki, Norio Shimizu, Kouji Yamawaki, Takeharu Mori and Masahiko Tanaka

PO4 **CDW FORMATION IN AN INCOMMENSURATE PHASE OF 1T-TaS2 STUDIED BY X-RAY THERMAL DIFFUSE SCATTERING**
Yo Machida, Satoshi Sasaki, Takayasu Hanashima, Kouichi Ohkubo, Kouji Yamawaki and Masahiko Tanaka

PO5 **CRYSTAL STRUCTURE OF ETHYL 4-(2,5-DIOXO-2,5-DIHYDRO-1H-PYRROL-1-YL) BENZOATE**
Vasu, K. A. Nirmala, M.Vishwas and Deepak Chopra

PO6 **X-RAY DIFFRACTION, XANES AND XMCD STUDIES ON THE SITE PREFERENCE AND VALENCE STATE OF Co AND Fe IONS IN IRON COBALTITE**
Kouji Yamawaki, Norio Shimizu, Satoshi Sasaki, Takayasu Hanashima, Tomoaki Watanabe, Masahiro Yoshimura and Masahiko Tanaka

PO7 **FERROMAGNETIC ORDERING MODEL OF A CoxTi1-xO2 THIN FILM (x = 0.07)**
Norio Shimizu, Satoshi Sasaki, Takayasu Hanashima and Kouji Yamawaki

PO8 **CRYSTAL STRUCTURE OF 2-AMINO-N-(2-CHLOROPHENYL)-5,6-DIHYDRO-4H-CYCLOPENTA[b]THIOPHENE-3-CARBOXAMIDE**
K.A.Nirmala, Vasu, S.Mohan, J.Saravanan and Deepak Chopra

PO9 **DEGREE OF DISORDER IN SPINEL-TYPE (Mn,Zn,Fe)3O4 EXAMINED BY THE TWO-WAVELENGTHS ANOMALOUS DISPERSION METHOD**
Syoichi Sakurai, Satoshi Sasaki, Kouji Yamawaki, Takayasu Hanashima and Norio Shimizu

PO10 **X-RAY STRUCTURAL STUDY OF IN-PLANE ATOMIC ARRANGEMENTS IN THE LAYERED COMPOUNDS MxTiS2 (M=Cu, Ni, Co)**
Ken-ichi Ohshima, Yoshinobu Kasuga, Tomoko Kusawake, Makoto Yasuda and Hiroki Uratani

PO11 **CRYSTAL STRUCTURE OF 7-METHYL 6, 8-DINITRO 4-BROMOMETHYL COUMARIN**
K.V.Ajuna Gowda, T.N.Guru Row, N.C.Shivaprakash and M.V. Kulkarni

PO12 **CRYSTALLOGRAPHIC ANALYSIS OF HYDROGEN BONDING IN SERIES OF CHOLEST-BASED STEROIDAL MOLECULES**
Dinesh and Rajnikant

PO13 **NEUTRON STUDIES OF CLUSTER BEHAVIOUR OF Pd40Ni22.5Fe17.5P20 SPIN GLASS**
E.P. Gilbert, R. Woodward, D.H. Yu and R. A. Robinson

PO14 **AB-INITIO PHASING AT 1.7Å RESOLUTION OF A PROTEIN FERREDOXIN I BY COMBINED REAL SPACE - RECIPROCAL SPACE APPROACH**
Krishna Chowdhury, Soma Bhattacharya and Monika Mukherjee

PO15 **DIFFUSE NEUTRON SCATTERING FROM d-BENZIL, C14D10O2, USING TIME-OF-FLIGHT LAUE DIFFRACTION**
T. R. Welberry, D. J. Goossens, W. I. F. David, M. J. Gutmann, M. J. Bull and A. P. Heerdegen

PO16 **S-SAD PHASING BY OASIS2004**
J. W. Wang, Y. X. Gu, C. D. Zheng, F. Jiang and H. F. Fan

PO17 **TREATMENT OF EXPERIMENTAL ERRORS IN DIRECT-METHOD SAD PHASING**
S. Huang, J. W. Wang, Y. X. Gu, D. C. Xian, H. F. Fan and M. M. Woolfson

PO18 **EFFECT OF SULFUR-ANOMALOUS SCATTERING SIGNAL ON SAD PHASING IN THE PRESENCE OF IRON ATOMS**
D. Q. Yao, J. R. Chen, J. W. Wang, C. D. Zheng, Y. X. Gu, F. Jiang, H. F. Fan and D. C. Xian

PO19 **SYNCHROTRON X-RAY POWDER DIFFRACTION STUDY OF THE STRUCTURAL PHASE TRANSITION IN CaBr2**
Brendan J. Kennedy and Christopher J. Howard

PO20 **CHARACTERIZATION OF THE Δ' PHASE- MATRIX INTERFACE IN 1420 ALUMINIUM ALLOYS BY SAXS**
Chai Zhi-Gang

PO21 **CATION ORDERING IN PENTLANDITE (Fe,Ni)(Fe,Ni)8S8**
Kia S. Wallwork, Allan Pring and Christophe Tenailleau

PO22 **THREE-BEAM DIFFRACTION ANOMALOUS FINE STRUCTURE OF THIN FILMS**
Hsueh-Hung Wu, Yen-Ru Lee, Hsin-Hung Chen, Wen-Shien Sun and Shih-Lin Chang

PO23 **CRYSTAL STRUCTURES OF ANHYDROBARAKOL AND ANHYDROBARAKOL HYDROCHLORIDE; AN EVIDENCE OF EXCEPTIONAL C=O/C-OH QUINONE CHARACTERISTIC**
P. Chimsook, N. Ngamrojnavanich, C. Chaichantipyuth, N. Chaichit, P. Kongsaeree, A. Petsom, N. Muangsin

PO24 **THE CLEAVAGE OF DIPEPTIDES BY Co(III) COORDINATION COMPOUNDS**
Ivan Bernal, Manas Saha and Uday Mukhopadhyay

PO25 **STRUCTURAL AND CONFORMATIONAL STUDIES OF DIHYDROPYRIMIDINES**
G.Y.S.K. Swamy and K.Ravikumar

PO26 **TWO- AND THREE- DIMENSIONAL ORGANICALLY TEMPLATED OPEN-FRAMEWORK LANTHANIDE SULFATES: EFFECTS OF "LANTHANIDE CONTRACTION" ON THE FRAMEWORK ARCHITECURES**
Jiang-Gao Mao and Yan-Ping Yuan

PO27 **THE CRYSTAL STRUCTURES OF HYDRAZINIUM 2,3-PYRAZINEDICARBOXYLATES, N2H5Hpyz(COO)2, (N2H5)2pyz(COO)2 and N2H5Hpyz(COO)2.H2pyz(COO)2**
T. Premkumar, S. Govindarajan, and Nigam P. Rath

PO28 **NEW TEN COORDINATED LANTHANUM 2-PYRAZINECARBOXYLATE DIHYDRATE CONTAINING HYDRAZINIUM CATION**
S. Govindarajan, T. Premkumar , V. Manivannan , K.R. Radhakrishnan and Jonathan W. Steed

PO29 **LADDER NETWORKS IN INCLUSION COMPLEXES OF 4,4-BIS(4-HYDROXYPHENYL) CYCLOHEXANONE**
Srinivasulu Aitipamula, Ashwini Nangia, Mariusz Jaskólski and Ram Thaimattam

PO30 **π-STACKING IN NOVEL FLUORESCENT NAPHTHALIMIDE SYSTEMS**
Jim Simpson, C. John McAdam, Joy L. Morgan and Brian H. Robinson

PO31 **DL-THREONINE AND DL-PHENYLALANINE COMPLEXES WITH TRICHLOROACETIC ACID**
K.Rajagopal, R.V.Krishnakumar, K.Ravikumar and S.Natarajan

PO32 **COMPARATIVE INVESTIGATION FOR THE CRYSTAL STRUCTURE OF THE COORDINATION COMPOUNDS OF THE RARE EARTH AND SHORT CHAIN ETHER EO2 , EO3**
Jianming Gu and Xiurong Hu

PO33 **REVERSIBLE SOLID-VAPOR SUBSTITUTION REACTIONS OF LAYERED CADMIUM ORGANOSULFONATES**
Jinsen Zhou, Li Wang and Jiwen Cai

PO34 **CONSTRUCTION OF SILVER (I) COLUMN WITH ENCAPSULATED ACETYLENEDIIDE AND A HYDROPHOBIC SHEATH PROVIDED BY ANIONIC AND ZWITTERIONIC CARBOXYLATE LIGATION**
Xiao-Li Zhao and Thomas C. W. Mak

PO35 **STUDIES ON IRON(III) COMPLEXES OF 2-PYRIDYL-6-(2-PYRIDYLCARBONYL)-2-PYRIDYLMETHANONE**
Xu-Dong Chen and Thomas C. W. Mak

PO36 **SUPRAMOLECULAR STABILIZATION OF OXOCARBON ANIONS IN UREA HOST FRAMEWORKS**
Chi-Keung Lam, Thomas C. W. Mak

PO37 **SYNTHESIS, STRUCTURE, AND DNA CLEAVAGE OF AN OPTICAL REACTIVE SPIROPENTACOPPER CLUSTER**
Szu-Miao Chen, Yu Wang and Kuan-Jiuh Lin

PO38 **CHARGE DENSITY STUDY AND ROLE OF HYDROGEN BOND IN TRAN-[Ni(cyan-kN)2(NH3)4] : COMPARISON BETWEEN EXPERIMENT AND THEORY**
Hsin-Hui Shen and Yu Wang

PO39 **PHOTOCHROMISM OF SALICYLIDENEANILINES DEDUCED BY THE ACID-BASE COMPLEX FORMATION**
Kohei Johmoto, Hidehiro Uekusa and Yuji Ohashi

PO40 **SOLVOTHERMAL INDUCED TRANS-CIS ISOMERIZATION OF [Fe(TZPY)2(NCS)2] (TZPY=3-(2-PYRIDYL)[1,2,3]TRIAZOLO[1,5-A]PYRIDINE)**
K. W. Chen , C. F. Sheu , G. H. Lee and Y. Wang

PO41 **A UNPRECEDENTED HOMOCHIRAL OLEFIN-COPPER(I) 2D COORDINATION POLYMER**
Ren-Gen Xiong and Xi-Sen Wang

PO42 **FERROELECTRIC COPPER QUININE COMPLEXES**
Ren-Gen Xiong and Hong Zhao

PO43 **STRUCTURE OF AN COMPLEX COMPOSED OF METHACRYLIC ACID AND PYRIDINE**
K. Yoshida, H. Uekusa, and Y. Ohashi

PO44 **X-RAY ANALYSIS OF REACTION PROCESS THROUGH ARYLNITRENE**
Takahiro Mitsumori, Hidehiro Uekusa and Yuji Ohashi

PO45 **X-RAY DIFFRACTION STUDY OF THE CRYSTALLINE-STATE PHOTORACEMIZATION OF A BULKY ALKYL CROUP IN A COBALOXIME COMPLEX**
H. Takeoka, H. Uekusa and Y. Ohashi

PO46 **IONIZATION STATES, STOICHIOMETRY AND HYDROGEN BONDING PATTERNS IN COMPLEXES OF AMINO ACIDS WITH CARBOXYLIC ACIDS**
R.V.Krishnakumar and S.Natarajan

PO47 **SYNTHESES AND STRUCTURES OF NaCd(H2O)2[BP2O8]·0.8H2O AND NaZn(H2O)2[BP2O8]·H2O AT ROOM TEMPERATURE AND AMBIENT PRESSURE**
Ming-Hui Ge, Wei Liu, Hao-Hong Chen, Xin-Xin Yang and Jing-Tai Zhao

PO48 **A MIXED CATIONS NICKEL DIPHOSPHATE WITH A LAYERED INTERGROWTH STRUCTURE: SYNTHESIS, STRUCTURAL AND MAGNETIC CHARACTERIZATION OF Na(NH4)[Ni3(P2O7)2(H2O)2]**
Wei Liu, Xin-Xin Yang, Hao-Hong Chen, Ya-Xi Huang, Walter Schnelle and Jing-Tai Zhao

PO49 **NH4[BPO4F]: A NOVEL OPEN-FRAMEWORK AMMONIUM FLUORINATED BOROPHOSPHATE WITH A ZEOLITE-LIKE STRUCTURE RELATED TO GISMONDINE TOPOLOGY**
Man-Rong Li, Wei Liu, Ming-Hui Ge, Hao-Hong Chen, Xin-Xin Yang and Jing-Tai Zhao

PO50 **TAILORING OF BOROPHOSPHATE STRUCTURES BY HALOGEN ANIONS AND/OR ORGANIC TEMPLATES**
Jing-Tai Zhao Wei Liu, Man-Rong Li, Ya-Xi Huang, Ming-Hui Ge,Hao-Hong Chen and Xin-Xin Yang

PO51 **SYNTHESIS AND CHARACTERIZATION OF SILVER(I) 1,3-BUTADIYNEDIIDE AND ITS RELATED SILVER(I) DOUBLE SALTS CONTAINING THE C42- DIANION**
Liang Zhao and Thomas C. W. Mak

PO52 **STRUCTURAL CHARACTERIZATION OF SPIN CROSSOVER COMPLEX TRANS-[Fe(TZPY)2(NCS)2] (TZPY = 3-(2-PYRIDYL)[1,2,3]TRIAZOLO[1,5-A]PYRIDINE)**
C. F. Sheu, J. J. Lee, G. H. Lee, I. J. Hsu, Y. C. Lin, K. Toriumi, Y. Ozawa and Y. Wang

PO53 **CHARGE DENSITY INVESTIGATION OF A NON-CENTROSYMMETRIC MN COMPLEX : Mn(mal)(H2O)2**
Yen-Chen Lin, I-Jui Hsu, Gene-Hsiang Lee and Yu Wang

PO54 **CRYSTAL ENGINEERING WITH SCORPIONATE LIGANDS**
Stuart R. Batten and Martin B. Duriska

PO55 **CRYSTAL STRUCTURE AND MELTING POINT CORRELATIONS OF ACETIC ESTERS**
Hidehiro Uekusa, Hirokazu Suzuki and Yuji Ohashi

PO56 **COORDINATION POLYMER WITH ZEOLITE OR ZEOLITE-LIKE TOPOLOGIES**
Yun-Qi Tian, Lin-Hong Weng, Zhen-Xia Chen, Dong Yuan Zhao and Xiao-Zeng You

PO57 **CRYSTAL STRUCTURES OF COMPLEXES OF AMINO ACIDS WITH ZINC AND CADMIUM CHLORIDES : IONIZATION STATES, STOICHIOMETRY, COORDINATION AND CRYSTAL PACKING**
R.V.Krishnakumar, M.Subha Nandhini and S.Natarajan

PO58 **CRYSTAL AND MOLECULAR STRUCTUR OF BIS(HYDRAZINIUM) BIS(OXALATO)NICKEL(II) DIHYDRATE AND BIS(HYDRAZINIUM) BIS(MALONATO)COBALT(II) DIHYDRATE**
V. Manivannan, K.R. Radhakrishnan, K. Saravanan, S. Govindarajan and J.J. Vittal

PO59 **SYTHESIS AND CRYSTAL STRUCTURES OF POLYNUCLEAR TITANIUM(IV) AND ZIROCONIUM(IV) COMPOUNDS SUPPORTED BY AN OXYGEN TRIPODAL LIGANDS**
Xiao-Yi Yi, Tony C. H. Lam, E. Y. Y. Chan, Qian-Feng Zhang, Ian D. Williams and Wa-Hung Leung

PO60 **DIRECT OBSERVATION OF DIFFERENT REACTION ROUTE DUE TO STERIC HINDRANCE IN CRYSTALLINE-STATE PHOTOISOMERIZATION**
Yuji Ohashi, Akira Hirano and Hidehiro Uekusa

PO61 **NOVEL BIS-DIDENTATE NITROGEN LIGAND DERIVED FROM 1,4-DIHYDRAZINOPHTHALAZINE**
Ling-Kang Liu and Wen-Fu Chang

PO62 **SOLID CRYSTALLINE FORMS OF DICLOFENAC SODIUM AND DICLOFENAC ACID**
Chuttree Phurat, Narong Praphairaksit, Malatee Taiyaqupt and Nongnuj Muangsin

PO63 **SELF-ASSEMBLY OF FOUR METAL-SQUARATE (Cd(II) AND Zn(II)) COORDINATION POLYMERS WITH FLEXIBLE 1,2-BIS(4-PYRIDYL)ETHANE LIGAND (DPE)**
Chih-Chieh Wang, Hui-Wun Lin, Chin-Hui Liao, Cheng-Han Yang and Gene-Hsiang Lee

PO64 **HYDROTHERMAL SYNTHESIS, CHARACTERIZATION, AND SUPRAMOLECULAR STRUCTURE OF [Co(C6H4O2N)3]·H2O**
Kittipong Chainok and Kenneth J. Haller

PO65 **THE ORDER-DISORDER TRANSITION AT 150 K OF POLYMERIC AG(BIPY)NO3**
Weenawan Somphon, Kenneth J. Haller and A. David Rae

PO66 **SUPRAMOLECULAR STRUCTURE OF AZIDONITROSYLBIS (TRIPHENYLPHOSPHINE) NICKEL**
Nongnaphat Khosavithitkul and Kenneth J. Haller

PO67 **THE CRYSTAL STRUCTURE OF PYRIDINE-3,5-DICARBOXYLIC ACID**
Samroeng Krachodnok and Kenneth J. Haller

PO68 **INVARIOMS FOR AUTOMATED LOW ORDER DATA CHARGE DENSITY ANALYSI**
B. Dittrich, M. Spackman, P. Luger

PO69 **NEW FACE-CAPPING BONDING MODE FOR ARENES IN ORGANOMETALLIC METAL CLUSTERS**
Jasmine Po-Kwan Lau and Wing-Tak Wong

PO70 **STRUCTURAL STUDY OF COORDINATION NETWORK BASED ON METAL ORGANIC LIGANDS**
Lap Szeto, Yang-Yi Yang and Wing-Tak Wong

PO71 **POWDER NEUTRON DIFFRACTION STUDY OF A CRYSTALLINE-STATE REACTION OF AN UNSATURATED THIOAMIDE DERIVATIVE**
Takashi Ohhara, Susumu Ikeda, Kenichi Oikawa, Akinori Hoshikawa, Takashi Kamiyama, Takaaki Hosoya and Yuji Ohashi

PO72 **STRUCTURAL CHARACTERIZATION OF THREE CRYSTALLINE MODIFICATIONS OF CHLOROTHALONIL BY X-RAY POWDER DIFFRACTION**
Xiurong Hu Ziqin Yuan Jianming Gu Guanglie Lu Xiaoyan Tu

PO73 **CRYSTAL STRUCTURE AND CONFORMATION OF GEM-CHLORO NITROSO - CYCLODODECANE (CH2)n-1CNOCl, with n=12**
C.R. Girija and Noor Shahina Begum

PO74 **TOPOLOGICAL ANALYSIS OF [NH2Me2][H(HC4O4)2]**
Chi-Rung Lee, Ching-Yi Lee and Yu Wang

PO75 **SYNTHESIS AND CHARACTERIZATION OF TWO POLYMORPHS OF Fe(2,2'- bpy)(HPO4)(H2PO4)**
Wen-Jung Chang, Yau-Chen Jiang and Kwang-Hwa Lii

PO76 **SYNTHESIS AND CHARACTERIZATION OF THE FIRST METAL OXALATOPHOSPHONATE: (C3H12N2)0.5[Ga3(C2O4)(CH3PO3)4]·0.5H2O**
Chia-Hui Lin and Kwang-Hwa Lii

PO77 **SYNTHESIS AND STRUCTURAL CHARACTERIZATION OF A NEW URANIUM SILICATE: K6(UO2)2(Si4O13)**
Chih-Shan Chen and Kwang-Hwa Lii

PO78 **SYNTHESIS AND STRUCTURAL CHARACTERIZATION OF (H4APPIP)[V3(C2O4)2(HPO4)3(PO4)(H2O)]·6H2O (APPIP = 1,4-BIS(3-AMINOPROPYL)PIPERAZINE), A LAYERED VANADIU OXALATOPHOSPHATE CONTAINING DOUBLE-SIX-RING UNITS**
Ming-Feng Tang and Kwang-Hwa Lii

PO79 **ELECTRONIC STRUCTURES OF POLYMORPHS IN MONOHALOGENATED BENZYL DERIVATIVES of 2,5-DIAMINO-3,6-DICYANOPYRAZINE DYES**
Shinya Matsumoto, Yoko Uchida and Mitsuhiro Yanagita

PO80 **HYDROGEN BONDING PATTERN AND Π -Π- INTERACTIONS IN 1,7-BIS-(4-HYDROXY-3-METHOXYPHENYL)-HEPTA-3,5-DIONE (TETRA HYDRO CURCUMIN)**
Noor Shahina Begum, C. R. Girija and A .A. Syed

PO81 **LANTHANIDE CONTRACT AND pH VALUE CONTROLLED STRUCTURES CHANGE IN A SERIES OF RARE EARTH COMPLEXES WITH P-AMINOBENZOIC ACID, CRYSTAL STRUCTURE AND LUMINESCENCE PROPERTY**
Jun-Ran Li, Hao-Ling Sun, Chao-Hong Ye, Xin-Yi Wang and Song Gao

PO82 **BIS(ALKYNYL) MERCURY(II) COMPLEXES OF OLIGOTHIOPHENES AND BITHIAZOLES**
Wai-Yeung Wong, Ka-Ho Choi and Guo-Liang Lu

PO83 **COMPARISON OF MOLECULAR PACKING MODES OF CHOLESTEROL DERIVATIVES**
Young Ja Park

PO84 **STUDIES ON THE WEAK HYDROGEN BONDS IN CRYSTAL**
Zhong-Yuan Zhou, Wing-Kong Kwan, Chi-Hung Yeung and Albert S. C. Chan

PO85 **FIRST OBSERVATION OF HELICAL BUNDLES IN CRYSTAL STRUCTURE OF HELICAL PEPTIDE SCAFFOLDS CONTAINING A, B- DEHYDROPHENYLALANINE RESIDUE**
M. Gupta, Rudresh, S. Ramakumar and V. S. Chauhan

PO86 **NEW STRATEGY TO SYNTHESIZE OSMABENZYNES**
Ting Bin Wen, Wai Yiu Hung, Herman Ho Yung Sung, Ian D. Williams and Guochen Jia

PO87 **SYNTHESIS AND NLO PROPERTIES OF NEW OCTUPOLAR MOLECULES**
Quanyuan Hu, George K. L. Wong, Herman Ho Yung Sung, Ian D. Williams and Guochen Jia

PO88 **HEXAMERIZATION OF ALKYNES MEDIATED BY OsCl(PCP)(PPh3) (PCP = 2,6- (Ph2PCH2)2C6H3)**
Ting Bin Wen, Zhong Yuan Zhou and Guochen Jia

PO89 **OSMABENZENES FROM THE REACTIONS OF HC≡CCH(OH)C≡CH With OsX2(PPh3)3 (X = Cl, Br)**
Haiping Xia, Guomei He, Hong Zhang, Ting Bin Wen, Herman Ho Yung Sung, Ian D. Williams and Guochen Jia

PO90 **RUTHENIUM-CATALYZED DIMERIZATION OF TERMINAL ALKYNES**
Peng Xue, Hoi Yan Leung, Ka Yin Cheng, Wai Bong Wong, Herman Ho Yung Sung, Ian D. Williams and Guochen Jia

PO91 **DILEAD μ9-L-TARTRATE: A CHIRAL METAL-ORGANIC FRAMEWORK WITH NONA-COORDINATION OF A SINGLE LIGAND**
Andy L-F. Leung, Ricky W. Li, Herman H-Y. Sung and Ian D. Williams

PO92 **ORGANO-CERAMIC SYNTHESIS: STRUCTURE OF A HYBRID SOLID with [Ln4(μ3-OH)4] LANTHANUM-HYDROXIDE TETRAHEDRA**
Candy Z-J. Lin, Herman H-Y. Sung and Ian D. Williams

PO93 **A NOVEL POLYMORPHIC PHASE TRANSITION IN A CADMIUM POLYMER [Cd(H2O)(2,6-NAP)] INVOLVING A 7 -> 5 COORDINATION NUMBER SWITCH**
Carly H-W. Tse, Samuel M-F. Lo and Ian D. Williams

PO94 **SELECTIVE SYNTHESIS OF POLYOXOMETALLATE CLUSTERS USING STRUCTURE-DIRECTING ORGANIC AND INORGANIC CATIONS**
Icy C-P. Lau, Yi Yu, Herman H-Y. Sung and Ian D. Williams

PO95 **CHIRAL COORDINATION POLYMERS BY HYDROTHERMAL SYNTHESIS: CRYSTALLIZATIONS OF ALKALINE EARTH TARTRATES**
Yu-Fong Yen, Andy L-F. Leung, Carly H-W. Tse, Ricky W. Li and Ian D. Williams

PO96 **HYDROTHERMAL CRYSTALLIZATION AND STRUCTURE OF LUMINESCENT 1-D LANTHANIDE POLYMERS [Ln2(BIPHENATE)3(H2O)2]**
Samadara Thushari, Herman H-Y. Sung, Kam-Sing Wong and Ian D. Williams

PO97 **STRUCTURES OF IMIDAZOLE MANGANESE VANADATES: CRYSTALLIZATION OF TEMPLATED VERSUS HYBRID SOLIDS**
Yi Yu, Teresa S-C. Law, Herman H-Y. Sung and Ian D. Williams

PO98 **METAL FORMATE NETWORK SOLIDS: SOLVOTHERMAL SYNTHESIS, STRUCTURES AND MAGNETIC PROPERTIES OF α-[Co(O2CH)2],β-[Ni(O2CH)2] And [M(OH)(O2CH)] M = Co, Ni**
Alvin W-H. Siu, Ian D. Williams, Herman H-Y. Sung, John A. Cha, Candy Z-J. Lin and Xi Xiang Zhang

PO99 **1:1 AND 1:2 ADDUCTS OF BIPYRIDINES WITH BIPHENIC ACID**
Fanny L-Y. Shek, Wan-Yee Wong, Samuel M-F. Lo, Herman H-Y. Sung and Ian D. Williams

PO100 **EFFECT OF SOLVothermal CONDITIONS ON CRYSTALLIZATION OF METAL COORDINATION POLYMERS: EXAMPLES OF THE ZINC AND COBALT PYROMELLITATE - BIPYRIDINE SYSTEMS**
Samuel M-F. Lo, Stephen S-Y. Chui, and Ian D. Williams

PO101 **A CHIRAL ORGANIC SALT FROM HYDROTHERMAL REACTION OF 4,4-BIPYRIDINE AND L-TARTARIC ACID WITH 50% PROTON TRANSFER**
Wan-Yee Wong, Fanny L-Y. Shek, Samuel M-F. Lo, Herman H-Y. Sung and Ian D. Williams

PO102 **S-AKYLATION OBSERVED ON TRI(2-THIOPHENYL)PHOSPHINO Tin COMPLEXES**
Michael Y. Chiang, Chi-Hui Chang and Jing-Wei Lin

PO103 **ELECTRON DENSITY DISTRIBUTIONS ON WEAK INTERMOLECULAR INTERACTIONS: CH...O INTERACTIONS IN TEMPO RADICALS**
Masanori Yasui, Kansui Takino, Fujiko Iwasaki and Daisuke Hashizume

PO104 **RAPID DISMUTATION OF H2O2 BY COFACIAL BIS-CORROLE CATALASE MODELS**
Fei Yam, Nga-Chun Ng, Hai-Yang Liu, Lam-Lung Yeung and C. K. Chang

PO105 **TWO NEW DITERPENOIDS FROM EUPHORBIA EBRACTEOLATA: STRUCTURAL STUDIES OF A DIASTEREOMERIC PAIR**
Herman H-Y. Sung, Ian D. Williams, Hai-Ming Shi, Hua-Xu Zhu, Nancy Y. Ip and Zhi-Da Min

PO106 **X-RAY ABSORPTION FINE STRUCTURE INVESTIGATION OF VANADIUM ON TiO2/SiO2 AND SiO2 SUPPORTS**
Hsiu-Mei Lin, Sheng-Tsang Kao, Jen-Ray Chang and Shin-Guang Shyu

PO107 **THE RESEARCH OF CRYSTAL STRUCTURES BY ELECTRON CRYSTALLOGRAPHY TECHNIQUE**
Liping You, Junliang Sun, Zhaofei Li, Guobao Li and Jianhua Lin

PO108 **SYNTHETIC ROUTES TO A NEW CLASS OF BLUE-EMITTING OLIGOACETYLENIC SILANES**
Suk-Yue Poon and Wai-Yeung Wong

PO109 **TRIPLET EMISSION IN SOLUBLE MERCURY(II) POLYYNE POLYMERS**
Li Liu and Wai-Yeung Wong

PO110 **GRAFTING TiO2 ON MCM-41 AS A TiO2 SUPPORT FOR VANADIA FOR CATALYTIC OXIDATION OF ETHANOL—EXAFS AND XANES ANALYSES OF VANADIUM**
Hsiu-Mei Lin, Sheng-Tsang Kao, Jen-Ray Chang and Shin-Guang Shyu

PO111 **DIRECT OBSERVATION OF THE HYDROGEN TRANSFER IN THE SOLID-STATE ORGANIC PHOTOREACTION WITH NEUTRON DIFFRACTION METHOD**
Hosoya Takaaki, Uekusa Hidehiro, Ozeki Tomoji, Ohashi Yuji, Ohhara Takashi, Tanaka Ichiro and Niimura Nobuo

PO112 **SYNCHROTRON STRUCTURE DETERMINATIONS OF INORGANIC GIANT MOLECULES**
Tomoji Ozeki, Shin-ichi Adachi and Toshihiro Yamase

PO113 **CRYSTAL STRUCTURES OF TWO ALDOL CONDENSATION PRODUCTS**
Yin-Su WU and Jiwen Cai

PO114 **SEPARATION AND CHARACTERIZATION OF CRYSTALLINE CEFUROXIME AXETIL DIASTEREOMERS**
Chuan-Qi Zheng and Jiwen Cai

PO115 **THE CRYSTAL STRUCTURES OF A SREIES OF DINICKEL COMPLEXES BRIDGED BY UNUSUAL (N,O,O')- COORDINATED AMINO ACIDS**
Li Wang, Jiwen Cai and Jin-Wang Huang

PO116 **VARIATION IN THE COORDINATION MODES OF DIFFERENT ARENEDISULFONATES TO TRANSITION METAL IONS**
Dong-Sheng Deng and Jiwen Cai

PO117 **A CONTEMPORARY APPROACH TO MORPHOLOGICAL CONTROL OF NANOCRYSTALS**
Mingmei Wu, Xianfeng Yang, Gan Lin, Caihong Wang, Wenjiao Lin, Lifang Liang, Xijiang Chen, Ningsheng Xu and Qiang Su

PO118 **CRYSTAL STRUCTURES AND MAGNETISM OF A SERIES OF TETRANUCLEAR HETEROMETALLIC Co(III)-Ln(III) COMPLEXES**
Feng He, Yang-Yi Yang and Xiao-Ming Chen

PO119 **CRYSTAL STRUCTURE OF DINUCLEAR COPPER (II) COMPLEX OF DIMETHYLGLYOXIME WITH BRIDGING CHLORIDE**
J. Kowiththaya, S. Siripisarnpipat, V. Ngumviriyakul, N. Chaichit andS. Sukvinich

PO120 **CONFORMATION OF EIGHT MEMBERED RING : 6-[BIS (2-CHLORO ETHYL)AMINO]-12 - OXO - DIBENZO [d,g],[1,3,2] DIOXAPHOSPHOCIN 6- OXIDE**
M.Krishnaiah and N.Jagadeesh Kumar.

PO121 **ELECTRON DENSITY AND ELECTRONIC CONFIGURATION OF BIOMIMETIC MODEL DINITROSYL IRON COMPLEX [S5Fe(NO)2]-**
I.-Jui Hsu, Jey-Jau Lee, Chung-Hung Hsieh, Tze-Yuan Wang, Gene-Hsiang Lee, Jin-Ming Chen, Jyh-Fu Lee, Shyue-Chu Ke, Wen-Feng Liaw and Yu Wang

PO122 **MULTIPLE-WAVE X-RAY DIFFRACTION AT RESONANCE: AN ITERATIVE BORN APPROXIMATION**
W.-H. Sun , Y.-R. Lee, S.-C. Weng, S.-Y. Cheng, W.-C. Sun and S.-L. Chang

PO123 **C-C BOND CLEAVAGE OF ALKYL AND ARYL CYANIDES BY A DINUCLEAR COPPER(II) CRYPTATE**
Tongbu Lu, Xiaomei Zhuang, Danni Que, Yanwu Li, RuoQqiu Wu, and Shi Chen

PO124 **CRYSTAL STRUCTURE AND CHARACTERIZATION OF A NEW CARBOXYLATO-MPO ORGANIC-INORGANIC HYBRID MATERIAL**
Yueh-Chun and Sue-Lein Wang

PO125 **STRUCTURAL CHARACTERIZATION OF TWO ORGANICALLY TEMPLATED GALLIUM PHOSPHATE**
Yu-Lun Lai and Sue-Lein Wang

PO126 **MIMICRY OF DIMETALLIC HYDROLASES: SYNTHESES, STRUCTURES AND ACTIVITIES OF ASYMMETRIC HOMO- AND HETERO-DINUCLEAR MODELS**
Gen-qiang Xue, Ian D. Williams and Xiao-Yuan Li

PO127 **STRUCTURAL ANALYSIS OF FIVE-COORDINATE TRANSITION METAL BORYL COMPLEXES WITH DIFFERENT D-ELECTRON CONFIGURATIONS**
King Chung Lam, Wai Han Lam, Zhenyang Lin, Todd B. Marder and Nicholas C. Norman

PO128 **X-RAY CRYSTAL STRUCTURE OF PLASMODIUM VIVAX DIHYDROFOLATE REDUCTASE: ANTIFOLATE RESISTANCE MECHANISM**
Palangpon Kongsaeree, Puttapol Khongsuk, Ubolsree Leartsakulpanich, Penchit Chitnumsub and Yongyuth Yuthavong

PO129 **SELF-ASSEMBLY OF MULTINUCLEAR RUTHENIUM THIOSALICYLATE SUPRAMOLECULES**
Stephen Sin-Yin Chui, Sharon Lai-Fung Chan and Chi-Ming Che

PO130 **THE CRYSTAL STRUCTURE OF SODIUM DIVANADYLDICITRATE DODECAHYDRATE**
Pham Thanh Huyen and Kenneth J. Haller

PO131 **TROILITE WITH SPACE GROUP P31c FOUND IN METEORITE**
Takeshi Nakagawa, Michael E. Zolensky, Katsuhiro Kusaka, Yoshikazu Miyatac and Kazumasa Ohsumi

PO132 **A RE-INVESTIGATION OF THE CRYSTAL STRUCTURE OF NATURAL CHEVKINITE**
Li Guowu, Ma Zhengsheng, Shi Nicheng, Xiong Ming and Fan Haifu

PO133 **STRUCTURE CHANGE OF Mn_2O_3 UNDER HIGH PRESSURE CAUSED BY CHARGE DISPROPORTIONATION**
Takamitsu Yamanaka, Takaya Nagai, Tomoo Fukuda and Koichi Kittaka

PO134 **THE STRUCTURAL BASIS OF STABILITY AND SUBSTRATE SPECIFICITY OF A PLANT CYSTEINE PROTEASE FROM AN INDIGENOUS FLOWERING PLANT, ERVATAMIA CORONARIA**
Chandana Chakrabarti, Piyali Guha Thakurta, Sampa Biswas and J.K. Dattagupta

PO135 **STRUCTURAL BASIS FOR CATALYTIC RACEMIZATION AND SUBSTRATE SPECIFICITY OF N-ACYLAMINO ACID RACEMASE FROM DEINOCOCCUS RADIODURANS**
Wen-Ching Wang, Wei-Chun Chiu, Chun-Li Wu, Cheng-Yu Chen, Jai-Shin Liu, and Wen-Hwei Hsu

PO136 **COMPARISON OF THE STRUCTURE AND FUNCTION OF INFLUENZA VIRUS NEURAMINIDASE AND PARAINFLUENZA VIRUS HAEMAGGLUTININ-NEURAMINIDAS(HN)**
P.M. Colman

PO137 **STRUCTURAL INVESTIGATION OF MYCOBACTERIUM SMEGMATIS DPS**
Siddhartha Roy, Satyabrata Das, Surbhi Gupta, K . Sekar, Dipankar Chatterji and M. Vijayan

PO138 **AWAY FROM THE EDGE: SAD PHASING FROM THE SULFUR ANOMALOUS SIGNAL MEASURED IN-HOUSE WITH CHROMIUM RADIATION**
C. Yang, J. W. Pflugrath, D. A. Courville, C. N. Stence, S. P. Williams, K. P. Madauss and J. D. Ferrara

PO139 **CRYSTAL STRUCTURE OF DISINTEGRIN A DOMAIN SWAPPED HOMODIMER FROM SAW-SCALED VIPER (ECHIS CARINATUS) AT 2.5Å RESOLUTION**
Punit Kaur, Sameeta Bilgrami, Shailly Tomar, Savita Yadav, Janesh Kumar, Talat Jabeen, Sujata Sharma and T. P. Singh

PO140 **INTRODUCTION OF THE PROTEIN DATA BANK JAPAN (PDBJ)**
T. Kosada, R. Igarashi, Y. Kengaku, S. Saeki, Y. Morita, M. Kusunoki, K. Kobayashi, A. Paehler, N. Ito and H. Nakamura

PO141 **REFOLDING, PURIFICATION AND CRYSTALLIZATION OF APICAL MEMBRANE ANTIGEN 1 FROM PLASMODIUM FALCIPARUM**
Tao Bai, Aditi Gupta and Adrian H. Batchelor

PO142 **CRYSTAL STRUCTURE OF A NOVEL SIGNALLING GLYCOPROTEIN FROM BOVINE REVEALS A NEW RECOGNITION SITE**
Janesh Kumar, Jayshankar Jasti, Sujata Sharma, Bhaskar Singh, Asha Bhushan and Tej P. Singh

PO143 **CRYSTAL STRUCTURE OF THE SMALL FORM OF GLUCOSE-INHIBITED DIVISION PROTEIN A FROM THERMUS THERMOPHILUS HB8**
W. Iwasaki, H. Miyatake and K. Miki

PO144 **CRYSTAL STRUCTURE OF SPHERICAL PARTICLE OF TOBACCO NECROSIS VIRUS COAT PROTEIN LACKNG N-TERMINAL ARM AT 2.6 Å RESOLUTION**
Keiichi Fukuyama, Shu Ishitobi and Kazuhiko Saeki

PO145 **X-RAY CRYSTAL STRUCTURE ANALYSIS OF A COMPLEX BETWEEN CARBOXYPEPTIDASE Y AND A PROTEIN INHIBITOR**
Yasuo Hata, Minoru Hayashida, Tomomi Fujii, Joji Mima, Rikimaru Hayashi and Yoshimi Ueda

PO146 **CRYSTALLIZATION AND PRELIMINARY X-RAY STUDY OF CARNOSINASE FROM MICE**
Tetsuo Yamashita, Hiroto Otani, Genji Kurisu, Masamni Kusunoki, Nobuaki Okumura and Katsuya Nagai

PO147 **FACTORS THAT INFLUENCE SUCCESS IN PROTEIN CRYSTALLIZATION**
Heather M. Baker, Ivan Ivanovic and Edward N. Baker

PO148 **CONCENTRATION AND CALCIUM DEPENDENT MONOMER-DIMER AND ACTIVITY-INACTIVITY TRANSITIONS IN PHOSPHOLIPASE A2: CRYSTAL STRUCTURE OF A CALCIUM INDUCED DIMER AT 1.6 Å RESOLUTION**
Talat Jabeen, Sujata Sharma, Nagendra Singh, Rajendra K. Singh, Punit Kaur and Tej P. Singh

PO149 **NATIVE PEPTIDES AS POTENT INHIBITORS OF SERINE PROTEASES: CRYSTAL STRUCTURE OF A COMPLEX FORMED BETWEEN a-CHYMOTRYPSIN AND ITS AUTOCATALYTICALLY PRODUCED OCTAPEPTIDE AT 2.2Å RESOLUTION**
Nagendra Singh, Talat Jabeen, Sujata Sharma, Ipshita Roy, M. N. Gupta, Sameeta Bilgrami, A. P. Baxla, Sharmistha Dey, Marcus Perbandt, Ch. Betzel and Tej P. Singh

PO150 **ANAEROBIC AND AEROBIC STRUCTURES OF FERREDOXIN II FROM DESULFOVIBRIO GIGAS REVEAL ELECTRON TRANSFER MECHANISM**
Chun-Jung Chen, Yin-Cheng Hsieh, Ming-Yih Liu and JeanLeGall

PO151 **CRYSTAL STRUCTURE OF CHORISMATE SYNTHASE: A NOVEL FMN-BINDING FOLD AND FUNCTIONAL INSIGHTS**
Se Won Suh and Hyung Jun Ahn

PO152 **PROBING THE DNA KINK STRUCTURE INDUCED BY THE HYPERTHERMOPHILIC CHROMOSOMAL PROTEIN SAC7D USING SITE-DIRECTED MUTAGENESIS AND X-RAY CRYSTALLOGRAPHY**
Chin-Yu Chen, Ting-Wan Lin, Chia-Cheng Chou, Tzu-Ping Ko and Andrew H.-J. Wang

PO153 **SECONDARY BINDING SITE OF TRYPSIN REVEALED BY CRYSTAL STRUCTURE OF TRYPSIN-OVOMUCOID INHIBITOR COMPLEX**
B. Syed Ibrahim and Vasantha Pattabhi

PO154 **CRYSTAL STRUCTURE OF THERMOSTABLE LIPASE FROM NEW SPECIES OF GEOBACILLUS STRAIN T1**
Raja Noor Zaliha Raja Abd. Rahman, Takahiko Yamamoto, Leow Thean Chor, Abu Bakar Salleh, Mahiran Basri, Kazufumi Takano, Shigenori Kanaya, Hiroyoshi Matsumura, Tsuyoshi Inoue and Yasushi Kai

PO155 **STUDIES ON THE CRYSTAL STRUCTURE AND FUNCTION OF CUCURMOSIN, A RIBOSOME-INACTIVATING PROTEIN FROM SARCOCARP OF CUCURBITA MOSCHATA**
Ming-Huang Chen, Shan Liu, Zhi-Ren Wang and Liqing Chena

PO156 **CRYSTAL STRUCTURE OF INORGANIC PYROPHOSPHATASE FROM HELICOBACTER PYLORI**
Y.-J. Sun, T.-C. Chao, C.-Y. Huang and H.-M. Huang

PO157 **AVAILABILITY OF THE X-RAY DATA COLLECTED WITH A CR ROTATING-ANODE FOR PHASING PROTEIN CRYSTALS**
Takashi Yamane, Atsuo Suzuki, Seiji Okazaki, Hideki Tanizawa, Tatsuo Hikage, Venkatachalam Rajakannan, Devadasan Velmurugan and Kanagaraj Sekar

PO158 **FIRST DETERMINATION OF THE INHIBITOR COMPLEX STRUCTURE OF HUMAN HEMATOPOIETIC PROSTAGLANDIN D SYNTHASE**
Yuji Kado,a Tsuyoshi Inoue, Yousuke Okano, Kousuke Aritake, Daisuke Irikura, Nobuko Uodome, Nobuo Okazaki, Shigehiro Kinugasa, Hideyuki Shishitani, Hiroyoshi Matsumura, Yasushi Kai and Yoshihiro Urade

PO159 **THE NEW MACROMOLECULE CRYSTALLOGRAPHY BEAMLINE 3W1A AT BSRF**
Peng Liu, YuHui Dong, Sheng Huang, DeQiang Yao and DingChang Xian

PO160 **CRYSTAL STRUCTURE OF A DISSIMILATORY NITRITE REDUCTASE FROM HYPHOMICROBIUM DENITRIFACANS**
Yong Xie, Tsuyoshi Inoue and Yasushi Kai

PO161 **CRYSTAL STRUCTURE OF THE SHANK PDZ-LIGAND COMPLEX REVEALS A CLASS I PDZ INTERACTION AND A NOVEL PDZ-PDZ DIMERIZATION.**
Y.J. Im, J.H. Lee, S.H. Park, S.J. Park, S.H. Rho, G.B. Kang, E. Kim and S.H. Eom

PO162 **THE STRUCTURE OF IMPORTIN-β BOUND TO SREBP-2 : INSIGHTS INTO NUCLEAR TRANSPORT OF A TRANSCRIPTION FACTOR**
Soo Jae Lee, Toshihiro Sekimoto, Eiki Yamashita, Emi Nagoshi, Atsushi Nakagawa, Naoko Imamoto, Masato Yoshimura, Hiroaki Sakai, Khoon Tee Chong, Tomitake Tsukihara and Yoshihiro Yoneda

PO163 **MOLECULAR REPLACEMENT SOLUTION FOR AN ACYLPHOSPHATASE FROM PYROCOCCUS HORIKOSHII**
Yuk-Yin Cheung and Kam-Bo Wong

PO164 **CRYSTALLIZATION, DIFFRACTION AND MOLECULAR REPLACEMENT OF A NOVEL ORANGE FLUORESCENT PROTEIN FROM CERIANTHUS SP.**
Denis T.M. Ip, David C.C. Wan and Kam-Bo Wong

PO165 **APPLICATIONS OF ACORN TO ATOMIC RESOLUTION DATA / TRUNCATED DATA AT 1.5 Å RESOLUTION OF CATALASE (~57 kDa)**
S. Selvanayagam, D. Velmurugan and T. Yamane

PO166 **STRUCTURAL BASIS OF NLS - BINDING SPECIFICITY OF IMPORTIN α ISOFORMS**
S.N.Y. Yang , J. Harris and B. Kobe

PO167 **STRUCTURAL AND FUNCTIONAL INSIGHT INTO NONSPECIFIC NUCLEASES INVOLVED IN CELL DEFENSE**
Hanna S. Yuan, Chia Lung Li, Kuo-Chiang Hsia and Woei-Chyn Chu

PO168 **CRYSTAL STRUCTURE AND CONFORMATION ANALYSIS OF A TETRAPEPTIDE BOC-B-ALA-LEU-AIB-VAL-OME**
R. S. Rathore

PO169 **CRYSTAL STRUCTURE OF THIAPYRAN REVEAL HERRING-BONE P ··· P INTERACTIONS**
T. Narasimhamurthy, J. C. N. Benny, K. Pandiarajan and R. S. Rathore

PO170 **SINGLE-CRYSTAL NEUTRON DIFFRACTION STUDIES OF RUBREDOXIN AND OTHER SMALL PROTEINS.**
Robert Bau

PO171 **WATER ENHANCED CRYSTALLINITY IN CYRTOPHORA SPIDER DRAGLINE**
Hwo-Shuenn Sheu, Khin Win Phyu, Yung-Ping Chiang, Yuch-Cheng Jean and I-Min Tso

PO172 **TWISTING OF PEPTIDE BOND BY HYDRATION WATERS AND LOCALIZATION OF DEUTERIUM ATOMS OBSERVED IN HUMAN LYSOZYME BY NEUTRON CRYSTALLOGRAPHY**
Kaori Chiba-Kamoshida, Takuro Matsui, Toshiyuki Chatake, Takashi Ohhara, Andreas Ostermann, Ichiro Tanaka, Katsuhide Yutani and Nobuo Niimura

PO173 **DESIGN OF PEPTIDES WITH a, b - DEHYDRO-RESIDUES: SYNTHESES, CRYSTAL STRUCTURES AND MOLECULAR CONFORMATIONS OF TWO TETRAPEPTIDES : Cbz - DVal - Val - DPhe - Ile - OCH3 AND Cbz - DVal - Leu - DPhe - Leu - OCH3**
V. K. Goel, A. P. Baxla, R. K. Somvanshi, R. Padma , S. Dey and T. P. Singh.

PO174 **EXPRESSION, PURIFICATION AND CRYSTALLIZATION OF MOB1 FROM *Sacchromyces cerevisiae***
Shannon W. N. Au, J. Wade Harper and David Barford

PO175 **THE C-TERMINAL REGION IN TRICHOSANTHIN IS IMPORTANT FOR ACTIVITY AND CONFORMATIONAL STABILITY**
Hiu-Mei Too,Yi Ding, Siu-Hong Chan, Zhilong Wang, Yiwei Liu, Mark Bartlam, Yicheng Dong, Kam-Bo Wong, Zihe Rao and Pang-Chui Shaw

PO176 **PURIFICATION AND STUDY OF ITS EFFECT OF POLYTYPISM IN SOLUTION GROWN CADMIUM IODIDE CRYSTALS USING X-RAY DIFFRACTION**
S.K.Chaudhary and Harjeet Kaur

PO177 **PHENOMENON OF POLYTYPISM IN MELT-GROWN LAYERED CRYSTAL OF CdI2 , PbI2 AND CdBr2.**
S.K.Chaudhary and Harjeet Kaur

PO178 **CRYSTALLIZATION OF SOME ORGANIC CONSTITUENTS OF URINARY STONES IN GEL AND CHARACTERIZATION**
E. Ramachandran and S. Natarajan

PO179 **SOME AZIDO-BRIDGED COORDINATION POLYMERS: STRUCTURES AND MAGNETISM**
Song Gao, Hao-Ling Sun, Yuan-Zhu Zhang and Bao-Qing Ma

PO180 **BISMUTH DISORDER IN PYROCHLORE OXIDES**
Brendan J Kennedy, Leqing Li and Qingdi Zhou

PO181 **XRD, FTIR AND TGA/DTA STUDIES OF GEL GROWN GLYCINE AND DL-SERINE**
E. Ramachandran and S. Natarajan

PO182 **CRYSTAL GROWTH BY CHEMICAL TRANSPORT OF PEROVSKITE TUNGSTEN BRONZES, LixWO3, AND THEIR OPTICAL PROPERTIES**
K. R. Dey, A. Hussain and C. H. Rüscher

PO183 **3X3X1 SUPERSTRUCTURE OF LITHIUM MANGANESE SPINEL**
Nobuo Ishizawa, Douglas du Boulay, Kenji Tateishi, Katsumi Suda and Shuji Oishi

PO184 **MICRO-STRUCTURAL STUDY ON THE ALLOY MLNi3.75CO0.75Mn0.3Al0.2 (ML: LA-RICH MISCH METAL) DURING THE HYDROGEN ABSORPTION AND DESORPTION CYCLING**
Guanglie Lu and Zhiqing Yuan

PO185 **RESIDUAL STRESS MEASUREMENT FOR GRANITE BY TOF NEUTRON DIFFRACTION METHOD**
T. Ishigaki, H. Obana, J. Kodama, S. Harjo and T. Kamiyama

PO186 **HYDROGEN-BONDED CRYSTALLINE FRAMEWORK BASED ON RESORCIN[4]ARENE AND 4,4'-BIPYRIDINEDIENE**
Shu-Qun Liu, Qian-Feng Zhang and Wa-Hung Leung

PO187 **OXYGEN-INDUCED FORMATION OF A NOVEL TETRA-NUCLEAR P-CYMENE RUTHENIUM COMPLEX WITH OXO BRIDGES**
Lihua Liu, Qian-Feng Zhang and Wa-Hung Leung

PO188 **CRYSTALLOGRAPHY OF MICROSTRUCTURAL TRANSITIONS IN COPPER BASED SHAPE MEMORY ALLOYS**
O. Adıgüzel

PO189 **POSITIONAL DISORDER AND DIFFUSION PATH IN OXIDE-ION CONDUCTORS**
Masatomo Yashima, Katsuhiro Nomura, Daiju Ishimura, Syuuhei Kobayashi, Hiroyuki Kageyama, Wataru Nakamura, Kenjiro Oh-uchi and Kenji Ohoyama

PO190 **HIGH-TEMPERATURE NEUTRON POWDER DIFFRACTION STUDY OF CERIA UP TO 1500C**
Syuuhei Kobayashi, Masatomo Yashima, Daiju Ishimura, Kenjiro Oh-uchi, Wataru Nakamura, Kenji Ohoyama, Katsuhiro Kawachi and Tadahi Yasui

PO191 **STRUCTURAL CHANGE OF THE Li-DOPED LANTHANUM TITANATE PEROVSKITE La2/3-xLi3xTiO3**
Wataru.Nakamura, Masatomo Yashima, Daiju Ishimura, Syuuhei Kobayashi, Kenjiro Oh-uchi, Mitsuru Itoh and Kenji Ohoyama

PO192 **AN ORGANICALLY TEMPLATED NICKEL GALLOPHOSPHATE WITH A UNIQUE LAYER STRUCTURE**
Chia-Her Lin, Yu-Lun Lai and Sue-Lein Wang

PO193 **GRASS FORMIG AT THE LIMIT: HOW GLASS FORMS WHEN THERE IS INSUFFICIENT NETWORK FORMER TO GO AROUND**
Shinji Kohara, Kentaro Suzuya, Ken Takeuchi, Chun-Keung Loong, Marcos Grimisditch, J.K. Richard Weber, Jean A. Tangeman and Thomas S. Key

PO194 **NEW RESULTS BY USING TEM TO STUDY OF THE MAGNETIC MATERIALS NbFeB**
V. Vong, D.M. Thuy and N.V. Vuong

PO195 **ROLE OF THE DOPED ELEMENTS IN MATERIALS FOR GAS SENSORS**
V. Vong and L.T. Hung

PO196 **CRYSTAL STRUCTURE X-RAY ANALYSIS OF TWO SPIRO-BIFLUORENE COMPOUNDS WITH REMARKABLE INTENSE SOLID-STATE RED FLUORESCENCE**
Chin-Ti Chen, Chih-Long Chiang, Wei-Ching Wu and Yuh-Sheng Wen

PO197 **CORRELATION BETWEEN CRYSTAL STRUCTURE AND FERROELECTRIC PHASETRANSITION TEMPERATURE FOR KTP MATERIALS.**
Stefan T. Norberg, Joacim Gustafsson and Nobuo Ishizawa

PO198 **SYNTHESIS, STRUCTURE, AND PHASE RELATIONSHIP IN LITHIUM MANGANESE OXIDE SPINEL**
Masao Yonemura, Atsuo Yamada, Stefanus Harjo, Takashi Kamiyama and Ryoji Kanno

PO199 **CRYSTAL STRUCTURE ANALYSIS OF Ti-Cr-Mo HYDROGEN ABSORBING ALLOYS**
K.Iwase, Y.Nakamura, E.Akiba and T.Kamiyama

PO200 **CARBON MICRO-RODS IN LOW-TEMPERATURE HYDROGENATED AMORPHOUS CARBON**
Prabal Dasgupta, D.P. Bhattacharyya, Nikhilesh Chowdhuri and Arup Banerjee

PO201 **EVOLUTION OF GROWTH MODE, MICROSTRUCTURE, AND PHOTOLUMINESCENCE IN MG- DOPED GAN EPILAYERS ON AI2O3 (0001)**
Hsueh-Hsing Hung, Chin-Pin Chuang and Ling-Yun Jang

PO202 **STRUCTUAL ANALYSIS OF SLIDE-RING GEL BY SMALL ANGLE X-RAY SCATTERING AND CONTROL OF THE PULLEY EFFECT**
Kentaro Kayashima, Yuya Shinohara, Eiji Takeuchi, Yoshiyuki Amemiya, Yasushi Okumura and Kohzo Ito

PO203 **METAL-BASED MOLECULAR FUNCTIONAL MATERIALS OF FLUORENES**
Wai-Yeung Wong

PO204 **CRYSTAL STRUCTURES OF MOLECULAR COMPLEXES BETWEEN SURFACTANTS AND HYDROQUINONE**
Akiko Sekine, Yuko Fujimura, Hidehiro Uekusa, Yuji Ohashi and Nahoko Iimura

PO205 **LITHIUM DIFFUSION IN LITHIUM MANGANESE SPINEL**
Kenji Tateishi, Douglas du Boulay and Nobuo Ishizawa

PO206 **NUMERICAL CONVERSION BETWEEN THE PEARSON VII AND THE VOIGT FUNCTIONS**
H. Wang and J. Zhou

PO207 **ON EQUIVALENCE OF COLORINGS OF PATTERNS ASSOCIATED WITH DECOMPOSITIONS OF THEIR SYMMETRY GROUPS**
Rene P. Felix and Maria Veronica P. Quilinguin

PO208 **THE AUSTRALIAN REPLACEMENT RESEARCH REACTOR**
R. A. Robinson and S. J. Kennedy

PO209 **IMPROVEMENT OF SPATIAL RESOLUTION OF IMAGES TAKEN WITH X-RAY CCD DETECTOR BY MAXIMUM LIKELIHOOD METHOD**
Y. Shinohara, E. L. Kosarev, Y. Ueji,a K. Uesugi, Y. Suzuki, N. Yagi and Y. Amemiya

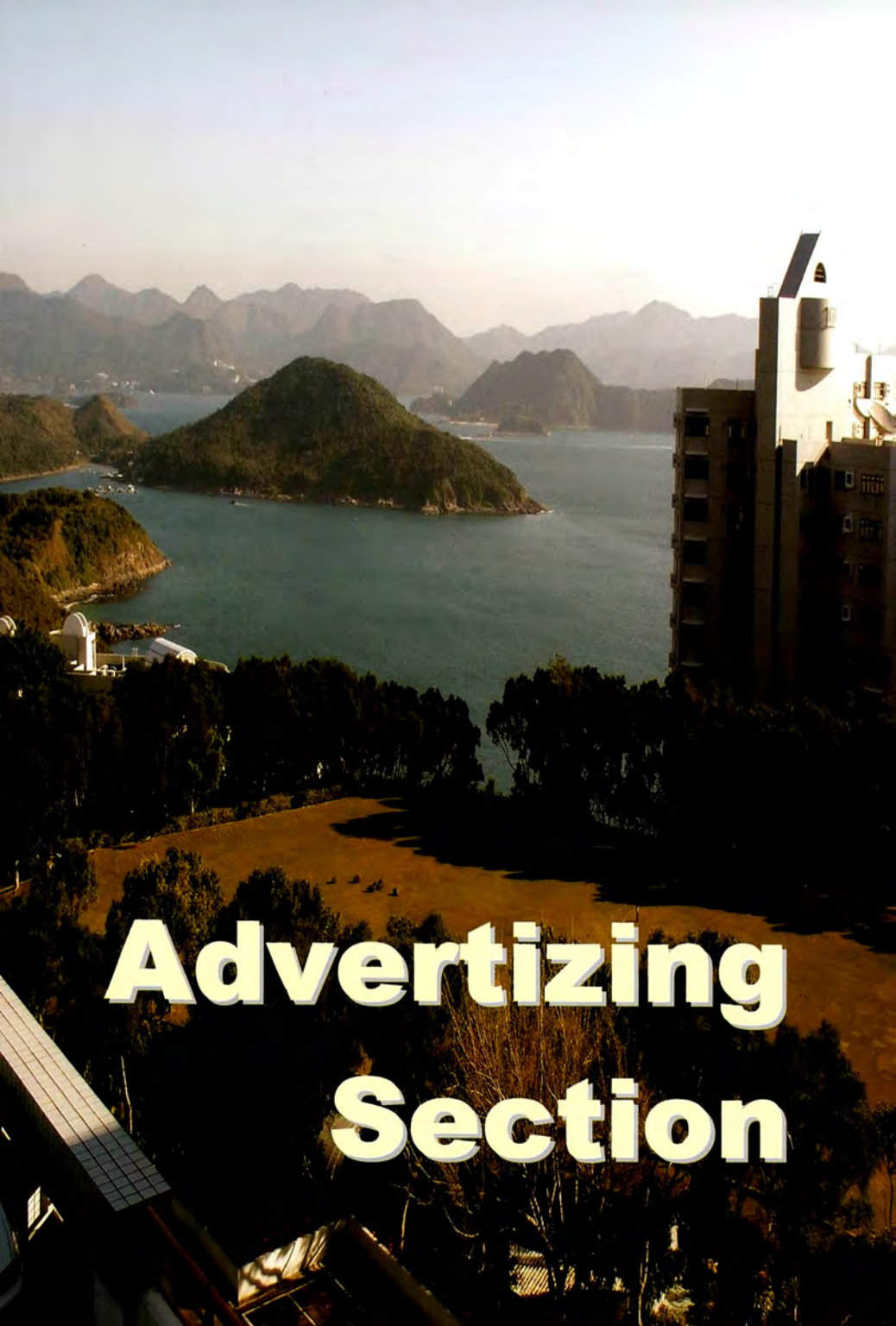
Advertizing
Section

FOX 2D focusing x-ray optic...

... simply unique

The **UNIQUE** combination of the precision graded multilaye
coating along the mirror length with a **SINGL**
mirror substrate allows the capture
a part of the source larger tha
any other multilayer mirr
system of equivalent length.

The single reflection brings more flux to your sample

- enhanced useful flux compared to standard tw reflection designs
- reduced collection time
- enhanced lifetime and lower cost of ownership (unc vacuum)
- compact mechanical design
- easy to align (10 minutes procedure)
- adaptable to all X-ray generators(rotating anode generators, sealed tubes or micro-focus sources)

Data courtesy of R. Kahn, L. Nauton, IBS Grenoble

Before upgrade with classical confocal multilayer system	Lysozyme crystal 0.4x0.4x0.4 mm and Gd as a phasing agent Unit cell (Å) a=b=77.12 c=38.6	After Upgrade with Fox 2D single reflection multi-layer optic from Xenocs
3 Minutes Exposure	Data collection: 360 images at 1° steps	1 Minute Exposure
0.55	Mosaicity	0.55
0.209	Rsym from 1.86 to 1.75	0.209
0.262	Rsym from 1.75 to 1.66	0.27
0.053	Rsym mean	0.048
0.053	Rfac	0.048
0.074	R ano	0.074
99.8	Completion	99.9
23.4	Multiplicity	23.3
9.0	Imean/Sig	10.2
2.5	I/Sig from 1.75 to 1.66	3.3

Xenocs

www.xenocs.com sales@xenocs.com
phone +33 4 76269540 fax +33 4 7626954

INTERNATIONAL TABLES for CRYSTALLOGRAPHY

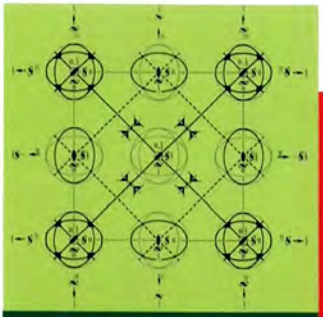

Volume A
Space-group symmetry

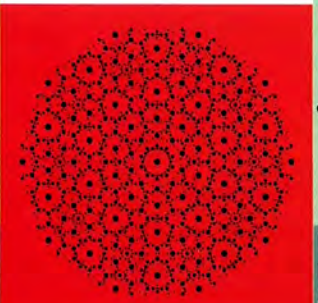

Volume B
Reciprocal space

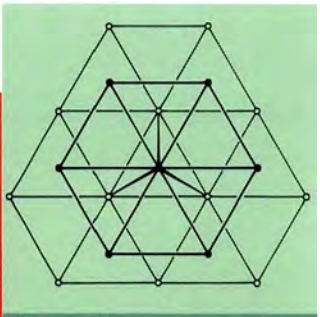

Volume C
Mathematical, physical and chemical tables

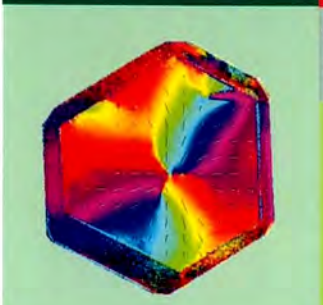

Volume D
Physical properties of crystals

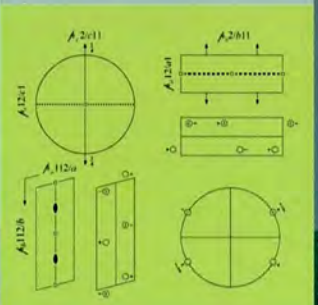

Volume E
Subperiodic groups

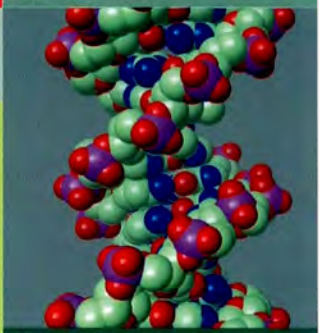

Volume F
Crystallography of biological macromolecules

Coming soon

Volume A1
Symmetry relations between space groups

Volume G
Definition and exchange of crystallographic data

www.iucr.org/it

An advanced analytical tool to deal with a broad, in-depth analysis

Rigaku

Multi purpose X-ray Diffractometer

D/MAX-Ultima III

The D/MAX-Ultima III is a versatile X-ray diffractometer equipped with crossbeam optics, an incident optical system unique to Rigaku. This analytical tool, as a single unit, can handle a wide variety of analyses ranging from routine powder sample analysis to thin film material evaluation analysis by in-plane measurement.

High-resolution parallel beam optics

Quite effective for high-precision analysis of organic compounds, ceramics, samples characterized by strong preferred orientation, those difficult for crushing and shaping, as well as structure analysis.

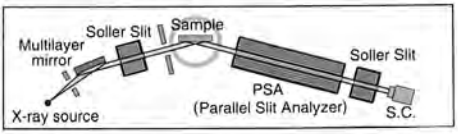

Comprehensive analysis software for X-ray powder diffraction patterns,

JADE 6.5

JADE 6.5 provides comprehensive information on crystals simply, accurately and rapidly just by clicking the aimed program. Included are qualitative and quantitative analysis, crystallite size calculation, lattice parameter refinement, structure analysis with powder patterns, and much more.

Rigaku Corporation
Beijing Office : Rm.1505, No.22, FANLI Bldg., Chaowai Street, Chaoyang District, Beijing 100020, China
Phone: 86-10-6588-3370 Fax: 86-10-6588-3372
http://www.rigaku.com.cn/

Rigaku/MSC, Inc.
9009 New Trails Drive The Woodlands, TX 77381-5209, USA
Phone: 281-363-1033 Fax: 281-364-3628
e-mail: info@rigakumsc.com
http://www.rigakumsc.com/

To meet the needs for high throughput crystallography...

Rigaku

Rigaku offers a new standard for the structure analysis of living macromolecules.

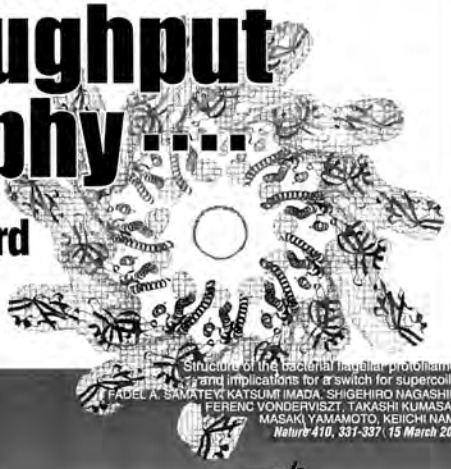

Structure of the bacterial flagellar protofilament and implications for a switch for supercoiling
FADEL A. SAMATEY, KATSUMI IMADA, SHIGEHIRO NAGASHIMA, FERENC VONDERVISZT, TAKASHI KUMASAKA, MASAKI YAMAMOTO, KEIICHI NAMBA
Nature 410, 331-337 (15 March 2001)

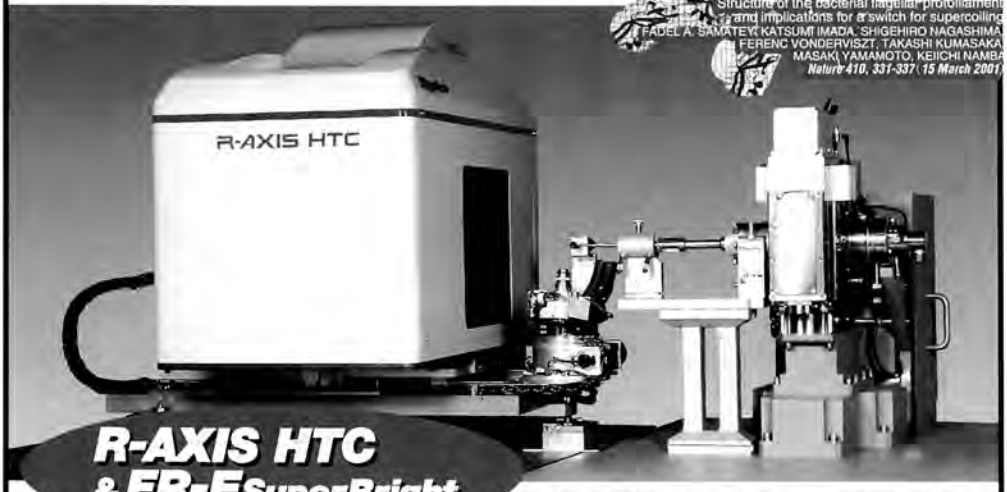

R-AXIS HTC & FR-E SuperBright

- Innovative three IP design with 10 second deadtime and dual read heads, provides the throughput of a CCD with the large aperture and superlative dynamic range of an image plate detector.
- Fitted with a partial-*χ*, 3-axis goniometer to provide for full sampling of reciprocal space.
- Suitable for the high intensities of a synchrotron or the perfect complement to the Rigaku FR-E SuperBright high brilliance rotating anode generator and high-throughput crystallography.

ACTOR
Automated Crystal Transport, Orientation, and Retrieval

Rigaku Corporation
Beijing Office : Rm.1505, No.22, FANLI Bldg., Chaowai Street, Chaoyang District, Beijing 100020, China
Phone: 86-10-6588-3370 Fax: 86-10-6588-3372
http://www.rigaku.com.cn/

Rigaku/MSC, Inc.
9009 New Trails Drive The Woodlands, TX 77381-5209, USA
Phone: 281-363-1033 Fax: 281-364-3628
e-mail: info@rigakumsc.com
http://www.rigakumsc.com/

FUJIFILM
I&I - Imaging & Information

富士フイルムの技術紹介（材料開発技術）

富士フイルムでは、有機化学から生物・環境化学までを技術のベースとして銀塩感光材料、磁気記録材料、非銀塩記録材料、産業材料、フラットパネルディスプレイ（FPD）材料等、高機能性材料の要素・基礎・商品化研究を行なっています。

◆必要とされる専攻分野

化学、応用化学、生物化学、薬学、物質工学、材料工学、物理学、
応用物理学、金属工学など

ナノ粒子合成技術

FePt系ナノ粒子は熱揺らぎに強く、サイズ4nmぐらいにしても強磁性を示すことが知られています。このため、将来の超高密度磁気記録媒体用の磁性体として有望視されています。当社は、FePt系ナノ粒子を逆ミセル法によって合成し、粒径および組成の両方について変動の小さい、単分散で均一組成のナノ粒子を得ています。また、これらの粒子を3～9nmの範囲で、自由にサイズ制御して合成できるようになっております。さらに、超常磁性から強磁性に変化する変態温度を大きく低下させることができています。

色材技術

富士フイルムが求め続けてきた、より美しくより長持ちする写真。そこで培ってきた色材の色相制御技術、堅牢化技術、分子配列制御技術、有機合成技術が、今、銀塩写真の究極を極めると共に、新しい出口を求めて様々な分野へと広がってきています。インクジェットなどのデジタルイメージング分野、DVD－Rなどの高密度光記録分野など、色素を扱う領域で当社の技術は幅広く貢献して行きます。

液晶用光学補償フイルム

TFT方式の液晶ディスプレイ（LCDパネル）は、斜め方向から観察するとコントラストが急激に低下したり、反転現象を起こして見づらくなることが欠点でした。富士フイルムは独自に、視野角を大幅に拡大する「WVフイルム」を開発しました。モニター・ノートパソコン分野では現在デファクト化しています。液晶テレビ分野でも、あらゆる液晶モードに対応するため、当社の機能性材料技術の優位性を活かした商品開発を進めています。

分析・解析技術と計算化学

解析技術センターは、最先端の解析技術を駆使して機能性材料・デバイスの機能やそのメカニズムを解明し、商品開発研究を先導することが使命です。解析技術は、分離・構造解析、無機・形態解析、表面・界面解析、物理化学的解析と理論計算から成っています。私たちは優れた材料開発を効率よく行なうために、大学等と連携して解析技術の継続的な強化を進め、研究を通して経営に貢献することを目指しています。

富士写真フイルム株式会社
東京都港区西麻布2-26-30　〒106-8620
人事部：神原　Tel: 03（6418）2896
応募はHP（http://www.fujifilm.co.jp/）の採用情報/経験者採用/オンライン応募をご覧下さい。

タンパク質構造解析ソフトウェア

〈NMR用〉

DYNAMO *Molecular Structure Engine*

DYNAMOは、シュミレーテッドアニーリング法
を使う構造計算プログラムです.

- ●極座標系と二面角の角度の分子動力学
- ●NMRによる構造の決定のための単純化された力場
- ●原子座標のファイルと制限の入力
- ●制限のバイオレーションの出力
- ●高度なコマンド言語
- ●インタラクティブなパラメータ表示

・NOEから算出される水素間の距離制限
・NMRから算出される二面角制限
・2H/Cα同位体シフト制限
・13Cα、13Cβシフト値と1Hシフト値
・クロスコリレーションスピン緩和速度
・(φ、ψ)の二面角相関ポテンシャルデータベース
・3Jカップリング定数、1JCα/Hカップリング定数
・双極子カップリング

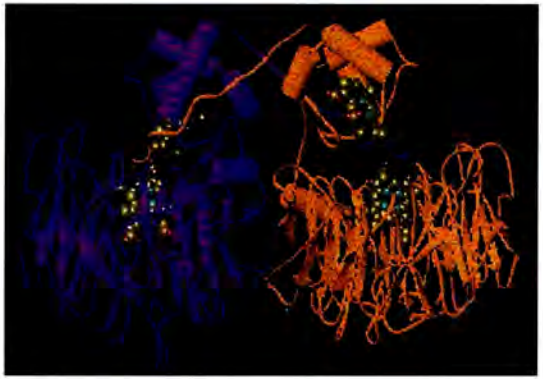

〈X線用〉

TURBO-FRODO

分子設計支援, 分子表示ソフトウェア

Turbo-Frodoは、分子モデリングを支援する
分子表示ソフトウェアです.

- ●フルスクリーンでの分子表示をサポート
- ●CPKモデル, 二十面体モデル, Ball and Stickを表示
- ●αヘリックスやβシートをリボンで表示
- ●作成した分子をHeapファイル, PB, PDB形式へ保存

X線回折データ処理をサポート

- ●X線回折の電子密度マップの読み込み・表示
- ●電子密度マップへの分子アサイン
- ●溶媒接触領域に基ずく分子のフォールディング
- ●構造を決定するのに必要な拘束ファイルの読み込み
- ●各原子にかかる拘束条件を色分け表示

LAS

株式会社エルエイシステムズ

〒323-0022 栃木県小山市駅東通り1-6-2 ｸﾞﾚｲｽﾋﾞﾙ5F
TEL:0285-24-9731　FAX:0285-24-9751　URL:www.las.jp　E-mail:support@las.jp

CHEMICAL COMPUTING GROUP INC.
Scalable eSoftware Scalable eScience

Molecular Operating Environment

カナダCCG社製統合計算化学システム

MOE

自らの手で進化させる新しい計算化学環境

MOEは創薬研究のための機能を統合したソフトウェアパッケージです。
開発環境と実行環境を一体化することにより、従来のソフトウェアの常識を超えた、
まったく新しい計算化学システムを提供します。

基本機能

■グラフィクス
低分子からタンパク質、DNA、RNA等の生体高分子、各種複合体を様々な手法で表示。
分子構築、編集機能を搭載。

■分子データマネージメント
分子構造から数値データまで、スプレッドシート形式で一括管理できるデータ管理システムを搭載。
PCでも数百万件分子の処理が可能。

■高機能言語SVL搭載
独自言語SVLとアプリケーションの開発環境も合わせて提供。MOEのアプリケーションはSVLで記述され、ソースコードのまま提供されるため、ユーザーの改変も自在。

分子モデリング・シミュレーション

- 分子力学、動力学計算
- 配座解析
- 分子アラインメント
- 静電ポテンシャル計算
- ドッキングシミュレーション

定量的構造活性相関（QSAR）

- 分子記述子の算出
- QSARモデルの構築・評価
- Recursive partitioning法
- 活性予測

コンビナトリアルケミストリー・HTS解析

- コンビケムライブラリー構築
- クラスター解析
- フィンガープリントの算出
- Similarity/Diversity解析
- 確率モデルによる大規模化合物ライブラリー活性解析

立体構造に基づくドラッグデザイン

- タンパク質表面解析
- リガンド結合部位探索
- グリッドドッキング
- ファーマコフォアモデルに基づく3Dデータベース検索

3Dバイオインフォマティクス

- アミノ酸配列のマルチアラインメント
- アミノ酸側鎖ロータマーライブラリー
- タンパク質構造ファミリーデータベース
- タンパク質ホモロジーモデリング
- 突然変異体のモデリング
- タンパク質構造解析

クロスプラットフォーム

- Windows 98以降
- Linux（Redhat6.2以降）
- SGI IRIX 6.5以降
- HP HP-UX11以降
- SUN Solaris 5.8以降
- クラスター対応

CCG社 日本総代理店

Ryoka Systems Inc.

株式会社 菱化システム　科学技術システム本部　計算科学部
〒279-0012　千葉県浦安市入船1-5-2 明治安田生命新浦安ビル4F
TEL：047-380-1231（直）　FAX：047-380-1239（直）
E-mail：ccg@cubs.bio.rsi.co.jp　URL：http://www.rsi.co.jp/science.html

タンパク質結晶化サポートシステム

クリスタルファインダー

特長

❶ 各プレートをプログラムに応じて観察し、結晶の有無を自動判別します。
❷ 観察画面の自動取込みが可能です。
❸ 粘度の違う溶液も精度良く分注できます。
❹ SBSプレートにも対応可能です。

結晶化プレート CF2002-P

特許出願中

観察光路を全てガラス（ロアガラス、アッパーガラス）で
構成しているため光学的な乱れのないドロップ観察を実現

結晶プレート

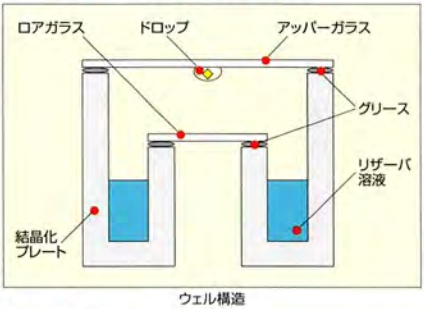

ウェル構造

●本装置は理化学研究所（播磨研究所）と共同で開発しました。

石川島検査計測株式会社
営業部
〒140-0014 東京都品川区大井1-22-13 米山ビル　TEL (03)3778-7925　FAX (03)3778-7952　ホームページ：http//www.iic-hq.co.jp

HITACHI

Hitachi High-Technologies

Unmatched analytical results produced with ease

Features

1. Quick observation
2. Automated columun alignment
3. Automated image viewing functions
4. High resolution STEM and SEM images
5. Nano-area electron diffraction: Simultaneous display with STEM image*
6. High sensitivity EDX analysis*
7. High speed and high sensitivity Hitachi EELS imaging system*

* Option

Hitachi Ultra-Thin Film Evaluation System

HD-2300

Hitachi High-Technologies Corporation

Tokyo, Japan

http://www.hitachi-hitec.com

24-14 Nishi-Shimbashi 1-chome, Minato-ku, Tokyo, 105-8717, Japan

Tel: +81-3-3504-7111 Fax: +81-3-3504-7123

AsCA-2004

第６回アジア結晶学会連合会議

２００４年６月２７日（日）～６月３０日（水）　　於：香港（中国）

（出席旅行のご案内）

前略

国際会議センターは、シンガポール大会（９２年）、バンコク大会（９５年）、マレーシア大会（９８年）、バンガロール大会（０１年）、そしてプルーム大会（０３年）の実績と経験より今回も結晶学会運営委員会のご協力を頂き、添乗員同行の出席旅行団を企画することになりました。

できるだけ多くの方々にご参加賜りたく、何なりと担当者までご相談ください。　　草々

■ AsCA-2004

・会　期：2004年6月27日（日）～30日（水）
・開催地：中国・香港
・学会場：香港科技大学（HKUST）
・利 用 ホ テ ル：日航香港（香港科技大学の宿泊施設も手配致します。）
・演題提出締切日：2004年2月15日
・学会登録費（弊社にて送金手続中／ご利用下さい。）

	4月1日以前	4月1日以降
Full participant	US$225.-	US$275.-
Student participant	US$125.-	US$175.-
Accompanying person	US$100.-	US$100.-

■ 会議出席基本日程表　┌ 日本結晶学会一般会員価格（10万円／航空機+日航ホテル）
　　└ 日本結晶学会学生会員価格（ 6万円／航空機のみ）

日次	月日（曜日）	都　市　名	交通機関	時　間	摘　　要
1	6月27日(日)	東京発 — 香港着	JL－731	(09：45／13：15)	空路、香港へ
		大阪発 — 香港着	JL－701	(09：45／12：35)	
		名古屋発 — 香港着	CX－533	(10：00／13：35)	着後、専用バスでホテルへ
2	6月28日(月)				第6回アジア結晶学会連合会議
3	6月29日(火)	香港滞在			（ツアーデスクにてオプショナル企画）
4	6月30日(水)				日航ホテル滞在
5	7月 1日(木)	香港発 — 名古屋着	CX－532	(16：15／21：00)	空路、帰国の途へ
		香港発 — 大阪着	JL－702	(15：05／19：35)	
		香港発 — 東京着	JL－732	(14：30／19：40)	着後、通関解散

上記以外のコースや個人行動の方、出発日・帰国日のご変更も承ります。
上記料金には空港税、航空保険料及び一人部屋利用料金（￥28,000）は含まれません。

お問い合せ・お申し込み

■■■ 株式会社グロリアツーリスト ■■■
JATA・国土交通大臣登録旅行業第343号

〒103－0013　東京都中央区日本橋人形町2－33－8　泉人形町ビル2F
TEL：03－5641－1225、1201　FAX：03－5641－1223
(E-mail) t.watanabe@gloria-tourist.co.jp　担当：渡辺（敏）、地曳、磯山

RICOH

Corporate Philosophy

The Spirit of Three Loves

Love your neighbor
Love your country
Love your work

RICOH COMPANY,LTD.
http://www.ricoh.com/

CCP4

Collaborative Computational Project Number 4

http://www.ccp4.ac.uk
Contact: ccp4@ccp4.ac.uk

Software Development in Macromolecular Crystallography

for 25 yrs

New CCP4 version 5.0
CCP4 software package includes:

- Data Processing with MOSFLM 6.2.4
- Molecular Replacement with Molrep 7.5
- Structure Refinement with Refmac5.2
- Binaries for common platforms; windows, OS X, linux

Chair of WG1 and Executive Committee: Professor J. Naismith, St.Andrews, UK
Chair of WG2: Dr P. Evans LMB-Cambridge, UK.
CCP4 is supported by the BBSRC
For academic and commercial enquiries please contact ccp4@ccp4.ac.uk

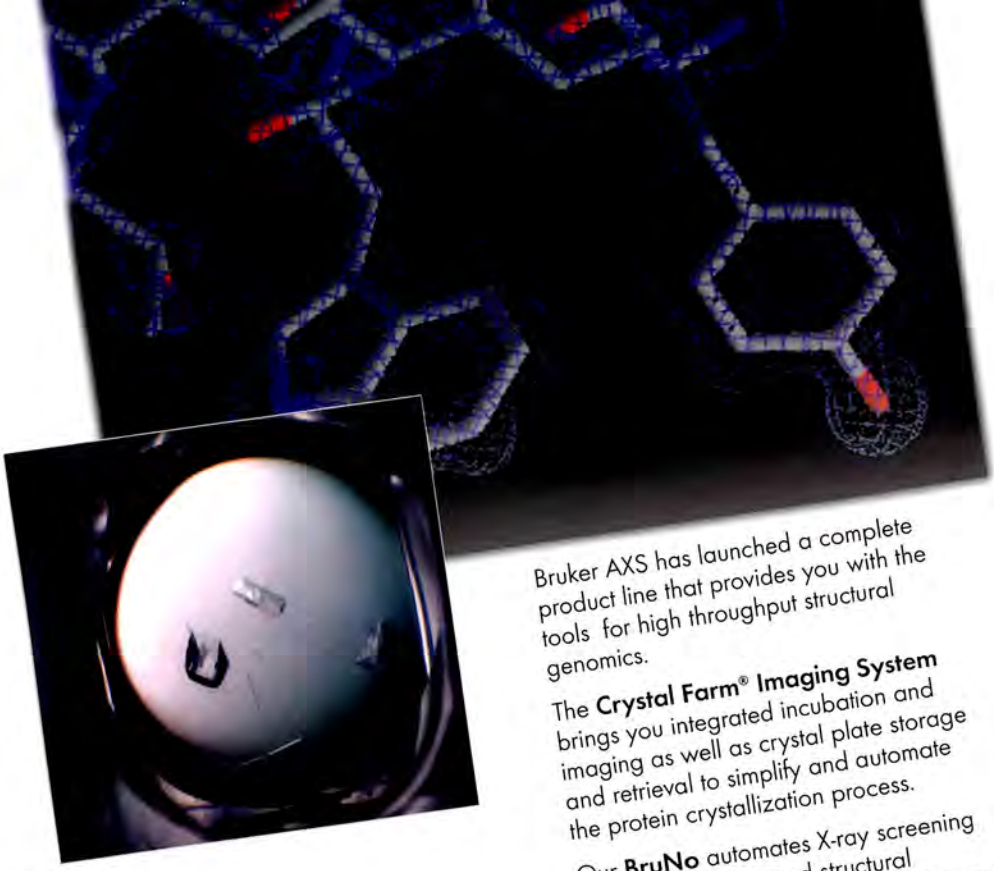

Bruker AXS has launched a complete product line that provides you with the tools for high throughput structural genomics.

The **Crystal Farm® Imaging System** brings you integrated incubation and imaging as well as crystal plate storage and retrieval to simplify and automate the protein crystallization process.

Our **BruNo** automates X-ray screening needed for high speed structural genomics, to rank which crystal of many is to be used for full data collection

Our **PROTEUM** home laboratory research system collects complete X-ray data better and faster, using the latest high brilliance MICROSTAR source and the highest sensitivity, fast readout PROTEUM CCD detector to see diffraction higher resolution.

Contact us now to learn more about these exciting new solutions for high-throughput Life Science applications!

HIGH THROUGHPUT BIOLOGICAL CRYSTALLOGRAPHY TOOLS

DISCOVERY PARTNERS INTERNATIONAL

BRUKER ADVANCED X-RAY SOLUTIONS

BRUKER NONIU

North America: BRUKER AXS INC. ▪ Tel. (+1) (608) 276-3000 ▪ Fax (+1) (608) 276-3006 ▪ www.bruker-axs.com ▪ info@bruker-axs.com

The Netherlands: BRUKER NONIUS B.V. ▪ Tel. (+31) (15) 269 8400 · Fax (+31) (15) 262 7500 ▪ www.bruker-axs.com ▪ info@bruker-nonius.com

Even the best can be improved upon, and we won't argue the fact. Especially, since we have introduced a better version yet of the best CCD detector for Chemical and Materials Crystallography – the new APEX II

New low noise 4K chip
Large 62 mm chip requires no taper

APEX II

The Best is Better

- Still the ultimate sensitivity
- Better spatial resolution
- Still no spatial distortion
- Lower dark noise and deeper cooling for long exposures
- New electronics with 4-port readout and user selectable speeds for ultra low noise applications

Contact us now or visit our web site to learn more about our ultimate solutions for crystallography.

BRUKER NONIUS

BRUKER ADVANCED X-RAY SOLUTIONS

North America: BRUKER AXS INC. n Tel. (+1) (608) 276-3000 n Fax (+1) (608) 276-3006 n www.bruker-axs.com n info@bruker-axs.com
The Netherlands: BRUKER NONIUS B.V. n Tel. (+31) (15) 2152 400 n Fax (+31) (15) 2152 500 n www.bruker-axs.com n info@bruker-nonius.com
Germany: BRUKER AXS GMBH n Tel. (+49) (721) 595-2888 n Fax (+49) (721) 595-4587 n www.bruker-axs.de n info@bruker-axs.de

marresearch

marcsc / marmosaic

Cryogenic sample changer **Ultrahigh-performance X-ray**

marresearch

marmosaic

mar345

marccd

World Leaders in X-ray Detectors

Liquid nitrogen free

...but cooler than ever

Introducing the Cobra, the new NON-LIQUID Cryostream from Oxford Cryosystems...

Cryostream-like efficiency and reliability without the liquid: Cobra truly offers the best of both worlds.

The Cobra offers:

- Temperature range 80-500K
- Fast cool down time (30 mins to 100K)
- Complete programmability from a Cryostream-style controller
- Turbo mode (10L/min gas flow) for fast cooldown

The Cobra can be supplied with or without a nitrogen gas generator, so you can use your laboratory dry nitrogen gas supply if available.

We will even offer you a trade-in on your old nitrogen system – just contact us for details.

We look after our technology so you can look after yours!

OxfordCryosystems

Head Office
3 Blenheim Office Park
Lower Road · Long Hanborough
Oxford · OX29 8LN · UK
T. +44 (0)1993 883488
F +44 (0)1993 883988
E. info@OxfordCryosystems.co.uk

North American Office
7 Jackson Road · Devens
MA 01432 · USA
T. 1-866-OXCRYO-8
978 772 7930
F. 978 772 7945
E. Info@OxfordCryosystems.corn

www.OxfordCryosystems.com

Using liquid nitrogen to heat the sample...

...now why didn't we think of it before?

It might sound illogical, but it works!

The new Cryostream Plus is as stable at 500 Kelvin (227°C) as it is at 80 Kelvin (-193°C), giving you the flexibility to heat & cool your sample at the touch of a button.

Maintaining the low nitrogen consumption, high stability and excellent performance for which the Cryostream is renowned, the Plus simply offers that little bit more: 100° C more to be precise.

And with generous options available for trading in or upgrading your old system, this could be the perfect opportunity to turn up the heat on your research!

We look after our technology so you can look after yours!

OxfordCryosystems

North American Office
220 Wood Road · Braintree
MA 02184-2403 · USA
T. 1-866-OXCRYO-8
781-843-5900
F. 781-843-5945
E. Info@OxfordCryosystems.com

Head Office
3 Blenheim Office Park
Lower Road · Long Hanborough
Oxford · OX29 8LN · UK
T. +44 (0)1993 883488
F +44 (0)1993 883988
E. info@OxfordCryosystems.co.uk

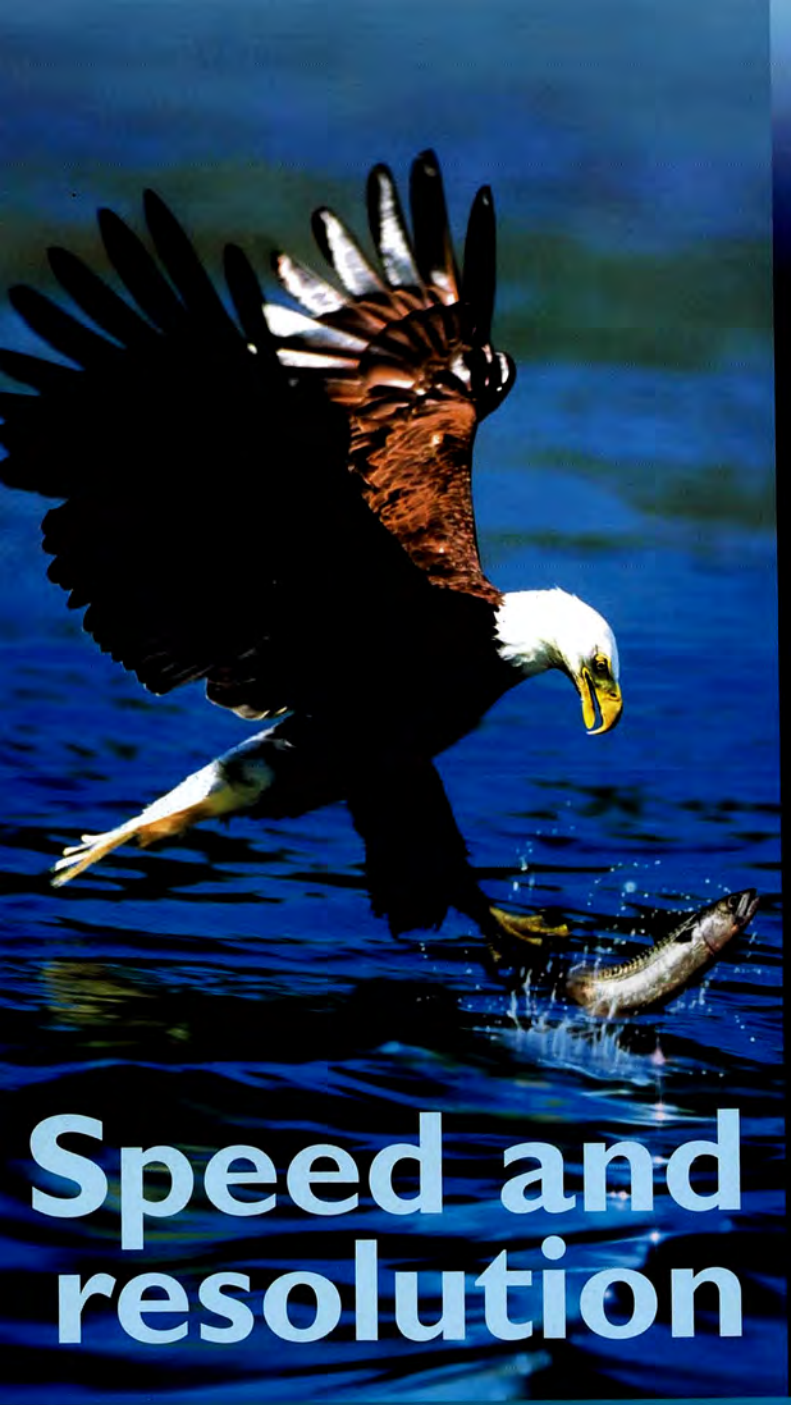

Speed and resolution

X'Celerator optimizes X-ray powder diffractometers' instrumental resolution

The sea eagle spots its prey from far above the water's surface - compensating for the diffraction of light in water - dives with breathtaking pace and catches it with amazing accuracy. A solution demanding not only speed, bu also resolution.

The X'Celerator, PANalytical' ultra fast X-ray detector, combines these two demands in one device. Thanks to RTMS (Real Time Multiple Strip) detection technology, t detector's recording speed is u to one hundred times faster than conventional detection systems. This advantage can b exploited to operate the diffractometer with high resolution settings, resulting i a data quality that can only b exceeded with diffractometers coupled to a synchrotron X-r source.

Why apply for synchrotron beam time while you could collect high-quality powder diffraction data in your own laboratory?

PANalytical, Spectris Pte Ltd
No 31 Kaki Bukit Road 3
#06-04/05, Lobby B - Techlink
Singapore 417818
Tel.: Main +65 6741 2868
Fax.: +65 6741 2166
e-mail: info@panalytical.com

www.panalytical.com

Winning by Sharing

PANalytic

X'Pert Software with XML: Leading the way forward in data sharing

X'Pert Software for XRD data

A complete family of analytical software

Whether you're in research, development or production control, there are PANalytical X'Pert Software packages to support your XRD data collection and analysis. The complete range, which centers on the X'Pert Data Collector, is based on the XRDML data platform.

A universal standard for structured data

PANalytical is the first company in the XRD community to bring you an open format based on the universal XML standard: XRDML. It ensures that your data remain accessible, transparent and secure and it guarantees total reproducibility. Information on instrument type, settings, test conditions and experimental parameters is included. Moreover, XML files are human readable.

To get on the way forward in data sharing, visit:

www.xrdml.com

PANalytical
Lelyweg 1, 7602 EA Almelo
The Netherlands
Tel.: +31 546 534 444
Fax.: +31 546 534 598

Regional sales offices
Americas
Europe, Middle East, Africa
Asia Pacific

E-mail: info@panalytical.com

www.panalytical.com

Winning by Sharing

PANalytical

You don't need a rotating anode!

Designed for protein crystallography, the **Xcalibur PX Ultra** has all the benefits of a rotating anode plus:

- Comparable performance to a 5kW rotating anode with CMF optics
- Large area 165mm Onyx CCD
- Compact, self-contained X-ray enclosure
- Low cost of ownership
- Low maintenance

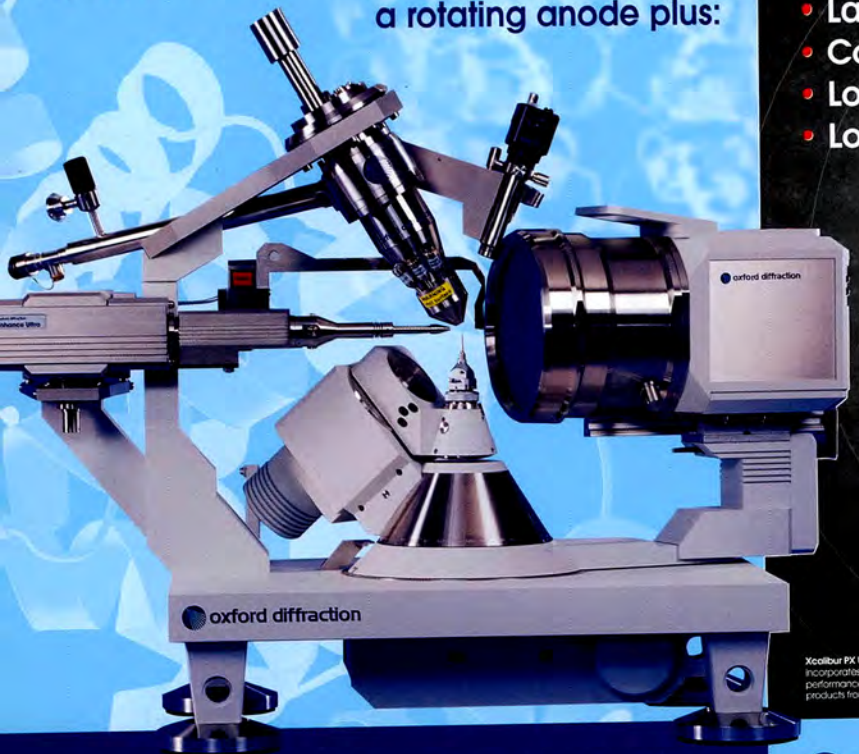

Xcalibur PX Ultra incorporates high performance products from Osmic

"Now I can concentrate on the science rather

oxford diffraction

Oxford Diffraction Ltd
68 Milton Park
Abingdon
Oxfordshire OX14 4RX

Oxford Diffraction Inc
130A Baker Avenue
Concord MA 01742
USA

Oxford Diffraction
Rethelstrasse 4
50933 Cologne
Germany

Oxford Diffraction Poland Sp. z o.o.
ul. Rogowska 127 A
54-440 Wroclaw
Poland

IPDS 2T

Single Crystal Diffractometer System

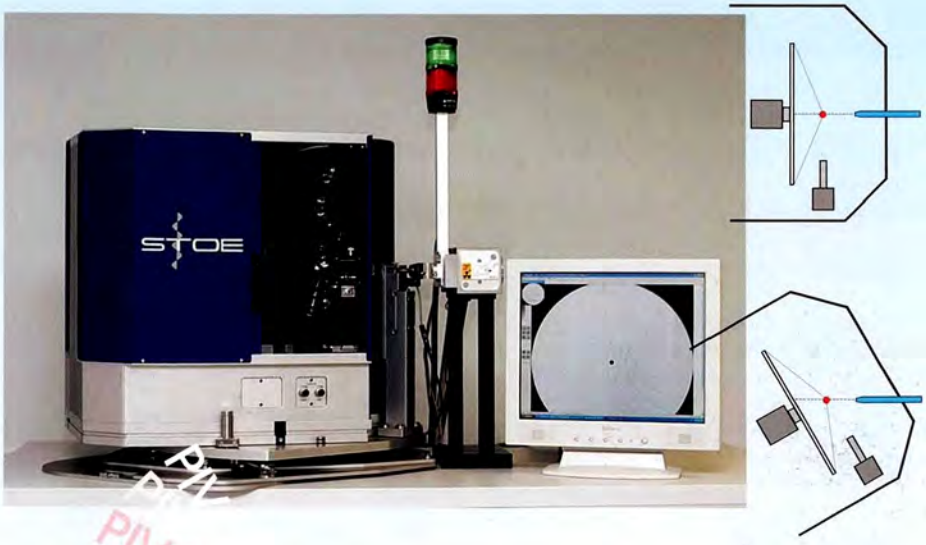

PIVOTING TO HIGHEST VERSATILITY

- 340mm imaging plate
- Dynamic range > $1x10^5$
- Two circle goniometer, ω from 0 - 180°, φ unlimited
- 5 positions: 0°, 15°, 30°, 45°, 60° 2θ
- 2θ max. = 137°
- Structure solutions for small molecules as well as for proteines
- Electron density calculations
- Investigations of powder samples
- High- and low-temperature attachments

STOE & Cie GmbH P.O.Box 101302 D-64213 Darmstadt
Phone: (+49) 6151 98870 Fax: (+49) 6151 988788
E-mail: stoe@stoe.com Homepage: http://www.stoe.com

Fluidigm

Let TOPAZ™ take you from screen to beam

The TOPAZ™ System for protein crystallization

Only one system addresses your needs from crystallization setup to diffraction data. Every system component has been optimized around our proven chip technology for free interface diffusion. You'll appreciate the very small sample requirements (nanogram quantities) and the integrated hardware and software that streamline your projects. With Topaz products, you can easily screen thousands of reagents per day to identify promising conditions, automatically scan for and score crystallization activity, and grow large, high-quality crystals for diffraction studies. And because the Topaz system has an open architecture, you can interface it with third-party pipetting robotics to further supercharge your throughput. In so many ways, we keep you moving toward your ultimate goal—reliable structural data.

If you're ready for a complete solution—from screen to beam—visit www.fluidigm.com/TOPAZ or call us today at 1-866-FLUIDLINE to learn more.

TOPAZ™

PROTEIN CRYSTALLIZATION BY **FLUIDIGM**

Frost & Sullivan
Scientific American 50
2003 Technology Award

www.fluidigm.com

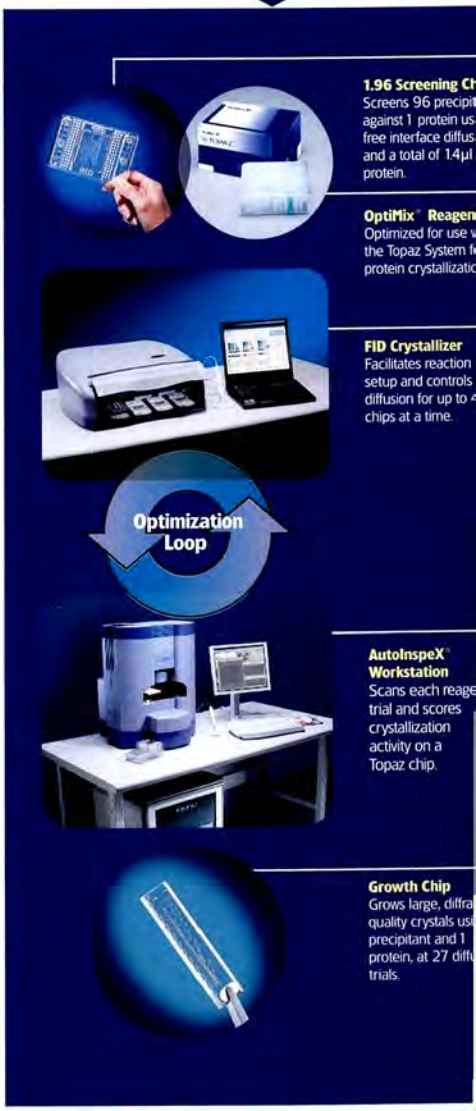

CAMPUS MAP

THE HONG KONG UNIVERSITY OF SCIENCE AND TECHNOLOGY

Academic Building Directory

THE HONG KONG UNIVERSITY OF SCIENCE AND TECHNOLOGY

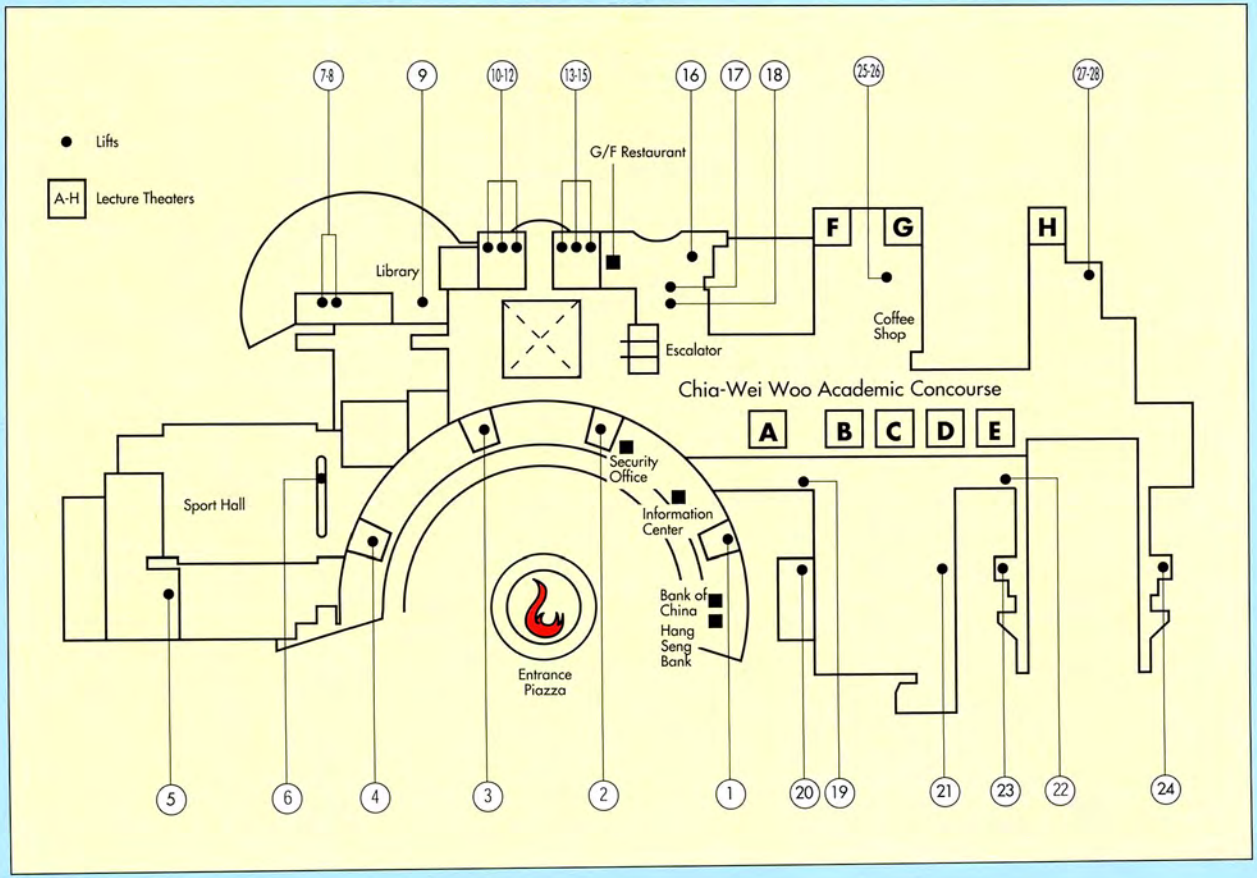

Oral Abstracts

PL1

SUPERCONDUCTIVITY OF BORIDE AND CARBIDE SYSTEMS

Jun Akimitsu

Department of Physics, Aoyama-Gakuin University, 5-10-1, Fuchinobe, Sagamihara, Kanagawa, Japan, 229-8553 (jun@phys.aoyama.ac.jp)

After the discovery of MgB_2, much attention has been paid to the boride and carbide systems. In this conference, we mainly review the following themes.

(1) First is the present situation of the superconductivity of MgB_2, which can be mainly interpreted in terms of BCS-type phonon mediate pairing.
In particular, we will focus on the relationship between the superconductivity and the change of crystal structure in MgB_2.

(2) We review our present status for the new superconductors including the boron and carbon systems found in my laboratory.
We should emphasize here that we discovered the superconductivity at 18 K in Y_2C_3, although this material with a maximum T_c of 11.5 K has already investigated by Krupka *et al* (J. Less-Common Met. **17** (1969) 91) (Fig.1). The crystal structure of Y_2C_3 is body centered cubic (Pu_2C_3-type) structure, and Y^{3+} ions are one-dimensionally aligned along [111] axis (Fig. 2). The lattice parameters, *a*, obtained in our work exist between 0.818-0.823 nm, and are smaller than those previously reported (0.821-0.825 nm).

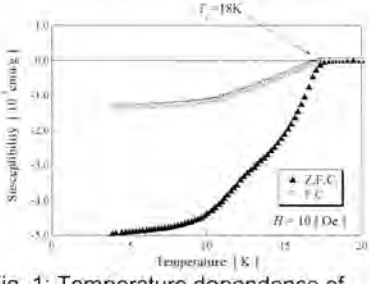

Fig. 1: Temperature dependence of susceptibility in Y_2C_3.

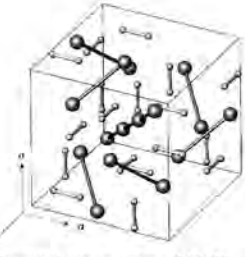

Fig. 2: Crystal structure of Y_2C_3. The large circles show Y atoms and the small circles show C atoms.

PL2

STRUCTURES OF NOVEL SIGNALING PROTEINS SECRETED DURING INVOLUTION AND INVOLVED IN APOPTOSIS

T. P. Singh

Department of Biophysics, All India Institute of Medical Sciences, New Delhi 110 029, India. (tps@aiims.aiims.ac.in)

A novel class of 40 kDa glycoproteins (SPX-40) have been detected in the dry secretions of non-lactating animals, culture supernatants of MG-63 human osteosarcoma cell lines, cultures of human synovial cells and human cartilage cells. The increased levels of similar protein have also been reported in certain types of breast and colon cancers. These proteins are implicated as protective signaling factor that determines which cells are to survive during the processes of drastic tissue remodeling. Sequence analysis and biochemical characterization have revealed a moderate similarity with chitinases and chitinase-like proteins but has indicated a completely altered combination of the so called active site residues. The three-dimensional structures, functions, nature of ligands and mode of ligand binding of these proteins are not yet known. In order to develop a detailed structure-function relationship, mechanism of ligand binding and their precise physiological role, we have determined structures of several of these proteins from a number of species. The detailed structure analyses has shown that these proteins contain a classical $(\beta\alpha)$ 8 barrel fold of triose phosphate isomerase (TIM) with an insertion of a small α/β domain similar to that of chitinases. Although, the TIM barrel in these proteins is very similar in shape to those of chitinases and chitinase-like proteins but it is packed very differently indicating that these proteins might be involved in a different kind of recognition. Unlike chitinases and chitinase-proteins, these proteins are glycosylated. The glycan moieties in these proteins contribute to the final folding particularly to the neighboring chains of the molecules. We speculate that these proteins may interact with cell surface receptors through protein-protein interactions as their carbohydrate binding capabilities appear to be greatly impaired due to a tightly packed TIM barrel. It is probable that the proteins of SPX-40 family might have originally evolved from chitinases, retained some sequence homologies and maintained similar structural framework but changed selectively and critically to acquire new functions.

PL3

FROM METAL STRING COMPLEXES TO METAL WIRES

Chih-Chieh Wang and Shie-Ming Peng

Department of Chemistry, National Taiwan University, Taipei, Taiwan
Tel No.: 886-2-23638305; Fax No.: 886-2-83693765 (smpeng@ntu.edu.tw)

Owing to their fascinating bonding nature, the metal-metal (M-M) multiple bonds in dinuclear metal complexes have been an interesting and vital research topic. During the past decade, our seminal and systematic approaches on the all-*syn* oligo-(α-pyridyl)amido ligands coordinated metal ions have successfully opened up a new chapter, extending this territory from dinuclear to linear oligonuclear metal complexes. Their unique features in structures and bonding characterization have been thoroughly investigated, which, according to the M-M bonding strength, can be classified into two categories, namely the oligonickel(II) complexes lacking an M-M bond and the oligochromium(II) complexes with a strong M-M bonding formation. Depending on the specificity and number of metal ions, structures and magnetic behaviors of the corresponding metal complexes are systematically analyzed. Their potential application as a molecular metal wire is conveyed on the basis of the band structures calculated from hypothetical one-dimensional metal strings. Moreover, self-assembled monolayers of *n*-alkanethiols are employed as a two-dimensional matrix to isolate the metal string complexes, of which the scanning tunneling microscopy (STM) image exhibits remarkable protrusion characteristics. For tricobalt and trichromium complexes, the topographic STM images reveal that the protruding features are, respectively, 0.3 nm and 0.6 nm higher than that of the trinickel complexes. The trend of increasing conductivity correlates well with their associated bond orders, and is also in consistence with qualitative EHMO approaches.

Keyword: Metal String Complex, Molecular Metalwire, STM Spectroscopy

References

1 Lin S. Y.; Chen I W.; Chen C. H.; Hsieh M. H.; Yeh C.Y.; Lin T. W.; Chen Y. H.; Peng S. M., *J. Phys. Chem. B*, **2004**, *108*, 959-964.

PL4

HIGH-THROUGHPUT PROTEIN CRYSTALLOGRAPY

Isao Tanaka

Division of Biological Sciences, Graduate School of Science, Hokkaido University, Sapporo, 060-0810, Japan (tanaka@castor.sci.hokudai.ac.jp)

The genome-sequencing projects have determined a plenty of DNA sequences of the genomes including entire human genomes or those of many important microbial pathogens and useful organisms. The information of these sequences will benefit on a variety fields like medical science, agriculture and fundamental biology. In this post-genomic era, an enormous number of genes can be target for the research. The term "structural genomics" is meant to be used for this situation in the field of protein crystallography. Thus, the structural genomics requires the determination of protein structures in a high-throughput manner with respect to sample preparation, crystallization, diffraction data collection, and structure analysis.

Japanese structural genomics project has been established in fiscal 00 under the name of "National Project on Protein Structural and Functional Analyses." In this project, our consortium "The Structural Genomics Consortium for research on Gene Expression System (SGCGES)" aims to elucidate the structures and functions of the proteins that are involved in gene expression. As one of the centers for the structural genomics project, we have been developing an automatic system for high-throughput protein crystallography.

Since protein crystallization is influenced by a number of parameters, development of a small-scaled and automated crystallization method is necessary. We have been working on the development of a micro-array chip device for high throughput screening for protein crystallization condition. In order to hold various precipitant solutions in gels, the hollow fibers arrayed on the chip are used. We have already determined polymerization conditions of gels for almost all precipitants with wide range of pH conditions. The prototype device has already been made.

For realizing the manual-intervention-free refinement, we have developed a Local-correlation-coefficient-based Automatic FItting for REfinement program (Lafire). This system consists of evaluation of existing model, automatic model modification, partial model building, a graphic monitor system and an interface with existing refinement programs. For the model modification, the backbone and side chains are independently fitted to the electron density based on the correlation coefficient. In addition, the system can build the regions (like loop regions) that are not able to be built by the automatic programs like Solve/Resolve or ARP/wARP. In conjunction with the refinement programs such as CNS and REFMAC, Lafire system has been successfully used to refine more than ten protein structures nearly in full-automatic manner.

PL5

CRYSTALLOGRAPHY WITHOUT CRYSTALS

Jianwei Miao,[a] Keith O. Hodgson,[a,b] Tetsuya Ishikawa,[c] Bart Johnson,[a] Yoshiki Kohmura,[c] and Yoshinori Nishino[c]

[a]Stanford Synchrotron Radiation Laboratory, Stanford Linear Accelerator Center, Stanford University, Stanford, CA 94309-0210, USA; [b]Department of Chemistry, Stanford University, Stanford, CA 94305, USA; [c]SPring-8/RIKEN, 1-1-1, Kouto, Mikazuki, Sayo gun, Hyogo 679-5198, Japan. (Miao@SLAC.Stanford.EDU)

When a coherent diffraction pattern is sampled at a spacing sufficiently finer than the Bragg peak frequency (*i.e.* the inverse of the sample size), the phase information is in principle embedded inside the diffraction pattern, and can be directly retrieved by using an iterative process. In combination of this oversampling phasing method with either coherent X rays or electrons, the methodology of crystallography has recently been image nano crystals, nanostructured materials and biological samples. In this talk, I will present the principle of the oversampling method, discuss the first demonstration experiment, and illustrate some applications in nanoscience and biology.

References

1 Miao, J., Charalambous, P., Kirz, K. and Sayre, D. (1999) *Nature* **400**, 342-345.
2 Miao J., Ishikawa T., Johnson B., Anderson E.H., Lai B. and Hodgson K.O. (2002) *Phys. Rev. Lett.* **89**, 088303(1-4).
3 Miao J., Hodgson K.O., Ishikawa T, Larabell C.A., LeGros M.A. and Nishino Y. (2003) *Proc. Natl. Acad. Sci. USA* **100**, 110-112.

PL6

GRID-ENABLED HIGH THROUGHPUT CHEMICAL CRYSTALLOGRAPHY: A NEW OPPORTUNITY FOR STRUCTURAL CHEMISTRY

Michael B. Hursthouse

School of Chemistry and Combinatorial Centre of Excellence,
University of Southampton, UK. (mbh@soton.ac.uk)

The great sensitivity of current CCD X-ray detectors and the availability of highly organised structure determination software packages facilitate rapid X-ray structure determination. The ever increasing demand from the synthesis labs for characterisation support is proving to be a challenge, but this can also be viewed as an opportunity – to accumulate structural knowledge at a pace greater than ever before. We are attempting to meet this challenge and take the opportunity provided with both hands. We have put in place procedures and equipment to provide a fully automated capability – from mounted crystal to validated and archived structure data with minimal operator intervention. The impact of this for structural science will be two-fold. Characterisation studies will become even faster and inexpensive, providing further valuable support for chemical structure-property studies, but with reduced operator overload. At the same time, the increasing volume of available structural data will offer more scope for increasing our structure-property knowledge.

However, high throughput data gathering then requires automated help in the sifting and assessment processes. In our lab we are focussing some of our work on the latter area. In the Comb-*e*-Chem project we are exploring the feasibility of an e-Science approach to provide an integrated, GRID-enabled, Chemical Structure and Property Environment, incorporating our high-throughput structure determination and some associated high-throughput property measurement capability, with distributed structure and property calculations and data-base mining. As an example of this approach, we are developing new software to search for patterns in crystal structures, with a view to learning more about crystal structure assembly, polymorphism and materials properties. At the same time, we are investigating alternative ways to disseminate structural results, recognising the fact that current publication strategies are unable to cope with current output, let alone increasing future output. This presentation will report and review the status of all of these activities.

MS01-1

CRYSTAL STRUCTURE OF A HEMOLYTIC LECTIN CEL-III FROM MARINE INVERTEBRATE *CUCUMARIA ECHINATA* AT 1.7 Å RESOLUTION

Tatsuya Uchida[a], Tomomitsu Hatakeyama[b], Takayuki Yamasaki[b], Seiichiro Eto[b], Hajime Sugawara[c], Kurisu Genji[a], Atsushi Nakagawa[a], and Masami Kusunoki[a]

[a]Institute for Protein Research, Osaka University, 3-2 Yamadaoka, Suita Osaka 565-0871 Japan, [b]Faculty of Engineering, Nagasaki University, Bunkyo-machi 1-14, Nagasaki 852-8521,Japan, [c]Plant Science Center, RIKEN, 1-7-22 Suehiro-cho, Tsurumi-ku, Yokohama City, Kanagawa 230-0045, Japan
(kusunoki@protein.osaka-u.ac.jp)

The lectin CEL-III derived from the marine invertebrate Holothuroidea *Cucumaria echinata* binds *N*-acetylgalactosamine or galactose-containing carbohydrates and causes hemolysis or hemagglutination toward erythrocytes Ca^{2+}-dependently(1). Here we report the X-ray crystal structure of CEL-III at 1.7 Å resolution determined by single isomorphous replacement with anomalous dispersion of a Pb derivative.

The protein consists of two b-trefoil domains on the N-terminal side and a C-terminal domain, the latter of which is composed of two a helices and one large b-sheet. No sequence homology was found for the C-terminal domain with other proteins. Five calcium ions bound to five of the six 3_{10} helices in the two b-trefoil domains. We assume that these ions are important for the structural integrity of CEL-III and are directly involved in the carbohydrate-binding, considering the structural and carbohydrate-binding similarity of this protein with other lectins, ricin B-chain and ebulin B-chain, with the same b-trefoil folds. The b-sheet of the C-terminal domain has large regions of non-polar residues on the domain surfaces and there are no disulfide bonds between the two b-trefoil domains and the C-terminal domain. This strongly suggests together with our biochemical data that upon binding of CEL-III to the erythrocyte membrane, six to seven molecules of CEL-III oligomerize by forming hydrophobic bonds between these molecules accompanied by some conformational change, leading to hemolysis by forming ion-permeable pores in the membrane.

Reference

1 Kouzuma, Y., Suzuki,Y., Nakano, M., Matsuyama, K., Tojo, S., Kimura, M., Yamasaki, T., Aoyagi, H. and Hatakeyama, T. (2003) *J. Biochem.* **134**, 395-402.

CRYSTAL STRUCTURES OF ARTOCARPIN-SUGAR COMPLEXES: VARIATION IN THE LENGTH OF A LOOP AS A STRATEGY FOR GENERATING LIGAND SPECIFICITY

M. Vijayan, Anand Srivastav, A. Surolia and A. Arockia Jeyaprakash

Molecular Biophysics Unit, Indian Institute of Science, Bangalore 560 012, INDIA (mv@mbu.iisc.ernet.in).

Lectins are carbohydrate binding proteins which exert their effects through specific recognition of different sugar structures. They adopt widely different folds and quaternary structures. For example, plant lectins, the most widely studied group in the family, exhibit five different folds. One of them, the β-prism I fold, was first identified in jacalin[1], one of the two lectins found in the seeds of jackfruit. The carbohydrate specificity of this lectin has been thoroughly characterized[2]. The other lectin from jackfruit seeds, artocarpin, also adopts β-prism I fold, although it has different carbohydrate specificities[3]. The structures of the complexes of artocarpin with mannotriose and mannopentose reported here show that the lectin has a deep-seated binding site formed by three loops. The primary site made up of two loops forms hydrogen bonds with the sugars while the second site comprising the third loop has mainly van der Waals interactions with them. A detailed comparison with the sugar complexes of heltuba, the only other mannose specific jacalin-like lectin with known three-dimensional structure in sugar-bound form, establishes the role of the sugar binding loop constituting the secondary site, in conferring different specificities at the oligosaccharide level. This loop is four residues longer in artocarpin than in heltuba, providing an instance where variation in loop length is used as a strategy for generating carbohydrate specificity.

References

1 Sankaranarayanan, R., Sekar, K., Banerjee, R., Sharma, V., Surolia, A. & Vijayan, M. (1996). *Nat. Struct. Biol.* **3**, 596-603.

2 Jeyaprakash, A. A., Katiyar, S., Swaminathan, C. P., Sekar, K., Surolia, A. and Vijayan, M. (2003). *J. Mol. Biol.* **332**, 217-228.

3 Pratap, J. V., Jeyaprakash, A. A., Rani, P. G., Sekar, K., Surolia, A. & Vijayan, M. (2002). *J. Mol. Biol.* **317**, 237-247.

MS01-3

CRYSTAL STRUCTURE OF ZINC CONTAINING MONOFERRIC C-LOBE OF BOVINE LACTOFERRIN AT 1.9 Å RESOLUTION

Sujata Sharma, Talat Jabeen, Jayashankar Jasti, Janesh Kumar, Ashok K. Mohanty and Tej P. Singh

Department of Biophysics, All India Institute of Medical Sciences, New Delhi-110 029, India (afrank2@hotmail.com)

Lactoferrin is an 80 kDa glycoprotein with two homologous lobes each containing a single ferric ion. The purified samples of bovine lactoferrin were incubated with proteinase K in 50 mM Tris-HCl, 5 mM $CaCl_2$, pH 8.0 at a 100:1 ratio. The hydrolyzed product contained N-lobe, C-lobe and inactive proteinase K. The N- and C-lobes were purified to homogeneity. The purified iron saturated samples of C-lobe were crystallized in 0.1 M MES buffer, pH 6.5 containing 25 % v/v polyethylene glycol monomethyl ether 550 and 0.01 M zinc sulphate heptahydrate. The structure was determined by molecular replacement and refined to an R-factor of 0.193 for all the data to 1.9 Å resolution. The final model comprises 2593 protein atoms (residues 342-676 and 681-685), 124 carbohydrate atoms (from 10 monosaccharide units, in three glycan chains), 1 Fe^{3+}, $1CO_3^{2-}$, 2 Zn^{2+} and 230 water molecules. The C-lobe folds in a similar manner as observed for the C-lobes of other lactoferrins. The domain orientation is characterized by six interdomain hydrogen bonds. The presence of two Zn^{2+} ions at sites other than the iron-binding site is a novel feature of this structure. This structure is also notable for extensive intermolecular hydrogen bonding in the crystals. This appears to be one of the best packed crystal structures among the proteins of transferrin superfamily.

STRUCTURAL BASIS OF BACTERIAL LIPOPROTEIN TRANSPORT

Kazuki Takeda[a], Hideyuki Miyatake[a],
Naoko Yokota[b], Shin-ichi .Matsuyama[b], Hajime Tokuda[b], and Kunio Miki[a, c]

[a]RIKEN Harima Institute/SPring-8, Hyogo, Japan, [b]Institute of Molecular and Cellular Biosciences, University of Tokyo, Tokyo, Japan, [c]Department of Chemistry, Graduate School of Science, Kyoto University, Kyoto, Japan,
(miki@kuchem.kyoto-u.ac.jp)

Bacterial lipoproteins are anchored on the membranes with acyl chains attached to cysteine residue at the N-termius. In Gram-negative bacteria such as *Escherichia coli*, the transport of hydrophobic lipoproteins from the inner membrane to the outer membrane through the periplasm is mediated by Lol system. The Lol system is composed of a periplasmic lipoprotein carrier LolA, a lipoprotein receptor LolB, and the LolCDE complex (ABC transporter).

The structures of LolA and LolB are surprisingly similar to each other and characterized by an unclosed β-barrel and three α-helices plugging the sheet, while the sequence identity between two proteins is about 8% [1]. For both proteins, the inner surface of the β-sheet and α-helices consist of hydrophobic residues. The cavities are possible binding sites of the lipid moiety of the lipoprotein. In the LolA structure, the side chain of Arg43 is oriented toward the interior of the molecule, and is hydrogen bonded to the main chain of residues in the helices. The helices are expected to undergo opening and closing upon the accommodation and release of lipoproteins, respectively. LolA(R43L) with a mutation at the residue in question can bind a lipoprotein but cannot transfer the associated lipoprotein to LolB [2], and the LolA(R43L)-lipoprotein complex accumulates in the periplasm. In the structure of the mutant, three α-helices are highly disordered.

References

1 Takeda, K., Miyatake, H., Yokota, N., Matsuyama, S., Tokuda, H. and Miki, K. (2003) *EMBO J.* **22,** 3199-3209.
2 Miyamoto, A., Matsuyama, S. and Tokuda, H. (2001) *Biochem. Biophys. Res. Commun.* **287**, 1125-1128.

MS01-5

CRYSTAL STRUCTURE OF LEUA, AN ESSENTIAL BIOSYNTHETIC ENZYME FROM *MYCOBACTERIUM TUBERCULOSIS*

Edward N. Baker,[a] Nayden Koon,[a] and Christopher J. Squire[a]

[a]School of Biological Sciences, University of Auckland, Private Bag 92019, Auckland, New Zealand (ted.baker@auckland.ac.nz).

Mycobacterium tuberculosis, the cause of TB, is responsible for more deaths worldwide than any other infectious agent. With the rise of multi-drug resistance and the long treatment regimes currently required, there is an urgent need for the development of new therapeutic drugs. As part of a structural genomics initiative focused on M. tuberculosis, we have targeted enzymes from the amino acid biosynthesis pathways.

LeuA (α-isopropylmalate synthase) is a dimeric (2 x 70 kDa) enzyme that catalyses the first committed step in the biosynthesis of the amino acid leucine, and has been shown to be essential for the viability of the organism. Since there is no equivalent enzyme in humans, LeuA is a potential drug target. The gene encoding LeuA in M. tuberculosis (Rv3710) was cloned and the protein expressed in *E. coli*, purified and crystallized. The selenomethionine (SeMet)-substituted protein was also prepared, purified and crystallized, seeding with the native crystals [1]. The structure was then solved by MAD methods, using synchrotron data collected at 3 wavelengths and refined at 2.0 Å resolution in complex with its substrate, α-ketoisovalerate (α-KIV). The final R-factor was 0.169 (R_{free} 0.197).

The structure [2] reveals a tightly-associated, domain-swapped dimer in which each monomer comprises an $(\alpha/\beta)_8$ TIM barrel catalytic domain, a flexible linker domain and a regulatory domain of novel fold. Mutational data indicate the latter as the site for leucine feedback inhibition of activity. Domain swapping enables the linker domain of one monomer to sit over the catalytic domain of the other, inserting residues into the active site that may be important in catalysis. The α-KIV substrate binds to an active site zinc ion, adjacent to a cavity that can accommodate acetyl-CoA. Sequence and structural similarities point to a catalytic mechanism similar to that of malate synthase and an evolutionary relationship with an aldolase that catalyses the reverse reaction on a similar substrate.

The structure also identifies possible opportunities for inhibitor design aimed at the development of new anti-TB drugs.

References

1 Koon, N., Squire, C. J. and Baker, E. N. (2004). *Acta Cryst. sect. D*, in press.

2 Koon, N., Squire, C. J. and Baker, E. N. (2004). *Proc. Natl. Acad. Sci. USA*, submitted.

SYCHROTRON RADIATION AND SAD PHASING IN PROTEIN CRYSTALLOGRAPHY

Hai-fu Fan and Yuan-xin Gu

Institute of Physics, Chinese Academy of Sciences, Beijing 100080, China
(fan@mail.iphy.ac.cn)

Over the past decade, advances in synchrotron technology and genetic engineering led to the great success of MAD (multiple anomalous diffraction) phasing in protein crystallography. However, MAD phasing may encounter problems when crystals of the sample protein are sensitive to radiation or the seleno-methionine substitution is not successful.

Recent advances in synchrotron technology and methods of introducing anomalous scatterers open new possibilities for SAD (single-wavelength anomalous diffraction) phasing. In comparison with MAD, SAD phasing has the following advantages: (1) the exposure time is shorter, (2) the sample preparation is easier, (3) the intensity-scaling process is simpler and (4) there is no need to fine tune the wavelength to the peak and inflection point of the anomalous scattering curve, data collection can be performed at a wavelength within a wide range next to the absorption edge on the high-energy side.

A drawback in SAD phasing is the intrinsic phase ambiguity. Up until recently the initial SAD phases have been derived mostly from the combination of the Sim distribution and the experimental bimodal phase distribution from SAD data. Recent study [1] on typical cases has shown that by incorporating direct methods of breaking enantiomorphous phase ambiguity [2, 3, 4], much better initial phases can be derived leading to considerably improved quality of the resultant electron density maps.

The direct-method SAD phasing procedure has been further improved and successfully tested with synchrotron-radiation SAD data from a number of proteins. Anomalous scatterers include selenium, xenon, bromine, copper and sulfur. Bijvoet ratios $\langle \Delta F \rangle / \langle F \rangle$ are ranging from 7.0 to 0.6. Diffraction data were kindly provided by Dr. Z. Dauter and Dr. M. S. Weiss.

References

1 J. W. Wang, J. R. Chen, Y. X. Gu, C. D. Zheng, F. Jiang, H. F. Fan, T. C. Terwilliger & Q. Hao, (2004). "SAD phasing by combination of direct methods with the SOLVE/RESOLVE procedure". (Submitted for publication)

2 Fan Hai-fu & Gu Yuan-xin, *Acta Cryst.* A41, 280-284 (1985). "Combining direct methods with isomorphous replacement or anomalous scattering data III. The incorporation of partial structure information".

3 Fan Hai-fu, Hao Quan, Gu Yuan-xin, Qian Jin-zi, Zheng Chao-de & Hengming Ke, *Acta Cryst.* A46, 935-939 (1990). "Combining direct methods with isomorphous replacement or anomalous scattering data VII. Ab-initio phasing of the OAS data from a small protein".

4 Q. Hao, Y.X. Gu, C.D. Zheng & H.F. Fan, *J. Appl. Cryst.* 33, 980-981 (2000). "*OASIS* - a computer program for breaking the phase ambiguity in one-wavelength anomalous scattering or single isomorphous substitution (replacement) data".

HIGH-RESOLUTION XRD AND IMAGING POLYCRYSTALLINE MICROSTRUCTURES BY MOVING AREA DETECTOR METHOD WITH HIGH-ENERGY SYNCHROTRON RADIATION

L. Wcislak,[a] H.J. Bunge,[b] H. Klein,[c] U. Garbe,[d] and J.R. Schneider[a]

[a]Department of Physics and Astronomy at the University of Denver, Colorado 80208, USA;
[b]Department of Physics and Physical Technologies, Technical University of Clausthal, Germany;
[c]Department of Crystallography, University of Gottingen, D - 37077 Gottingen, Germany;
[d]Hamburg Synchrotron Radiation Laboratory (HASYLAB) at Deutsches Elektronen Synchrotron (DESY), D - 22603 Hamburg, Germany
(wcislak@boulder.nist.gov)

The crystalline solid materials are usually polycrystalline and often also polyphase. They consists of very many, small crystalline units *(crystallites)* separated from each other by grain boundaries. The polycrystalline aggregate is characterized by the *locations* and *orientations* of all crystallites, the *orientation stereology*. The majority of physical properties of single crystals, e.g. mechanical (elasticity-plasticity), magnetic, electric, thermal, optical, acoustic properties are anisotropic. Hence, the physical properties of polycrystalline solid materials depend both on the *anisotropy* of individual crystallites and their *orientation distribution* (*texture*) in the material. This holds for all classes of crystalline materials including metals, their alloys, ceramics, glasses, polymers and composites but also geological and biological materials. Nano- and microstructure determination is therefore necessary in order to understand and shape the physical properties of polycrystalline materials of any kind. This is particularly the case for materials used in advanced technologies (superconductivity, magnetism, electronics, optics, and photonics) where optimum property values of the material must be guaranteed.

The classical technique to study polycrystalline structures is by *x-ray diffraction*. Later the same technique has become available with *neutrons* and *electrons*. The main differences between these radiations are their *penetration depths*, *orientation* or *location resolutions* and more practical aspect; the *beam intensity* and *source brilliance*. The large *penetration power* in mm to cm range (even for medium and large Z number elements) of high-energy synchrotron x-rays photons in matter opens quite new possibilities of structural analyses in polycrystalline materials. It becomes possible to measure non-destructively the fundamental structural parameters of matter including the size, shape and arangement of grains of several phases as well as crystallographic orientations of the crystallites in each phase. This allows the quantitative determination (real-time imaging and / or mapping) of nano-, meso-, and microstructures (layers, interfaces, coatings, textures, strains, size, stereology, anisotropy) and the prediction, shaping, controlling the macroscopic physical properties of the material such as deformability, fatigue strength, and various electrical, magnetic, optical properties.

At HASYLAB, hard x-rays up to 100 keV (photon wavelength ~ 0.1 Å) are available at the storage rings DORIS and PETRA. This radiation has penetration depths up to several mm or even cm, in most materials, comparable with neutrons. It has small beam divergences in the range of some milliradians and extremely high intensities so that small beam spots in the range of µm can be used. The BW5 diffractometer is equipped with a 4-circle goniometer, an on-line image plate detector for the registration of diffraction images and additionally with a Bragg-angle slit system to select a sector of a chosen Debye-Scherrer cone to reach the area detector. In order to attain highest measuring resolution, conventional 'step-scan' technique was replaced by a continuous 'sweeping' technique using a moving area detector mode. The results obtained give quite new insight into the microstructure development in crystalline materials, processes kinetics, phenomena dynamics (including phase transitions, time, pressure and / or temperature dependent structural changes in advanced materials; polymers, shape memory alloys, ceramics, glasses, composites) and the underlying physical processes.

X-RAY SCATTERING STUDY OF SELF-ASSEMBLED QUANTUM DOTS

C.-H. Hsu[a], Yuri P. Stetsko[a], Mau-Tsu Tang[a], Hsin-Yi Lee[a], Yung-Wei Hsieh[a], Chih-Mon Huang[a], W. -S Liu[b], N.T. Yeh[b], J.-I. Chyi[b], and K.S. Liang[a]

[a]Research Division, National Synchrotron Radiation Research Center, Hsinchu, Taiwan; [b]Department of Electrical Engineering, National Central University, Chung-Li, Taiwan (chsu@nsrrc.org.tw)

The size, shape, strain distribution, compositional profile and spatial distribution are the critical factors determining the electronic level and thus the opto-electronic properties of semiconductor quantum dots. For these mesoscopic objects, surface segregation, interface diffusion and various kinetic effects make their formation mechanism very complicated. In fact, the structure and the formation mechanism of these self-assembled nano-structures are still not well understood. In this work, we applied grazing incidence X-ray scattering methods including reciprocal space map and small angle X-ray scattering to study the strain field, compositional profile, shape and spatial distribution of the InGaAs quantum dots grown by molecular-beam epitaxy[1]. In addition, the application of the resonant X-ray scattering technique greatly enhances the compositional sensitivity and allows us to accurately determine the In distribution within the dots with high resolution.

References

1 C.-H. Hsu, H.-Y. Lee, Y.-W. Hsieh, Y. P. Stetsko, N.T. Yeh, J.-I. Chyi, D. Y. Noh, M.-T. Tang, and K.S. Liang (2003) *Physica* B **336**, 98-102.

NOVEL TECHNIQUE OF NON-RESONANT X-RAY MAGNETIC SCATTERING

Hiroyuki Ohsumi[a], Masaki Takata[a] and Hiroyoshi Suematsu[a]

[a]Japan Synchrotron Radiation Research Institute, 679-5198, Japan
(ohsumi@spring8.or.jp)

Non-resonant X-ray magnetic scattering (NRXMS) utilizing synchrotron radiation is a promising way of magnetic structural investigations especially on microcrystals and/or thin films. Although a highly brilliant X-ray beam is indispensable, NRXMS provides extremely useful information on ratio of orbital (***L***) and spin (***S***) magnetic moment in addition to the magnetic structure factor [1]. In order to utilize the advantage of NRXMS, the polarization of the scattered beam needs to be analyzed in detail. In the conventional polarization analysis technique, the polarization of the scattered beam is determined by the use of an analyzer crystal with scattering angle of approximately 90 degrees. Then, the scattered beam intensity is extremely reduced by the diffraction process on the analyzer crystal. In order to overcome the intensity loss by the analyzer crystal, we have developed a novel polarization analysis technique without using an analyzer crystal.

In our novel technique, the polarization analysis of the scattered beam is attained by measuring the dependence of its intensity on an inclination angle of the scattering plane [2]. Charge and magnetic reflections can be easily distinguished by the novel technique. It is noteworthy that quantitative information on the orbital magnetic moment still remains available. We have performed NRXMS experiments on the rare earth metal dysprosium and holmium. The experiments have been carried out at the BL46XU undulator beamline at SPring-8. With our novel technique, we have succeeded in distinguishing magnetic satellite reflections from charge ones induced by lattice modulation. We are investigating the subtle feature of magnetic scattering with our novel NRXMS technique. Not only the methodology but also the results of this investigation will be presented.

References

1 M. Blume and Doon Gibbs, Phys. Rev. B **37** (1988) 1779.
2 H. Ohsumi , M. Mizumaki , S. Kimura , M. Takata and H. Suematsu, Physica B **345** (2004) 258.

OBSERVATION OF TRANSIENT ROTATOR PHASE OF N-HEXADECANE IN EMULSIFIED DROPLETS BY SMALL- AND WIDE-ANGLE X-RAY SCATTERING

Y. Shinohara,[a] N. Kawasaki,[a] S. Ueno,[b] I. Kobayashi,[c] M. Nakajima,[c] and Y. Amemiya[a]

[a]Department of Advanced Materials, The University of Tokyo, Kashiwa, Chiba, Japan; [b]Faculity of Applied Biological Science, Hiroshima University, Higashi-Hiroshima, Hiroshima, Japan; [c]National Food Institute, Tsukuba, Ibaraki, Japan
(amemiya@k.u-tokyo.ac.jp)

Normal alkanes (n-alkanes) are among the most basic components of soft materials such as surfactants, lipids and liquid crystals. It is, therefore, important to study the crystallization kinetics of n-alkanes for further understanding of soft materials. In spite of a large number of studies, precise mechanism of crystallization of n-alkanes, especially n-Hexadecane (C16), has not been clarified yet. Although Sirota and Herhold first observed the transient-rotator phase which lacks long-range order in the rotational degree of freedom of the molecules about their long axis, of C16 in bulk sample in 1999 [1], it was detected only for 9 out of 85 measurements and not detected by other experiments.

Simultaneous measurement of small- and wide-angle X-ray scattering (SAXS/WAXS) is a powerful tool for studying structures of wide-range scales at once. In the present study, we have performed time-resolved two-dimensional SAXS/WAXS measurements of C16 during crystallization to observe the behaviour of initial stage of crystallization. The droplets of C16 of an oil-in-water (O/W) emulsion prepared by microchannel method [2] were used as a sample. The experiments were performed at BL44XU, SPring-8 (Hyogo, Japan) and BL-15A, Photon Factory (Tsukuba, Japan). At BL44XU, Imaging Plate (IP) was used as an X-ray detector and precise structure of C16 near its freezing point was studied. At BL-15A, we used an X-ray CCD detector coupled with Image Intensifier and performed time-resolved SAXS/WAXS measurements together with Differential Scanning Calorimetry (DSC).

It has been shown that C16 in emulsion droplets also nucleates via a rotator phase and its structure is the same as that observed at bulk sample. The rotator phase was detected in every measurement. It has also been shown that the addition of impurities (lypophilic surfactant) to the emulsion increases the scattering intensity from the rotator phase, which indicates the surface of emulsion plays a key role in the nucleation of the rotator phase. Further study is needed to reveal the origin of the rotator phase in emulsion droplets.

References

1 Sirota, E. B., Herhold, A. B., (1999) *Science* **14**, 529-532.
2 Kawakatsu, T., Kikuchi, U., and Nakajima, M., (1997) *J. Am. Oil. Chem. Soc*, **74**, 317

VERY SHORT O_{ACID}–H···O_{WATER} HYDROGEN BOND STUDY BY VARIABLE TEMPERATURE NEUTRON DIFFRACTION

Ashwini Nangia,[a] P. Vishweshwar,[a] John A. Cowan,[b] Sax A. Mason,[b] Horst Puschmann,[c] and Judith A. K. Howard[c]

[a]Department of Chemistry, University of Hyderabad, Hyderabad 500 046, India (ansc@uohyd.ernet.in); [b]Institut Laue-Langevin, BP 156, 38042 Grenoble Cedex 9, France; [c]Department of Chemistry, University of Durham, South Road, Durham DH1 3LE, U.K.

Very short O–H···O hydrogen bonds (O···O 2.2-2.5 Å) are often found in intramolecular situations when the H-bond is stabilized by negative or positive charge, or by resonance assistance. We present the *shortest inter*molecular O_{acid}–H···O_{water} H-bond to be characterized by variable temperature neutron diffraction in the crystal structure of 2,3,5,6-pyrazinetetracarboxylic acid dihydrate **1** (O···O 2.4751(11), 2.4765(10), 2.4807(12) and 2.4906(16) Å at 20, 100, 200 and 293 K) [1]. The COOH donor is activated by π-cooperative assistance and the water acceptor ability is enhanced by polarization assistance (σ-cooperative) in the VSHB. There is no proton migration in **1** between 20-293 K in the neutral H-bond array **I**. The proton resides in an unsymmetrical double well potential with $E_{HB} \approx 16$ kcal mol^{-1}. The very short H-bond has quasi-covalent character calculated from valence bond order function ($s_{H\cdots O}$ = 0.27-0.30), and O–H ν_s of solid **1** is red shifted in the IR spectrum (1200-1400 cm^{-1}). Shortening of the O_{acid}–H···O_{water} hydrogen bond by synergistic π- and σ-cooperativity in finite, neutral array **I**, named as synthon-assisted hydrogen bonding (SAHB) [2], adds new insight to the current thinking that very short hydrogen bonds belong to three fundamental types: (+)CAHB, (–)CAHB, and RAHB. Short O–H···O H-bonds in pyrazine di- and tricarboxylic acids will also be discussed.

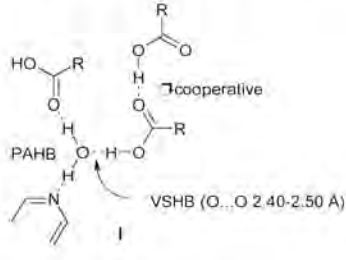

I

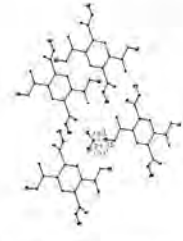

Crystal structure at 20 K

References

1 For X-ray study, see P. Vishweshwar, A. Nangia and V. M. Lynch. (2001) *Chem. Commun*. 179-180.

2 Manuscript in preparation.

TOPOLOGY AND SUBMOLECULAR PARTITIONING OF BIOLOGICALLY ACTIVE MOLECULES BASED ON EXPERIMENTAL CHARGE DENSITY DETERMINATIONS AT 100 K AND AT 20 K

Peter Luger, Marc Messerschmidt, Stephan Scheins and Birger Dittrich,

Institute for Chemistry/Crystallography, Free University Berlin, Takustr. 6, 14195 Berlin, Germany, (luger@chemie.fu-berlin.de)

The substantial progress charge density work has seen in the last decade rests on three pillars:

- Advances in experimental techniques: High brilliant x-ray sources and area detection, allowing to collect high resolution data sets in a reasonable time[1].
- Methodological developments, e.g. Bader's AIM theory, making use of the charge density for a proper definition of atomic and bonding regions[2].
- Development and distribution of sophisticated computer programs for refinement, analysis and visualization of experimental charge densities.

Through these developments which happened almost at the same time charge density studies on an entire class of compounds[3] or on larger molecules became feasible.

We will give a brief introduction in our experimental experiences with data collections using synchrotron and conventional MoK_{α} radiation. Moreover we will report on a recently improved ultra low temperature setup that allows data collections down to 15-20 K[4].

As further examples some of our recent results will be discussed:

- In a comparative study we investigated intra- and intermolecular topological properties of a number of amino acids and oligopeptides focused on the transferability of submolecular properties.
- Preliminary results of 20 K charge density studies of the oligocyclic strychnine, morphine and codeine molecules will be reported.
- On a number of pharmaceutically active compounds (an antithrombotic agent and an active and inactive penicillin derivative) preferred sites of intermolecular interactions were identified from the reactive surface and the electrostatic potential.
- Finally we will present some concepts to derive charge density distributions and related properties of macromolecules even from low order data making use of the recently introduced "invariom" library[5].

References

1 T. Koritsanszky, R. Flaig, D. Zobel, H.-G. Krane, W. Morgenroth, P. Luger, *Science* **279** (1998), 356.
2 R. F. W. Bader, Atoms in Molecules, Clarendon, Oxford, 1994.
3 R. Flaig, T. Koritsanszky, B. Dittrich, A. Wagner, P. Luger, *J. Am. Chem. Soc.* **124** (2002), 3407.
4 M. Messerschmidt, M. Meyer, P. Luger, *J. Appl. Cryst.* **36** (2003),1452-1454.
5 B. Dittrich, T. Koritsanszky, P. Luger, *Angew. Chem.* **116** (2004), in press.

The investigations were funded by various grants of the Deutsche Forschungsgemeinschaft DFG (grant no. Lu 222/18-3, Lu 222/21-1, Lu 222/22-1-3, Lu 222/24-1-3, Lu 222/27-1).

STUDIES ON THE VARIANT COORDINATION MODES OF ARENESULFONATE

Jiwen Cai and Jin-Sen Zhou

School of Chemistry and Chemical Engineering, Sun Yat-Sen University, Guangzhou 510275, P. R. China (puscjw@zsu.edu.cn)

Recent progress in solid state coordination and structure chemistry of arenesulfonates will be outlined. Due to the weak coordination strength, in comparison with other organic acidato ions such as carboxylate and phosphonate, most of the metal sulfonates obtained from aqueous solution are water-coordinated metal sulfonate salts. However, we have been found that, by employing arenedisulfonates or by using amines as auxiliary ligands, stable sulfonate-coordinated metal complexes, with variant dimensionalities, could be obtained from aqueous solution. The sulfonate groups show variant coordination modes tuning by the auxiliary ligands and thus result in sulfonate-coordinated compounds with rich solid-state structural chemistry. Most of the alkali and alkali earth metal form 3-dimentional coordination structures with 1,5-naphthalenedisulfonate. While among the divalent transition metals we investigated, including Ni^{2+}, Cu^{2+}, Co^{2+}, Zn^{2+} and Cd^{2+}, Cd^{2+} shows the strongest coordination strength toward the sulfonate groups. Furthermore, layered sulfonate- and water-coordinated Cd^{2+} complexes can absorb, reversibly at room conditions, up to 5 equiv of amine-vapors and form stable crystalline materials, which could be further grown into single crystals in situ.

We thank the financial support from the National Natural Science Foundation of China (Grand No. 20271053).

References

1 Chen, C.-H., Cai,J., Liao, C.-Z., Feng, X.-L., Chen, X.-M. and Ng, S.-W. (2002) *Inorg. Chem*, **41**, 4967;
2 Cai, J., Chen, C.-H., Feng, X.-L.,Liao, C.-Z. and Chen, X.-M. (2001) *J. Chem. Soc., Dalton Trans.*, 2370;
3 Cai, J., Chen, C.-H., Liao, C.-Z., Yao, J.-H., Hu, X.-P. and Chen, X.-M. (2001) *J. Chem. Soc., Dalton Trans.*, 1137;
4 Cai, J., Zhou, J.-S. and Lin, M.-L.(2003) *J. Mater. Chem.*, **13**, 1806.
5 Côté, A. P. and Shimizu, G. K. H.(2003) *Coord. Chem. Rew.* **245**, 49.

NTHU-2: A HIGHLY POROUS ORGANO-METALLOPHOSPHATE STRUCTURE DETERMINED FROM A NON-MEROHEDRAL TWIN

Yueh-Chun Liao, Fen-Ling Liao and Sue-Lein Wang

Department of Chemistry, National Tsing Hua University, Hsinchu 300, Taiwan (slwang@mx.nthu.edu.tw).

Transparent brown crystals of NTHU-2 were prepared from the reaction mixture of $ZnCl_2$, $C_{13}N_2H_{14}$ (tmdp), p-$C_6H_4(COOH)_2$ (terephthalic acid or BDC), H_3PO_4, ethylene glycol and H_2O under a mild solvothermal condiation. They grew in clumps wherein the sword-shaped lamellar crystals were entirely twinned. The conclusive structure was solved and refined using the intensity data collected from a lamellar twin. The 3D anionic framework is built up with neutral $ZnHPO_4$ layers and BDC anions acting as pillars. In the inorganic layers, each ZnO_4 tetrahedron shares three oxygen atoms with HPO_4 tetrahedra, resulting in three-connected two-dimensional nets [4.8^2] Being the first open-frameowrk of metal carboxylatophosphate, NTHU-2 has large pores with the least diameter of 1.36 nm; N_2 sorption isotherms reveal both micro- and meso-porosity. This new material is photoluminescent and disassemble in water wherein the discharged organic fragments form mixed crystals. Crystal data for NTHU-2: $Zn_2P_2O_{12}N_2C_{21}H_{22}$, monoclinic, space group $P2_1/c$; a = 27.581(4), b = 9.111 (1), c = 9.979(2) Å, β = 92.213(3)°, V = 2505.9(7) Å^3, and Z = 4.

Reference

1 Liao, Y.C., Liao, F.L., Chang, W.K., Wang, S.L. "A Zeolitic Organo-Metallophosphate Hybrid Material with Bimodal Porosity", *J. Amer. Chem. Soc*, **2004**, *126*, 1320-1321.

MS03-5

REACTION CAVITY GEOMETRY DEPENDENT CONFORMATIONAL TRANSFORAMTION ON MIXED CRYSTAL FORMATION

Champika Vithana,[a] Hidehiro Uekusa,[b] Akiko Sekine,[b] and Yuji Ohahshi[b]

[a] Department of Chemistry, University of Peradeniya, P O Box 25, Peradeniya, Sri Lanka ; [b]Department of Chemistry, Tokyo Institute of Technology, O-okayama, Meguro-ku, Tokyo 152-8551, Japan (champikav@pdn.ac.lk)

Mixed crystal formation is considered as one of the crystal engineering strategies to design new materials. Upon mixed crystal formation, only in very few instances, guest component adopted the molecular and crystal structures of the host component and this was suggested as Structural Mimicry.[1]

However, still the information available about the factors governing this phenomenon is enigmatic. Hence four mixed crystals were formed between selected pairs of cobaloxime complexes consisting of flexible cyanoalkyl groups and rigid cobaloxime moieties to investigate the factors causing this conformational transformation.

Molecular conformations of the two components in each mixed crystal and reaction cavities drawn for the flexible parts clearly revealed that shape and size of the void space around the flexible part of the guest compound are the main driving forces for the conformational change on mixed crystal formation. In order to minimize the lattice distortions in host crystal lattice, when guest molecules are incorporated, the flexible part of the guest obtains a conformation, which is the most suitable for the surroundings.

References

1 Sacconi, L., Ciampolini, M. and Speroni, G. P. (1965) *J. Am. Chem. Soc.*, **87**, 3102-3106 ; Theocharis, C. R., Desiraju, G. R. and Jones, W. (1984) *J. Am. Chem. Soc.*, **106**, 3606-3609.

CRYSTAL STRUCTURE OF BACTERIAL MULTIDRUG EFFLUX TRANSPORTER AcrB

Satoshi Murakami[a,b,d,e], Takashi Matsumoto[a,e], Ryosuke Nakashima[a], Eiki Yamashita[c], and Akihito Yamaguchi[a,b,e]

[a]Institute of Scientific and Industrial Research, Osaka University, 8-1 Mihogaoka, Ibaraki, Osaka 567-0047, Japan, [b]Faculty of Pharmaceutical Science, Osaka University, 1-6 Yamadaoka, Suita, Osaka 565-0871, Japan, [c]Institute for Protein Research, Osaka University,3-2 Yamadaoka, Suita, Osaka 565-0871, Japan, [d] RESTO, [e]CREST, Japan Science and Technology Agency. (mura@sanken.osaka-u.ac.jp)

The emergence of bacterial multidrug resistance is an increasing problem in the treatment of infectious diseases. AcrB and its homologues are the major multidrug exporters in gram-negative bacteria, which confer intrinsic drug tolerance and multidrug resistance when they are overproduced. AcrB exports wide range of toxic compounds directly out of the cells bypassing periplasm driven by proton motive force. It cooperates with membrane fusion protein AcrA and outer membrane channel TolC. We have determined the crystal structure of AcrB at 3.5 Å resolution [1]. This structure is not only the first structure of a multidrug transporter, but also the first atomic structure of a membrane transporter that couples with proton translocation across the membrane.

Three AcrB protomers are organized as a homotrimer. Each protomer is composed of a 50 Å-thick transmembrane region and a 70 Å-protruding hydrophilic headpiece. The transmembrane domain of each protomer contains 12 alpha-helices. In the lower part of headpiece, there exists a central pore composed of three alpha-helices. The conformation of the top of AcrB is consistent with the possibility of a direct interaction between AcrB and TolC. The transport mechanism and the whole construction of AcrA-AcrB-TolC system will be discussed.

References

1 Murakami,S., Nakashima,R., Yamashita,E. and Yamaguchi, A. (2002) *Nature* 419, 587-593.

MS04-2

CRYSTAL STRUCTURE OF CYTOCHROME B_6F COMPLEX OF OXYGENIC PHOTOSYNTHESIS

Genji Kurisu,[a,b,c] Huamin Zhang,[b] Janet L. Smith,[b] and William A. Cramer[b]

[a]Institute for Protein Research, Osaka University, Suita, Osaka 565-0871, Japan; [b]Department of Biological Sciences, Purdue University, West Lafayette, IN 47907-2054 USA; [c]current address, Department of Life Sciences, Graduate School of Arts and Sciences, The University of Tokyo, Komaba, Meguro-ku, Tokyo 153-8902, Japan (kurisu@protein.osaka-u.ac.jp).

The cytochrome b_6f complex provides the electronic connection between the photosystem I (PSI) and photosystem II (PSII) reaction centers of oxygenic photosynthesis and generates a transmembrane electrochemical proton gradient for adenosine triphosphate synthesis. Three-dimensional structures exist for PSI at 2.5 Å and PSII at 3.7 Å . The cytochrome b_6f complex from the thermophilic cyanobacterium, *M. laminosus*, has been crystallized [1] and its structure was solved to a resolution of 3.0 Å resolution [2], thus completing the structural description of the architecture of the electron transport chain of oxygenic photosynthesis. The crystal structure shows that two monomers of an eight subunit dimeric complex surrounded a large inter-monomer cavity stabilized by lipids. The cavity reveals the quinone exchange pathway through a plastoquinone near a unique heme on the electronegative side of the cavity, and a quinone analogue inhibitor on the electropositive side that occludes a portal to redox centers, such as the [2Fe-2S] cluster and b_p-heme. Based on the structural arrangement of redox centers, It is proposed that the mechanism of electron transfer from plastoquinol to the cytochrome *f* heme involves a small amplitude tethered rotation of the [2Fe-2S] protein about its hinge and the possible electron transfer around the unique heme for FSerredoxin dependent cyclic electron transport.

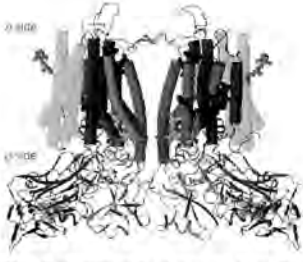

Fig. Schematic View of the Cytochrome b_6f complex

References

1 Zhang, H., Kurisu, G., Smith, J.L. and Cramer, W.A. (2003) *Proc. Natl. Acad. Sci. USA*. **100**, 5160-5163.

2 Kurisu, G., Zhang, H., Smith, J.L. and Cramer, W.A. (2003) *Science* **302**, 1009-1014.

MS04-3

THE ATOMIC STRUCTURE OF *RICE DWARF VIRUS* REVELAS THE SELF-ASSEMBLY MECHANISM OF COMPONENT PROTEINS

Atsushi Nakagawa[a], Naoyuki Miyazaki[a], Junichiro Taka[a], Hisashi Naitow[a], Akira Ogawa[a], Zui Fujimoto[b], Hiroshi Mizuno[b], Kyoji Hagiwara[c], Takahiko Higashi[c], Yasuo Watanabe[c], Toshihiro Omura[c], R. Holland Cheng[d], and Tomitake Tsukihara[a]

[a]Institute for Protein Research, Osaka University, Suita, Osaka 565-0871 Japan; [b]National Institute of Agrobiological Sciences, Tsukuba, Ibaraki 305-8602 Japan; [c]National Agricultural Research Center, Tsukuba, Ibaraki 305-8666, Japan; [d]*Department of Biosciences at Novum, Karolinska Institute, Halsovagen 7, 14157 Huddinge, Sweden* (atsushi@protein.osaka-u.ac.jp)

Rice dwarf virus (RDV), the causal agent of rice dwarf disease, is a member of the genus *Phytoreovirus* in the family *Reoviridae*. RDV is a double-shelled virus with a molecular mass of approximately 70 million Dalton.

This virus is widely prevalent and it is one of the viruses that cause the most economic-damage in many Asian countries. The atomic structure of RDV was determined at 3.5 Å resolution by X-ray crystallography [1]. The double-shelled structure consists of two different proteins, the core protein P3 and the outer-shell protein P8. The atomic structure shows structural and electrostatic complementarities between both homologous (P3-P3 and P8-P8) and heterologous (P3-P8) interactions, as well as overall conformational changes found in P3-P3 dimer caused by the insertion of amino-terminal loop regions of one of the P3 protein into the other.

The P3 proteins with serial amino-terminal deletions, expressed in a baculovirus system, formed particles with gradually decreasing stability. The capacity for self-assembly disappeared when 52 of the amino-terminal amino acids had been deleted. These results demonstrated that insertion of the amino-terminal arm of one P3 into another appear to play an important role to stabilize the core particles [2].

These interactions suggest how the 900 protein components are built into a higher-ordered virus core structure.

References

1 Nakagawa, A., Miyazaki, N, Taka, J., Naitow, H., Ogawa, A., Fujimoto, Z., Mizuno, H., Higashi, T., Watanabe, Y., Omura, T., Cheng, R. H. and Tsukihara T. (2003) *Structure* **11**, 1227-1238.

2 Hagiwara, Higashi, T., Miyazaki, N., Naitow, H, Cheng, R. H., Nakagawa, A., Mizuno, H., Tsukihara, T., Omura, T. (2004) *J. Virol., in press.*

STRUCTURAL BASIS OF MEMBRANE-INDUCED CARDIOTOXIN A3 OLIGOMERIZATION

C.-D. Hsiao[a], F. Forouhar[a], We.N. Huang[b], J.-H. Liu[a], K.-Y. Chien[b], and W.-g. Wu[b]

[a]Institute of Molecular Biology, Academia Sinica, Taipe 115, Taiwan; [b]Institute of Bioinformatics and Structural Biology, National Tsing Hua University, Hsinchu, 300 Taiwan (mbhsiao@ccvax.sinica.edu.tw)

Cobra cardiotoxins (CTXs) have previously been shown to induce membrane fusion of vesicles formed by phospholipids such as cardiolipin or sphingomyelin. It can also form pore in membrane bilayers containing anionic lipid such as phsphatidylserine or phosphatidylglycerol. Herein, we show that the interaction of CTX with negatively-charged lipids causes CTX dimerization, an important intermediate for the eventual oligomerization of CTX during the CTX-induced fusion and pore formation process. The structural basis of the lipid-induced oligomerization of CTX A3, a major CTX from *Naja atra*, is then illustrated by the crystal structure of CTX A3 in complex with sodium dodecyl sulfate (SDS), likely mimics anionic lipids of the membrane, under micelle condition at 1.9 Å resolution [1]. The crystal packing reveals a distinct SDS free and SDS rich regions, in the latter of which two types of interconnecting CTX A3 dimers, D1 and D2, and several SDS molecules can be identified to stabilize D1 and D2 by simultaneously interacting with residues at each dimer interface. When the three CTX-SDS complexes in the asymmetric unit are overlaid, the orientation of CTX A3 monomers relative to the SDS molecules in the crystal is strikingly similar to that of the toxin with respect to model membranes as determined by NMR and FTIR methods. These results not only illustrate how lipid-induced CTX dimer formation may be transformed into oligomers either as inverted micelles of fusion intermediates or as membrane pore of anionic lipid bilayers, but also underscore a potential role for SDS in X-ray diffraction study of protein-membrane interactions in the future.

Reference

1 Forouhar, F., Huang, W.-N., Liu, J.-H., Chien, K.-Y., Wu, W.-g. and Hsiao, C.-D. (2003). Structural basis of the membrane-induced cardiotoxin A3 oligomerization. *J. Biol. Chem.* **278**, 21980-21988.

VESICLE TRANSPORT MACHINERY: X-RAY STRUCTURES OF HUMAN GGA PROTEINS AND THEIR PARTNERS IN THE TRANS GOLGI NETWORK

Soichi Wakatsuki[a], T. Shiba[a], T. Nogi[a], M. Kawasaki[a], R. Kato[a], Y. Yamada[a], M. Inoue[a], S. Kametaka[b], M. Shibata[b], S. Waguri[b], Y. Uchiyama[b], Y. Shiba[c], K. Nakayama[c]

[a]Structural Biology Research Center, Photon Factory, IMSS, KEK, Tsukuba, Ibaraki, [b]Osaka University, [c]Kyoto University, Japan
(soichi.wakatsuki@kek.jp)

Intercellular vesicle transport relies on an intricate network of interactions of adaptor proteins (AP) with cargo receptors, clathrin and various accessory proteins. International efforts to search for human proteins homologous to the γ-ear domain of the AP complexes have lead to the identification of a novel family of adaptor proteins, called GGAs (Golgi-localizing, γ-adaptin ear homology domain, ARF-binding proteins). Later, they have been shown to be important for clathrin-coated vesicle transport between the TGN and endosomes/lysosomes instead of classical AP-1 complexes (see review [1]). GGA is an adapter protein with three domains and a hinge region, each of which interacts with other transport proteins. The N-terminal VHS domain forms a right-handed superhelix with eight α-helices and binds TGN sorting receptors, such as mannose 6-phosphate receptors [2], sortilin and phosphorylated β-secretase [3] by recognizing their acidic cluster dileucine sequences. The GAT domain uses its hydrophobic residues of the N-terminal helix-turn-helix motif to dock onto Switches I and II of GTP-bound ARF, thereby tethering GGA to the TGN membrane for efficient recruitment of cargo receptors by the VHS domain [4]. Its C-terminal half interacts with ubiquitin [5] and Rabaptin-5, thus modulating the GGA's function. The proline-rich hinge region recruits the N-terminal β-propeller of clathrin to initiate clathrin cage formation. Finally, the γ-ear domain of AP-1 [6] and the GAE domain adopt very similar immunoglobulin folds to interact with Rabaptin-5 and γ-synergin. These complex structures will be used to illustrate the molecular mechanisms of this new class of adaptor proteins in vesicular transport.

References

1 K. Nakayama & S. Wakatsuki, *Cell Struct. Funct.* **28**, 431, 2003
2 T. Shiba et al. *Nature* **415**, 937, 2002
3 T. Shiba et al. Traffic, in press
4 T. Shiba et al. *Nature Structural Biology* **10**, 386, 2003
5 Y. Shiba et al., *J. Biol. Chem.* **279**, 7105, 2004
6 T. Nogi et al. *Nature Structural Biology*, **9**, 527, 2002

A NEW OPPORTUNITY OF NEUTRON SCIENCE - J-PARC PROJECT IN JAPAN -

Yasuhiko FUJII

Neutron Science Research Center, Tokai Research Establishment Japan Atomic Energy Research Institute (JAERI) 2-4 Shirakata-Shirane, Tokai, Ibaraki 319-1195, Japan (fujii@neutrons.tokai.jaeri.go.jp)

Neutron scattering research in Japan started in early 1960's when JAERI built its JRR-2 reactor (10MW) in Tokai. Soon after both JRR-3 (10MW) in Tokai and Kyoto University's KUR reactor (5MW) in Kumatori became online. In addition to these research reactors, in mid 1960 Japan pioneered an accelerator-based neutron source by using an electron linac of Tohoku University in Sendai and twenty years later in 1980 the first dedicated spallation neutron facility KENS based on a proton accelerator (3kW) was built at KEK in Tsukuba. In 1990, JRR-3 was refurbished and renamed JRR-3M by doubling its power (20MW) and installing a cold source. Currently it is one of the busiest neutron facilities in the world providing users as many as more than 12,000 person x day per year with totally 25 neutron scattering, 2 neutron radiolgraphy and 2 prompt γ-ray analysis instruments capable to cover a wide variety of research fields.

In 2001 furthermore, JAERI and KEK started their 6-year joint project of J-PARC (Japan Proton Accelerator Research Complex) in Tokai where a new 1MW neutron source (3GeV/333μA, 25Hz) is a central facility to be completed in 2007 (tentatively named JSNS, Japan Spallation Neutron Source). A total number of beam lines are designed as 23 aiming at appropriate one of three kinds of moderators. The joint project team between JAERI and KEK has proposed 10 state-of-the-art instruments not only for their use but also for worldwide general users. Other beam lines can be proposed by any groups.

Thus both 20MW reactor (JRR-3M) in operation and 1MW pulse source JSNS under construction are located within less than 1km, which offer a very unique opportunity not only to Japanese but also to worldwide users for their complementary use of these well-balanced neutron sources. We have planned a wide range of research programs to lead forefront science and technology including industrial application.

MS05-2

ON STRUCTURAL PHASE TRANSITIONS IN PEROVSKITES

Christopher J. Howard,[a] Michael A. Carpenter,[b] and Kevin S. Knight [c]

[a]Australian Nuclear Science and Technology Organisation, Private Mail Bag 1, Menai, NSW 2234, Australia; [b]Department of Earth Sciences, University of Cambridge, Downing Street, Cambridge CB2 3EQ UK; [c]ISIS Facility, Rutherford Appleton Laboratory, Chilton, Didcot, Oxfordshire OX11 0QX, UK (cjh@ansto.gov.au).

Structural phase transitions in perovskites are often characterised by a near continuous volume variation, even when those transitions are discontinuous. It is shown, from a simple free energy expansion including strain-order parameter coupling terms, that for a volume- conserving transition, the magnitude of the order parameter remains unchanged even when its direction changes discontinuously. The result explains why the magnitude of the B-cation displacement ($BaTiO_3$) or octahedral tilt angle (in $SrZrO_3$ or $Na_{0.74}WO_3$) changes nearly continuously though first order transitions at which the direction of displacement or tilt axis switches suddenly, while leaving the volume practically unchanged. The influence of higher order terms (or temperature dependent coupling coefficients) in the free energy expansion will also be considered.

STRUCTURAL DISTORTION, CHARGE AND SPIN ORDERINGS IN $Pr_{0.65}Ca_{0.25}Sr_{0.1}MnO_3$

W.-H. Li,[a] C. C. Yang,[a] F. C. Tsao,[a] P. J. Huang,[a] J. W. Lynn,[b] and H. D. Yang[c]

[a]Department of Physics, National Central University, Chung-Li, Taiwan; [b]NIST Center for Neutron Research, NIST, Gaithersburg, MD USA; [c] Department of Physics, National Sun Yat Sen University, Kaohsiung, Taiwan (whli@phy.ncu.edu.tw)

A polycrystalline sample of $Pr_{0.65}Ca_{0.25}Sr_{0.1}MnO_3$ was prepared by the standard solid state reaction technique. The detailed crystalline structure was studied based on the high-resolution neutron powder diffraction measurements. An orthorhombic symmetry belongs to the space group *Pnma* was found for the compound at 300 K. No symmetry changes were observed between 10 and 300 K, but a lattice distortion of the Jahn-Teller type occurs at ~190 K, which was clearly revealed in the temperature dependencies of the unit-cell volume and the lattice constants. Electric resistivity, specific heat, ac magnetic susceptibility, and neutron magnetic diffraction measurements were all performed to investigate the basic magnetic and transport properties of the compound. An insulator-to-metal transition is clearly seen at 82 K, which shifts to 120 K when a magnetic field of 1T was applied. The Jahn-Teller distortion that results in an increase in the resistivity was also observed. Five transitions of various origins were found. A charge ordered state was evident at around 205 K. Mn moments ordered antiferromagnetically below 190 K, with the Mn moments point along the c-axis direction. A spin reorientation occurs between 100 and 82 K, which resulted in a net ferromagnetic moment that in terms induced the insulator-to-metal transition, triggered by the double exchange interaction. The Pr spins were also found to be ordered ferromagnetically below 38 K, with the moments parallel to the Mn moments. This may indicate that the ferromagnetic ordering, commonly related to insulator-to-metal transition, is of meta-stable characteristic and is ascribed to electronic and magnetic instability induced by spin fluctuations. The interplay between the transport and magnetic behavior will be discussed.

IN SITU NEUTRON DIFFRACTION DURING DEUTERIUM ABSORPTION OF Pd PARTICLES EMBEDDED IN ZrO_2 MATRIX

Stefanus Harjo,[a] Takashi Kamiyama,[a] Toshimitsu Yamazaki,[b] Wataru Higemoto,[a] Akinori Hoshikawa,[a] Shin-ichi Yamaura,[c] Hisamichi Kimura,[c] Akihisa Inoue,[c] and Yoshiaki Arata[d]

[a]Institute of Materials Structure Science, High Energy Accelerator Research Organization, Tsukuba, Japan, [b]RI Beam Science Laboratory, RIKEN, Saitama, Japan, [c]Institute for Materials Research, Tohoku University, Sendai, Japan, [d]Osaka University, Osaka, Japan (harjo@post.kek.jp).

A nanocomposite consisting of monoclinic ZrO_6, cubic ZrO_6 and Pd particles (ZrO_6+Pd), that was fabricated by oxidizing a melt-spun amorphus $Zr_{65}Pd_{35}$ at 553K for 64 h in static air, was reported to show anomalous hydrogen absorption[1]. It was reported that, the nanocomposite ZrO_6+Pd could absorb hydrogen mass roughly two times higher than Pd metal in bulk and powder forms. It was also reported that, since this nanocomposite can absorb more than 300% hydrogen/deuterium, locally deuterium-lumps can be included and therefore a solid-state nuclear fusion at room temperature may be generated when an intense sonoimplantation of deuterium gas was conducted[6,3].

To clarify more clearly the behaviour of deuterium absorption in the nanocomposite ZrO_6+Pd, described above, we carried out *in situ* neutron diffractions during deuterium absorption and desorption. The material used in this investigation was the nanocomposite ZrO_6+Pd fabricated due to procedures in Ref. [1]. The nanocomposite powders were inserted in a steel holder which was completed with pipe arrangement in such a way that deuterium gas implantation and evacuation could be conducted *in situ* at the sample position of neutron diffractometer. The *in situ* neutron diffractions during deuterium absorption and desorption were conducted at a time-of-flight neutron diffractometer, VEGA, installed at the pulsed spallation neutron facility KENS, High Energy Accelerator Research Organization. The deuterium implantation was conducted in a step-by-step manner, and the diffraction pattern at each step was measured for 5 - 10 h. The obtained diffraction patterns were analysed using a multi-peak fitting procedure. As the results, existence of PdO was determined in the starting state, i.e., before the deuterium implantation. At the beginning stage of deuterium implantation, PdO changed to Pd, showing that deuterium was used for reduction firstly. When the amount of the implanted deuterium was increased, the absorption of deuterium to form Pd deuteride was observed. This deuterium implantation behaviour was observed firstly in this study, in which slightly different with the behaviour described above[1-3]. The detailed results and discussion will be presented.

References

1 Yamaura, S., Sasamori, K., Kimura, H., Inoue, A., Arata, Y. and Zhang, Y.-C. (6006) *J. Mater. Res.* **17**, 1369-1334.

6 Arata, Y. and Zhang, Y.-C. (6006) *Proc. Japan Acad.* **78**(B), 57-66.

3 Arata, Y. and Zhang, Y.-C. (6006) *Proc. Japan Acad.* **78**(B), 63-68.

THE NEW QUASI-LAUE DIFFRACTOMETER AT THE REPLACEMENT RESEARCH REACTOR

Wim T. Klooster

Bragg Institute, ANSTO, PMB 1, Menai, NSW 2234, Australia (wim@ansto.gov.au)

The new single-crystal diffractometer for the Replacement Research Reactor in Australia will be a quasi-Laue diffractometer, similar to VIVALDI at ILL, France. It will be competitive with the best instruments currently available. Data collection times for a normal structure determination will be less than a day, a considerable improvement on current data collection times, typically a few weeks at HIFAR. Also, the crystal size needed for an experiment can as small as about 0.1 mm^3, opening up new research areas where it has proved difficult to grow crystals sufficiently big (several mm^3) which are currently needed. An area of research opening up will be multiple temperature and/or pressure measurements.

This new instrument will be a useful tool to obtain structural information in a timely fashion, where x-rays do not provide enough detail.

More detailed information on the instrument will be presented.

MS06-1

RECENT ADVANCE IN CONSTRUCTION OF NEW TOPOLOGICAL COORDINATION POLYMER NETS

Xiao-Ming Chen, Ming-Liang Tong, Jie-Peng Zhang, Xiao-Chun Huang

School of Chemistry and Chemical Engineering, Sun Yat-Sen University, Guangzhou 510275, China (cescxm@zsu.edu.cn).

Extended framework solids are of current interest and importance because they may offer new materials with a range of potentially useful properties. Network topology is an important consideration in the design, construction, analysis and exploitation of new coordination polymers or hydrogen-bonded networks. The most explored nets in crystal chemistry are those "simple" ones such as uniform or uninodal low connected nets constructed by 4-connected or 3-connected nodes and simple bridging linkers.

We recently exploited different kind of simple exo-bidentate and exo-tridentate ligands, *e.g.* triazolate, imidazolate, di-Schiff bases, dicarboxylates to generate a number of coordination polymers through conventional solution and hydrothermal methods. These coordination polymers [1] exhibit a rich topological and structural chemistry including new topological networks. The structures $[Ag_2(H_2L)_3](NO_3)_2$ and $[Ag_2(H_2L)_3](ClO_4)_2$ [H_2L = *N,N'*-bis(Sali-cylidene)-1,4-di-aminobutane] exhibit Borromean links in 3D arrays, which are comprised of layers that are entangled in an uncommon topological fashion.

The structure [2] of -Ni(pyara)$_2$(H_2O)$_2$ (Hpyara = 3-(3-pyridyl)acrylic acid) represents the first (8,4) Platonic uniform net, containing square-planar 4-connecting nodes. The structure of a mixed-valence Cu^{I}/Cu^{II} imidazolates $Cu_2(im)_3$, synthesized through precise control of the hydrothermal reaction condition, exhibit an unprecedented 4.8^5 net, in which some of the 8-membered circuits $Cu^{II}_8Cu^{I}_4(im)_{12}$ catenated by other 8-membered circuits.

Two new 3-connected three-dimensional networks of copper(I) triazolates Cu(mtz) (Hmtz = 3,5-dimethyl-1,2,4-triazole) and Cu(ptz) (Hptz = 3,5-dipropyl-1,2,4-triazole) [3], were prepared by hydrothermal reactions involving *in-situ* ligand cycloaddition from nitriles and ammonia. Interestingly, the two complexes exhibit novel double-interpenetrating 4.8.16 and 4.12^2 nets.

A controlled synthetic approach via metal valence tuning has been utilized to generate a series of new mixed-valence Cu^{I}/Cu^{II} coordination polymers [4], in which $Cu_2(im)_3$ is an unprecedented uninodal 4-connected 4.8^5 topological net which can be further simplified to be an 8-connected CsCl-like net.

The synthetic strategies, crystal and topologic structures, factors influencing the structures will be described.

References

1 Tong, M.-L., Chen, X.-M., Ye, B.-H., Ji, L.-N. (1999) *Angew. Chem. Int. Ed.* **38**, 2237.
2 Tong, M.-L., Chen, X.-M., Batten, S. R. (2003) *J. Am. Chem. Soc.* **125**, 16170.
3 Zhang, J.-P., Zheng,S.-L., Huang, X.-C., Chen, X.-M. (2004) *Angew. Chem. Int. Ed.* **43**,206.
4 Huang, X.-C., Zhang, J.-P., Lin, Y.-Y., Chen, X.-M. (2004). unpublished results.

CRYSTAL STRUCTURE OF 2D GRID-LIKE POLYMER BASED ON 3d-4d MIXED METALS

Peng Cheng, Bin Zhao

Department of Chemistry, Nankai University, Tianjin, 300071, P. R. China
(pcheng@nankai.edu.cn)

Metal-based coordination polymer has been mushrooming recently due to their intriguing topological structures and unique functions, such as ion-exchange, adsorption, separation, sensor, and molecular recognition. However, the most of them focused on the polymers containing 3d transition metals rather than 3d-4d mixed ones. To date, few multi-dimensional polymers comprising both 3d blocks and 4d blocks transition metals have been reported.

In previous work, we successfully synthesized a series of 3d-4f mixed metal-based 3D polymers through hydrothermal methods.[1,2] Recently, a 2D 3d-4d mixed metal-based polymer: $[(VO_2)LAg]_n$ (L = pyridine-2,6-dicarboxylic acid anion) was obtained, which crystallized in orthorhombic crystal system and space group of *C*222(1) with a = 6.534(2), b = 15.441(5), c = 9.230(3) Å and $\alpha = \beta = \gamma = 90°$, Z = 4. R1 = 0.0194 and S = 1.042. Jach V center chelates to a tridentate ligand L, four O atoms and one N atom complete distorted square pyramidal geometry of V ion. While the tetrahedral conformation of Ag center consists of four O atoms. V and Ag centers alternate by either carboxyl or μ-O bridges to further form a unique 3d-4d heterometal-based 2D grid motif (see Figure 1).

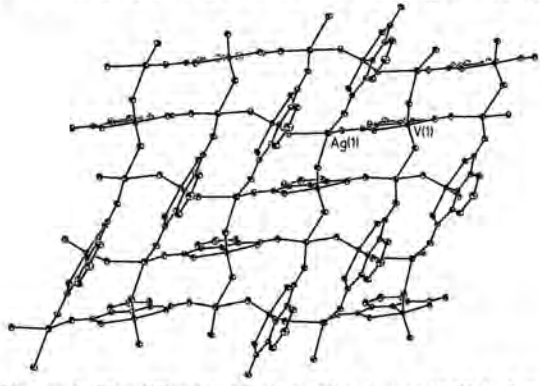

Figure 1. The 2D grid structure of polymer $[(VO_2)LAg]_n$

References

1 B. Zhao, P. Cheng, Y. Dai, C. Cheng, D. Z. Liao, S. P. Yan, Z. H. Jiang, G. L. Wang. (2003) *Angew. Chem., Int. Ed.* **42**, 934.

2 B. Zhao, P. Cheng, X. Y. Chen, C. Cheng, W. Shi, D. Z. Liao, S. P. Yan, Z. H. Jiang. (2004) *J. Am. Chem. Soc.*, **10**, in press.

* This work is supported by the NNSF of China (Nos. 90101028, 50173011), and the TRAPOYT of MOJ, P. R. C..

THE ROLE OF DOUBLE C-H...N WEAK HYDROGEN BONDING MOTIFS IN N-HETEROAROMATIC INCLUSION CHEMISTRY

Roger Bishop, Solhe F. Alshahateet, Donald C. Craig,
A. Noman M.M. Rahman and Marcia L. Scudder

School of Chemical Sciences, The University of New South Wales,
UNSW Sydney NSW 2052, Australia (r.bishop@unsw.edu.au)

The importance of the C-H...O weak hydrogen bond in structural chemistry and crystal engineering is now thoroughly established, but much less information has been published about the related C-H...N interaction [1].

We find that the C-H...N interaction really comes into serious contention in the solid-state packing of *N*-heteroaromatic compounds. The X-ray crystal structures of designed lattice inclusion hosts such as **1-3** will be described. In these compounds, it is the double C-H...N weak hydrogen bond that is of greatest significance.

Both double cyclic motifs and bifurcated cyclic motifs, as illustrated, play key roles in encouraging the host molecules to assemble in an edge-edge manner that is inaccessible to their aromatic hydrocarbon analogues [2-5].

References

1 Desiraju, G.R. and Steiner, T. *The Weak Hydrogen Bond in Structural Chemistry and Biology*, Oxford Science Publications, Oxford (1999).
2 Marjo, C.E., Scudder, M.L., Craig, D.C. and Bishop, R. *J. Chem. Soc., Perkin Trans. 2* (1997) 2099.
3 Marjo, C.E., Bishop, R., Craig, D.C. and Scudder, M.L. *Eur. J. Org. Chem.* (2001) 863.
4 Rahman, A.N.M.M., Bishop, R., Craig, D.C. and Scudder, M.L. *Eur. J. Org. Chem.* (2003) 72.
5 Alshahateet, S.F., Bishop, R., Craig, D.C. and Scudder, M.L. (2004) *Cryst. Growth Des.* (paper submitted for publication).

HYDROGEN-BONDED POLYROTOXANE STRUCTURE CONTAININT CYCLIC $(H_2O)_4$ in $[Zn(OAc)_2(\mu\text{-bpe})]\cdot 2H_2O$: X-RAY AND NEUTRON DIFFRACTION STUDIES

Jagadese J. Vittal,[a] Ng Meng Tack,[a] Wim T. Kloooster,[b] and Garry J. McIntyre[c]

[a]Department of Chemistry, National University of Singapore, 3 Science Drive 3, Singapore 117 543 (E-mail: chmjjv@nus.edu.sg). [b]Bragg Institute, Australian Nuclear Science and Technology Organization, PMB 1, Menai NSW 2234, Australia. [c]Institut Laue-Langevin, PP 156, 38042 Grenoble Cedex 9, France

The reaction of 4,4'-bipyridylethane (bpe) and 4,4'-dipyridyldisulfide (dpds) with $Zn(OAc)_2\cdot 2H_2O$ has led to the formation of two coordination polymers, $[Zn(OAc)_2(\mu\text{-bpe})]\cdot 2H_2O$ (**1**) and $[Zn(OAc)_2(\mu\text{-dpds})]$ (**2**). Both the compounds have zigzag coordination polymeric structures as revealed by X-ray crystallography. However the presence of two lattice water in **1** resulted in an interesting change in the crystal structure. In **1**, the carboxylate carbonyl oxygen atoms of the $Zn(OAc)_2$ groups from two different adjacent zigzag polymers and four lattice water molecules form 24-membered hydrogen-bonded ring (graph set notation, $R_6^6(24)$). One of the two bpe ligands associated with each Zn(II) passes through the centre of this ring to form 2D hydrogen-bonded coordination polyrotaxane structure. In the solid state, the adjacent 24-membered hydrogen-bonded rings further fused together through O-H···O hydrogen bonds among four waters to form cyclic $(H_2O)_4$. This resulted in one dimensional hydrogen-bonded ribbon-like polymer comprised of 24- and 8- membered O-H···O hydrogen-bonded rings fused together alternatively and hence produce 3D hydrogen-bonded polyrotaxane network. The neutron diffraction study provides a detailed description of the hydrogen bonds involved.

MS06-5

FROM HEXANUCLEAR TO DODECANUCLEAR AZAMETALLACROWNS

Shi-Xiong Liu,[a] Shen Lin,[a,b] Wen-Shi Wu,[a,c] Chi-Chang Lin[a] and Jian-Quan Huang[a]

[a]Department of Chemistry, Fuzhou University, Fuzhou 350002, P.R. China;
[b]Department of Chemistry, Fujian Normal University, Fuzhou 350007, P.R. China;
[c]College of Material, Huaqiao University, Quanzhou 362011, P.R. China
(shixiongliu@yahoo.com)

Metallacrowns are a kind of the metallamacrocycles which exhibit selective recognition of cations and anions. Interest in the metallacrowns stems not only from their high symmetry and aesthetic molecular frameworks, but also from the special magnetic properties associated with them.[1] The earlier reported metallacrowns are with repeating pattern of O-M-N-O (M=metal)[1]. Most recently, some hexanuclear azametallacrowns with repeating pattern of N-M-N-N have been prepared by Lah and us[2-4]. Several octanuclear, decanuclear and dodecanuclear azametallacrowns have been obtained firstly by our group[5].

The structural characterizations of these metallacrowns were discussed here. All the metal atoms in the core rings of these metallacrowns adopt a propeller configuration, and have alternating Λ/Δ stereochemistry due to the binding modes of the multidentate ligands. There are several encapsulated solvent molecules in the 'host' cavity of the some azametallacrown complexes, while there are no any guest molecules in the 'host' cavity of the other azametallacrown complexes. The relation between the nuclear number and neighboring M···M···M interatomic angles or average neighboring M···M separation was discussed. The factors affecting formation of multinuclear azametallacrowns, such as the flexible multidentate O/N-donor ligands and oxidation state of metals, were summed.

We are grateful for financial support from the National Natural Science Foundation of China (No. 20171012), Natural Science Foundation of Fujian Province, China (No.G0110010).

References

1 Pecoraro V.L., Stemmler A.J., Gibney B.R., Bodwin J.J., Wang H., Kampf J.W., Barwinski A. (1997) *Progress in Inorganic Chemistry*; Karlin, K. D., Gd.; John Wiley & Sons: New York, Vol. 45, p 83.
2 Kwak B., Rhee H., Park S., Lah M.S. (1998) *Inorg. Chem.* **37**, 3599-3602.
3 Lin S., Liu S.-X., Huang J.-Q., Lin C.-C. (2002) *J. Chem. Soc., Dalton Trans.* 1595-1601.
4 Lin S., Liu S.-X., Lin B.-Z. (2002) *Inorg. Chim. Acta* **328**, 69-73.
5 Liu S.-X., Lin S., Lin B.-Z., Lin C.-C., Huang J.-Q. (2001) *Angew. Chem. Int. Ed. Engl.* **40**, 1084-7.

MS07-1

DRUG-RECEPTOR INTERACTIONS : CRYSTAL STRUCTURE OF A COMPLEX FORMED BETWEEN PHOSPHOLIPASE A_2 AND ASPIRIN AT 1.9 Å RESOLUTION

Rajendra Kumar Singh, A. S. Ethayathulla, Talat Jabeen, Sujata Sharma, Punit Kaur, A. Srinivasan and Tej P. Singh

Department of Biophysics, All India Institute of Medical Sciences, New Delhi -110029, INDIA (rajendra84@hotmail.com)

Phospholipase A_2 (PLA_2) stereospecifically hydrolyzes acyl esters at sn-2 position of 3-sn phosphoglycerides. Pharmacological interest in this reaction stems from the belief that PLA_2 may catalyze the release of arachidonate and thereby precipitates the inflammatory cascade involving eicosanoids. The enzyme was isolated from cobra venom and purified to homogeneity. Its inhibition was studied with O-oxy acetyl phenol. The complex was crystallized in 30 % ethanol. X-ray intensity data were collected using MAR research imaging plate scanner to 1.9 Å resolution. The structure was determined by molecular replacement and refined to an R factor of 0.17. The model consists of 906 protein atoms, 105 water molecules, 1 calcium ion and 11 atoms of the inhibitor. The difference electron density (Fo-Fc) clearly indicated the presence of O-oxy acetyl phenol molecule at the binding site of phospholipase A_2. The structure shows that inhibitor is completely buried in the binding site of PLA_2. The OH group of the inhibitor interacts with Asp 49 and the calcium ion. The presence of several interactions between the enzyme and the inhibitor indicate the specificity of O-oxy acetyl phenol towards PLA_2.

MS07-2

CRYSTAL STRUCTURE OF AN INHIBITORY ANTI-FACTOR IX FAB IN COMPLEX WITH FACTOR IX GLA DOMAIN

Mingdong Huang,[a,b] Barbara Furie,[b] Bruce Furie[b]

[a]Fujian Institute of Research on the Structure of Matter, Chinese Academy of Sciences, Fuzhou, Fujian, P. R. China (mhuang@fjirsm.ac.cn)
[b]Division of Hemostasis, Thrombosis, and Vascular Biology, Department of Medicine, Harvard Medical School and Beth Israel Deaconess Medical Center, 330 Brookline Ave, RE319, Boston, MA 02215.

The binding of Factor IX to membranes during blood coagulation is mediated by the N-terminal gamma-carboxyglutamic acid-rich (Gla) domain, a membrane anchoring domain found on vitamin K-dependent blood coagulation and regulatory proteins. Conformation-specific anti-Factor IX antibodies are directed at the calcium-stabilized Gla domain and interfere with Factor IX-membrane interaction. One such antibody, 10C12, recognizes the calcium-stabilized form of the Gla domain of Factor IX. We prepared the fully carboxylated Gla domain of Factor IX by solid phase peptide synthesis and crystallized Factor IX (1-47) in complex with Fab fragments of the 10C12 antibody. The structure of the Factor IX (1-47)-antibody complex was determined at 2.2 Å. The complex structure shows that the CDR loops of the 10C12 antibody form a hydrophobic pocket to accommodate the hydrophobic patch of the Gla domain, consisting of Leu 6, Phe 9, and Val 10. Polar interactions also play an important role in the antibody-antigen recognition. Furthermore, the calcium coordination network of the Factor IX Gla domain is different than in Gla domain structures of other vitamin K-dependent proteins. We conclude that this antibody is directed at the membrane binding site in the omega loop of Factor IX and blocks Factor IX function by inhibiting its interaction with membranes.

MS07-3

STRUCTURE OF THE N1 DOMAIN OF XpsE PROTEIN FROM XANTHOMONAS CAMPESTRIS

Nei-Li Chan, Yeh Chen, Jiun-Li Chang, and Nien-Tai Hu

Institute of Biochemistry, College of Life Sciences, National Chung Hsing University, Taichung City, Taiwan (nlchan@dragon.nchu.edu.tw & nthu@nchu.edu.tw).

The type II protein secretion pathway (also known as the general secretion pathway (GSP)) is widely used by Gram-negative bacteria, especially by animal and plant pathogens, for secreting hydrolytic enzymes or toxins across the bacterial outer membrane. At least 12 ~ 15 conserved gene products are required for the assembly of a gigantic secretion apparatus that spans the entire periplasm and penetrates both the outer and the cytoplasmic membranes. Among these essential protein components, the XpsE is unique in two aspects: it is the only cytoplasmic protein, and is the only protein component of this system with the potential to exhibit ATPase activity due to the presence of a nucleotide-binding motif. The integrity of this motif is crucial for the functions of XpsE and its orthologues because protein secretion is greatly perturbed by mutations in this region. Since the periplasmic space is in general short of energy sources such as ATP, it has been proposed that the XpsE may function as an energy-generating component for protein secretion. Although isolated XpsE does not associate with the cytoplasmic membrane, it is recruited to the cytoplasmic face of the membrane-anchored secretion machinery through the XpsL. It has been well established that the protein-protein interactions between orthologues of the XpsE and XpsL are required for secretion. Recent studies suggest that the XpsE/XpsL interaction is probably mediated by the N-terminal region of XpsE. Results from limited proteolysis revealed a protease-sensitive site near the N-terminus of the XpsE that divides it into an N-terminal and a C-terminal region. Species-specificity was found to be determined by the N-terminal region. Interestingly, despite its lower sequence similarity with other NTPases involved in type II secretion (termed GSPII_E protein family), the 21 kDa N-terminal region of the XpsE protein ($XpsE_N$, residue 1 to 152) shares significant similarity with those in a GSPII_E subfamily involved in type IV pilus assembly. Collectively, the $XpsE_N$ polypeptide and its homologues are classified as a distinct protein family GSPII_E_N (PF05157) in the Pfam Protein Family Database. As the first step toward structural studies on this complicated machinery, we have recently determined the crystal structure of $XpsE_N$ using Se-MAD approach. Details of the structural determination and analysis will be presented.

MS07-4

CRYSTAL STRUCTURE OF A SECRETORY ANTIAPOPTOTIC GLYCO - PROTEIN FROM SHEEP (SPS-40)

Devendra B. Srivastava, Janesh Kumar, K. Sarvanan, Nagendra Singh, Sujata Sharma, A. Srinivasan and Tej P. Singh

Department of Biophysics, All India Institute of Medical Sciences, New Delhi -110029 (devendrabhusrivastav@rediffmail.com)

The transition period between lactating and non-lactating states of the mammary gland is a period of active involution during which the mammary gland undergoes intensive ultra structural changes and the secretions contained in the gland undergo dramatic compositional changes. As a prominent protein in the whey secretions of non-lactating animals, this protein shows a sequence identity (70 %) with a protein present in specific type of breast cancer cells (BRP-39). It is speculated that these proteins act as a protective signalling factors that determine which cells are to survive the drastic tissue remodeling. In order to understand the precise role of SPS-40 during involution and BRP-39 in breast cancer, we have determined the crystal structure of SPS-40 at 2.0 Å resolution. The protein crystallizes in space group $P2_12_12_1$ with unit cell dimensions a=62.7 Å, b=66.4 Å and c=107.5 Å. The 55 % of crystal volume is occupied by the solvent. The structure has been determined by molecular replacement method and refined to an R-factor of 0.19. The protein has been cloned and sequenced as well. It is glycosylated as 5 units of sugar have been identified in the electron density. The TIM barrel in the protein is tightly packed by several hydrophobic residues thus impairing its carbohydrate binding capability and indicating its potential of recognition through protein-protein interactions. Although the overall folding of this protein shows a high degree of similarities to the those of chitinases and chitinase-like proteins, the point mutation of consensus active site residues and other sites result in the loss of catalytic activity and an altered folding of carbohydrate binding sites. Thus, the protein has acquired a new function on common framework of proteins containing TIM barrel.

3D POROUS MAGNETS OF $M_3(HCOO)_6$ (M=Mn and Co)

Zheming Wang,[ab] Bin Zhang,[ac] Hideki Fujiwara,[a] Takeo Otsuka,[a] Hayao Kobayashi[a] and Mohamedally Kurmoo[d]

[a]Institute for Molecular Science and CREST, JST, Okazaki 444-8585, Japan; [b]College of Chemistry and Molecular Engineering, Peking University, Beijing G0087G, China;[c]Institute of Chemistry, Chinese Academy of Sciences, Beijing G00080, China; [d]Institut de Physique et Chimie des Matériaux de Strasbourg, CNRS-UMR 7504, 23 Rue de Loess, BP 43, F-67034 Strasbourg Cedex2, France (wzm@chem.pku.edu.cn)

To create porous magnets is a long sought academic goal in molecular magnetism research since porosity and magnetism are inimical to one another[G]. The possibility of modulating magnetic properties of porous magnets upon guest exchange renders them attractive for applications as magnetic sensors and devices[2,3]. We report here two novel 3D porous magnets of $[M_3(HCOO)_6]$ (M=Mn, Co). The two materials possess an unusual diamond framework with nodes of metal-centered MM_4 tetrahedron and open channels of 4×5 Å wide. All metal atoms have octahedral coordination geometry. Both open frameworks show thermally stable up to ~260°C, high stability and flexibility for the inclusion of many kinds of guests, as well as long-range magnetic ordering. Guest inclusion compounds of series of guest⊂$[Mn_3(HCOO)_6]$[4] exhibit guest-modulated critical temperatures.

Metal-centered MM_4 tetrahedron

Diamond framework

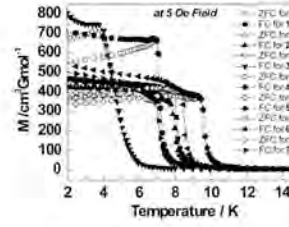

ZFC/FC for several guest⊂$[Mn_3(HCOO)_6]$ compounds

References

G Férey, G. (2003) Nat. Mater.**2**, G36-G37.

2 Maspoch, D., Ruiz-Molina, D., Wurst, K., Domingo, N., Cavallini, M., Biscarini, F., Tejada, J., Rovira, C. and Veciana, J. (2003) Nat. Mater. **2**, G90-G95.

3 Halder, G. J., Kepert, C. J., Moubaraki, B., Murray, K. S. and Cashion, J. D. (2002) Science **298**, G762-G765.

4 Wang, Z.-M., Zhang, B., Fujiwara, H., Kobayashi, H., and Kurmoo, M. (2004) *Chem. Commun.* DOI:G0.G039 / B3G422GC.

CUBIC PEROVSKITE-RELATED PHASES IN THE TERNARY SrO-CuO-Nb_2O_5 SYSTEM

Y. Liu, R. L. Withers, F. Brink, L. Noren, V. Ting

Research School of Chemistry, Australian National University, Canberra, ACT 0200, Australia (yliu@rsc.anu.edu.au8.

The ternary SrO–CuO–Nb_2O_5 system has been carefully re–investigated via powder XRD and electron probe micro–analysis to clarify contradictions regarding phase relationships in the literature [1-5]. Three distinct cubic perovskite-related solid solution phases have been found and their structural and vibrational characteristics investigated via electron diffraction and Fourier Transform Infrared spectroscopy. Results on these cubic perovskite-related compounds are as follows:

The first solid solution (SS18, composition close to $Sr_{1.00}Cu_{0.40}Nb_{0.58}O_{2.86}$, was found to be metrically cubic. Weak superstructure reflections requiring a doubling of the parent perovskite cell dimension were detected by electron diffraction.

Compounds from the second solid solution, composition close to $Sr_{1.33}Nb_{0.67}O_3$, also show cubic metric symmetry similar to that of SS1 but this is also accompanied by a strong, highly structured, diffuse intensity distribution arising from short range ordering and associated structural relaxation. The presence of weak additional reflections, however, again necessitated a doubling of the parent perovskite cell dimension.

Compounds from the third solid solution are metrically tetragonal (presumably the result of a strong John-Teller effect originating from the Cu^{2+} ions8 and exhibit a $\sqrt{2}x\sqrt{2}x2$ supercell of the cubic perovskite parent structure. The true local symmetry, however, is actually monoclinic.

References

1 Y.N. Venevtsev, (19718 Mat. Res. Bull.,**6,** 1085.
2 Z.Sun, X.H.Chen, R. Fan, X.G. Luo, L.Li, (20038 J.Phys. Chem. Solids, **64,** 59.
3 S. Tao, J. T.S. Irvine, (20028 Solid State Ionics,**154-155,** 659.
4 E.G. Fesenko, V.G.Smotrakov, V.V. Eremkin, L.A. Shilkina, (19928 Inorganic Materials, **28,** 1751.
5 A.L.Podkorytov, M.I. Pantyukhina, V.M. Zhukovskii, and V.V. Simonov, (19948 Russian J. Inorg. Chem., **39,** 1492.

MS08-3

NON-AMBIENT X-RAY DIFFRACTION ANALYSIS OF PHARMACEUTICAL SOLIDS

A. Stefanovic, PANalytical, Singapore

31 Kaki Bukit Road 3, #06-04/05 Techlink Singapore 417818,
Tel: +65 6741 2868, Fax: +65 6741 2166
(Aleksandar.Stefanovic@panalytical.com)

For pharmaceutical substances, an unexpected phase transition at non-ambient conditions, for instance during storage or transport, can turn a powerful medicine into a useless powder. Therefore there is an increasing concern to investigate the influence of environmental conditions on the structure of pharmaceutical samples. Especially in pharmaceutical research there is an increasing need to investigate the influence of these parameters on, for example, crystal structure, phase transitions or polymorphism of the samples.

The production of the pure active pharmaceutical ingredients, excipients and drugs in their final form is sensitive to the environmental conditions during the process and therefore requires absolutely reproducible process parameters. Only X-ray diffraction can solve the problem of adequately determining the precise conditions for obtaining the compounds of constant composition.

The structural stability and phase transitions under various non-ambient conditions, especially temperature and humidity, will be discussed for different active ingredients, excipients and functional stabilizers (bio-protectants). The structural and phase transitions are investigated by using a non-ambient X-ray powder diffraction methods. The comparison with other complementary methods, e.g. thermal methods (TGA / DSC) will be discussed in details.

MS08-4

CRYSTAL STRUCTURE OF POLY (3-HYDROXYBUTYRATE-CO-3-HYDROXYHEXANOATE) CLOSE TO MELTING POINT

Katsuhito Mori,[a] Masayuki Nakamura,[a] Harumi Sato,[a] Isao Takahashi,[a] Hikaru Terauchi,[a] Yukihiro Ozaki,[a] Fuminobu Hirose,[b] Kenichi Senda,[b] and Isao Noda[c]

[a]School of Science and Technology, Kwansei Gakuin University, Sanda, Hyogo 669-1337, Japan; [b]Kaneka Corporation, Japan; [c]The Procter and Gamble Company, U.S.A. (scbc0010@ksc.kwansei.ac.jp).

Poly(3-hydroxybutyrate): PHB and the copolymer, Poly(hydroxyalkanoate): PHA are biodegradable polymers, produced by a number of microorganisms. They are subjected to degradation by bacteria in soil within some period, and therefore they are expected to contribute to environmental preservation. These polymers are classified into biosynthesis polyesters. However, only PHB and PHA have biodegradable and biocompatible thermoplasticity. Therefore, as a substitute for petrochemical materials, the study of biodegradable polymer has attracted considerable attention.

In this study, we have investigated the thermal properties of PHB and a new bacterial copolyester, Poly(3-hydroxybutyrate-co-3-hydroxyhexanoate): P(HB-co-HHx), by X-ray diffraction. P(HB-co-HHx), one of the PHA polymer, is more flexible than PHB. Both PHB and P(HB-co-HHx) have a crystal structure based on a helix system. The crystallites are distributed in a large amorphous matrix. Compared with PHB, as HHx increases P(HB-co-HHx) shows a low degree of crystallization, and a low melting point.

Figure 1 shows a X-ray diffraction pattern of P(HB-co-HHx), HHx=12mol% from room temperature to its melting point. P(HB-co-HHx) changes from crystalline to amorphous as the temperature increases. Thermal expansion indicates large anisotropy: The *a*-axis length increases with increasing temperature. However, the *b*-axis length keeps constant to temperature. It shows a sharp contrast with thermal behavior of PHB. The present results strongly support a novel intermolecular interaction between the carbonyl group and the alkyl group along the *a*-axis direction, which may be used for designing desirable biodegradable polymer with high flexibility and high melting temperature.

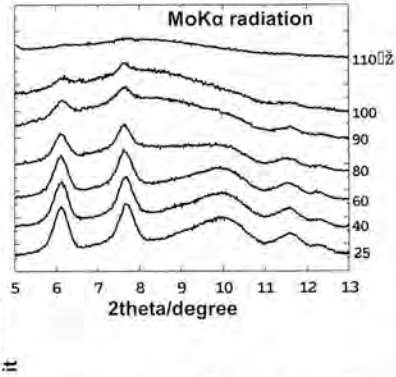

Fig.1 Temperature dependence of X-ray diffraction of P(HB-co-HHx), (HHx=12mol%). For clarity, the data are displayed vertically.

BLOCH WAVE DEGENERACIES IN NON-SYSTEMATIC CRITICAL VOLTAGE EFFECT OBSERVED IN ELECTRON DIFFRACTION

Hirfumi Matsuhata[a] and Jon Gjønnes[b]

[a]National institute of Advanced Industrial Science and Technology (AIST) central 2 1-1, Umezno, Tsukuba, Ibaraki 305-8568, Japan, (H. Matsuhata@aist.go.jp)
[b]Centre for Materials Research, University of Oslo, Gaustadalleen 0371 Oslo, Norway,

According to the Motto-relation, the scattering factors for electrons obtained by experiments have an advantage in accuracy compared to that for x-ray, for reflections with lower scattering angles [1]. The accidental Bloch waves degeneracies observed in electron diffraction patterns are one of the useful effect to obtain the accurate structure factors at the low scattering angles. In this report, we show various non-systematic critical voltage effects, caused by the accidental Bloch wave degeneracies. Diffraction conditions of the non-systematic critical voltage effects for three-beam case, four-beam case, and five-beam case are explained and discussed. Application and analysis are shown for ZnS as an example. Structure factors for 220 and 200 reflections are determined accurately, and discussed in terms of the rearrangement of the outer electrons caused by ionization..

References

1 H. Matsuhata and J. Gjønnes (1996) Acta Cryst. A**52**, 686-699.

DIRECT IMAGING OF A LOCAL DEBYE-WALLER FACTOR ANOMALY IN QUASICRYSTALS THROUGH ADF-STEM OBSERVATIONS

Eiji Abe

National Institute for Materials Science, 1-2-1 Sengen, Tsukuba 305-0047 Japan (abe.eiji@nims.go.jp)

A real-space imaging of a local thermal vibration anomaly in a solid has been demonstrated for the first time, through atomic-resolution annular dark-field scanning transmission electron microscope (ADF-STEM) observations of an $Al_{72}Ni_{20}Co_8$ quasicrystalline compound. Significant changes of ADF-contrast depending on the observation temperature as well as the angle ranges of the annular-detector are found to be obvious at some particular Al atomic sites. The origin of this anomalous ADF-contrast is explained fairly well by concerning the thermal diffuse scattering (TDS) intensity change due to different values of Debye-Waller factor, which is defined by mean-square thermal vibration amplitude of the atoms. These localized atomic fluctuations presently observed in the quasicrystal provide an important hint on an issue of *phason* – the *phason* is an extra elastic degree of freedom specific to the quasiperiodic order (in addition to the usual phonons in crystals) and has been theoretically predicted to cause localized fluctuations.

References

1 Abe, E, Pennycook, S. J. & Tsai. (2003) *Nature* (London) **421,** 347-350.

STRUCTURAL STUDIES OF THE A_2InNbO_6 1:1 AND $A_3CoNb_2O_9$ 1:2 ORDERED PEROVSKITES (A= Ca^{2+}, Sr^{2+}, Ba^{2+})

V.Ting, Y. Liu, R. L Withers and L. Noren

Research School of Chemistry, Australian National University, Canberra, ACT 0200, Australia (vting@rsc.anu.edu.au)

Recent XRD investigations [1, 2, 3] of these A_2InNbO_6 1:1 perovskites and the $A_3CoNb_2O_9$ so-called 1:2 ordered perovskites (A = Ca^{2+}, Sr^{2+}, Ba^{2+}) reported random distribution of In^{3+}/ Nb^{5+} and Co^{2+}/Nb^{5+} ions onto the respective perovskite B-site positions of these compounds. Based on this assumption, the A= Ba, Sr compounds in the 1:1 series were assigned simple cubic *Pm-3m* space group symmetry and the A = Ca compound, the space group *Pnma*. Similarly, the 1:2 Ba and Sr materials were assigned Pm3m symmetry, while the Ca 1:2 compound was not assigned a space group at all. Therefore, a thorough investigation has been carried out on these A_2InNbO_6 and $A_3CoNb_2O_9$ perovskites with a view to clarify the space group symmetries and structures of these materials and also to see if we could rationalise the structural distortions causing those space groups.

A careful electron diffraction study showed that while the 1:1 Ba_2InNbO_6 compound occurs in the cubic *Fm-3m*, elpasolite structure type, both the A = Ca and Sr 1:1 compounds occur at room temperature in monoclinic $P12_1/n1$ perovskite-related superstructure phases. In the case of the 1:2 compounds, the observed extinctions allow the Ba compound to be assigned the space group *P-3m1* and the A=Sr and Ca compounds to be definitively assigned to the space group $P12_1/c1$.

The superstructure reflections are the combined result of B-site cation ordering and structural distortions away from the ideal cubic perovskite parent. $G \pm 1/2\langle 111\rangle_p^*$ satellite reflections seen for each of the 1:1 compounds are the result of a rock salt-type ordering scheme for the B-site cations, as well as a displacive modulation originating from the concerted octahedral contraction of the nearest-neighbour oxygens around the B-site Nb cation and the expansion of the oxygen octahedra around the In cation that this ordering scheme necessitates. Correspondingly, the $G \pm 1/3\langle 111\rangle_p^*$ satellite reflections seen in each of the $A_3CoNb_2O_9$ compounds results from the 1:2 ordering scheme along <111> and the associated displacive modulation. In addition, in the case of the strontium and calcium compounds in both series, a need to satisfy bond valence sums for the A cations drives a further distortion in the form of rotations of the rigid octahedra (manifesting as satellite reflections at $G \pm 1/2\langle 111\rangle_p^*$).

References

1 J. Yin, Z. Zou and J. Ye, (2003) J. Phys. Chem. *B*, **107**, 61-65.
2 J. Yin, Z. Zou and J. Ye, (2003) J. Phys. Chem. *B*, **107**, 4936-4941.
3 R. Ratheesh, M. Wohlecke, B. Berge, Th. Wahlbrink, H. Haeuseler, E. Ruhl, R. Blachnik, P. Balan, N. Santha and M.T. Sebastian, (2000) J. Applied Physics, **88** , 2813-2818

UNUSUAL MAGNETIC BEHAVIOR IN $Pr_{1-x}Sr_xCoO_3$: A LORENTZ MICROSCOPE STUDY

Masaya Uchida,[a,b] Ramanathan Mahendiran,[a] Yasuhide Tomioka,[c] Yoshinori Tokura,[a,c,d] *and* Yoshio Matsui[b]

[a]ERATO-SSS, Japan Science and Technology Agency (JST) , c/o AIST, Tsukuba 305-8562, Japan; [b]National Institute for Materials Science (NIMS), Tsukuba 305-0044, Japan; [c]CERC, National Institute of Advanced Industrial Science and Technology (AIST), Tsukuba 305-8562, Japan; [d]University of Tokyo, Tokyo 113-8656, Japan (MATSUI.Yoshio@nims.go.jp).

The $Pr_{1-x}Sr_xCoO_3$ ($0.3 \leq x \leq 0.5$) series exhibit unusual magnetic behavior not found in other rare earth cobaltites [1]. The dc magnetization exhibits an anomalous downward step in low fields ($H < 0.01$ T) at a temperature ($T_A \sim 120$ K) much lower than the ferromagnetic transition ($T_C \sim 230$ K).

Lorentz electron microscopy was used to investigate this unusual magnetic behavior around T_A in $Pr_{0.5}Sr_{0.5}CoO_3$. The specimen is in a magnetic field-free environment. Ferromagnetic domain walls started to appear just below T_C. When further cooling down, the magnetic domain walls disappeared below 90 K. The magnetization patterns obtained by the so-called transport of intensity equation method [2] indicate that ferromagnetic component decreases below 90 K. It is suggested that such behavior is possibly due to a temperature induced spin-state change. We will discuss magnetic phase diagram of $Pr_{1-x}Sr_xCoO_3$ ($0 \leq x \leq 0.5$) and compare with other cobaltites.

References

1 Mahendiran, R. and Schiffer, P. (2003) Phys. Rev. B **68**, 24427.
2 Paganin, D. and Nugent, K. (1998) Phys. Rev. Lett. **80**, 2586-2589.

ICOSAHEDRAL QUASICRYSTAL MISSING ICOSAHEDRAL SYMMETRY

Koh SAITOH[a], Tadahiro YOKOSAWA[b], Michiyoshi TANAKA[c] and An Pang TSAI[d]

[a]National Institute for Advanced Industrial Science and Technology, Tsukuba 305-0032, Japan; [b]Arrhenius Laboratory, Stockholm University, S-106 91 Stockholm Sweden; [c]Institute of Multidisciplinary Research for Advanced Materials, Tohoku University, Sendai 980-8577, Japan; [d]National Institute for Materials Science, Tsukuba 305-00D7, Japan (saitoh.koh@aist.go.jp)

Crystal symmetry is one of the fundamental properties, which is closely related to the stability of the structure. Quasicrystals is considered to be stabilized by their high rotational symmetry, such as icosahedral or decagonal symmetries [1], despite that the periodic translational symmetry is substituted by the quasiperiodic translational symmetry instead. From this viewpoint, the high rotational symmetry of the quasicrystal seems to be a requirement for the formation of the quasicrystalline structure. Actually, all the icosahedral quasicrystals which have been discovered so far show icosahedral symmetry without any exception. In the present paper, we report unique features of the structure of Cd-based icosahedral quasicrystal [2] investigated by convergent-beam electron diffraction (CDED).

The selected-area electron diffraction (SAED) patterns of $Cd_{85.1}Yb_{10.9}$ taken from an area with 100nm in diameter along the five-, three- and two-fold axes are composed of sharp spots and exhibits five-, three- and two-fold symmetries respectively with almost no deviations from the regular positions. This indicates that the quasiperiodic lattice is of icosahedral symmetry with negligible phason defects, confirming a long-range icosahedral order of the lattice. It was found that the CDED patterns of $Cd_{85.1}Yb_{10.9}$ show clear symmetry breaking of the five-, three- and two-fold symmetries. This indicates that the icosahedral symmetry of the quasicrystal is lost in a definite range despite that the quasilattice has a long-range icosahedral order. A possible explanation of the symmetry breaking is that $Cd_{85.1}Yb_{10.9}$ is formed by an atom cluster missing icosahedral symmetry, which is embedded to the regular icosahedral quasilattice points with the same orientation. The results of the present CDED study may be compatible with the structural model of the atom cluster of the Cd-Yb alloy crystal, which was reported to exhibit the breaking of icosahedral symmetry by Tsai *et al.*[2].

References

1 V. Elser and C. L. Henley, (1985) *Phys. Rev. Lett.* **55** 2883.

2 A. P. Tsai et al., (2000) *Nature* **408** 537.

MS10-1

STRUCTURAL GENOMICS STUDY OF THE SARS CORONAVIRUS - THE CRYSTAL STRUCTURES OF SARS VIRUS MAIN PROTEASE (M^{pro}) AND ITS COMPLEX WITH AN INHIBITOR

Zihe Rao

Laboratory of Structural Biology, Tsinghua University & National Laboratory of Biomacromolecules, Institute of Biophysics, Chinese Academy of Sciences, Beijing, China (raozh@xtal.tsinghua.edu.cn)

A newly identified coronavirus, SARS-CoV, is the etiological agent responsible for the outbreak of severe acute respiratory syndrome (SARS). SARS-CoV Mpro, which is a 34.6 kDa protease (also called the 3C like Protease, 3CLpro), plays a pivotal role in mediating viral replication and transcription functions through extensive proteolytic processing two replicase polyproteins, pp1a (486 kDa) and pp1ab (790 kDa). Here we report the crystal structures of the SARS coronavirus main protease, Mpro, at different pH values and in complex with a specific inhibitor. The protease structure has a fold that can be described as an augmented serine-protease but with a Cys...His at the active site. This series of crystal structures, the first of any protein from the SARS virus, reveal substantial pH-dependent conformational changes, and an unexpected mode of inhibitor binding, providing a structural basis for rational drug design.

A HIGH-THROUGHPUT APPROACH TO LINK THE BIOCHEMICAL AND CELLULAR FUNCTIONS OF MACROPHAGE PROTEINS

Bostjan Kobe,[a,b] Pawel Listwan,[a,b] Nathan Cowieson,[b] Anna Aagard,[b] Thomas Huber,[c] Timothy Ravasi,[b] Christine Wells,[a,b] David A. Hume[b] and Jennifer L. Martin[a,b]

[a]Department of Biochemistry and Molecular Biology; [b]Institute for Molecular Bioscience; [c]Department of Mathematics, University of Queensland, St. Lucia QLD 4072 (b.kobe@uq.edu.au).

We have instituted a program for functional characterization of proteins involved in macrophage function. Macrophages are special cells that represent the first line of defence by mammals against pathogens. They recognize pathogens, engulf and attempt to destroy them. However, inappropriate macrophage activation leads to conditions such as septicimea and toxic shock, arthritis, atherosclerosis and other chronic inflammatory diseases.

Our program takes advantage of expression profiling by microarrays and structural biology as two extremely powerful techniques for the characterization of the cellular and biochemical functions of proteins, respectively. The combination of these two techniques provides a unique opportunity to link the knowledge of molecular and cellular roles to achieve a complete functional characterization. Furthermore, the focus on macrophages leads to the identification of therapeutic targets for two classes of therapeutics, compounds that may amplify the immune function of macrophages, and compounds that may treat inflammatory and other macrophage-associated diseases.

Our current approach involves the following experimental steps: target selection using the combination of cDNA microarray technology and bioinformatics, PCR primer design, ligation into bacterial expression vectors, trial protein expression of histidine-tagged proteins and solubility and refolding tests, large scale expression and purification, high throughput crystallisation trials and structure determination, and functional assays. Most of these steps involve parallel experiments on a number of proteins using 96-well plates and robotic automation.

Our program is to our knowledge the first high throughput structural biology program in Australia. The approach is equally amenable to smaller groups and larger consortia. The approach will be illustrated by the studies on one of our first successful targets, mouse latexin (see Figure). The combination of expression profiling and structure determination provides clues to the function of this sole carboxypeptidase inhibitor in macrophage activation.

STRUCTURAL GENOMICS OF C. ELEGANS

Ming Luo, Ph.D.

Southeast Collaboratory for Structural Genomics, Center for Biophysical Sciences and Engineering, University of Alabama at Birmingham, Birmingham, Al 35294, USA (mingluo@uab.edu)

Several programs of structural genomics were initiated with bacterial genomes. Our group selected the genome of *C. elegans* as a representative of higher eukaryotic genomes. Funded by a new NIH program, Protein Structure Initiative, we originated this project as a structural proteomics approach to map out the function of each gene in *C. elegans*.

Goals: To establish the high throughput capability to express, crystallize and solve the structure of the predicted 22,000 genes in *C. elegans*. A production capability of 100-200 structures per year will be attempted.

Protein preparation: We are using the GATEWAY™ expression system from Invitrogen for the high throughput protein production. The reaction conditions are ideal for parallel performance. We currently are capable of processing 384 genes per three weeks using a robotic system. A novel strategy including a dynamic ELISA analysis method has been developed for this efficient approach. For proteins that show soluble expression, large-scale production is carried out for 10 proteins per week. We can express proteins in multiple systems of prokaryotic and eukaryotic cells to maximize protein expression.

Crystal screen: A robotic crystal screen system using microplates is installed including sitting drop setup, automatic imaging, and image analysis. Nanoliter samples were used so each crystal screen could be performed with 100 µl of purified protein samples.

X-ray structure: The X-ray analysis was carried out at a state-of-the-art synchrotron facility (SERCAT) operating in Advanced Photon Source, Argonne National Laboratory. This facility will allow automated operation to collect X-ray diffraction data in a timely fashion. New phasing methods by single wavelength anomalous dispersion (SAD) were implemented to solve structures using protein crystals from recombinant or natural sources based on hetero-atoms such as Fe, Ca, or S without heavy atom isomorphous phasing or selenium substitution.

Results: Over 6,500 genes from the *C. elegans* genome have been tested in the HTP facility for protein expression. 3,000 proteins were expressed, among which 446 were soluble. 63 proteins have been crystallized. The system met the basic criteria we designed for. Structural studies are now in progress. Progress will be discussed at the conference

AN INTEGRATED APPROACH FOR SYNCHROTRON BASEDSTRUCTURAL PROTEOMICS ON PROTEIN GLYCOSYLATION AND TRANSPORT

Soichi Wakatsuki[a], M. Kawasaki[a], R. Kato[a], M. Hiraki[a], N. Matsugaki[a], N.Igarashi[a], & M. Suzuki[a]

[a]Structural Biology Research Center, Photon Factory, IMSS, KEK, Tsukuba, Ibaraki, Japan. (E-mail: soichi.wakatsuki@kek.jp)

Glycosylation is one of the most important post-translational modifications carried out by an intricate network of glycosyltransferases, glycosidases, transporters, and transport proteins in the endoplasmic reticulum (ER) and the Golgi apparatus. Here, vesicular transport machineries play crucial roles for protein glycosylation as well as protein transport such as endocytosis, exocytosis, and autophagy. We are pursuing a target-oriented structural proteomics project on the molecular mechanisms of protein glycosylation and transport as part of the Japanese national project, Protein 3000. The project is benefiting from an integral approach which combines efforts in protein overexpression, purification, crystallization, synchrotron beam line development and rapid data collection, structure solution, and biological assays.

The structures of the three domains of GGA, a new class of adapter proteins of vesicular transport [*Nature* 415, 937, 2002; *Traffic* in press; *Nature Structural Biology*, 9, 527, 2002; *ibid.* 10, 386, 2003] will be used to illustrate our approach. In addition, several other examples of recent X-ray structures will be chosen from plant lectins responsible for trafficking of glycosylated proteins, mammalian glycosyltransferases [J.Biol.Chem. *in press*] and glycosidases.

In the area of structure determination, we are developing a number of high-throughput technologies to assist not only our structural genomics projects but also general users from Asia and Oceania. These include two new insertion-device MAD beam lines (PF BL-5 & PF-AR NW12) which can produce high quality data sets in 5 to 30 minutes with user-friendly software and highly accurate (1 to 2 microns rotational error) diffractometers, an extremely large scale crystallization robot (200,000 conditions/day) and robotics for crystal harvesting and cryo-protectant exchange. We are also developing a next generation X-ray area detector called X-ray HARP which will enable continuous and super-fine phi slicing data collection (for example 180 degree oscillation in one rotation) from weakly diffracting crystals.

MAGNETIC STRUCTURE ANALYSIS OF ANTIFERROMAGNETIC AND FERROELECTRIC COMPOUND $ERMN_2O_5$ AND YMN_2O_5

Y. Noda,[a] S. Kobayashi, [a] T. Osawa, [a] Y. Fukuda, [a] H. Kimura, [a] I. Kagomiya [b] and K. Kohn [b]

[a]Institute of Multidisciplinary Research for Advanced Materials, Tohoku University, Sendai 980-8577, Japan; [b]Department of Physics, Waseda University, Shinjuku-ku, Tokyo 169-8555, Japan (ynoda@tagen.tohoku.ac.jp).

The family of RMn_2O_5 compounds (R=Y and rare earth elements) was recently payed much attention because magnetic order and ferroelectric order strongly couple each other. For instance, in Y and Er compounds, the anti-ferromagnetic phase transition occurs at about T_N=44K with doubly modulated incommensurate magnetic phase ($\mathbf{q}_M$=(1/2+x, 0, 1/4+z)). On further cooling, the modulation wave vector locks-in the commensurate ones sequentially, first lock-in on q_z and then lock-in on q_x at about T_D=41K and T_{CM}=40K, respectively. Simultaneously, electric spontaneous dipole moment shows up and dielectric constant peaks at the lock-in transition of q_z=1/4[1-3].

We have performed crystal and magnetic structure analyses of YMn_2O_5 and $ErMn_2O_5$ at the commensurate magnetic phase, at 25K and 20K respectively. R-factors of crystal and magnetic structure analyses are 4.5% and 8.6% for YMn_2O_5, and 2.8% and 5.5% for $ErMn_2O_5$. W obtained the magnetic moment as each component of $8Mn^{4+}$, $8Mn^{3+}$ and $8Er^{3+}$ independent atoms(Fig.1), but no magnetic moment in Y atoms. We found the magnetic moment on Mn^{4+} and Mn^{3+} are sinusoidally modulated and the moment of Er^{3+} has mainly z-component (longitudinal wave character). The difference between Er and Y compound is that the node of the sinusoidal wave is between Mn^{4+} atoms (magnetic Er atom layer) for Er compound, while it is on the Mn^{4+} atom for Y compound.

References

1 I. Kagomiya, H. Kimura, Y. Noda and K. Kohn, *J. Phys. Soc. Jpn.* **70** (2001) Suppl. pp.145-147

2 Y. Noda, Y. Fukuda, H. Kimura, I. Kagomiya, S. Matsumoto, K. Kohn, T. Shobu and N. Ikeda, *J. Korean Phys. Soc.* **42**(2003) S1192-1195.

3 S. Kobayashi, T. Osawa, H. Kimura, Y. Noda, I. Kagomiya and K. Kohn *J. Phys. Soc. Jpn.* **73**(2004)NO4 in press

RESONANT X-RAY SCATTERING FROM Fe_3O_4 SINGLE CRYSTAL: A SCENARIO OF ELECTRONIC PHASE SEPARATION BELOW THE VERWEY TRANSITION

Hsueh-Hsing Hung [a]

[a]National Synchrotron Radiation Research Center, Hsinchu Science Park, 30077, Taiwan (hhh@nsrrc.org.tw).

Origin of the Verwey transition in magnetite is unsolved for more than 60 years [1]. At the room temperature, magnetite forms a cubic lattice of inverse spinel structure: $(Fe_A^{3+}O)(Fe_B^{3+}Fe_B^{2+}O_3)$. As generally considered, the electronic fluctuation among the octahedral B-site iron ions reasons out the metallic phase above the Verwey temperature, T_V=122K. Regarding the unoccupied valence states and whether or not long-range charge ordering below T_V, there have been two recent letters of work at ESRF just standing up for an opposite point of view [2, 3]. One observation, based on single-crystal results of resonant X-ray scattering (RXS) from "forbidden" (002) as well as (006) reflection, claimed that *no charge separation below T_V in magnetite* because of neither change of the 1s to 3d nor to 4p resonant electronic excitation been captured in their measurement. The other one, derived from a best-fit model with two sets of Fe_B-O bond length to match the data of X-ray and neutron powder diffraction, however, supported *a possible evidence of charge separation below T_V*.

In our RXS work at the BL15B beamline of NSRRC, but under an exact way to access this problem, distinctive changes in feature of resonant electronic excitations through the Verwey transition are disclosed without ambiguities. Particularly, as following the in-plane (1-10) rhombohedral distortion, continuous structural transformation as well as charge localization is initialized at 4 degrees above the expected Verwey temperature and, thus, electronic phase separation is abruptly formed at T_V due to the bond dimerization.

References

1 E. J. W. Verwey, Nature (London) **144**, 327 (1939).
2 J. Garcia, et al., PRL **85**, 578 (2000); PRB **63**, 054110 (2001).
3 J.P. Wright, J.P. Attfield, and P.G. Radaelli, PRL **87**, 266401 (2001); PRB **66**, 214422 (2002).

CORRELATIONSHIP BETWEEN CRYSTAL STRUCTURE AND PIEZOELECTRICITY IN LANGASITE WITH FOUR CATIONS

H. Ohsato[a], T. Iwataki[a], N. Araki[a], H. Morikoshi[b] and K. Kakimoto[a]

[a]Nagoya Institute of Technology, Gokiso-cho, Showa-ku, Nagoya 466-8555, Japan; [b]Materials Research Center, TDK Co., 570-2, Matugashita, Minamihatori, Narita 286-8588, Japan (ohsato.hitoshi@nitech.ac.jp).

Recently, one of promising piezoelectric materials for higher frequencies, wider bandwidth and higher-bit rates digital communication is $La_3Ga_5SiO_{14}$ (LGS) designated as langasite applied SAW filter. It has larger electromechanical coupling factor than quartz and also has nearly the same temperature stability as quartz. LGS crystal with $Ca_3Ga_2Ge_4O_{14}$-type crystal structure was synthesized and the crystal structure is analyzed by Mill [1]. It is also important feature that the growth of the single crystal is easy. In the case of three-elements compounds such as $[R_3]_A[Ga]_B[Ga_3]_C[GaSi]_DO_{14}$ (R=La, Pr and Nd), the piezoelectric constant increases with the ionic radius of R [2-4]. In this study, crystal structures of four-element compounds such as $[A_3]_A[B]_B[Ga_3]_C[Si_2]_DO_{14}$ (A=Ca or Sr, B=Ta or Nb) are analyzed by single crystal X-ray diffraction, and the mechanism and properties of the piezoelectricity depend on the species of cation was clarified based on the crystal structure.

This crystal structure with $P321$ space group belongs to trigonal crystal system with three-hold axes in a primitive hexagonal lattice. The crystal structure formulae presented in this paper are shown as $[R_3]_A[Ga]_B[Ga_3]_C[GaSi]_DO_{14}$ for three-elements compounds RGS and $[A_3]_A[B]_B[Ga_3]_C[Si_2]_DO_{14}$ for four-elements components ABGS. Here, A: Sr and Ca, B: Ta and Nb. There are four independent cation sites: A-dodecahedron, B-octahedron, C-, and D-tetrahedron. In the large cation layer with A- and B-polyhedra, a characteristic empty space locates, which play an important role in the mechanism of piezoelectricity.

When a force is added to the [100] direction, polarization occurred on the [100] due to the destruction of charge balance. The space releases for repulsion of large cations. We also measured the piezoelectric constants and electromechanical coupling factor for RGS and ABGS. We found a parameter which these properties are depend on. These properties are located on the line as a function to the parameter.

Acknowledgements

A part of this work was supported by a grant from the NITECH 21st Century COE Program "World Ceramics Center for Environmental Harmony" from Japanese Ministry of Education, Science, Sports and Culture and by a Grant-in Aid for Science Research (C) from Japan Society for the Promotion of Science.

References

1 B.V.Mill *et al.*, Doklady Akademii Nauk USSR, **264** (1982) 1385-89.
2 J.Sato *et al.*, J. Crystal Growth, **191**(1998)746-53.
3 T. Iwataki, H. Ohsato, *et al.*, J. Euro. Ceram. Soc. **21**, (2001)1409-1412.
4 H. Ohsato, *et al.*, Abstract for 4th Asian Meeting on Ferroelectrics, pp232, 12-15, Dec. 2003 Bangalore, India.

CRYSTAL STRUCTURES AND PHASE TRANSITIONS IN THE SYSTEM $SrTiO_3$-$La_{2/3}TiO_3$

Christopher J. Howard,[a] A. Gregory R. Lumpkin,[ab] Ronald I. Smith,[c] and Zhaoming Zhang [a]

[a]Australian Nuclear Science and Technology Organisation, Private Mail Bag 1, Menai, NSW 2234, Australia; [b]Department of Earth Sciences, University of Cambridge, Downing Street, Cambridge CB2 3EQ UK; [c]ISIS Facility, Rutherford Appleton Laboratory, Chilton, Didcot, Oxfordshire OX11 0QX, UK (cjh@ansto.gov.au).

The distribution of A-site cations in the perovskite system $La_xSr_{1-3x/2}TiO_3$ depends on the concentration of La^{3+} ions and associated vacancies. For smaller x ($x \leq 0.2$) the substitutions are random. For $x \geq 0.55$, the cations are ordered in such a way that successive layers are occupied to a greater (close to fully occupied) and lesser (this layer contains most of the vacancies) degree, and this ordering drives a tetragonal distortion. For x from about 0.25 to 0.5, the X-ray patterns show diffuse peaks indicative of similar ordering, but this is not long range order and no tetragonal distortion results. The lower temperature structures also exhibit out-of-phase tilting of the TiO_6 octahedra, setting in at temperatures varying practically linearly with composition from 105 K for $x = 0$ to about 650 K at $x = 2/3$.

MS11-5

ANTIPHASE DOMAINS AND B-SITE ORDERING IN $Pb(Mg_{1/3}Nb_{2/3-\delta})O_3/SrTiO_3$ THIN FILMS

Seon Hee Seo,[a] Suraj Yadav,[a] Do Young Noh[a]* and Kiyotaka Wasa[b]

[a]Department of Materials Science and Engineering, Kwangju Institute of Science and Technology, Kwangju, Korea 500-712; [b]Faculty of Science, Yokohama City University, 22-2 Seto Kanazawaku, Yokohama, Japan (dynoh@kjist.ac.kr)

Anti-phase domains and 'B-site' ordered nanoregions are found in $Pb(Mg_{1/3}Nb_{2/3-\delta})O_3$ (PMN) thin films in a synchrotron x-ray scattering experiment. Epitaxial PMN(001) thin films grown by radio frequency magnetron sputtering evolve from tetragonal to pseudo cubic structure as the film thickness increases due to the strain relaxation. In films with intermediate thickness, antiphase domain boundaries (ADB) with 1/2[110] displacement appear. The lattice in the B-site ordered regions in the films with ADBs is much more distorted than average lattice. The ADB phase shares common features with the monoclinic phase observed in bulk relaxsor PMN.

* Author to whom correspondence should be addressed; electronic mail: dynoh@kjist.ac.kr

MULTIPLE OPEN READING FRAMES, CODON BIOS AND AMINO ACID USE AND THE EVOLUTION OF THE GENETIC CODE.

W. L. Duax[a,c], R. Huether[a], L. Habegger[a], S. Connare[a], V. Pletnev[b] and J. Schaber[a]

[a]Structural Biology Dept. Hauptman-Woodward Inst., 73 High St., Buffalo, NY 14203, [b]Shemyakin-Ovchinnikov Inst., Moscow, Russia Federation and [c]SUNY, Dept of Structural Biology, Buffalo, NY. (duax@hwi.buffalo.edu)

Examination of the complete genome of *S. coelicolor* reveals that the antisense strands of 70% of the 7555 genes (5277) contain no stop codons and could in principle be open reading frames (ORFs). Furthermore 2174 genes have a third full length ORF, 228 have a fourth ORF and 56 have five ORFs (no stop frames). We previously detected multiple ORFs (MORFs) and a bias in codon usage in the short chain oxido reductase (SCOR) enzyme family. Of 1651 predicted or known gene products in species from bacteria, archaea, and eukaryotes, 84 SCOR genes having triple ORFs (TORFs) were found to be encoded almost exclusively by the 32 of the 64 codons that are GC-only or GC-rich (2 out of 3 nucleic acids in a codon being G or C) in composition. Examination of the MORFs in *S. coelicolor* revealed a similar bias in codon use and a DNA triple bias that is most severe in the QORFs and PORFs. The 228 QORF genes vary in length from 28 to 464 amino acid, 87% of the coding is from the GC-rich half of the genetic code and 82% of the protein sequences are composed of 10 amino acids (GPASTDLVER). Only eighteen of the expected gene products are characterized. These include two ABC transport proteins, a cyclase, a kinase, a synthetase, a two component regulator, a carbohydrate transport protein, an oxidoreductase and the L12 ribosomal protein. Further investigation reveals a high incidence of MORFs, codon bias and amino acid bias in most prokaryotic ribosomal proteins. Regardless of overall GC content many ribosomal proteins have genes containing DORFs and have no cysteines or tryptophans in their amino acid composition. The MORFs in the SCOR enzymes and *S. coelicolor* appear to identify a subset of the codon system that evolved first, and a subset of amino acids that may have constituted the earliest folded proteins. This work is supported by NIH Grant No. DK26546.

STRUCTURE BASED 'PUNCTUTATION MARKS' IN GENOMIC DNA

Manju Bansal[a] and Aditi Kanhere[a]

[a] Molecular Biophysics Unit, Indian Institute of Science, Bangalore-560012
(mb@mbu.iisc.ernet.in)

Recognition of genomic signals by RNA polymerase is an important first step in transcription initiation but exactly how RNA polymerase locates these signals in the stretch of genomic sequence remains unclear. Are there any punctuation marks other than the known hexameric sequence motifs at -10 and -35 positions? We have analyzed 279 *Escherichia coli* promoter sequences for various structural properties like curvature, flexibility and stacking energy. Overall, the promoter sequences show presence of a curved region covering the -10 and -35 signals. Our study shows that the mean curvature of upstream sequences is more than that of the downstream coding sequences and there are also clear differences in stacking energy of the two regions. Thus, analysis of curvature and stacking energy in the promoter DNA sequences reveal certain signals, which could be used to identify such regions in a genomic sequence.

MS12&13-3

BIOINFORMATICS IN STRUCTURAL GENOMICS OF C. ELEGANS

Jun Tsao, Ph.D., David H. Johnson, and Mike Carson, Ph.D.

Southeast Collaboratory for Structural Genomics, Center for Biophysical Sciences and Engineering, University of Alabama at Birmingham, Birmingham, Al 35294, USA (juntsao@uab.edu)

Our NIH funded program on Structural Genomics of *C. elegans* is a part of the Protein Structure Initiative. A relational database has been developed to capture all experimental data and to mine data with regard to target selection, protein expression conditions, crystallization conditions and structural analyses (website: *http://sgce.cbse.uab.edu*). Over 16,000 Open Reading Frame (ORF) clones of *C. elegans* have been stored and their experimental results are presented. Trends of successful protein production and crystallization could be observed. Our results could serve as reference gages to avoid pitfalls in selecting other eukaryotic ORFs for structural analysis.

SSEP: SECONDARY STRUCTURAL ELEMENTS OF PROTEINS

K. Sekar, V. Shanthi, P. Selvarani, Ch. Kiran Kumar and C.S.Mohire

Bioinformatics Centre and Supercomputer Education and Research Centre, Indian Institute of Science, Bangalore 560 012, INDIA (sekar@physics.iisc.ernet.in)

SSEP is a comprehensive resource for accessing information related to the secondary structural elements present in the 25% and 90% non-redundant protein chains. The current version provides information about the a-helical segments, b-strand fragments, 3_{10}-helices, b and n-turns and hairpin loops of varying lengths. The free graphics program RASMOL has been interfaced with the search engine to visualize the three-dimensional structures of the user queried secondary structural fragment. In addition, the package can be used to extract the three-dimensional atomic coordinates of the defined secondary structural elements. The database is updated regularly and is available through Bioinformatics web server at http://cluster.physics.iisc.ernet.in/ssep/ or http://144.16.71.148/ssep/. The details and the newly added options will be presented.

Reference

1 V. Shanthi, P. Selvarani, Ch. Kiran Kumar, C.S. Mohire and K. Sekar. (2003) *Nucl. Acids. Res.* **31(1)**, 448-451.

THE ROLE OF DATA DICTIONARIES IN KNOWLEDGE RETENTION

Sydney R Hall[a] and Nick Spadaccini[b]

[a] School of Biomedical & Chemical Sciences, University of Western Australia, Nedlands 6009; [b] School of Computer Science & Software Engineering, University of Western Australia, Nedlands 6009, Australia. (syd@crystal.uwa.edu.au)

Data dictionaries are electronic files that contain precise computer-readable information about data items used in a particular field. These dictionaries are of increasing importance in science as the basis for the seamless interchange of data between laboratories, journals and databases.

In crystallography, data dictionaries exist for a number of sub-discipline areas, as well as for the "core" data items common to many aspects of crystal structures and their analysis. CIF dictionaries are available for the discipline areas of structure analysis, macromolecular structure, powder diffraction, symmetry, incommensurate structures, and precision density studies. These are described in detail in the soon to be published *International Tables Volume G* [1].

The primary function of data dictionaries is to precisely identify and characterise frequently used data items. This characterisation, which includes the definition of attributes such as dependencies between data items; whether they are numbers or text; and allowed enumeration, forms the basis for data validation processes critical to journals and databases accepting deposited data.

Data attributes in the next generation of data dictionaries (generally referred to as 'domain ontologies') provide much more *semantic* information about data items. This information is usually expressed as 'methods' which determine the relationship of *derivative* data items to *primitive* (i.e. measured or postulated) and other derivative data. Methods scripts may be expressed in various ways, but their common purpose is to provide functional algorithms that allow non-primitive information to be evaluated. Methods may be applied to data classes as well as individual items, and are particularly important because they preserve executable knowledge about the data items they determine. The 'ontology evaluation' approach differs from conventional software because methods only link items, or classes of items, to the next level of data higher in the derivation chain. The sequence of evaluation steps is not predetermined as it is in computer programs.

This paper will describe an ontology approach to knowledge retention based on the *StarDDL* and *dREL* languages[2], and demonstrate how these are applied to data evaluation and validation.

References

1 *International Tables for Crystallography Volume G* (2004) Eds. S R Hall and B McMahon. Kluwer Academic Press: London.

2 Spadaccini, N., Hall, S.R. and Castleden, I.R. (2000) *J. Chem. Inform. & Computer Sci.* **40**, 1289-1301.

3D STRUCTURAL ANALYSIS OF PROSITE PATTERNS

Sukanta Mondal,[a] Vasanthakumar.B,[b] S. P. Jaishankar[b] and S. Ramakumar[a,b]

[a] Department of Physics, Indian Institute of Science, Bangalore-560 012, India.
[b] Bioinformatics Centre, Indian Institute of Science, Bangalore-560 012, India.(suku@physics.iisc.ernet.in)

True positive hits of PROSITE patterns are expected to have a characteristic three-dimensional structure. The combined sequence-structure attributes of PROSITE patterns can be used for function prediction of an uncharacterized protein with known primary and three-dimensional structure, a situation that might arise in structural genomics projects. We have analyzed the structural features of variable length sequence patterns as well as fixed length sequence patterns from different categories of Enzyme classification in PROSITE. The results of the analyses for the variable length patterns show that conserved residues in the pattern can adopt well-defined backbone conformation. In general, conserved residues in variable length patterns are likely to be completely buried or partially solvent exposed. Key residues for metal binding are from conserved positions in the variable length pattern and ligands are mostly interacting with conserved residues. We have found specific examples of true hits of PROSITE fixed length patterns displaying structural plasticity by assuming significantly different local conformation depending upon the context. Our work highlights the importance of taking into account all the known distinct conformations of PROSITE patterns while creating a sensitive 3D template for the pattern for use in functional annotation.

MATCHING STRUCTURE TO CELL DISTORTION IN TWINNED CRYSTALS

A. David Rae[a]

[a] Research School of Chemistry, The Australian National University, ACT 0200, Australia (rae@rsc.anu.edu.au).

When twin related reciprocal lattices coincide sufficiently well for all intensities to be collected as the sum of two components, there is the possibility that the wrong one of two cells might be chosen to go with the fractional coordinates determined for the structure. This is often recognised by obtaining a satisfactory refinement with the twin ratio reversed compared to expectation. Demands of cell conventions and standard space groups may require changing fractional coordinates and equivalent positions rather than the cell to correct such problems. The problem arises naturally when a structure is obtained by relating it to an already known structure of higher symmetry rather than trying to untwin intensities to obtain an initial solution (a procedure that is less reliable as 1:1 twinning is approached).

Many structures can be described as an occupancy modulation of an idealised 1:1 disordered parent structure of higher symmetry corresponding to the Fourier transform of a subset of the observed reflections or a symmetrised component of the observed reflections. Symmetry elements destroyed by ordering the structure may reappear as a mechanism for polytypism, stacking faults or twinning. An example where all 3 phenomena can occur, sometimes in the same "crystal", is 9,10 phenanthrenequinone [1]. A 1:1 disordered parent structure of $P2_1/c$ symmetry can be ordered to form different orientations of a *Cc* structure with *a* and *b* doubled or different orientations of a *F-1* structure with *a*, *b* and *c* all doubled. In the triclinic case and are no longer exactly 90 °. For the 100 K structure of $Ag(bipy)NO_3$, bipy = 4,4'-bipyridine [2] the only extra reflections occur from the loss of systematic absences when the symmetry is lowered from *Fddd* to *F12/d1* and is no longer 90 °. In both compounds the use of standard settings of standard space groups, viz *P-1* and *C2/c* helps disguise the existence of an idealised parent structure of higher symmetry.

Choices are made when these structures are ordered. The choice of cell can be replaced by a choice between pseudo symmetry related sets of equivalent positions of the parent structure. The requirements of standard space group settings may complicate this choice. Using no restraints or constraints refinements can be performed that are identical except that the twin ratio is reversed. However a sensible use of constraints and restraints produces a preference for one structure and helps explain the cell distortion. The above compounds will be used to illustrate appropriate procedures.

References

1 Rae, A. D. and Willis, A.C. (2003) *Z. Kristallogr.* **218**, 221-230.

2 Somphon, W., Haller, K.J. and Rae, A. D. (2004) *AsCA'04 Abstracts.*

DATA BASE OF HYDROGEN AND HYDRATION IN PROTEINS

N. Niimura[a], I.Tanaka[b], K.Kurihara[b],T.Chatake[b] and M.Maeda[b]

[a]Faculty of Engineering, Ibaraki University, Naka-narusawa, 4-12-1, Hitachi, Ibaraki, 316-8511, Japan. TEL +81-294-38-5254 (niimura@mx.ibaraki.ac.jp)

[b]Neutron Science Research Center, Japan Atomic Energy Research Institute, Tokai-mura, Ibaraki-ken, 319-1195, Japan. TEL: +81-29-282-5906, FAX: +81-29-284-3822

Neutron diffraction provides an experimental method of directly locating hydrogen atoms in proteins, and the development of the neutron imaging plate (NIP) became a breakthrough event in neutron protein crystallography. Several high resolution neutron diffractometers dedicated to biological macromolecules (BIX-2, BIX-3 and BIX-4) with the NIP have been constructed at the Japan Atomic Energy Research Institute and these have enabled high resolution (such as from 1.5Å to 2.0Å) structural analyses of several proteins to have been carried out. The crystal structures of myoglobin, rubredoxin (wild & mutant), hen egg-white lysozyme (at pH4.9 and 7.0) and, human lysozyme, cubic insulin, DsrD and oligomer DNA have been determined using BIX. From these studies, all the hydrogen and hydration in these proteins have been summarized as data base, and by using them, very interesting topics relevant to hydrogen and hydration in proteins, such as hydrogen bonds (bifurcated H-bondings and very few example of co-linear H-bondings arrangement of X-H ----Y) and dynamical behaviors of hydration structures including hydrogen have been extracted from the analytical procedure of the Data Base.

The part of this work is supported by ORCS and JST data base promotion funding.

AB INITIO STRUCTURE DETERMINATION OF $Co(dt)_2$ BY GENETIC ALGORITHM

Makoto Sakata[a], Yuichi Fujishiro[a], Eiji Nishibori[a], Masaki Takata[b], Akiko Kobayashi[c], Hayao Kobayashi[d].

[a]Department of Applied Physics, Nagoya University, Nagoya 464-8603, Japan; [b]Japan Synchrotron Research Institute, Kouto, Mikazuki-cho, Sayo-gun, Hyougo 679-5198, Japan; [c]Research Centre for Spectro-chemistry, The University of Tokyo, Hongo, Bunkyo-ku, Tokyo 113-0033, Japan; [d]Institute for Molecular Science and CREST, Myodaiji, Okazaki 444-8585, Japan(sakata@cc.nagoya-u.ac.jp).

As a related material to single component molecular conductor $Ni(tmdt)_2$[1] (tmdt= tetra-thiafulvalene-trithiolate),a cobalt complex with extended-TTF ligand, $Co(dt)_2$ (dt= tetra-thiafulvalene-dithiolate), was synthesized under the expectation of the magnetic molecular conductor by changing central metal atom and ligand. Electrical resistivity of $Co(dt)_2$ pellet sample was 1.9S cm^{-1} which showed fairly metallic at room temperature. The magnetic susceptibility at room temperature was too small, 3.5×10^{-4} emu mol^{-1}. The crystal structure determination of this material was required for understanding very low magnetic susceptibility. However, single crystal of $Co(dt)_2$ has never been synthesized and only small amount of powder sample was obtained. In this study, ***ab initio*** structure determination of $Co(dt)_2$ was successfully carried out by using third generation synchrotron powder diffraction data. The structure was determined by genetic algorithm(GA) and refined by MEM/Rietveld method[2].Eventually precise charge densities of was $Co(dt)_2$ obtained.

The powder diffraction pattern of $Co(dt)_2$ was measured at SPring-8, BL02B2. The wavelength of incident x-ray was 1.0Å. The powder data was indexed using the program DICVOL on the basis of the first 24 observable peaks, giving the triclinic unit cell : a=11.7164(2)Å, b=10.9496(1)Å, c= 7.7319(7)Å , α=79.731(1)°, β=96.481(2)°, γ=113.9686(9) °. A planer molecular structure model of $Co(dt)_2$, which is similar to $Ni(tmdt)_2$ were used in the process of structure determination by GA. The GA analysis was carried out for both ***P1*** and ***P-1*** triclinic space group. The reliability factor of GA solutions based on weighted profile, Rwp, was 14% for ***P1*** and 15% for ***P-1*** respectively. Each solution gave almost identical structure. Then, it is concluded that solution of ***P-1*** space group, which has higher symmetry, was the final result by GA.

The structure refinement by MEM/Rietveld analysis was carried out based on GA result. The reliability factors of final Rietveld refinement based on Bragg intensities, RI, and weighted profiles, Rwp, were RI=6.4% and Rwp=3.6%, respectively. Each of two extended TTF-ligands of $Co(dt)_2$ molecule was distorted in opposite direction and inter molecular distance from nearest neighbor molecule was as small as 3.12 from Rietveld refinement. Furthermore, the MEM charge density of cobalt atom was connecting to not only four S atoms which belong to same molecule but also S atom belonging to nearest neighbor molecule. It was concluded that $Co(dt)_2$ forms a dimeric molecule that two molecules are parallel to each other. It is considered that the dimer formation suppress the magnetic moment of Co ions by anti-ferromagnetic interactions of two $Co(dt)_2$ molecules.

References

1. H. Tanaka., et al., (2001) *Science* ***291***, 285-287.
2. M. Takata., et al., (1995) *Nature* **377**, 46., M. Takata, et al., (2001) *Z. Kristallogr.* **216**, 71.

APPLICATIONS OF LARGE 2D DETECTORS FOR NEUTRON POWDER DIFFRACTION.

Alan W. Hewat

Institut Laue-Langevin, BP 156X Grenoble Cedex 9, 38042 France (hewat@ill.fr).

1D electronic position sensitive detectors were first developed for neutron powder diffraction in the late 1960's in Grenoble, and for the first time made it possible to study very small samples, chemical kinetics etc. using Rietveld refinement. A few years later, linear wire detectors became available for X-ray powder diffraction. Recently we have built a large high-resolution 2D neutron detector (super-D2B), and we have approval for a project to build an even large high flux 2D neutron detector (DRACULA), with a prototype already working (D19).

In this presentation we will describe some of the new science that might be done with such detectors, and show that they will allow powder diffractometers on high flux reactors such as at ILL in France, or the new reactors FRM-II in Germany and RRR in Australia, to compete successfully with machines on the new American and Japanese pulsed neutron sources.

SCREENING STABILIZING POLYMERS FOR DRUG DEVELOPMENT USING VARIABLE TEMPERATURE X-RAY DIFFRACTION

Z. Ping Wu, R. Hart, and D. Stirling

Pharmaceutical Sciences, Pfizer Global Research & Development, 10777 Science Center Dr, San Diego, CA 92122, USA; (zhen.wu@pfizer.com).

The performance of pharmaceutical solid dosage forms often are affected by the solid state form of the drug used in the formulation[1]. Amorphous materials are often used in drug formulation due to their higher solubility and absorbability. However these materials need to be stabilized with a polymer since they tend to be physically and chemically less stable. We report here a method to quickly screen polymers for use as a stabilizer in drug formulation.

The method described here is the Non-ambient X-ray Diffraction (NA-XRD) technique.[2] This is a powerful new tool for identifying new solid forms and characterizing their stability. This technique allows the x-ray powder pattern of a sample to be recorded at selected temperatures and relative humidities, where physical or chemical transformations of the sample may occur. A commercially available drug Indomecathin was used as a model in this study. Mixtures of Indomecathin with various polymers were prepared and their stability was quickly determined under accelerated conditions using NA-XRD. The results demonstrate that this technique allows rapid identification of potential polymers for further evaluation in drug development.

References

1 Chemburkar et al, (2000) Org. Proc. Res. Dev., **4**, 417.
2 Fawcett et al, (1986) Adv. X-ray Anal., **29**, 323.

STUDY OF CRYSTAL STRUCTURE IN $LaMn_{1-x}Cu_xO_3$ COMPOUNDS

S. Ravi and Manoranjan Kar

Department of Physics, Indian Institute of Technology Guwahati, Guwahati – 781039, India (sravi@iitg.ernet.in)

$LaMnO_3$ is an antiferromagnetic insulator with antiferromagnetic transition at around 141K [1]. The substitution of Cu in place of Mn can introduce the mixture of Mn^{3+} and Mn^{4+} ion in the compound. The ferromagnetic double exchange interaction between Mn^{3+} and Mn^{4+} in the Mn-O-Mn (Mn^{3+} - O^{2-} - Mn^{4+}) network play the key role for ferromagnetic metal (FMM) to paramagnetic insulator (PMI) transition, and the colossal magneto-resistance (CMR) property in the vicinity of FMM to PMI transition temperature in mixed valence manganite perovskites [2]. Simultaneously, the substitution of Cu in place of Mn will not affect the crystal structure, as the size of Cu ion is comparable to that of Mn ions. Here we have reported the crystal structure of $LaMn_{1-x}Cu_xO_3$ by analyzing XRD patterns. $LaMn_{1-x}Cu_xO_3$ compounds were prepared for x = 0, 0.10, 0.15, 0.20 and 0.30 by solid-state route. The final sintering in pellet form was carried out at 1200°C in air for over 60hrs with intermediate grindings. XRD patterns were recorded at room temperature using a Seifert 3003-TT XRD machine by employing CuK_α radiation. The samples are mostly in single phase form. XRD patterns were analyzed with the help of fullprof program by employing rietveld refinement technique [3]. The patterns for all the samples could be refined using *Pbnm* space group. The typical lattice parameters are found to be a = 5.543Å, b = 5.510Å, and c = 7.816Å for x = 0.15. It has been found that the lattice parameters and unit cell volume is almost constant for all the samples. It could be due to the two competing effects, such as smaller ionic size of Mn^{4+} ions compared to Mn^{3+} ions and larger ionic size of Cu^{2+} ions compared to Mn^{3+} or Mn^{4+} ions. The average Mn-O bond lengths and Mn-O-Mn bond angles have been calculated from the rietveld refined parameters. The particle size has been calculated from XRD pattern using the Scherrer formulae [4]. It has been found that particle size increases with the increase of Cu concentration. DC electrical resistivity measurements down to low temperature show semiconducting behaviour for all the samples. Temperature variations of ac susceptibility down to 30K were measured at an ac field amplitude of 5.3Oe. The above Cu doped samples show paramagnetic to ferromagnetic transitions. The paramagnetic to ferromagnetic transition temperature (T_c) decreases with the Cu concentration. It could be due to the increase of antiferromagnetic superexchange interaction between the Cu and Mn ions. The reentrant spin glass like behaviour has been observed at low temperature.

References

1 Wollan, J. E. O. and Koehler, W. C. (1955) Phys. Rev., 100 545.
2 Jin, S., Tiefel, T. H., McCormack, M., Fastnacht, R. A., Ramesh, R. and Chen, L. H. (1994) *Science*, 264, 413.
3 Young, R. A. (1996) "The Rietveld Method" International Union of Crystallography. (New York, Oxford University Press).
4 Taylor, A. (1961) X – ray Metallography (Wiley, New York).

POWDER DIFFRACTION STUDIES OF BISMUTH DOUBLE PEROVSKITE $Ba_2A^{3+}B^{5+}O_6$

Qingdi Zhou[a], Brendan J. Kennedy [a]

[a] Centre for Structural Biology and Structural Chemistry and Centre for Heavy Metals Research, School of Chemistry, The University of Sydney, Sydney, NSW, 2006, Australia (q.zhou@chem.usyd.edu.au)

The double perovskite compounds of $Ba_2A^{3+}B^{5+}O_6$ (A = Bi, Sc, B = Ta, Sb, Bi) have been synthesized and their structures have been determined by synchrotron X-ray and neutron powder diffraction techniques. These studies seek to establish the effect of Bi valence on the structures and phase transitions in these double perovskites. At room temperature, the compound Ba_2ScBiO_6 is cubic in space group *Fm3m*, whereas Ba_2BiSbO_6 and Ba_2BiTaO_6 have a rhombohedral structure in space group *R*3. Variable temperature synchrotron powder diffraction studies show that heating Ba_2BiTaO_6 result in an, apparently, continuous transition to the cubic structure near 250 °C (Figure 1). Ba_2BiSbO_6 becomes cubic above 300 °C. For both these compounds the Bi–O bond distances are indicative of trivalent Bi. In comparison, $Ba_2Bi_2O_6$ is monoclinic at room temperature, *I*2/*m*, as a result of both $Bi^{III/V}$ charge ordering and tilting of the BiO_6 octahedral. This undergoes a first order transition near 150 °C to the rhombohedral structure. These experimental results are consistent with a group theoretical analysis of the PT in rock-salt ordered double perovskites[1].

References

1 Howard, C.J.; Kennedy, N.J.; and Woodard, P.M. (2003) *Acta Cryst. B59*, 463-471.

MOLTEN SALT SYNTHESIS AND CRYSTAL STRUCTURES OF PALLADIUM PHOSPHATES AND ARSENATES

Kwang-Hwa Lii,[a,b] Ling-I Hung,[c] and Sue-Lein Wang[c]

[a]Department of Chemistry, National Central University, Chungli; [b]Institute of Chemistry, Academia Sinica, Taipei; [c]Department of Chemistry, National Tsing Hua University, Hsinchu, Taiwan, R.O.C. (liikh@cc.ncu.edu.tw)

All elements in the first transition series and most elements in the second and third series form crystalline phosphates. However, few phosphates of the platinum-group metals, namely Ru, Os, Rh, Ir, Pd and Pt, have been reported. Solid phosphates of osmium and iridium are actually not known. The structural chemistry of the corresponding arsenates is even more limited. This presentation reports the results of our exploratory synthesis of palladium phosphates and arsenates by molten flux reactions. Six compounds with the general formula $A_2Pd_3(X_2O_7)_2$ (A = monovalent metal cations) and five different structural types have been characterized. For example, the structure of $Cs_2Pd_3(P_2O_7)_2$ consists of discrete $Pd^{II}O_4$ squares which are linked by P_2O_7 groups *via* corner-sharing to generate a 3D framework containing 12-ring channels in which Cs^+ catons are located. Much to our surprise the arsenate analogue, $Cs_2Pd_3(As_2O_7)_2$, with the same general formula adopts a 2D layer structure with the interlayer space filled with Cs^+ cations. Within a layer there are PdO_4 squares and As_2O_7 groups fused together *via* corner-sharing. Adjacent layers are stacked such that strings of Pd atoms are formed. The PdO_4 squares show eclipsed and staggered stacks with alternate short and long Pd···Pd distances. The structure of $Cs_2Pd_3(As_2O_7)_2$ is shown below.

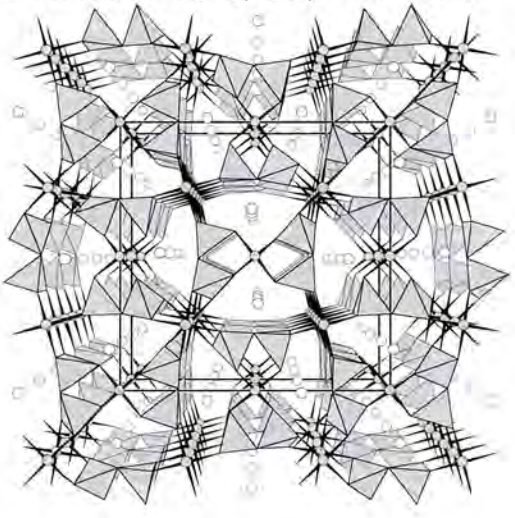

SPIN DENSITY AND CHARGE DENSITY STUDIES ON AN ORGANIC MAGNET

Jey-Jau Lee[a] and Yu Wang[b]

[a]National Synchrotron Radiation Research Center, Hsinchu 300, Taiwan; [b]Department of Chemistry, National Taiwan University, Taipei, Taiwan =jjlee@spring8.or.jp)

Spin density and electron density studies of organic radical compound have been carefully investigated by Polarized Neurton diffraction, Neurton diffraction and X-ray diffraction method at very low temperature =2K, 20 K and 125 K respectively). Electron density and spin density distribution based on multipole model will be presented.

The PND experiment data are actually measuring the flipping ratio, R, of bragg reflections, =hkl). This ratio is defined as the ratio of the diffracted intensities and with incident neutron beam polarized in spin up, I⁺=hkl), and down, I⁻=hkl), respectively. The *flipping ratios* of a Bragg reflection, R=hkl) is then given by=

$$R(\mathrm{hkl}) = \frac{I^{+}}{I^{-}} = \frac{F_N^2 2 + \sin^2\alpha\ F_M^2 + 2\sin^2\alpha\ F_N F_M}{F_N^2 + \sin^2\alpha\ F_M^2 - 2\sin^2\alpha\ F_N F_M}$$

A total of 585 such flipping ratios are collected up to sin=θ)/λ=0.80 Å^{-1}. The magnetic structure factor, F_M, deduced from the flipping ratios, is the Fourier component of the spin density S=ρ). After the analyses, there are significant spin density distribution =0.07e) at the hydrogen atom of the phenyl group.

According to the results of the PND and three MO calculations, Significant spin density are located at the nitroxide group and they are perpendicular to the N-O bonds but directly point toward the hydrogen atom of the phenyl group. The DFT/Dmol calculation on the dimer of this radical also indicates significant spin density population on the hydrogen-bonded hydrogen atom. Based on the spin density measurement and the MO calculations, the transmittance of the magnetic behavior of the title compound is believed to be due to the intermolecular hydrogen bond, N-O…H-C and can be well identified. .

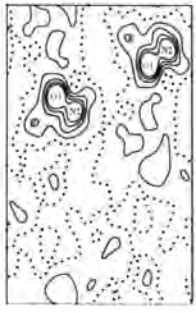

Figure.spin density distribution on y=1/4 plan

	DFT calculations			Expt.
	monomer	dimer	Xtal	PND
First Molecule				
O1	0.5264	0.5258	.446	.3721
N5	0.4301	0.4308	.500	.3211
H22(H8)	0.	0.0025	.005	-.02
H23(H7)	0.	0.0013	.003	.07
Second Molecule				
O45	-	0.5045		
N49	-	0.4489		
H66(H8)	-	0.		
H67(H7)	-	0.		

Table. Theoretical and experimental spin density population on selected atoms.

MS15-3

A NOVEL ALUMINOBORATE MOLECULAR SIEVERS CONTAINING OCTAHEDRAL FRAMEWORKS OF 3D TUNNEL STRUCTURE

Jianhua Lin and Jing Ju

State Key Laboratory of Rare Earth Materials Chemistry and Applications, College of Chemistry and Molecular Engineering, Peking University, Beijing 100871, P. R. China (jhlin@chem.pku.edu.cn)

A new microporous aluminoborate family, i.e., $HAl_3B_6O_{15}(OH)_4$ (PKU-1), $Al_5B_5O_9(OH)_3$ (PKU-5), $Al_4B_6O_{15}$ (PKU-5) and $HAl_5B_3O_8$ (PKU-6), have been synthesized in the boric acid flux by direct reactions with aluminum salts in a closed system at the temperatures slightly above the melting point of boric acid. The structures of these aluminoborates were established by using powder X-ray diffraction techniques. PKU-1, PKU-5 and PKU-5 crystallize in trigonal structures consisting of borate groups and porous octahedral frameworks with 18-, 54-and 10-membered octahedral tunnels. In the structures, the Al-octahedra share edges, respectively, in *cis*- and *trans*-fashions, forming the octahedral frameworks. The borate groups, all in triangular geometry, share oxygens with the octahedral frameworks thus to compensate the negative charge of the frameworks. The structure principle of PKU-6 is different from that of other members of PKU family. The aluminum atoms are all 5-coordinated with pyramid geometry. The Al-polyhedra share edges forming one-dimensional chains that are linked to one-dimensional pore framework via triangular borate (B_3O_7). Two structure units are fundamental in the PKUs structures, i.e., the 3-membered ring units 5Al+B and Al+5B, which, as we believe, are crucial to stabilize these unusual octahedral frameworks. PKU-5 is stable up to 800°C; while the frameworks of PKU-1 and PKU-5 collapse at about 600 and 400°C respectively. PKU-6 discomposes at about 650 °C. These compounds exhibit typical microporous behavior.

References

1 Jing Ju, Jianhua Lin*, Guobao Li, Tao Yang, Hongmei Li, Fuhui Liao, Chun–K. Loong, and Liping You, Octahedra-based Molecular Sieves with 18-Octahedral-atom Frameworks, *Angew. Chem. Int. Ed.* **42**, 5607 (5003); *Angew. Chem.*, **115,** 5765(5003)

MODULATED STRUCTURES IN THE Ta_2O_5-WO_3 SYSTEM FROM X-RAY AND NEUTRON POWDER DIFFRACTION DATA

Siegbert Schmid[a] and Anja Binder[b]

[a]School of Chemistry, The University of Sydney, NSW 2006, Australia; [b]Institute for Inorganic Chemistry, University of Tübingen, Germany (s.schmid@chem.usyd.edu.au-.

Systems that form modulated structures are a fascinating class of materials, which lack lattice periodicity but may still be perfectly long-range ordered [1]. Such systems exist across the whole range of chemical disciplines from organic conductors to high-T_c superconductors and minerals. The importance of modulated structures has been recognised, but there have been few systematic studies across composition ranges of solid solutions that form modulated structures. Such a systematic investigation is expected to further our understanding of crystal chemical and structural aspects of modulated structures as well as the reasons for their existence.

One example for a modulated structure, the wide-range, non-stoichiometric solid solution ($1\text{-}x\text{-}Ta_2O_5 \cdot xWO_3$, $0 \leq x \leq 0.267$, has been subject to intensive investigation over many years [2]. Owing to the phase transition at 1360 °C, large single-crystals of L-Ta_2O_5 were impossible to grow. Thus, attempts were made to stabilise the phase by the addition of other oxides. For WO_3, a series of anion-deficient α-UO_3-related 'line phases' with basic structure dimensions very similar to those of L-Ta_2O_5 was found within the composition range ($1\text{-}x\text{-}Ta_2O_5 \cdot xWO_3$, $0 \leq x \leq 0.267$.

As part of a systematic study X-ray and neutron powder diffraction data for a number of compositions were collected at the Australian National Beamline Facility, Tsukuba, Japan and at the HIFAR facility, Lucas Heights, Australia, respectively. The results of the structure refinements using JANA [3] will be presented.

References

1 Withers, R. L., Schmid, S. & Thompson, J. G. (1998-. *Prog. Solid State Chem.* **26,** 1.
2 Schmid, S., Fütterer, K. & Thompson, J. G. (1996-. *Acta Cryst.* **B52,** 223.
3 Petricek, V. & Dušek, M. (2000-. JANA2000, Programs for Modulated and Composite Crystals, Institute of Physics, Praha, Czech Republic.

A CHIRAL METAL ZINCOBOROPHOSPHATE TEMPLATED BY ACHIRAL TRIAMINE: SYNTHESIS AND CHARACTERIZATION OF $(C_4N_3H_{16})[Zn_3B_3P_6O_{24}]\cdot H2O$

Wei Liu, Hao-Hong Chen, Xin-Xin Yang, Man-Rong Li, Ming-Hui Ge and Jing-Tai Zhao

The State Key Laboratory of High Performance Ceramics and Superfine Microstructure, Shanghai Institute of Ceramics, Chinese Academy of Science, Shanghai 200050, P. R. China (lw@mail.sic.ac.cn)

Organically templated metal borophosphates are of great current interest because of their novel structures and potential applications.[1] The first example of an organo-templated chiral zincoborophosphate, $(C_4N_3H_{16})[Zn_3B_3P_6O_{24}]\cdot H2O$ has been hydrothermally synthesized in the presence of structure-directing agent, DETA. It crystallizes in the hexagonal system, space group $P6_522$, a = 9.6677(14) Å, c = 14.860(3) Å, γ = 120°, V = 1202.8(3) Å^3, Z = 2. The structure is an infinite three-dimensional zeolite-analogous open-framework structure built from corner-sharing ZnO_4, BO_4 and PO_4 tetrahedra. Two types of channel systems exist in the structure along the *c* axis. Besides the large channels built from the borophophate chains $_\infty{}^1\{[B_3P_6O_{24}]^{3-}\}$, the other one-dimensional opening is made up of two twisted corner-sharing tetrahedral helices connecting through ZnO_4 tetrahedra. Protoned DETA molecules are arranged along 6_1 or 6_5 axis and are located in the free spaces of borophosphate helical chains to form a novel chiral organic-inorganic channel system. It is the first example of an organically templated borophosphate derivative having such a chiral arrangement of organic molecules in the crystal. The terminal $(H_3DETA)^{3+}$ groups connect adjacent borophosphate helical ribbons via N–H...O hydrogen bonds while water molecules are also supported by hydrogen bonds with the organic molecules. Thermal investigations show that this compound can lose the water molecules in the channels up to 200°C and obtain a dehydrated microporous phase. The crystalline dehydration product is a microporous borophosphates with helical hollow channel structure and can be stable up to 450°C in air, which have a potential application as a catalyst.

References

1 Anthony, K. C; Gérard, F.; Thierry, L. (1999) *Angew. Chem., Int. Ed. Engl.*, 38, 3268-?.

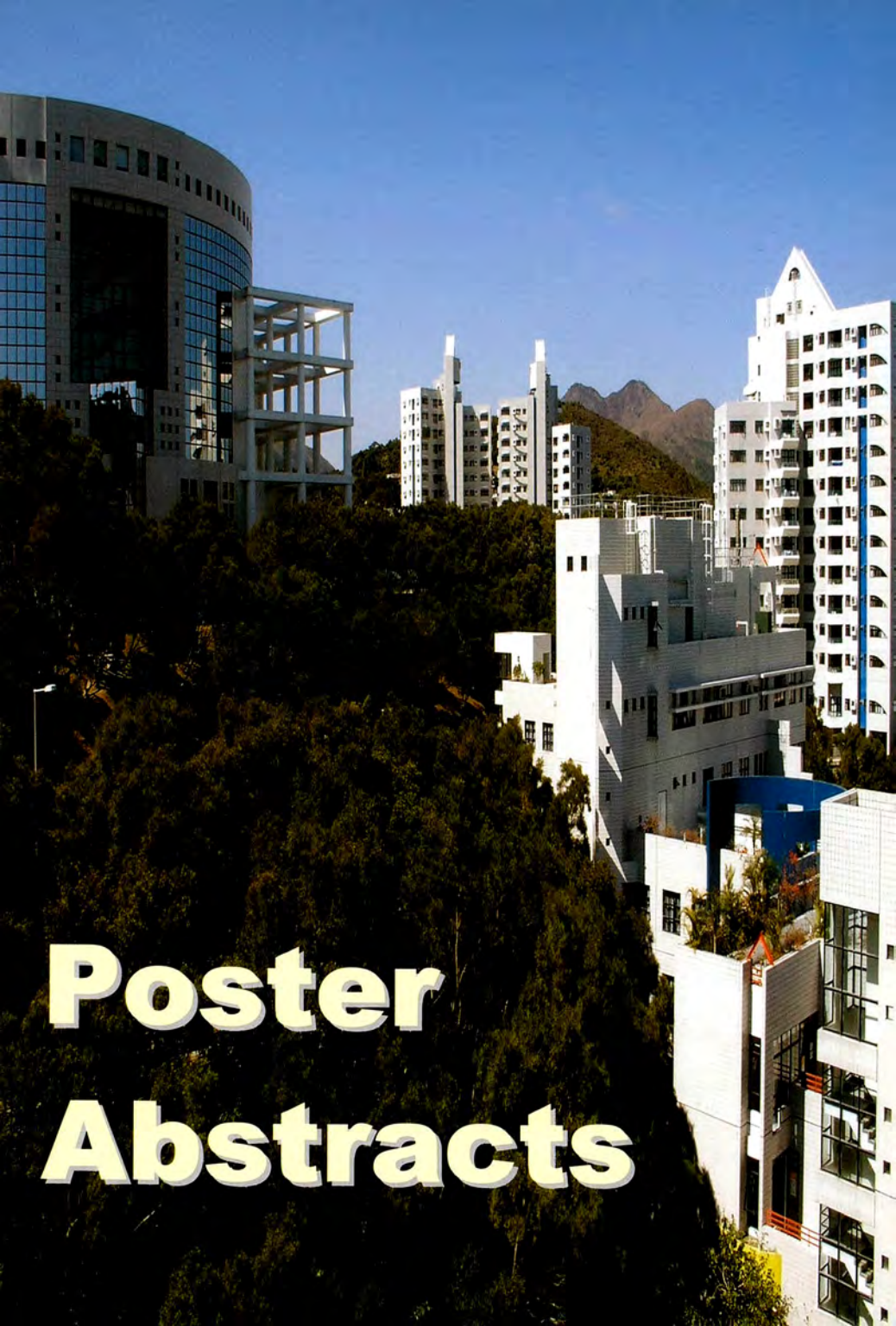

Poster Abstracts

PO1

ANALYSES OF HYDROGEN BONDS IN AMINO ACID – INORGANIC ACID 2:1 COMPLEXES

B.Sridhar [a] , K.Anitha and R.K.Rajaram[a]

[a]School of Physics, Madurai Kamaraj University, Madurai-625 021, India (sshiya@yahoo.com)

In an Amino acid-inorganic acid complex, when the number of hydrogen atoms attached to the inorganic acid is less than the number of amino acids, the hydrogen atom liberated from the inorganic acid is shared by the two amino acids through a short O-H...O hydrogen bond. The following crystal structures, L-methionine, L-aspartic acid, L-phenylalanine, L-proline, L-lysine hydrochloride, L-valine and β-alanine were grown in a stoichiometric ratio 2:1 with the inorganic acids like perchloric acid and nitric acid. In the case of hydrogen bis (L-phenylalanine) perchlorate, bis (L-proline) hydrogen perchlorate, L-valine L-valinium perchlorate monohydrate, D-serinium D-serine nitrate and bis (L-proline) hydrogen nitrate, the hydrogen bond linking the aminoacid residues may be termed as a nearly symmetric hydrogen bond, from the donor-hydrogen and hydrogen-acceptor distances. In the crystal structures of hydrogen bis(L-lysinium(+))dichloride perchlorate, hydrogen bis(L-lysinium(+))dichloride nitrate, hydrogen bis(L-phenylalanine) nitrate L-methionine L-methioninium perchlorate monohydrate and L-aspartic acid nitrate-L-aspartic acid, the hydrogen atoms may be termed as asymmetric bond, since hydrogen atom is closer to the donor carboxyl group. The structural details of the above complexes will be presented. A survey of similar compounds, in relation to the geometry of the carboxylate and carboxylic acid groups, will also be discussed

PO2

BONDING AND AGGREGATIONS OF SOME AMINO ACID - INORGANIC ACID COMPLEXES

B.Sridhar [a], K.Anitha and R.K.Rajaram[a]

[a]School of Physics, Madurai Kamaraj University, Madurai-625 021, India (sshiya@yahoo.com)

When the number of amino acid and hydrogen atoms liberated from the inorganic acids is equal, then these free hydrogen atoms, in general, link the amino acid and the inorganic acid through rather strong O-H...O hydrogen bonding (O...O distance ~ 2.6 Å). In this context, the crystal structures of L-threonine, L-tyrosine, DL-aspartic acid, L-methionine, L-phenylalanine, L-glutamic acid and L-isoleucine were grown in stoichiometric ratio of 1:1 with inorganic acids like sulfuric acid and ortho phosphoric acid. The crystal structures were solved using standard crystallographic methods. The packing diagram of the crystal structure reveals the aggregation pattern in the unit cell. Generally, hydrophobic α-amino acid like valine, leucine, phenylalanine and norleucine, aggregates as two-dimensional ordered layers. The examination of the packing diagram of tri (L-isoleucinium) sulfate bisulfate reveals the aggregation of hydrophilic zone interconnected by O-H...O and N-H...O hydrogen bonds in a cage like structure. The crystallographic features of the above structures will be presented.

ELECTRONIC STRUCTURES OF $La_{1-x}Sr_xCoO_3$ EXAMINED BY XMCD MEASUREMENS AT THE Co *K* ABSORPTION EDGE

Takayasu Hanashima,[a] Satoshi Sasaki,[a] Norio Shimizu,[a] Kouji Yamawaki,[a] Takeharu Mori,[b] and Masahiko Tanaka[b]

[a]Materials and Structure Laboratory, Tokyo Institute of Technology, Nagatsuta 4259, Midori, Yokohama 226-8503, Japan; [b]Institute of Materials Structure Science, High-Energy Accelerator Research Organization, Oho 1-1, Tsukuba 305-0801, Japan (sasaki@n.cc.titech.ac.jp)

The end-member compound $LaCoO_3$ is considered to be a nonmagnetic semiconductor in the low-spin state of Co^{3+} at low temperature. Magnetic susceptibility slowly increases with temperature and reaches a maximum of a broad peak at $T \sim 100$ K [1]. The nonmagnetic $LaCoO_3$ is considered to transform to paramagnetic with the spin-crossover phenomenon around the temperature. Also, an intermediate-spin ground state has been proposed to be stabilized for a Co^{3+} (d^6) system in $LaCoO_3$ or Co^{4+} (d^5) in $SrCoO_3$ [2,3]. When holes can be doped into $LaCoO_3$ by substituting Sr for La, the transition of $La_{1-x}Sr_xCoO_3$ compounds changes from nonmagnetic semiconductor to ferromagnetic metal for $x \geq 0.2$ up to the other end-member of $SrCoO_3$ [4].

We have studied the effect of Sr doping on the magnetic structure of $La_{1-x}Sr_xCoO_3$ ($x = 0$, 0.2, 0.3, 0.4, 0.5 and 0.6) by X-ray magnetic circular dichroism (XMCD) at the Co *K* absorption edge.

A negative peak of XMCD was clearly observed for pure $LaCoO_3$ at $E = 7.719$ keV within the threshold region, suggesting the existence of the intermediate-spin state of Co^{3+}. A positive peak appeared at $E = 7.723$ keV of the main edge by Sr substitution for La in $LaCoO_3$ ($x \geq 0.2$), which is in accord with the observation of Co^{4+} on X-ray absorption near edge structure. A negative peak observed at the pre-edge suggests the hybridization and super-exchange interaction between Co^{4+} and neighboring Co^{4+} with the positive main-edge peak. The dispersion-type XMCD signals at the main edge can be rationalized with the double-exchange interaction between Co^{3+} and Co^{4+}.

References

1 Yamaguchi, S., Okimoto, Y., Taniguchi, H. and Tokura, Y. (1996) *Phys. Rev. B* **53**, R2926-R2929.
2 Goodenough, J.B. (1971) *Mater. Res. Bull.* **6**, 967-976.
3 Potze, R.H., Sawatzky, G.A. and Abbate, M. (1995) *Phys. Rev. B* **51**, 11501-11506.
4 Jonker, G.H. and van Santen, J.H. (1953) *Physica (Amsterdam)* **19**, 120-130.

CDW FORMATION IN AN INCOMMENSURATE PHASE OF 1T-TaS_2 STUDIED BY X-RAY THERMAL DIFFUSE SCATTERING

Yo Machida,[a] Satoshi Sasaki,[a,b] Takayasu Hanashima,[a] Kouichi Ohkubo,[a] Kouji Yamawaki,[a] and Masahiko Tanaka[c]

[a]Department of Materials Science and Engineering, Tokyo Institute of Technology, Nagatsuta, Yokohama 226-8503, Japan; [b]Materials and Structures Laboratory, Tokyo Institute of Technology, Nagatsuta, Yokohama 226-8503, Japan; [c]Institute of Materials Structure Science, KEK, Oho, Tsukuba 305-0801, Japan (sasaki@n.cc.titech.ac.jp)

Charge-density-wave (CDW) formation is considered as the consequence of the electron-phonon interaction. The layered transition-metal dichalcogenides such as TaS_2 have attracted much interest because of their unique electron properties associated with quasi-two-dimensional characters and phase transitions related to the CDW formation. 1*T*-TaS_2 has three stable phases, which are an incommensurate phase (IC), a nearly commensurate phase (NC) and a commensurate phase (C) with phase-transition temperatures of 350 K (IC to NC) and 190 K (NC to C) [1,2].

We have studied the dispersion curves of phonons by means of synchrotron x-ray thermal diffuse scattering (TDS), which relates quantitatively to the frequency and wavelength of traveling elastic waves in a crystal. Since the thermal vibration of the lattice can be described by a linear superposition of these waves, the TDS intensity gives the phonon dispersion curves [3]. The TDS intensity of the IC phase was measured at the BL-10A station of Photon Factory. Single crystals of 1*T*-TaS_2 were synthesized by the chemical vapor-transport method [4]. A single crystal in dimensions of 5 x 5 x 0.2 mm^3 was mounted with a small furnace in a vertical-type four-circle diffractometer. A satellite reflection was observed at $\boldsymbol{q} = 0.28\boldsymbol{a}^* + \boldsymbol{c}^*/3$. The TDS intensity around the 1 -1 0 reciprocal lattice point was measured within the temperature range between 300 and 460 K.

Least-squares analyses in terms of lattice dynamics yielded the dispersion curves of phonons, which revealed the Kohn anomaly both in the longitudinal acoustic (LA) and transverse acoustic ($TA_{//}$) modes. It is suggested that the rotation of the ordering vector in the nearly commensurate phase at low temperature is triggered by the softened ($TA_{//}$) modes.

References

1 Wilson, J.A., DiSalvo, F.J. and Mahajan, S. (1974) *Phys. Rev. Lett.* **32**, 882-885.
2 Scruby, C.B., Williams, P.M. and Parry, G.S. (1974) *Phil. Mag.* **31**, 235-274
3 Holt, M., Wu, Z., Hong, H., Zschack, P., Jemian, P., Tischler, J., Chen, H., and Chiang, T.-C. (1999) *Phys. Rev. Lett.* **83**, 3317-3319.
4 Endo, T., Nakao, S., Yamaguchi, W., Hasegawa, T. and Kitazawa, K. (2000) *Solid State Commun.* **116**, 47-50.

PO5

CRYSTAL STRUCTURE OF ETHYL 4-(2,5-DIOXO-2,5-DIHYDRO-1H-PYRROL-1-YL)BENZOATE

Vasu[a] , K.A.Nirmala* [b], M.Vishwas[c], Deepak Chopra[d]

[a] Vivekananda degree college Malleshwaram west Bangalore-560055,
[b] Reader in physics, Bangalore University, Bangalore-560056,
[c] Government college of Pharmacy Bangalore-560027,
[d] Indian Institute of Science, Solid State Chemistry Unit, Bangalore-560012,
(vasusriranga@rediffmail.com)

Succinimides are important medicinal agents in the therapy of diseases such as tuberculosis, convulsions and hypertension[1,2]. This application of the compound attracted us to take up the crystal and molecular structural work by X-ray diffraction method to know the conformational aspects. The title compound Ethyl 4-(2,5-dioxo-2,5-dihydro-1H-pyrrol-1-yl)benzoate is a derivative with an ester-substituted aryl maleimide. The yellow compound crystallizes in monoclinic system of space group $P2_1/c$ with number of molecules per unit cell four. The X-ray data was collected on SMART AXX CCD detector. The structure was solved using WINGX(1.64). The lattice parameters are **a**=12.028(6)Å, **b**=7.358(4)Å, **c**=13.561(7)Å, β=96.364(7)°. The refinement gave a final R-value 0.044 for 2328 unique reflections.

The angle between the mean planes passing through the benzene ring and the maleimide ring is 41.4(1)°, indicating the steric repulsion between the carbonyl groups and the benzene ring. The dihedral angle is small [2.5(2)°] in a similar structure without carbonyl groups[3].

Molecular chains are observed, via two different C-H...O hydrogen bonds running along the **a** and **c**-axes, respectively. The C-H...O hydrogen-bonded chain down the **a**-axis involves the ester carbonyl group, whereas the other down the c-axis employs one of the carbonyl groups of the maleimide ring.

We acknowledge DST(IRHPA) and Prof.T.N.Guru Row IISc.,(SSCU) for providing diffraction data. One of the authors Vasu acknowledges Vivekananda Degree College principal for the support.

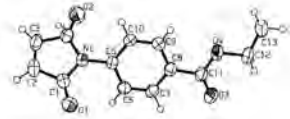

Fig : Molecular structure of the compound with 50% probability ellipsoid

References

1 Pandey, U.K., Lohani,H.C.& Agrawal.,A.K.(1984. Indian Drugs, 21,135-138
2 Crider,M. &EdwardO.M.(1977)J.Med.Chem.20,405-409.
3 Paulus,E.F.&Rivo,E.(1988) Acta Cryst C44 1242-1244.

X-RAY DIFFRACTION, XANES AND XMCD STUDIES ON THE SITE PREFERENCE AND VALENCE STATE OF Co AND Fe IONS IN IRON COBALTITE

Kouji Yamawaki,[a] Norio Shimizu,[a] Satoshi Sasaki,[a] Takayasu Hanashima,[a] Tomoaki Watanabe,[a] Masahiro Yoshimura,[a] and Masahiko Tanaka[b]

[a]Materials and Structures Laboratory, Tokyo Institute of Technology, Nagatsuta 4259, Midori-ku, Yokohama 226-8503, Japan; [b]Institute of Materials Structure Science, High-Energy Accelerator Research Organization, Oho 1-1, Tsukuba 305-0801, Japan (shimizu@lipro.msl.titech.ac.jp).

Iron cobaltite, $Fe_{1.2}Co_{1.8}O_4$, is a mixed-valence compound with the spinel structure. The cation distribution between tetrahedral A and octahedral B sites as well as the valence states of Co and Fe ions are indispensable to the interpretation of the magnetic properties of cobaltites.

The site occupancy of Fe and Co ions was determined with the anomalous scattering effects of synchrotron X-rays. Although it is generally difficult to grow single crystals of cobaltites, fortunately single crystals of $Fe_{1.2}Co_{1.8}O_4$ could be synthesized by the hydrothermal reaction. Diffraction data were collected at λ = 1.6182 Å, by using a vertical-type four-circle diffractometer at BL-10A in the Photon Factory. The chemical formula obtained in site-occupancy refinements is $[Fe_{0.72(4)}Co_{0.28}]^A[Fe_{0.48}Co_{1.52}]^BO_4$.

In order to determine the valence states of Fe and Co ions, the measurements of X-ray absorption near edge structure (XANES) and X-ray magnetic circular dichroism (XMCD) spectra were performed at Fe *K* and Co *K* edges at BL-3A. The Fe *K* XANES spectra indicate that all Fe ions exist as trivalent ones. On the other hand, a ratio of divalent and trivalent Co ions was estimated to be Co^{2+} : Co^{3+} = 1 : 8 from the Co *K* XANES data. The intensity variation of XMCD signals was used to determine the valences of Co ions on individual sites. Since the main-edge peak of XMCD spectra has been reported to originate Co^{2+} ions in the B sites for a series of iron-cobaltite studies [1], the occupation of Co^{2+} in $Fe_{1.2}Co_{1.8}O_4$ was determined from the estimation of the peak height. The results shows that only Co^{2+} ions occupy the A sites.

Thus, it is finally suggested that the most plausible chemical formula is $[Fe^{3+}_{0.72(4)}Co^{2+}_{0.28}]^A[Fe^{3+}_{0.48}Co^{2+}_{0.72}Co^{3+}_{0.80}]^BO_4$.

References

1 Kita, N., Shibuichi, N. and Sasaki, S. (2001) *J. Synchrotron Rad.*, **8**, 446-448.

PO7

FERROMAGNETIC ORDERING MODEL OF A $Co_xTi_{1-x}O_2$ THIN FILM (x = 0.07)

Norio Shimizu,[a] Satoshi Sasaki,[a] Takayasu Hanashima,[a] and Kouji Yamawaki[a]

[a]Materials and Structures Laboratory, Tokyo Institute of Technology, Nagatsuta 4259, Yokohama 226-8503, Japan (shimizu@lipro.msl.titech.ac.jp).

A Co-doped TiO_2 (anatase) thin film was discovered as a ferromagnetic and transparent semiconductor having T_c above 400 K [1]. The ferromagnetic properties were confirmed by hysteresis on the M-H loop from magnetic response measurements, hysteresis of Kerr loops or vibrating sample magnetometry.

Recently, fluorescence X-ray magnetic circular dichroism (XMCD) and absorption spectra at the Co *K* absorption edge were measured for a Co-doped anatase thin film on a $LaAlO_3$ (001) substrate [2]. Negative-to-positive dispersion-type XMCD spectra were clearly observed at E = 7.725 keV, suggesting the ferromagnetism at room temperature and unlikelihood on the existence of Co-metal clusters. XANES spectra support the Co^{2+} oxidation state and participation of a partial structure of ilmenite-type $CoTiO_3$.

We have proposed a crystal structure of Co-doped anatase films and the ferromagnetic order scheme by Co-Ti-O polysynthetic twin lamellae. A (012) $CoTiO_3$ layer interstitially distributes parallel to the (001) plane of anatase and replaces a quarter of the anatase cell at intervals of three and half times of the cell along the ***c*** axis. Thus, our sample has a CoO/TiO_2 ratio of 1/(4n+1) (n = 3) and $c = (2n+1)c_{an}/2$, which gave the best magnetic property as a result of the combinatorial crystal growth. The cell dimensions are a = 7.6, b = 3.8 and c' = 33 Å (c = 66 Å). The thin film forms an antiphase domain (APD), having (1) a repetition of 3.5 unit cells of TiO_2 toward the $\boldsymbol{c}_{an}$ axis, (2) an antiphase relationship by 2_1 screw rotation and (3) an out-of-step of $a_{an}/2$ for the APD boundary.

The above geometrical relationship is known as the polysynthetic twinning or tropochemical cell-twinning (TCT) [3]. The magnetic moments of Co^{2+} in $CoTiO_3$ are ferromagnetically coupled within a layer, where the direction of the magnetic moment lies along the ***c*** axis perpendicular to the plane of the Co-Ti-O layer. The adjacent Co-Ti-O layers are far enough to prevent the antiferromagnetic interaction. The isolated Co-Ti-O layer characterizes the magnetic moments of Co^{2+} by in-plane ferromagnetic ordering and is defined as the "ferromagnetic lamella".

References

1 Matsumoto, Y. *et al* (2001) *Science* **291**, 854-856.
2 Shimizu, N. *et al.* (2004) *J. Phys. Soc. Jpn*, **73**, *in press*.
3 Takéuchi, Y. (1997) *Tropochemical Cell-Twinning*, *MSMR Monographs*, Terra Scientific Publishing Co., Tokyo.

PO8

CRYSTAL STRUCTURE OF 2-AMINO-N-(2-CHLOROPHENYL)-5,6-DIHYDRO-4H-CYCLOPENTA[b]THIOPHENE-3-CARBOXAMIDE.

K.A.Nirmala,[a] Vasu,[b] S.Mohan,[c] J.Saravanan,[d] Deepak Chopra[e]

[a]professor, dept. physics, Bangalore University, Bangalore-560056, [b]Vivekananda degree college Malleshwaram west, Bangalore-560055, [c]P.E.S college of Pharmacy Hanumanthanagar Bangalore-560050, [d]M.S.Ramaiah college of pharmacy, Bangalore-560054, [e]Indian Institute of Science, Solid State Chemistry Unit, Bangalore-560012, (nirmalaka47@yahoo.com)

Schiff bases and their derivatives of thiophene possess antibacterial, antitubercular and antifungal properties[1,2,3]. Sulphur containing Schiff bases are most effective. The title compound shows the above mentioned properties. In view of this application of the compound, crystal and molecular structure work by X-ray diffraction method was taken up to understand the conformational aspects. The title compound synthesised by refluxing cyclopentanone and o-chloroacetanilide with diethylamine, sulphur powder with ethanol. Pale green crystals of the compound were grown by slow evaporation method using N,N-dimethyl Formamide and ethanol (1:1) as the solvents. The single crystal X-ray data was collected on a SMART AXX CCD detector. The crystals are in monoclinic system of space group $P2_1/c$ with two crystallographically independent molecules. The structure was solved using WINGX(1.64). The lattice parameters a =9.939(3)Å, b=29.449(8) Å, c=9.747(3) Å, β=111.912(4)°. The refinement gave a R-value 0.0568 for 5215 unique reflections.

The torsional angles between the thiophene moiety and the chlorophenyl ring in the 2 molelcules is -178.9(3)° and 173.3(3) ° respectively, thus indicating extensive electron delocalization over the entire molecule. There exists strong and highly directional intra and inter-molecular N-H...O hydrogen bonds which is responsible for the packing of molecules leading to needle crystals.

We kindly acknowledge DST(IRPHA) and Prof.T.N.Guru Row IISc.,(SSCU) in helping the data collection.

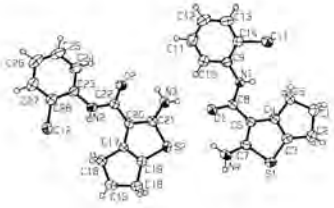

Referecnes

1 Csaszar,J.,&Morvay,J.(1983). Acta Pharmaceutica. Hungarica. 53(5),121-128.

2 Lakshmi,V.V., Sridhar, P.& Polasa,H.(1985). Indian J. of Pharmaceutical Sciences. 47,202-204.

3 Cohen,V.I., Rist,N.& Duponchel,C.(1977) J. of Pharmaceutical Sciences. 66, 1322-1334.

DEGREE OF DISORDER IN SPINEL-TYPE $(Mn,Zn,Fe)_3O_4$ EXAMINED BY THE TWO-WAVELENGTH ANOMALOUS DISPERSION METHOD

Syoichi Sakurai,[a] Satoshi Sasaki,[a] Kouji Yamawaki,[a] Takayasu Hanashima,[a] and Norio Shimizu[a]

[a]Materials and Structure Laboratory, Tokyo Institute of Technology, Nagatsuta 4259, Yokohama 226-8503, Japan (sasaki@n.cc.titech.ac.jp)

The spinel structure is divided into two extreme types in cation distribution between tetrahedral A and octahedral B sites. One is normal-spinel type of $[Y]^A[ZZ]^BO_4$ and the other is inverse-spinel of $[Z]^A[YZ]^BO_4$, where Y and Z are different kinds of cations. There are some reports on the existence of temperature dependence on the cation distribution in Mn ferrites [1,2]. It is an obvious result that the Mn-Zn-Fe ferrite synthesized by the Bridgman method and used for videotape recorder's heads belongs to a normal-spinel type of $[Mn_{0.54}Zn_{0.34}Fe_{0.12}]^A[Zn_{0.01}Fe_{1.99}]^BO_4$ [3]. However, recent EXAFS analyses have reported different cation distributions such as $[Mn_{0.25}Zn_{0.35}Fe_{0.40}]^A[Mn_{0.40}Fe_{1.59}]^BO_4$ (aqueous solution; heating at 500°C) and $[Mn_{0.21}Zn_{0.52}Fe_{0.27}]^A[Mn_{0.34}Fe_{1.66}]^BO_4$ (solid reaction) [4].

Since the cation distribution attracts our interest in understanding the magnetic properties of ferrites, it has been investigated with the two-wavelengths anomalous dispersion (TWAD) method of synchrotron x-rays [5]. Single crystals were grown in evacuated silica tubes at 1373 K for 180 hours. The chemical formula was obtained from the EDX analysis. The cell dimension and u parameter are a = 8.5000(5) Å and u = 0.2610(2), respectively. Diffraction experiments for $Mn_{0.80}Zn_{0.18}Fe_{2.02}O_4$ were performed using a spherical single crystal of 0.1 mm in diameter. Synchrotron experiments were carried out in a four-circle diffractometry at BL-10A of the Photon Factory. The wavelengths used in this study are 1.7535 and 1.2934 Å, which are 0.01 Å longer than those at Fe K and Zn K absorption edges, respectively. The TWAD method is indispensable to a ternary Mn-Zn-Fe system and allowed us to determine the cation distribution accurately with a large difference in atomic scattering factors. Least-squares refinements gave a final chemical formula of $[Mn_{0.71}Zn_{0.10}Fe_{0.19}]^A[Mn_{0.09}Zn_{0.08}Fe_{1.83}]^BO_4$, showing that about 17% of Mn and Zn ions exists as the inverse-spinel ingredient.

References

1 Yasuoka, H., Hirai, A., Shinjo, T., Kiyama, M., Bando, Y. and Takada, T. (1967) *J. Phys. Soc. Jpn.* **22**, 174-180.

2 Ohara, H., Mizobuchi, T., Matsumoto, K. and Sasaki, S. (2000) *Ferrite: Proc. of 8th Intern. Conf. Ferrite (ICF-8)*, 223-225

3 Okita, A., Saito, F., Sasaki, S. Toyoda, T. and Koinuma, H. (1998) *Jpn. J. Appl. Phys.* **37** (6A), 3441-3445.

4 Calvin, S., Carpenter, E.E., Harris, V.G. and Morrison, S.A. (2002) *Appl. Phys. Lett.* **81** (20), 3828-3830.

5 Tsukimura, K. and Sasaki, S. (2000) *Phys. Chem. Minerals* **27**, 234-241.

PO10

X-RAY STRUCTURAL STUDY OF IN-PLANE ATOMIC ARRANGEMENTS IN THE LAYERED COMPOUNDS M_xTiS_2 (M=Cu, Ni, Co)

Ken-ichi Ohshima, Yoshinobu Kasuga, Tomoko Kusawake, Makoto Yasuda and Hiroki Uratani

Institute of Materials Science, University of Tsukuba, Tsukuba 305-8573, Japan (ohshima@bk.tsukuba.ac.jp)

The layered disulphides of transition metals are intercalated with various ions and molecules between the sulphur layers which are normally separated throughout the Van der Waals interaction. These intercalation compounds are of interest because of their quasi-two-dimensional (2D) properties and because of their application as electrodes in cell.

We have performed the X-ray diffraction study to measure composition dependences of diffuse or superlattice scattering for single crystals of M_xTiS_2 (M=Cu, Ni, Co) compounds for understanding the local or ordered arrangements of the intercalated M atoms at room temperature.

1) Cu_xTiS_2 ($x<0.37$) : Two types of diffuse maximum due to the different in-plane correlations of Cu atoms appeared, depending on the composition. The maxima appeared at 1/2,0,1/2, 0,1/2,1/2 & equivalent positions and at 1/3,1/3,1/2,2/3,2/3,1/2 and equivalent positions for the lower content and for the highest composition, respectively. For the intermediate composition, the types of diffuse scattering coexist, with intensities depending on the composition. We expect the following in-pane ordered phases : 2x2 and $(3^{1/2}x3^{1/2})R30^\circ$ structures in Wood notation, whose stoichiometric composition x corresponds to 1/4 and 1/3, respectively [1,2].
2) Ni_xTiS_2 ($x<0.37$) : One type of diffuse maximum appeared at 1/3,1/3, 1/2, 2/3,2/3,1/2 and equivalent positions at around x=0.33. There is no extra scattering at lower content.
3) Co_xTiS_2 ($x<0.33$) : Two types of superlattice reflection due to the atomic ordered arrangements of Co atoms appeared at 1/2,0, 1/2, 0, 1/2, 1/2 & equivalent positions and 1/3,1/3, 1/2, 2/3,2/3,1/2 & equivalent positions for x= 1/4 and 1/3, respectively. As expected in the compounds Cu_xTiS_2, in-pane ordered phases, 2x2 and $(3^{1/2}x3^{1/2})R30^\circ$ structures, are confirmed to exist in the compounds Co_xTiS_2 at x=1/4 and 1/3.

Observed in-plane diffuse intensities are compared with the calculated ones, using a linearized mean-field approximation for the correlations of a binary Ising system well developed above T_c developed by Class and Moss [3].

References

1 Kusawake, T., Takahashi, Y., Ohshima, K. and Wey, M.-Y. (1999) *J. Phys.: Condens. Matter* **11**, 6121-6128.
2 Kusawake, T. and Ohshima, K. (2003) *J. Phys. Soc. Jpn.* **72**, 2829-2831.
3 Moss, S. C. and Clapp, P. C. (1966) *Phys. Rev.* **142**, 418-427.

PO11

CRYSTAL STRUCTURE OF 7-METHYL 6, 8-DINITRO 4-BROMOMETHYL COUMARIN

K.V.Ajuna Gowda[a,c], T.N.Guru Row[b], N.C.Shivaprakash[c] and M.V. Kulkarni[d]

[a]Department of Physics, S.J.C.I.T. ,Chickballapur, Kolar-562 101, India, [b]Solid State and Structural Chemistry Unit, Indian Institute of Science , Bangalore-560 012, India, [c]Department of Instrumentation , Indian Institute of Science , Bangalore-560 012, India, [d]Department of Chemistry, Karnataka University, Dharwad-580 003, India (shiv@isu.iisc.ernet.in).

Attempted nitration of 7-methyl-4-bromomethyl coumarin has resulted in the formation of 6,8-nitro product which has been confirmed by spectral methods[1]. The compound crystallizes as colourless plates in orthorhombic with space group Pbac and cell dimensions a = 8.122(2), b = 11.091(4), c = 27.723(6) Å. The Structure was solved by SHELX97 program (Sheldrick 1997) and refined to a R factor of 0.059. We have noticed that the allylic bromine is not in the plane of coumarine but is oriented at an angle of 104° with respect to the pyrone ring. The compound stabilzes with presence of four Br...Br weak interactions. The details of weak interactions are discussed in this paper.

References

1 Clayton A, (1910), J Chem Soc , 97, 1397- 1399.

PO12

CRYSTALLOGRAPHIC ANALYSIS OF HYDROGEN BONDING IN SERIES OF CHOLEST-BASED STEROIDAL MOLECULES

Dinesh* and Rajnikant

Condensed Matter Physics Group, Department of Physics, University of Jammu, Jammu Tawi 180 006, INDIA. (dine_nesh@rediffmail.com)

The work reported in this paper is based on a comparative analysis of C-H...O, N-H...O and N-H...N hydrogen bonded interactions which play an indispensable role in organic molecular assemblies. Both intra and intermolecular interactions have been examined in case of a series of cholest-based steroidal molecules. In view of some recent spurt in literature on weak interactions and their role in organic molecular assemblies, we have selected the C-H...O hydrogen bond as a prototype of the entire interaction type and have analysed it in case of series cholest-based steroids whose three-dimensional molecular and crystal structures have been elucidated by us. Taking into account the generalized distance and angle cut-off criterion for the intra and intermolecular interactions, as proposed by Desiraju and Stenier (1999), we have found that both these kinds of interactions in cholest-based steroids fall in the range of "intermediate to strong and weak interactions". Graphical projection of interaction data further authenticate our findings. Details will be presented.

References

1 Desiraju, G.R. & Steiner, T. (1999) *The weak hydrogen bond in structural chemistry and biology*, *IUCr, Oxford Press*, 10-11.

PO13

NEUTRON STUDIES OF CLUSTER BEHAVIOUR OF $Pd_{40}Ni_{22.5}Fe_{17.5}P_{20}$ SPIN GLASS

E.P. Gilbert,[a] R. Woodward,[b] D.H. Yu,[a] and R. A. Robinson[a]

[a]Bragg Institute, Australian Nuclear Science and Technology Organisation, Lucas Heights, NSW, 2234, Australia;
[b]School of Physics, University of Western Australia, Perth, 6009, Australia.

Magnetic metallic glasses have enormous technological importance in, for example, magnetic recording, magnetic refrigeration and the construction of electrical transformers and motors. Traditionally these amorphous materials were prepared by melt spinning (10^6 K s^{-1}) to form ribbons.

Bulk magnetic metallic glasses based on the quaternary alloy Pd-Ni-Fe-P exhibit interesting phase behaviour depending on temperature and applied magnetic field. For the alloy of $Pd_{40}Ni_{22.5}Fe_{17.5}P_{20}$, paramagnetic, superparamagnetic, ferromagnetic and spin glass regions are all evidenced [1]. It is proposed that the complex phase transitions in these kinds of materials may be due to the materials not being truly amorphous. The possible large-scale chemical inhomogeneities within the alloy may lead to clustering of magnetic ions. On cooling, frustration due to competing interactions between clusters may result in the observed spin glass-like behaviour.

We will present our first neutron-studies, employing small-angle neutron scattering, with polarised incident beam, on the alloy of $Pd_{40}Ni_{22.5}Fe_{17.5}P_{20}$ as a function of temperature (RT to 5K) and applied magnetic field (0 to 5T).

References

1 Shen T. D., Schwarz R. B. and Thompson J. D., *J. Appl. Phys.* **85**, 4110-4119, 1999.

PO14

AB-INITIO PHASING AT 1.7Å RESOLUTION OF A PROTEIN FERREDOXIN I BY COMBINED REAL SPACE – RECIPROCAL SPACE APPROACH

Krishna Chowdhury,[a] Soma Bhattacharya, [b] and Monika Mukherjee [a]

[a]Department of Solid State Physics, Indian Association for the Cultivation of Science, Kolkata 700 032, India; [b]Department of Physics, St. Xavier's College, Kolkata 700 016. (sspmm@iacs.res.in)

Ferredoxin I, an iron containing protein, is capable to interact and form electron transfer complexes with many different proteins and it's three dimensional structure is of fundamental importance to help these interactions. The structure of Ferredoxin I has been successfully redetermined ab-initio from a single native data set by a combined real space- reciprocal space approach. The protein contains 97 amino acid residues (733 non-H atoms) and a [2Fe-2S] cluster with 81 solvent water molecules. The complex crystallizes in space group $P2_12_12_1$ with cell parameters a=31.0, b=39.2, c=83.5Å and Z=4. X-ray diffraction data [1] extending to 1.7Å was obtained from protein data bank (PDB code: 1a70).

The direct method approach of MULTAN88 generated several thousand phase sets at 1.7Å with 1000, 1500, 2000 largest |E| values. The phase set with lowest mean phase error (MPE) of 68.91° gave an E-map that indicated positions of two Fe atoms. Successive weighted Fourier maps could reveal [2Fe-2S] bridge and few small fragments but not the entire protein model. The initial phase estimates using (Fe+4S) and (Fe+6S) coordinates obtained from the Fourier maps were subjected to 400 – 500 cycles of refinement with options for low density elimination and histogram matching using the program PERP [2]. MPE dropped from 62.2° to 45.5° and the map correlation coefficient (MCC) increased from 0.421 to 0.651 for 3922 reflections with |E|>1.0. The resultant phase set could yield an interpretable electron density map. The study reveals that even with knowledge of phases for 2% of the scattering material the real space – reciprocal space phasing approach can lead to proper model building for proteins diffracting at low resolution of 1.7Å.

References

1 Binda, C., Code, A., Aliverti, A., Zanetti, G., and Mattevi, A. (1998) Acta Cryst **D54**, 1353 – 1358.

2 Refaat, L.S., Tate, C., Woolfson, M.M. (1996) Acta Cryst. **D52**, 1119– 1124.

PO15

DIFFUSE NEUTRON SCATTERING FROM d-BENZIL, $C_{14}D_{10}O_2$, USING TIME-OF-FLIGHT LAUE DIFFRACTION

T. R. Welberry[a] D. J. Goossens[a] W. I. F. David[b] M. J. Gutmann[b] M. J. Bull[b] and A. P. Heerdegen[a]

[a]Research School of Chemistry, Australian National University, Canberra ACT 0200, Australia; [b]ISIS, Rutherford Appleton Laboratory, Milton, Didcot, Oxfordshire, UK (goossens@rsc.anu.edu.au).

Diffuse neutron scattering data have been recorded for the molecular crystal d-benzil, $C_{14}D_{10}O_2$, using time-of-Flight Laue diffraction on SXD and PRISMA at ISIS. Using SXD it was possible to access a large fraction of the total three-dimensional reciprocal space out to a **Q** value of 15 $Å^{-1}$, using only four individual exposures and by making use of the -3m Laue symmetry of the crystal. By binning the scattered data according to incident neutron energy, patterns were obtained using neutrons in the range of ~20 meV to 150 meV, which showed little sign of inelastic effects and so could be compared with previously analysed X-ray data. For neutron energies of <20 meV, inelastic effects were observed, which have been used to obtain an estimate for the energy of phonons associated with a particular vibrational mode. A model previously derived from analysis of X-ray data observed over a limited range of **Q** has been used to calculate neutron patterns over the full **Q** range. Comparison with the neutron data showed that while the model from X-ray data gives a good description of the form of the diffuse patterns, the magnitudes of the atomic displacements are underestimated by a factor of ~2.25.

We will discuss our latest results which test our model by using SXD to explore the temperature dependence of the diffuse scattering. Further, PRISMA has been used to measure phonon energies directly, allowing comparison with those energies inferred from the diffuse scattering.

S-SAD PHASING BY OASIS2004

J. W. Wang, Y. X. Gu, C. D. Zheng, F. Jiang, and H. F. Fan

Chinese Academy of Sciences, Institute of Physics, Beijing, 100080, P. R. China (jwwang@cryst.iphy.ac.cn).

OASIS [1] is a direct-method program in the CCP4 suite [2] for resolving the phase ambiguity in single-wavelength anomalous diffraction and in single isomorphous replacement of proteins. It has recently been modified in order to make the phasing procedure more efficient and automatic. The main modifications include: (1) automatically adjust the standard deviation D in the expression of lack-of-closure error; (2) fitting the direct-method figures-of-merit to a uniform distribution before they are output to density modification.

The new version of OASIS has been tested with sulphur single-wavelength anomalous diffraction (S-SAD) data from the protein Glucose isomerase and the protein Xylanase [3]. Diffraction data sets used in the following test were kindly provided by Dr. Z. Dauter.

Glucose isomerase crystallizes in space group I222 with unit cell a=92.90, b=97.95 c=102.71. Diffraction data at 2Å resolution were collected with synchrotron radiation at λ=1.54Å. The Bijvoet ratio (<ΔF>/<F>) is 0.60%, which is a rather low value among the others. S atoms were located by the program SHELXD, then the phases of the whole set of reflections were derived by *OASIS*. After density modification using the program DM in the CCP4 suite, the average phase error was decreased to 44°. The automatic model-building program ARP/wARP found 386 residues of the total of 388.

Xylanase crystallizes in space group $P2_1$ with unit cell a=41.19, b=67.18 c=50.88. beta=113.5°. Diffraction data at 1.63Å resolution were collected with synchrotron radiation at λ=1.743Å. The Bijvoet ratio (<ΔF>/<F>) is 0.69%. The 5 independent S atoms were located by SHELXD. OASIS phasing followed by DM led to an average phase error of 55°. The resultant map is easily interpreted.

The new version of *OASIS* will be released in due course, presumably first on the webpage *http://cryst.iphy.ac.cn*.

References

1 Hao, Q., Gu, Y. X., Zheng, C. D. & Fan, H. F. (2000) *J. Appl. Cryst.* **33**, 980-981.
2 Collaborative Computational Project, Number 4. (1994). *Acta Cryst.* **D50**, 760-763.
3 Ramagopal. U. A., Dauter, M., Dauter Z. (2003) *Acta Cryst.* **D94**, 1020-1027.

PO17

TREATMENT OF EXPERIMENTAL ERRORS IN DIRECT-METHOD SAD PHASING

S. Huang[a], J. W. Wang[b], Y. X. Gu[b], D. C. Xian[a], H. F. Fan[b] & M. M. Woolfson[c]

[a]Institute of High Energy Physics, Chinese Academy of Sciences, Beijing 100039, China. [b]Institute of Physics, Chinese Academy of Sciences, Beijing 100080, China. [c]Department of Physics, University of York, YO1 5DD, UK
(shuang@cryst.iphy.ac.cn)

In treating experimental errors in the magnitude of normalized structure factors, a weighting function is given to the three phase structure invariants $|E_{-h'}\cdot E_{h'}\cdot E_{h-h'}|$. The function is expressed as

$$W=\exp(-kV^{\frac{1}{2}})$$

where

$$V=\left(\frac{\sigma_{E_{-h'}}}{E_{-h'}}\right)^2+\left(\frac{\sigma_{E_{h-h'}}}{E_{h-h'}}\right)^2+\left(\frac{\sigma_{E_{h'}}}{E_{h'}}\right)^2+\left(\frac{\sigma_{E_{-h+h'}}}{E_{-h+h'}}\right)^2$$

and k is a constant to be determined in each test case.

Experimental single-wavelength anomalous diffraction (SAD) data from two proteins were used in our test:

Azurin [1] crystallizes in space group $P4_122$ with unit cell a=b=52.65, c=100.63Å. There is one Cu atom (anomalous scatterer) in the asymmetric unit. The Bijvoet ration $\langle\Delta F\rangle/\langle F\rangle$ at λ=0.97Å is 1.44%.

Rusticyanin [2] crystallizes in space group $P2_1$ with unit cell a=32.34, b=60.68, c=38.01Å, β=107.82°. There is one Cu atom (anomalous scatterer) in the asymmetric unit. The Bijvoet ration $\langle\Delta F\rangle/\langle F\rangle$ at λ=1.376Å is 2.36%.

Phases were derived by the program OASIS and improved by the program DM, both are supported programs of the CCP4 suite [3]. Test for each SAD data set was performed by comparing results of two identical phasing processes, one with and the other without the weighting function. Preliminary results showed that the use of the weighting function led to smaller averaged phase error and better electron density maps.

References

1 Dodd, F., Hasnain, S. S., Abraham, Z. H., Eady, R. R. & Smith, B. E. (1995). *Acta Cryst.* D51, 1052-1064.

2 Harvey, I., Hao,Q., Duke, E.M. H., Ingledew,W. J. & Hasnain, S. S. (1998). Acta Cryst. D54, 629-635.

3 Collaborative Computational Project, Number 4. (1994). *Acta Cryst.* **D50**, 760-763.

EFFECT OF SULFUR-ANOMALOUS SCATTERING SIGNAL ON SAD PHASING IN THE PRESENCE OF IRON ATOMS

D. Q. Yao[a], J. R. Chen[a], J. W. Wang[b], C. D. Zheng[b], Y. X. Gu[b], F. Jiang[b], H. F. Fan[b] & D. C. Xian[a]

[a] Institute of High Energy Physics, Chinese Academy of Sciences, Beijing 100039, China.
[b] Institute of Physics, Chinese Academy of Sciences, Beijing 100080, China.
(dqyao@cryst.iphy.ac.cn)

Recently there is a revival of single-wavelength anomalous diffraction (SAD) phasing in protein crystallography. So far in practice, successful SAD phasing accompanied with a Bijvoet ratio (<|DF|>/<F>) greater than 0.6%. The present work is to examine the effect of weak sulfur-anomalous scattering signals on SAD phasing in the presence of much stronger anomalous scattering atoms Fe. Test was performed with SAD data of the protein CAUFD. The experimental diffraction data was kindly provided by Dr. Z. Dauter.

CAUFD [1] crystallizes in space group $P4_32,2$ with unit cell a=b=33.95, c=74.82Å. Diffraction data at 0.94Å resolution were collected with the synchrotron radiation at λ=0.88Å. There are 8 Fe and 8 S atoms in the asymmetric unit. The Bijvoet ratio contributed from the Fe-substructure is 3.6%, while that from the S-substructure is 0.55%. Phases were derived based on the known substructure of anomalous scatterers by the program OASIS and improved by the program DM, both are supported programs in the CCP4 suite [2]. The result of SAD phasing based on Fe-anomalous scattering signals and that based on "Fe+S"-anomalous scattering signals were compared. Although either result led to nearly the complete structure, the electron density map of the latter contains evidently fewer spurious peaks. This implies that the contribution of sulfur-anomalous scattering signals with Bijvoet ratio as low as 0.55% is not negligible even in the presence of much higher anomalous scattering signals from Fe with the Bijvoet ratio as large as 3.6%.

Comparison of phase errors, correlation coefficients and electron density maps will be shown.

References

1 Dauter, Z., Wilson, K. S., Sieker, L. C., Meyer, J. & Moulis, J.-M. (1997). *Biochemistry*, **36**, 14493-14502.
2 Collaborative Computational Project, Number 4. (1994). *Acta Cryst.* **D50**, 760-763.

PO19

SYNCHROTRON X-RAY POWDER DIFFRACTION STUDY OF THE STRUCTURAL PHASE TRANSITION IN $CaBr_2$

Brendan J. Kennedy[a] and Christopher J. Howard[b]

[a]School of Chemistry, The University of Sydney, Sydney, NSW 2006 Australia; [b]Australian Nuclear Science and Technology Organisation, Private Mail Bag 1, Menai, NSW 2234, Australia (cjh@ansto.gov.au).

The structures of $CaBr_2$ have been investigated using high resolution powder synchrotron X-ray diffraction methods between room temperature and 800 °C. At room temperature $CaBr_2$ has an orthorhombic $CaCl_2$-type structure (*Pnnm* Z = 2) with *a* = 6.8847(1) *b* = 6.5806(1) and *c* = 4.3477(1) Å. Heating above 560 °C results in a continuous transition to a tetragonal rutile type structure (*P42/mnm* Z = 2) with *a* = 6.81095(7) and *c* = 4.41770(5) Å at 650 °C. Investigation, through either spontaneous strain or octahedral tilt angle, suggests that the transition is close to second order in nature, although the contribution from the sixth order term in the Landau potential cannot be neglected.

PO20

CHARACTERIZATION OF THE Δ' PHASE- MATRIX INTERFACE IN 1420 ALUMINIUM ALLOYS BY SAXS

Chai Zhi-Gang

Beijing Aeronautical Technology Research Center, Beijing 100076
People's Republic of China (chaizg@sina.com.cn)

The interface between the δ' phase and matrix in 1420 aluminium alloys, which were treated by 1) aging or 2) retrogression and re-aging (RRA) methods, have been characterized by means of the small angle X-ray scattering (SAXS) technique. The results indicate that a transition zone exists between the δ' phase and matrix for both treatment methods. The existence of a transition zone implies that the δ' phase is precipitated by spinoidal decomposition. The results also show that the RRA treatment can effect rapid disappearance of the interfacial transition zone.

PO21

CATION ORDERING IN PENTLANDITE $(Fe,Ni)(Fe,Ni)_8S_8$

Kia S. Wallwork[a], Allan Pring[b] and Christophe Tenailleau[b]

[a]ANSTO, PMB 1, Menai, NSW, 2234; [b]South Australian Museum, North Terrace, Adelaide, SA, 5000 (kiw@ansto.gov.au)

Pentlandite is the primary nickel mineral in nearly all Ni-sulphide deposits and is thus of enormous economic importance.

Pentlandite adopts a cubic structure based on a ccp array of S atoms with metals in $^1/_2$ the tetrahedral sites and in $^1/_8$ of the octahedral sites. Thus the formula can be written as $M^oM^t{}_8S_8$ where M^t is the metal in tetrahedral sites and M^o is a metal in the octahedral site. The structure consists of cubic clusters of tetrahedral metal ions $[M_8S_6]$ that are linked to MS_2 octahedra. Natural pentlandite contains roughly equal amounts of Fe and Ni, together with small amounts of Co and Cu, but pure Fe and Ni end-members are not stable.

Single crystal X-ray diffraction studies of two natural samples indicate that Fe can be preferentially ordered into the octahedral site, a process that occurs at lower temperatures [1,2]. Tsukimura [1] showed that the ordering was destroyed by annealing at 250 °C. Strain is associated with ordering of Fe/Ni between octahedral and tetrahedral sites and leads to an increase in the cell parameter. Etschmann *et al.* [3] and Wang *et al.* [4] annealed a number of synthetic pentlandite samples at low temperature (150 – 200 °C) for periods of up to five months and noted changes in the cell parameters that indicate some cation ordering may have occurred.

Using this collection of low temperature anneal/quench samples we have determined the cation distribution between the octahedral and tetrahedral sites and thus be able to determine the kinetics of cation ordering and the activation energy. This pentlandite/pyrrhotite system is one of the few sulphide systems in which cation ordering has been investigated. The low temperature (250 °C) at which the cation ordering is destroyed is indicative of the high metal mobility in sulphides at low temperatures. This can be compared with the rock forming silicates were cation ordering is destroyed at temperatures around 600 °C.

Due to the similarity of the Fe and Ni scattering curves for X-rays high resolution powder diffraction data were collected at a number of different energies in order to exploit anomalous dispersion effects.

References

1 Tsukimura, K. (1989) *Mineralogical Journal*, 14, 323-337.
2 Tsukimura, K. and Nakazawa, H. (1984) *Acta Crysatallographica*, B40, 364-367.
3 Etschmann B., Pring, A., Putnis A., Grguric, B.A., and Studer, A. (2004) *American Mineralogist*, 89, 39-50.
4 Wang, H., Ngothia, Y., O'Neill, B., Etschmann, B. and Pring A. (2003) Chemeca 2003, Proceedings Volume.
5 Zhang, Y., Wilkinson, A., Nolas, G., Lee, P. and Hodges, J. (2003) *Journal of Applied Crystallography*, 36, 1182-1189.

PO22

THREE-BEAM DIFFRACTION ANOMALOUS FINE STRUCTURE OF THIN FILMS

Hsueh-Hung Wu,[a] Yen-Ru Lee,[a] Hsin-Hung Chen,[a] Wen-Shien Sun,[a] and Shih-Lin Chang[a]

[a]Department of Physics, National Tsing Hua University, Hsinchu, Taiwan, 300, R.O.C. (d893308@oz.nthu.edu.tw)

Different from the usual two-beam DAFS (diffraction anomalous fine structure), we have recently developed the multi-beam DAFS (MDAFS) for observing the local structural environment of resonant atoms. With three-beam diffraction data for different photon energies, the visibility *Rv* of the intensity asymmetry related to the phases of structure-factor triplets involved in the three-beam diffraction can be determined. Analysis based on the dynamical diffraction theory and XAFS gives fine structures of DAFS spectra. In this paper, the three-wave diffractions of (100) *CdTe* thin films epitaxially grown on the (100) *InSb* substrates are measured for different photon energies covering all the L edges of the constituent atoms. The crystallographic phase of structure-factor triplets and the resonance phase shifts influenced by the substrate could be analyzed to give the interface structures in relation to the *CdTe* and *InSb*. Using this MDAFS technique, we have also extracted the information about the fine structures of Cd and Te around the interface.

PO23

CRYSTAL STRUCTURES OF ANHYDROBARAKOL AND ANHYDROBARAKOL HYDROCHLORIDE; AN EVIDENCE OF EXCEPTIONAL C=O/C-OH QUINONE CHARACTERISTIC

P. Chimsook[a], N. Ngamrojnavanich[a], C. Chaichantipyuth[b], N. Chaichit[c], P. Kongsaeree[d], A. Petsom[a], N. Muangsin[a]*

[a]Research Centre for Bioorganic Chemistry, Department of Chemistry, Faculty of Science, Chulalongkorn University, Bangkok 10330, Thailand, [b]Department of Pharmacognosy, Faculty of Pharmaceutical Sciences, Chulalongkorn University, Bangkok 10330, Thailand, [c]Department of Physics, Faculty of Science and Technology, Thammasart University, Bangkok 12121, Thailand, [d]Department of Chemistry, Faculty of Science, Mahidol University, Bangkok 10400, Thailand (44723304@Student.chula.ac.th, Ch_Piti@hotmail.com)

Barakol(**1**), (3a,4-dihydro-3a,8-dihydroxy-2,5-dimethyl-1,4-dioxaphenalene) [1a, 1b], is an active component extracted from *Cassia siamea*. It is used in traditional medicines for treating insomnia and other medicinal conditions [2]. Barakol is unstable and easily converted to anhydrobarakol(**2**). In order to study their physiochemical, physiological and pharmacological properties, anhydrobarakol hydrochloride (**3**), a stable salt form, is prepared. However, these properties are not clearly understood [3a, 3b, 3c, 3d]. The spectroscopic data including NMR and IR are unusual and ambiguous [1b]. The absorption band of C=O stretching at 1676 cm^{-1} was significantly red shifted from that of a typical C=O frequency (~1710 cm^{-1}). Moreover, the IR spectrum of **3** also shows unexpected n(C=O) stretching at 1671 cm^{-1}, similar to that of **2**. Therefore, it is necessary to obtain pure forms of **1** and **2**, and also their crystal structures in order to explain their properties.

We present a preparation method to obtain a pure form of **2** and the first successful crystal structures determination of **2** and **3**. They were crystallized in a monoclinic system, with space group $P2_1/c$ and $P2_1/n$, respectively. Their crystal structures reveal an interesting C=O and C-OH characteristic. As a consequence, the NMR and IR spectroscopic data can be explained. The molecular structure of **2**, shows the elongated C=O bond distance of 1.285(3) Å, which is longer than a normal carbonyl bond of 1.22 Å. For the crystal structure of **3**, it is interesting that C-OH bond distance of 1.3351(6) Å is significant shorter than that of a normal C-OH of hydroquinone (1.40 Å) [4], and dramatic longer than that of C=O in **2**.

Referrences

1 (a) Hassanali-walji, A., King, T.J., Wallwork, S.C. (1969) *J.Chem.Soc.ChemCommun.***12**, 678. (b) Bycroft, B.W., Hassanali-walji, A., Johnson, A.W., King, T.J. (1970) *J.Chem.Soc.* **12**, 1686-1689.

2 Kinghorn, A.D., Balandrin, M.F. (1992) Human Medicinal Agents from Plants (American Chemical Society , Washington, DC).

3 (a) Thongsaard, W., Deachapunya, C., Pongsakorn, S., Boyd, E.A., Bennett, G.W., Marsden, C.A. (1995) *Br.J.Pharmacol.* **114**, 284p. (b) Thongsaard, W., Deachapunya, C., Pongsakorn, S., Boyd, E.A., Bennett, G.W., Marsden, C.A. (1996a) *Pharmacol.Biochem.Behav.* **53**, 753-758. (c) Fiorino, D., Treit, D., Menard, D., Lermer, L. and Phillips, A. (1998) *Behavioural Pharmacology*. **9**, 375-378. (d) Sukma, M., Chaichantipyuth C., Murakami Y., Tohda M., Matsumoto K., Watanable H. (2002) *Journal of Ethnopharmacology*. **83**, 87-94.

4 Gilesdie, R.J., Popelier, P.L.A. Oxford New York: Oxford University Press, 2001.

PO24

THE CLEAVAGE OF DIPEPTIDES BY Co(III) COORDINATION COMPOUNDS

Ivan Bernal*, Manas Saha and Uday Mukhopadhyay

Chemistry Department, University of Houston, Houston, Tx 77204-5003.
(chem4m@pop.uh.edu)

Cleavage of peptide bonds occurs when [Co(tren)Cl2]+ or [Co(trien)Cl2]+ (tren = tris(2-aminoethyl)amine, trien = 1,4,7,10 tetraaza- decane) are allowed to react with dipeptide molecules such as b-alanyl-L-histidine (carnosine), glycyl-DL-methionine and L-alanyl-L-alanine at pH ~7.5. The cationic complexes that contain a fragmented amino-acid residue were isolated as the perchlorate salt or the mixed chloride perchlorate salt. b-alanyl-L-histidine (carnosine) reacts with [Co(tren)Cl2]+ to give the [Co(tren)(histidine)]2+**1** and [Co(tren)(b-alanine)]2+ **2**. Glycyl-DL-methionine reacts with [Co(tren)Cl2]+ or [Co(trien)Cl2]+ to produce [Co(tren)(methionine)]2+ **3**, [Co(tren)glycine]2+ **4** or [Co(trien)(methionine)]2+ **5** and [Co(trien)(glycine)]2+ **6**. Reaction between [Co(trien)Cl2]+ and b-alanyl-L-histidine produces [Co(trien)(histidine)]2+7 and a free b-alanyl molecule. [Co(tren)Cl2]+ or [Co(trien)Cl2]+ reacts with L-alanyl-L-alanine to yield [Co(tren)(alanine)]2+ **8** or [Co(trien)(alanine)]2+ **9**. All these cationic complexes were charactersied by analytical data, spectral studies and crystal structures. The structural illustrations provide important information regarding the mechanism and the streochemical aspects of such reactions. [Co(tren)(histidine)]2+ **1** crystallizes in the enantiomorphic space group P212121. The circular dichromism spectrum for **1** suggests that a very small extent of racemization of the amino acid takes place during the cleavage reaction between [Co(tren)Cl2]+ and b-alanyl-L-histidine. **2** and **5** crystallize in P21/c and **3**, **8** in P21/n space groups, respectively. **7** and **9** crystalize P212121 and P21, respectively. Circular dichroism spectral studies suggest that appreciable racemization of the amino acid takes place during the reaction between [Co(trien)Cl2]+ and b-alanyl-L-histidine and complete racemization was observed in case of reaction between [Co(tren)Cl2]+ and/or [Co(trien)Cl2]+ and L-alanyl-L-alanine.

PO025

STRUCTURAL AND CONFORMATIONAL STUDIES OF DIHYDROPYRIMIDINES

G.Y.S.K. Swamy and K.Ravikumar

Laboratory of X-ray Crystallography, Indian Institute of Chemical Technology, Hyderabad 500 007, India (swamygundimella@yahoo.com)

Quinazolin-4(1H)-ones commonly known as benzpyrimidones, form an important class of heterocyclic compounds. Substituted quinazolin-4(1H)-ones possess a wide range of pharmacological activities, such as antibacterial [1] and anti cancer[2]. Reported here are crystal structure of 2-(4-Dimethylamino-phenyl)-1-phenethyl-2,3-dihydro-1H-quinazolin-4-one and 1-Phenethyl-2p-tolyl-2,3-dihydro-1H-quinazolin-4-one. The structural analysis provides an opportunity to study biological activity and its implication in the structural requirement needed for binding to the receptors.

The most important aspect of the molecules concern from the pharmacological point of view is the disposition of the key functional group, which in turn depends on conformation of the central pyrimidine ring. The central dihydropyrimidine ring in both the structures are affected by conjugation. The sum of the valance angles around the nitrogen atoms N1,N2 & N3 is 360°, indicating that the state of hybridization of these is sp^2. The DHP ring is puckered in such a manner that the atoms N1,C6,C5,C3, & N2 are coplanar with the sixth atom C1 is displaced 0.605Å(0.18Å for compound II) above the least squares plane. The conformation of pyridine ring can be described as a sofa with asymmetric parameters ΔC_1= 6.09(compound I) & 4.73(compound II). Ring planarity with respect to torsion angles was correlated to pharmacological activity. The results were compared with related structural data. The phenethyl group has a fully extended conformation with respect to the central pyrimidine ring(N2-C11-C17-C13 174.95(3)° & 179.3(2)° for compounds I & II respectively). The dimethyl amino group of compound I is coplanar wth the phenyl ring with which it is attached and positioned equatorially at C1 of the dihydropyrimidine ring. This is defined by the average magnitude of C3-N2-C1-C12 and C6-N1-C1-C12 torsion angles(175.34(2)°). In the crystal packing, pseudo dimmers are forming along the a-axis through N-H-...O hydrogen bonding. Other ring conformations along with correlations with other similar structures will be presented.

References

1 Ager, I.R., Harrison, D.R., Kennewell, P.D. & Taylor, J.B. (1977). J. Med. Chem. **20**, 379-386.

2 Skula, S.K., Agnihotri, A.K. & Chowdhary, B.L. (1981). Indian Drugs,**19**, 59-60.

TWO- AND THREE- DIMENSIONAL ORGANICALLY TEMPLATED OPEN-FRAMEWORK LANTHANIDE SULFATES: EFFECTS OF "LANTHANIDE CONTRACTION" ON THE FRAMEWORK ARCHITECTURES**

Jiang-Gao Mao and Yan-Ping Yuan

State Key Laboratory of Structural Chemistry, Fujian Institute of Research on the Structure of Matter, Chinese Academy of Sciences, Fuzhou 350002, P. R. China (mjg@ms.fjirsm.ac.cn)

Materials with open-framework and microporous structures are promising candidates for hybrid composite materials in electro-optical and sensing applications in addition to their potential applications in the areas of catalysis, ion exchange, intercalation chemistry, photochemistry, and materials chemistry.[1-2] The study of metal open architectures making use of other oxy-anions such as group 16 elements has started to be flourishing since the pioneering works of Rao et al. on the preparation of organically templated open-framework cadmium sulfates.[3] The exploration for the organically templated metal sulfates has been expended to lanthanide and actinide metals recently, which exhibit different coordination chemistry from that of transition metals. An open framework solid of scandium sulfate-phosphate was reported by Wright's group.[4] One-, two- and three-dimensional organically templated lanthanum(III)) sulfates have also been structurally characterized, the open frameworks isolated are closely related to the "structure directing" template cations as well as the reaction conditions.[5] Herein we report two Nd(III) sulfates with layered and 3D open frameworks, and a layered Er(III) sulfate, namely, three-dimensional $\{C_2H_{10}N_2\}_2Nd_2(SO_4)_5(H_2O)_2$ **1**, $\{C_2H_{10}N_2\}_3Er_2(SO_4)_6(H_2O)_2$ **2** and $\{C_4H_{16}N_3\}Nd(SO_4)_3(H_2O)$ **3** with a layered structure.

All three lanthanide sulfates were synthesized by a similar method. A mixture of lanthanide((III) oxide, sulfuric acid, organic amine and 10 ml of water with a molar ratio of Ln: amine : sulfate = 1: 3 : 14 was sealed into an autoclave equipped with a Teflon liner (25 ml) and heated at 110 °C for 2 days. Needle shaped crystals of **1**, **2** and **3** were obtained as pure phases based on XRD powder diffraction and element analysis. Their structures have been established by single crystal diffraction.[6]

References

1 A. K. Cheetham, G. Ferey, T. Loiseau, *Angew. Chem. Int. Ed.* **1999**, *38*, 3268.

2 J. Zhu, X. Bu, P. Feng, G. D. Stucky, *J. Am. Chem. Soc.* **2000**, *122*, 11563.

3 (a) A. Choudhury, J. Krishnamoorthy, C. N. R. Rao, *Chem. Commun.* **2001**, 2610; (b) G. Paul, A. Choudhury, C. N. R. Rao, *J. Chem. Soc. Dalton Trans.* **2002**, 3859.

4 I. Bull, P. S. Wheatley, P. Lightfoot, R. E. Morris, E. Sastre, P. A. Wright, Chem. Commun. **2002**, 1180.

5 (a) Y. Xing, Y. Liu, Z. Shi, H. Meng, W. Pang, *J. Solid State Chem.* **2003**, *174*, 381; (b) Y. Xing, Z. Shi, G. Li, W. Pang, *Dalton Trans.* **2003**, 940; (c) T. Bataille, D. Louër, *J. Mater. Chem.* **2002**, *12*, 3487.

6 Crystal data: $C_4H_{24}N_4Nd_2O_{22}S_5$, **1**, *Mr* = 929.05, monoclinic, $P2_1/c$ with a = 6.6051(2) Å, b = 17.0238(7) Å, c = 20.4648(8) Å, β = 94.921(2) °, V = 2292.66(15) Å^3, Z = 4, μ = 5.045 mm^{-1}, ρ_{calc} = 2.692 g cm^{-3}. $C_6H_{34}N_6Er_2O_{26}S_6$, **2**, *Mr* = 1133.27, orthorhombic, *Pbca* with a = 9.6460(1) Å, b = 19.9459(4) Å, c = 30.3455(6) Å, V = 5838.42(18) Å^3, Z = 8, μ = 6.254 mm^{-1}, ρ_{calc} = 2.579 g cm^{-3}. $C_4H_{18}N_3NdO_{13}S_3$, **3**, *Mr* = 556.63, monoclinic, $P2_1$ with a = 6.6380(1) Å, b = 10.361(1) Å, c = 11.050(1) Å, β = 93.808(4) °, V = 758.2(1) Å^3, Z = 2, μ = 3.913 mm^{-1}, ρ_{calc} = 2.438 g cm^{-3}. Unique reflections: **1**, 3988(R_{int} = 4.72%); **2**, 5158(R_{int} = 6.65%); **3**, 3519(R_{int} = 2.07%). Observed reflections ($I>2\sigma(I)$): **1**, 3102; **2**, 4386; **3**, 3389. Final R1, wR2 for observed data: **1**, 0.0589, 0.1031; **2**, 0.0437, 0.0817; **3**, 0.0244, 0.0521 GOF: **1**, 1.155; **2**, 1.184; **3**, 1.046.

**This work was supported by National Natural Science Foundation of China (No. 20371047)

PO27

THE CRYSTAL STRUCTURES OF HYDRAZINIUM 2,3-PYRAZINEDICARBOXYLATES, $N_2H_5Hpyz(COO)_2$, $(N_2H_5)_2pyz(COO)_2$ and $N_2H_5Hpyz(COO)_2.H_2pyz(COO)_2$

T. Premkumar,[a] S. Govindarajan,[a]* and Nigam P. Rath[b]

[a]Department of Chemistry, Bharathiar University, Coimbatore 641 046, India; [b]Department of Chemistry, University of Missouri-St. Louis, MO 63121, USA
(premsrf@yahoo.co.in)

The crystal structures of hydrazinium hydrogen-2,3-pyrazinedicarboxylate $N_2H_5Hpyz(COO)_2$ (**1**), dihydrazinium 2,3-pyrazinedicarboxylate, $(N_2H_5)_2pyz(COO)_2$ (**2**) and hydrazinium hydrogen-2,3-pyrazinedicarboxylate 2,3-pyrazinedicarboxylic acid, $N_2H_5Hpyz(COO)_2.H_2pyz(COO)_2$ (**3**), where $H_2pyz(COO)_2$ = 2,3-pyrazinedicarboxylic acid, have been investigated by three-dimensional single-crystal X-ray data, collected at –25, –50 and –130°C, respectively. While Crystallographic data for salt **1** are orthorhombic, space group $P2_12_12_1$ with **a** = 6.8321(2), **b** = 19.2716(4), **c** = 25.6913(6) Å, Z = 16 and final R factor of 0.1688 based on 8141 independent reflections, **2** are monoclinic, space group $P2_1/c$ with **a** = 8.0171 (3), **b** = 15.3659 (7), **c** = 8.1431 (4) Å, β = 94.952 (3)°, Z = 4 and final R factor of 0.0892 (λ = 0.071073 Å) based on 1968 independent reflections. The salt **3** crystallizes in the triclinic space group P-1 with **a** = 7.3542 (9), **b** = 7.9617 (9), **c** = 8.3895 (10) Å, Z = 2 and final R factor of 0.0621 based on 1727 independent reflections. The structures of all the salts suggest that each contains $N_2H_5^+$ cation and a residue of $Hpyz(COO)_2^-$/$pyz(COO)_2^{2-}$ anion. In addition to the above, the salt **3** contains one molecule of parent acid. Though it has been speculated, such a type of acid rich hydrazinium salts has not been isolated so far. For the **first time**, we have not only isolated the same in the solid state but also studied crystallographically. Further, it is worth to mention here that, for the **first time** a successful attempt has been made to synthesize aforesaid all the three types of hydrazinium salts with 2,3-pyrazinedicarboxylic acid and proved crystallographically. It is observed that, in all these salts, there is a common arrangement of molecular packing. In all, there is an anionic chain running along one of the crystallographic axes formed through O-H...O and/or N-H...O hydrogen bonds. The hydrazinium ions sit at the space between the pyrazinedicarboxylic moieties in the crystal lattice so as to form multiple-hydrogen bonds leading to molecular network. The results will be presented.

PO28

NEW TEN COORDINATED LANTHANUM 2-PYRAZINECARBOXYLATE DIHYDRATE CONTAINING HYDRAZINIUM CATION

S. Govindarajan[a]*, T. Premkumar [a], V. Manivannan [b], K.R. Radhakrishnan [c] and Jonathan W. Steed [d]

[a]Department of Chemistry, Bharathiar University, Coimbatore 641 046, India; [b]Department of Physics, Presidency College, Chennai, 600 005, India; [c]Department of Physics, Government Arts College, Kumbakonam 612001,India; [d]Department of Chemistry, Kings College, Strand, London, WC2 R2LS, UK.
(drsgovind@yahoo.co.in)

New dihydrazinium lanthanum 2-pyrazinecarboxylate dihydrate, $(N_2H_5)_2[La(pyzCOO)_5].2H_2O$, (pyzCOO = 2-pyrazinecarboxylate) has been synthesized and its solid state structure determined from single crystal X-ray study. The crystals are monoclinic, space group $P2_1/n$ with a = 16.4018 (4), b = 22.8727 (6), c = 14.9608 (9) Å, β = 102.660 (2)°, Z = 8 and R = 0.0592. The structure analysis shows that the crystals consists of $N_2H_5^+$ cations, water molecules and the $[La(pyzCOO)_5]^{2-}$ anions. The asymmetric part contains two crystallographically independent lanthanum atoms having similar coordination. Interestingly, each lanthanum atom has ten coordination formed by five 2-pyrazinecarboxylate (bidentate chelate) ligands, via its N, O bonding moieties. The other pyrazine N atom present in the ring is not involved in coordination. The $N_2H_5^+$ ions and the water molecules are not coordinated to the metal. Coordination numbers from six to twelve have been established in lanthanide compounds but ten coordination appears rarely. It is worthwhile to mention here that, the ten coordination of hydrazinium lanthanide complexes with carboxylate anions have been observed for the first time. The structure is built up by lanthanum ions joined by 2-pyrazinecarboxylate groups forming two-dimensional sheets parallel to (001) plane. The space between the sheets is occupied by hydrazinium ions and lattice water molecules. The sheets are held together by the network of hydrogen bonds involving $N_2H_5^+$ ions, lattice water and 2-pyrazinecarboxylate oxygens. The complex anions are stacked one above the other along c-axis. As a whole the structure is stabilized by N-H...O_w, N-H...N, N-H...O and O_w-H...O hydrogen bonds. Further, from the X-ray powder patterns, it is evident that the corresponding Ce complex is isostructural with the titled compound. The results from the IR and thermoanalytical studies are in accordance with these isostructural groupings.

PO29

LADDER NETWORKS IN INCLUSION COMPLEXES OF 4,4-BIS(4-HYDROXYPHENYL)CYCLOHEXANONE

Srinivasulu Aitipamula,[a] Ashwini Nangia,[a] Mariusz Jaskólski,[b] and Ram Thaimattam[a]

[a]School of Chemistry, University of Hyderabad, Hyderabad 500 046, India; [b]Center for Biocrystallographic Research, IBCh, Polish Academy of Sciences and Department of Crystallography, Faculty of Chemistry, A. Mickiewicz University, Grunwaldzka 6, 60-780 Poznan, Poland. (che078s@uohyd.ernet.in).

Molecules with symmetrical molecular scaffold, a degree of rigidity, and good hydrogen bonding groups (OH, COOH, C=O) form open framework structures. For example, 1,1-bis(4-hydroxyphenyl)cyclohexane includes a variety of guest molecules [1]. We have undertaken a systematic study of 4,4-bis(4-hydroxyphenyl)cyclohexanone, **1**, and its inclusion complexes. The crystal structure of **1** has two independent molecules in the crystallographic asymmetric unit and the network associated with one of the symmetry independent molecules encircles the other molecule through O–H···O and C–H···O hydrogen bonds [2]. Inclusion complexes of **1** form two types of ladder networks assembled from the T-shaped tecton. In one case, molecules of **1** form the ladder network and the guest/solvent molecules bind to the host framework (G_1). In the second type, water expands the host framework along the ladder rungs and guest/solvent molecules are included in the voids (G_2). These structures represent two variants of ladder host-guest adducts built from a T-shaped tecton [3]. TGA/DSC measurements confirm the thermal stability and host-guest stoichiometry.

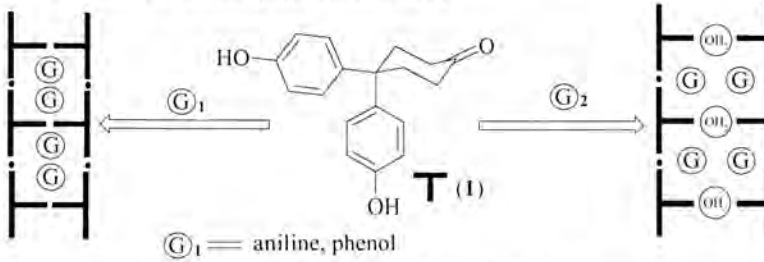

G1 = aniline, phenol

G2 = *o*-cresol+water, *m*-cresol+water, *p*-cresol+water, 2-chlorophenol+water

References

1 Caira, M. R., Horne, A., Nassimbeni, L. R. and Toda, F. (1997) *J. Mater. Chem.* **7**, 2145-2149.

2 Aitipamula, S., Desiraju, G. R., Jaskólski, M., Nangia, A. and Thaimattam, R. (2003) *CrystEngComm*, **5**, 447-450.

3 Kumar, V. S. S., Nangia, A., Kirchner, M. T. and Boese, R. (2003) *New J. Chem.*, **27**, 224-226.

PO30

π-STACKING IN NOVEL FLUORESCENT NAPHTHALIMIDE SYSTEMS

Jim Simpson, C. John McAdam, Joy, L Morgan and Brian H Robinson

Department of Chemistry, University of Otago, P.O. Box 56, Dunedin, NEW ZEALAND (jsimpson@alkali.otago.ac.nz)

Efficient energy transfer between redox and/or photoactive centres is an important goal for new materials incorporating both organic and organometallic species because of their potential technological applications. 1,8-naphthalimides are excellent candidates as components of donor acceptor arrays and, with appropriate substitution of the naphthalimide moiety, offer the possibility of significant charge separation in the excited state [1,2].

In the course of this work we have obtained the crystal and molecular structures of several naphthalimide derivatives with the general formula shown in the diagram [R = Me, C_6H_4CN, CH_2Fc (Fc = (η^5-$C_5H_4Fe(\eta^5$-$C_5H_5)$, R' = H, piperidine, *E*-CH=CH-piperidine, -C≡C-Fc, -C≡C-2,3,4,6-tetra-O-acetate-β-*D*-glucopyranoside, R' = H, NO_2] . A common thread is the stabilisation of these solid state structures by offset π-stacking interactions involving the naphthalimide rings, with substituents on the dicarboximide N-atoms and the naphthalene rings oriented to optimise the stacking interactions.

Interestingly, while the corresponding naphthaldiimides with R = Fc or Fc-CH_2- substituents on the imide N atoms can be prepared, the products are found to be totally intractable green solids that are insoluble in a wide range of solvents. It is postulated that strong π-stacking interactions promote aggregation in these materials.

References

1 McAdam, C.J., Robinson, B.H. and Simpson, J. (2000) *Organometallics* **19**, 3644-3653

2 McAdam, C.J., Morgan, J.L. Robinson, B.H., Simpson, J., Rieger, P.H., and Rieger, A.L. (2003) *Organometallics* **22**, 5126-5136

PO31

DL-THREONINE AND DL-PHENYLALANINE COMPLEXES WITH TRICHLOROACETIC ACID

K.Rajagopal[a], R.V.Krishnakumar[b], K.Ravikumar[c] and S.Natarajan[d]

[a]Department of Physics, Saraswathi Narayanan College, Madurai-625 022, India, [b]Department of Physics, Thiagarajar College, Madurai – 625 009, [c]Laboratory of Crystallography, Indian Institute of Chemical Technology, Hydrabad-500 007, India, [d]Department of Physics, Madurai Kamaraj University, Madurai-625 021, India (s_natarajan50@yahoo.com)

Amino acids and their complexes are of great chemical and biological interest. Hence, we have undertaken systematic and precise X-ray crystallographic investigations on several complexes of amino acids involving carboxylic acids with a view to study the geometry of amino acid molecules in different crystalline environments. This paper describes the crystal and molecular structures of DL-Threonine and DL- Phenylalanine with trichloroacetic acid. Trichloroacetic acid represents a class of simple organic molecules of the type $R\text{-}CO_2H$ (monocarboxylic acids) and assumes importance in the formation of hydrogen bonds with amino acids owing to the presence of a highly 'participating' carboxylic acid group and a relatively 'passive' R group (Cl_3, in the present case). Crystal structure elucidation of trichloroacetic acid itself was carried out in our laboratory recently [1]. The crystal structure elucidation of complexes of amino acids viz., DL-valine, DL-methionine, L-Proline, β-alanine and L-Phenylalanine, with trichloroacetic acid were also reported [2-6]. Interestingly, these complexes may also be depicted as proton transfer complexes of the type A.B, where A is a amino acid and B is a carboxylic acid.

Single crystals of the compounds were grown from saturated aqueous solution containing respective amino acids and trichloroacetic acid in a 1:1 stoichiometric ratio. DL-Threoninium trichloroacetate ($C_4 H_{10} N O_3^+ . C_2 Cl_3 O_2^-$) crystallizes in the monoclinic system, Space group $P2_1$ with a = 10.329(1) Å, b = 10.427(1) Å, c = 10.780(1) Å, β = 103.12(1)° and Z = 4. DL-Phenylalaninium trichloroacetate ($C_9 H_{12} N O_2^+ . C_2 Cl_3 O_2^-$) crystallizes in the monoclinic system, space group C2/c with a = 18.820(4) Å, b = 16.511(3) Å, c = 10.053(2) Å, β = 111.27(3)° and Z = 8. The structures were solved by direct methods and refined by full-matrix least squares on F^2 with R values 0.033 and 0.056, respectively. In both the structures, amino acid molecules exist as cations and trichloroacetic acid molecules as anions. The symmetry related amino acid cations and trichloroacetate anions are held together by N---H...O and O---H...O hydrogen bonds in addition to van der Waals interactions. The details of molecular aggregation and hydrogen bonding pattern will be presented.

References

1 Rajagopal, K., Mostad, A., Krishnakumar, R. V., Subha Nandhini, M. & Natarajan, S. (2003) Acta Cryst. E59, o316-o318.
2 Rajagopal, K., Krishnakumar, R. V., Subha Nandhini, M., Mostad, A. & Natarajan, S. (2002) Acta Cryst. E58, o279-o281.
3 Rajagopal, K., Krishnakumar, R. V., Mostad, A. & Natarajan, S. (2003) Acta Cryst. E59, o31-o33.
4 Rajagopal, K., Krishnakumar, R. V., Mostad, A. & Natarajan, S. (2003) Acta Cryst. E59, o277-o279.
5 Rajagopal, K., Krishnakumar, R. V., Subha Nandhini, M., Mostad, A. & Natarajan, S. (2003) Acta Cryst. E59, o206-o208.
6 Rajagopal, K., Krishnakumar, R. V., Subha Nandhini, M., Cameron, T. S. & Natarajan, S. (2003) Acta Cryst. E59, o1084-o1086.

PO32

COMPARATIVE INVESTIGATION FOR THE CRYSTAL STRUCTURE OF THE COORDINATION COMPOUNDS OF THE RARE EARTH AND SHORT CHAIN ETHER EO2 , EO3

Jianming Gu and Xiurong Hu

Analysis Center of Zhejiang University , Hangzhou 310028, P.R.China
(gujianming@zjuem.zju.edu.cn)

Aggregative glycol have more general character of crown ether and cryptate ether, composing easy and low toxicant, so they can be comprehensive studied because their important function in the field of chemistry and biology[1,2].

The crystal structure of $Nd(EO2)_3$ and $La(EO3)_3$ are investigated and compared[3,4]. The crystal $Nd(EO2)_3$ belongs to monoclinic system with space group $P 2_1/n$ and the cell are a=14.124(1), b=13.990(1), c=15.265(1)Å, β=96.78(1)°, V=3001.1(6) $Å^3$, All Oxygen on chain ether of the three groups were participate in coordinated, formed nine-coordination, and it's coordinating polyhedron showed tricapped trigonal prism, the ether link round the bond of C--C arrange into $ST\bar{T}S$ (Symmetry, Trans).

The crystal $La(EO3)_3$ belongs to monoclinic system with space group $P 2_1/c$ and the cell are a=15.474(2), b=11.386(1), c=20.481(4)Å, β=99.82(1)°,V=3618(1) $Å^3$, ten-coordination, it's coordinating polyhedron is biscapped tetrahedron antiprism, the arrangement of ether link round the bond of C--O are shown $GTT\bar{G}TT$ Gauche, Trans.

The negative ion ClO^{-4} does not take part in coordination.

References

1 Pedersen C.J., (1967) J.Am.Chem., **89**, 2495
2 Hirashima, et al , (1986) Bull. Chem. Soc. Jpn., **59**, 25
3 Gu Jianming, Hu Xiurong, (1998) (Chinese)J Inorganic Chem , **3**, 313-317
4 Gu Jianming, Hu Xiurong, (1996) Chinese J Structural Chem, **3**, 239-242

PO33

REVERSIBLE SOLID-VAPOR SUBSTITUTION REACTIONS OF LAYERED CADMIUM ORGANOSULFONATES

Jinsen Zhou, Li Wang, Jiwen Cai

School of Chemistry and Chemical Engineering, Sun Yat-Sen (Zhongshan) University, Guangzhou 510275, P. R. China (puscjw@zsu.edu.cn)

Layered [Cd(1,5-naphthalenedisulfonate)$(H_2O)_2]_n$ (**1**) and {Cd(μ_2-*p*-N,O-$NH_2C_6H_4SO_3)_2(H_2O)_2\}_n$ (**2**) can uptake amine quantitatively without dehydration, via solid-vapor reaction. The substitution reaction process is selective and reversible at room temperature. Remarkably, single crystals of the $C_2H_5NH_2$ and $C_3H_7NH_2$ adducts (**3,4**) grew into single crystal suitable for X-ray structure analysis, *in situ* of the solid-vapor reaction. The resulting adducts were also characterized by elemental analyses, IR and TGA. The reversible process was recorded by PXRD. The result represents the first crystalline metal sulfonate complex undergoing reversible solid-vapor substitution reaction with amines at room conditions. The difference in the physical properties, especially the conductivity of **2** as a neutral polymer and **3** as a salt, could be used to explore the potential application of the air-stable and easy-to-make crystalline material **2** as a chemical sensor or switch for volatile amines. We thank the financial support from the National Natural Science Foundation of China (Grand No. 20271053).

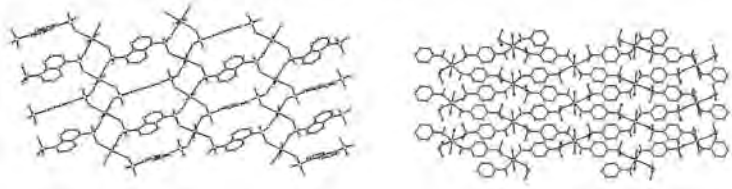

Figure 1. The 2-dimensional coordination network of **1** and **2**.

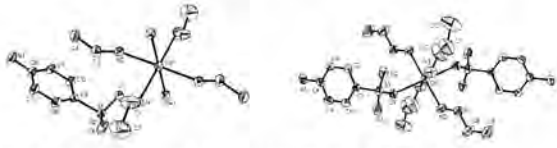

Figure 2. The coordination structure of **3** and **4**.

References

1 Jiwen Cai, Jin-sen Zhou and Mu-liang Lin. (2003) *J. Mater. Chem.* **13**, 1806-1811.

2 Jin-Sen Zhou, Jiwen Cai, Li Wang and Seik Weng Ng, (2004) *Dalton Trans.*, submitted.

PO34

CONSTRUCTION OF SLVER(I) COLUMN WITH ENCAPSULATED ACETYLENEDIIDE AND A HYDROPHOBIC SHEATH PROVIDED BY ANIONIC AND ZWITTERIONIC CARBOXYLATE LIGATION

Xiao-Li Zhao and Thomas C. W. Mak

Department of Chemistry, The Chinese University of Hong Kong, New Territories, Shatin, Hong Kong SAR, P. R. China
(tcwmak@cuhk.edu.hk)

Betaines are zwitterions having a carboxylate group and a quaternary ammonium group, with the presence of the carboxylate group, they belong to the family of carboxylate compounds and exhibit most of the common coordination modes. Owing to their permanent bipolarity and overall charge neutrality, betaine ligands are expected to be advantageous in the study of coordination polymers in several respects: 1) synthetic access to water-soluble polymeric metal carboxylates; 2) new structural varieties, such as complexes with metal centers bearing additional anionic ligands, and those with variable metal to carboxylate molar ratios; 3) easy synthetic modification of carboxylate ligands by varying the substituents on the quaternary nitrogen atom and the link between the two polar terminals.

In the course of our investigation on silver salts containing silver acetylide, two double salts of silver acetylide containing both anionic and zwitterionic carboxylate ligands, $[(Ag_2C_2)(AgCF_3CO_2)_4(H_2O)L^1]\cdot 2H_2O$(**1**) and $[(Ag_2C_2)_3(AgCF_3CO_2)_{14}(L^2)_4]$ (**2**) (L^1 = pridinioacetate
; L^2 = pyridiniopropionate) have been synthesized and structurally characterized. Each has a columnar structure generated from the fusion of silver cages with C_2^{2-} species embedded in its inner core and an exterior coat comprising anionic and zwitterionic carboxylates.

This work is supported by Hong Kong Research Grant Council Earmarked Grant Ref. No. CUHK 4268/00P.

PO35

STUDIES ON IRON(III) COMPLEXES OF 2-PYRIDYL-6-(2-PYRIDYLCARBONYL)-2-PYRIDYLMETHANONE

Xu-Dong Chen and Thomas C. W. Mak

Department of Chemistry, The Chinese University of Hong Kong, New Territories, Shatin, Hong Kong SAR, P. R. China (tcwmak@cuhk.edu.hk)

The structure diversity displayed by the metal complexes of di-2-pyridyl ketone, which stems from the ability of the doubly and singly deprotonated forms of the *gem*-diol form, or the monoanion of the hemiacetal form of this ligand, to adopt a variety of coordination modes, has drawn a great deal of interest of chemists in recent years.[1]

During our systematic studies of metal complexes of a new ligand, 2-pyridyl-6-(2-pyridylcarbonyl)-2-pyridylmethanone (**L**), it was found that reaction of **L** with $FeCl_3$ can be solvent-controlled, giving four crystalline compounds exhibiting two kinds of structures, among which is a linear tri-iron complex assembled with two deprotonated hemiacetals of **L** (**L"**). The three iron(III) atoms are bridged by oxygen atoms from both **L"** and μ-OCH_3 and the linear structure is terminated by two chloro ligands; the Fe2···Fe1···Fe3 angle is 152.6°, and the distance between Fe1 and Fe2, Fe3 are 2.897Å and 2.916Å, respectively. The other three crystals have the same structure containing a mononuclear iron(III) cation with only one carbonyl group taking the *gem*-diol form while the other remains intact.

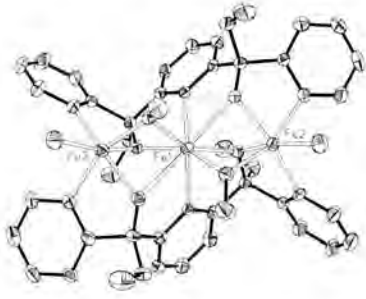

This work is supported by HongKong Research Grants Council Earmarked grant Ref. No. CUHK 402003.

Reference:

1 Papaefstathiou, G.S. and Perlepes, S.P., (2002), *Comments on Inorganic Chemistry*, **23**(**4**), 249-274.

PO36

SUPRAMOLECULAR STABILIZATION OF OXOCARBON ANIONS IN UREA HOST FRAMEWORKS

Chi-Keung Lam, Thomas C. W. Mak

Department of Chemistry, The Chinese University of Hong Kong, Shatin, New Territories, Hong Kong SAR, P. R. China (tcwmak@cuhk.edu.hk).

Our current interest is to generate new inclusion compounds [1] with oxocarbon anions [2] and urea derivatives plus other molecular species as the building blocks of various host lattices, using different types of quaternary ammonium cations as guest templates. In the course of our systematic studies, we found that an elusive species such as allophanate $NH_2CONHCO_2^-$ [3] or dihydrogen borate $BO(OH)_2^-$ [4] can be generated *in situ* and stabilized in a hydrogen-bonded urea host framework. Guided by this design strategy, the C_{2v} valence tautomeric structures of croconate [5] and the relatively unstable rhodizonate species [6] are subsequently stabilized in two novel crystalline inclusion compounds.

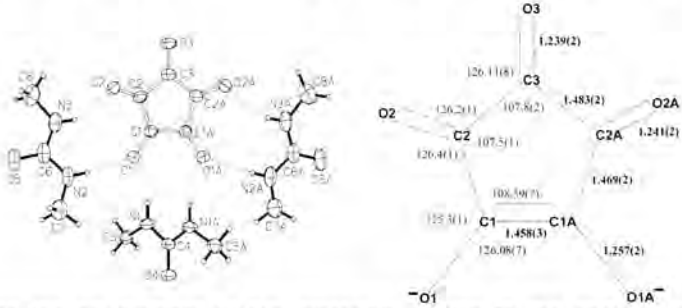

Hydrogen-bonding environment of the croconate dianion in the crystal structure of $[(C_2H_5)_4N^+]_2C_5O_5^{2-}\cdot 3(CH_3NH)_2CO$ (left); bond lengths (Å) and angles (°) of the C_{2v} valence tautomer of the croconate dianion with standard deviations enclosed in parentheses (right).

This work is supported by Hong Kong Research Grants Council Earmarked Grants CUHK 4268/00P and 402003.

References

1 Mak, T. C. W. and Li, Q. (1998) in *Advances in Molecular Structure and Research* (Eds.: M. Hargittai, I. Hargittai), JAI Press, Stamford, Connecticut, **Vol. 4**, pp. 151-225.

2 Lam, C. -K. and Mak, T. C. W. (1999) *Zh. Strukt. Khim.*, **40**, 883-891; (2000) *Cryst. Engng.*, **3**, 33-40, 225-226; (2000) *Tetrahedron*, **56**, 6657-6665.

3 Mak, T. C. W., Yip, W. -H. and Li, Q. (1995) *J. Am. Chem. Soc.*, **117**, 11995-11996.

4 Li, Q., Xue, F. and Mak, T. C. W. (1999) *Inorg. Chem.*, **38**, 4142-4145.

5 Lam, C. -K., Cheng, M. F., Li, C. L., Zhang, J. P., Chen, X. M., Li, W. K. and Mak, T. C. W. (2004) *Chem. Commun.*, 448-449.

6 Lam, C. -K. and Mak, T. C. W. (2001) *Angew. Chem. Int. Ed.*, **40**, 3453-3455.

PO37

SYNTHESIS, STRUCTURE, AND DNA CLEAVAGE OF AN OPTICAL REACTIVE SPIROPENTACOPPER CLUSTER

Szu-Miao Chen,[a] Yu Wang,[a*] and Kuan-Jiuh Lin[b*]

[a]Department of Chemistry, National Taiwan University, No.1, Sec. 4, Roosevelt Road, Taipei, Taiwan ; [b]Department of Chemistry, National Chung-Hsing University, 250,Kuo Kuang Road,Taichung, Taiwan. (d92223013@ntu.edu.tw)

Nature uses a self-assembly principle to build a supermolecular envelope around the metal center, therefore, metal ions are often found at the active site of many metalloenzymes to exhibit distinctive spectral and chemical features. Here we describe a self-assembly methodology to synthesize a spiropentacopper(II) cluster self-enclosed by pyroglutamic acid ligands, $K_2Cu_5(pGlu)_6(OH)_2 \cdot 10H_2O$, namely Spiro-$Cu_5$.

Spiro-Cu_5, synthesized by one-step solvothermal method, contains square planar, square pyramidal, and distorted octahedral configurations which are present simultaneously in three distinct Cu^{II} (d^9) ions in the asymmetric unit. The three mixed coordination geometries represent an entire spectra of nature Jahn-Teller distortion of Cu(II) electronic configuration for the first time. The intra-cluster metal-metal separations are of 2.992(2), 3.185(2), and 3.549(3) Å. Interestingly, it is found for the first time that the chiral pyroglutamic acid ligands appear to be in three different coordination types to encompass the novel spiropentacopper cluster with a center of symmetry($\bar{1}$) in the middle.

In the presence of H_2O_2, we propose that Spiro-Cu_5 would initiate hydroxy radicals (•OH) and transfer electron(s) to the phosphate backbone of nucleic acids, consequently cleave DNA. To our best knowledge, the spiropentacopper cluster is the first polynuclear species (M>3) capable of mediating DNA cleavage.

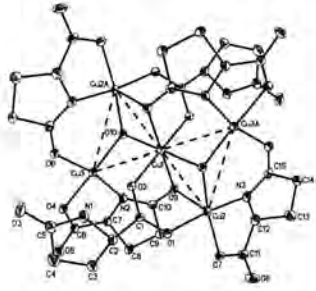

PO38

CHARGE DENSITY STUDY AND ROLE OF HYDROGEN BOND IN TRAN-[Ni(cyan-*k*N)$_2$(NH$_3$)$_4$] : COMPARISON BETWEEN EXPERIMENT AND THEORY

Hsin-Hui, Shen , Yu-Wang*

Department of Chemistry, National Taiwan University, Taipei 106, Taiwan
(r91223026@ntu.edu.tw)

The six-coordinated complex trans-[Ni(cyan-*k*N)$_2$(NH$_3$)$_4$] has been characterized in the solid state by X-ray diffraction at 100 K and 298 K. The space group at room temperature is Fmmm with a site symmetry of mmm. While lowering the temperature, the space group changes to Ccmm at 100K and the molecule is located at a site symmetry of 2mm. The main difference that involves phase transition at low temperature is the change of hydrogen-bonding patterns. In order to understand the chemical bonding of the nickel complex and various hydrogen-bonding in this complex, the electron density distribution of the complex is derived using both the single crystal X-ray diffraction and DFT calculations with different kinds of hydrogen bonds. The comparisons are made in d-orbital occupancies at the nickel center and the topological properties associated with the BCP. The pi-delocalization of the ligand will be discussed with reference to the bond ellipticity and Fermi-hole distribution. Results on the electron density distribution will be presented in the form of deformation density, Laplacian maps and the topological properties. The Laplacian maps derived from the experiments agree well with the maps derived theoretically.

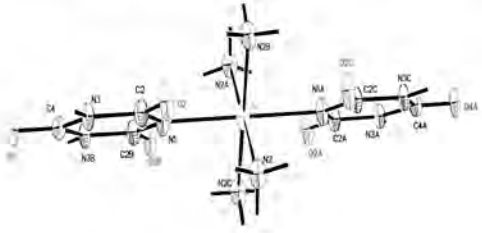

R.T. (Fmmm)

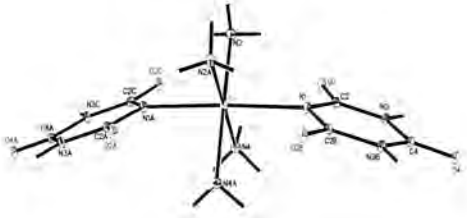

100K (Ccmm)

PO39

PHOTOCHROMISM OF SALICYLIDENEANILINES DEDUCED BY THE ACID-BASE COMPLEX FORMATION

Kohei Johmoto, Hidehiro Uekusa, Yuji Ohashi

Department of Chemistry and Materials Science, Graduate School of Science and Engineering, Tokyo Institute of Technology, Tokyo 152-8551, Japan
(kjomoto@chem.titech.ac.jp)

Light-induced reversible color change of substances is known as photochromism and has attracted attention due to their potential applications such as optical data storage etc. Salicylideneaniline (SA) derivatives have the property of photochromism or thermochromism, which is reversible color change with variation of temperature. The color change from stable yellow to unstable red is brought about by the change of molecular conformation. The planar conformation leads to thermochromism whereas non-planar one to photochromism. Moreover, the large cavity around the imine group makes the red form stable upon heating. Since SA has a non-planar conformation and large cavity, its red form has long lifetime.

N-salicylidene-4-carboxyaniline (4C-SA) has a planar conformation and shows thermochromism. It was found that 4C-SA formed an acid-base complex with dibenzylamine and that the complex crystal shows photochromism. The structure was analyzed by X-rays. The molecular conformation of 4C-SA in the complex crystal is changed to non-planar as shown in the Figure. Similar change was observed for the compound of 3C-SA and its complex with dibenzylamine. The complex formation is a powerful tool to obtain photochromism for the SA derivatives.

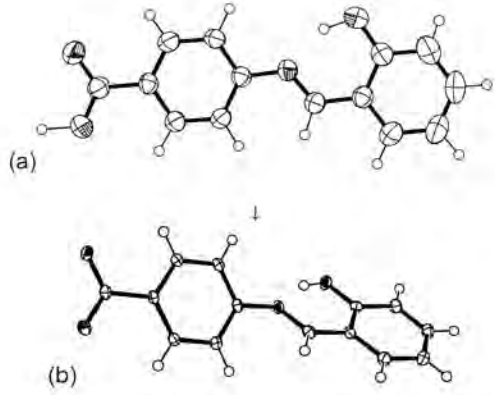

Figure. Molecular structures of (a) 4C-SA and (b) 4C-SA in the complex with dibenzylamine

PO40

SOLVOTHERMAL INDUCED TRANS-CIS ISOMERIZATION OF $[Fe(tzpy)_2(NCS)_2]$ (tzpy=3-(2-PYRIDYL)[1,2,3]TRIAZOLO[1,5-A]PYRIDINE)

K. W. Chen , C. F. Sheu , G. H. Lee ,Y. Wang*

Department of Chemistry, National Taiwan University, Taipei 106, Taiwan
(r90223020@ntu.ed.tw)

The novel complex *Cis*-$[Fe(tzpy)_2(NCS)_2]$(**1**) has been synthesized successfully from spin crossover *trans*-$[Fe(tzpy)_2(NCS)_2]$(**2**) isomer by solvothermal induced isomerization method. Single-crystal diffraction data was collected at 293 K by CAD-4 diffractometer. Complex (**1**) crystallizes in the monoclinic space group *C* 2/*c* with Z=4, a=14.828(4), b=11.485(5) Å ,c=15.071(2) Å, beta = 110.081(15) deg. The bond lengths of Fe-N are 2.249(4) Å, 2.197(4) Å, and 2.056(5) Å for complex **1** and 2.019(1) Å, 1.971(2) Å, and 1.933(1) Å for complex **2** at LS state. Both complexes have a similar pseudo-octahedral [FeN6] core with the NCS- groups in the cis arrangement in **1** but trans in **2**. Variable-temperature magnetic susceptibility measurement reveals that **1** staying in a high-spin state in the observed temperature range of 5-300 K. It is interesting to note that the differences of the crystal packing between the isomeric iron (Ⅱ) complexes result in a dramatic change in their magnetic properties. Further studies on the origin of the discrepancy in the crystal field responsible for this result are currently in progress.

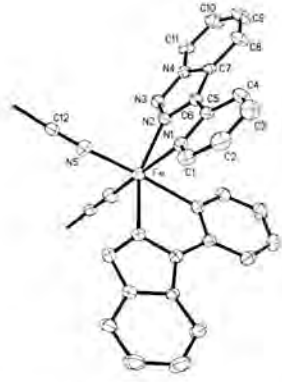

ORTEP diagram of *cis*-$[Fe(tzpy)_2(NCS)_2]$ (30%, 273 K)

PO41

A UNPRECEDENTED HOMOCHIRAL OLEFIN-COPPER(I) 2D COORDINATION POLYMER

Ren-Gen Xiong, Xi-Sen Wang

Coordination Chemistry Institute, The State Key Laboratory of Coordination Chemistry, Nanjing University, 210093 Nanjing, P. R. China, (xiongrg@netra.nju.edu.cn)

The reaction of 4-Vinylbenzylcinchonidinium chloride ([VB-N-CIN]Cl (**1**), a chiral phase transfer catalyst (CPTC), prepared from the corresponding cinchona alkaloid and 4-vinylbenzyl chloride in refluxing acetone and N,N-dimethylformamide, solvothermally reacts with CuCl to afford the unprecedented 2D layered homochiral copper(I)-olefin coordination polymer $Cu_5Cl_6(VB\text{-}N\text{-}CIN)_2 \cdot C2H5OH$ (**2**•EtOH), in which The five Cu(I) centers connect together by four μ2-Cl and two μ3-Cl linkers to result in the formation of two clusters composed of two triangles (Cu1-Cu2-Cu3 and Cu3-Cu1A-Cu2A), while two triangles share a corner of Cu3. Cu1 and Cu1A and Cu2 and Cu2A are all three -coordinated and coordinate to the N atom of the quinoline ring and olefin moiety of the quinuclidine ring to result in the formation of a 2D square-grid network. The remaining Cu3 only coordinates to four Cl atoms with a tetrahedral geometry. It is noteworthy that two adjacent layers are in an AA type arrangement and one ethanol molecule is intercalated between two layers of **2** as the framework. A preliminary enantioseparation investigation shows that the 2D layered network in **2** is capable of selectively intercalating (R)-2-butanol.

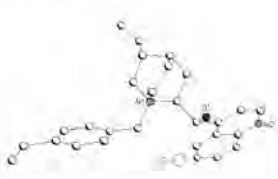

fig1a: the molecular for **1** fig1b an asymmetric unit of compound **2**

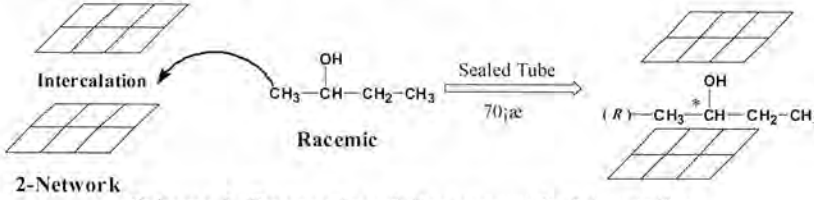

Scheme 1: Proposed resolution process by intercalation

Reference

1 Xie, Y.-R., Wang, X.-S., Xiong, R.-G., et.al., (2003), Organometallics, 22, 4396

FERROELECTRIC COPPER QUININE COMPLEXES

Ren-Gen Xiong, Hong Zhao

Coordination Chemistry Institute, The State Key Laboratory of Coordination Chemistry, Nanjing University, 210093 Nanjing, P. R. China(xiongrg@netra.nju.edu.cn)

The reactions of quinine with Cu(I)Cl and Cu(I)Br afford $Cu_5Cl_9(H_2Quinine)_2$ (1) and $Cu_3Br_7(H_2Quinine)_2(H_2O)$ (2), respectively, with 1D polymeric structures. The anionic chain in (1) contains $Cu_4Cl_6^{2-}$ adamantane-type aggregates that are linked to two identical units by $CuCl_3^{2-}$ bridges, and the Cu(I) centers in (2) have a distorted tetrahedral environment formed by bridging and terminal bromide ions. Given that the products (1) and (2) crystallize in a chiral space group (*C*2) which belong to a polar point group (C_2), their optical properties were studied. Reliminary examinations of a powdered sample indicate that both (1) and (2) are SHG-active with approximate responses 4.0 times that of KDP. The space group *C*2 is associated with the point group C_2, one of the 10 polar point groups (C_1, C_2, C_m, C_{2v}, C_4, C_{4v}, C_3, C_{3v}, C_6, C_{6v}) required for ferroelectric behavior. Experimental results indicate that (1) does indeed display good ferroelectric behavior while (2) shows relatively low ferroelectric responses. There is an electric hysteresis loop in (1), which is a typical ferroelectric feature with a remanent polarization (Pr) of 0.28 $\mu C \cdot cm^{-2}$ and coercive field (Ec) of 16 $kVcm^{-1}$.[8] . The saturation spontaneous polarization (Ps) of (1) is ca. 2.0 $\mu C \cdot cm^{-2}$ compared to ferroelectric KDP which is 5.0 $\mu C \cdot cm^{-2}$. (1) is the first homochiral metal-organic coordination polymer exhibiting ferroelectric behavior.

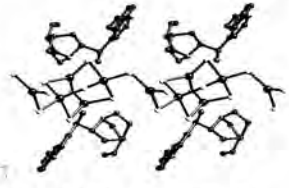

Figure 1. The structure of 1

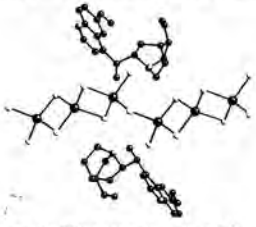

Figure 2. The structure of 2

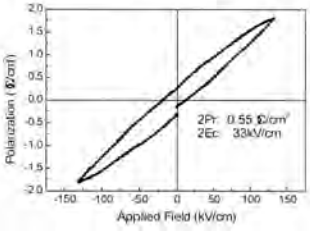

Figure 3. The electric hysteresis loop of a pellet of powdered 1 observed by Virtual Ground Mode using an RT6000 ferroelec- tric tester at room temperature.

Reference

1 Zhao, H.; Qu, Z.-R.; Xiong, R.-G., et al. (2003)*Chem. Mater.***15**, 4166-4168.

PO43

STRUCTURE OF AN COMPLEX COMPOSED OF METHACRYLIC ACID AND PYRIDINE

K. YOSHIDA, H. UEKUSA, Y. OHASHI

Department of Chemistry, Tokyo Institute of Technology, Tokyo 152-8551, Japan
:kyoshida@chem.titech.ac.jp)

Molecular complexes composed of low-molecular-weight acids and bases are good models to understand intermolecular acid-base interaction in crystalline state. Since the component molecules and the complex are liquid at room temperature, the complex crystal should be prepared on the diffractometer using the cooling equipment and then the intensity data should be collected with the diffractometer. In this work, the structure composed of methacrylic acid and pyridine, **1**, was analysed at three temperatures to investigate the effect of *p*Ka on intermolecular interaction.

Equimolar amount of methacrylic acid and pyridine was sealed in a capillary and the capillary was mounted on the Rigaku R-AXIS RAPID diffractometer. Using the cooling equipment, a single crystal of **1** :m.p. 250K) was grown in the capillary. The intensity data were collected with the diffractometer at 223, 173 and 123K. The complex crystal belongs to the monoclinic system and the space group is $P2_1/n$.

The methacrylic acid and pyridine molecules make the 1:1 complex with the O-H...N hydrogen bond. However, the structure is disordered as shown in Fig. 1. The disordered structure is composed of two modes as shown in Fig. 2. At 223 K, the ratio of mode I to II is 7:3 and the O1-H...N and O2-H...N distances in mode I and II are 2.69 and 3.14Å, respectively. At 123 K, the ratio comes close to 5:5 and the two O-H...N bonds have the similar distances. This indicates that the disorder is a dynamic one and that the pyridine molecule shows the in-plane flip-flop motion to make the hydrogen bonds with both of O1 and O2. The crystal structure is shown in Fig. 3.

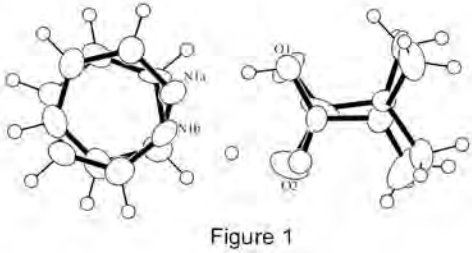

Figure 1

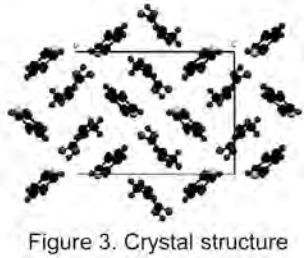

Figure 3. Crystal structure

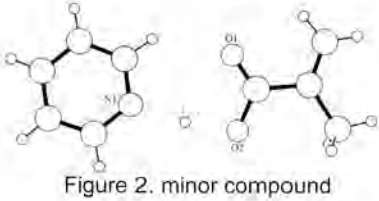

Figure 2. minor compound

X-RAY ANALYSIS OF REACTION PROCESS THROUGH ARYLNITRENE

Takahiro Mitsumori, Hidehiro Uekusa, Yuji Ohashi

Department of Chemistry and Materials Science,Graduate School of Science and Engineering, Tokyo Institute of Technology, Tokyo 152-8551,Japan
(tmitsumo@chem.titech.ac.jp)

When arylazide is irradiated with UV light, it is dimerized to azo compound through arylnitrene as shown in the Scheme. When the crystal of the acid-base complex composed of m-carboxyphenylazide and dibenzylamine was irradiated with UV light, the structure of the intermediate nitrene was analyzed by X-rays at 80 K.[1] For the crystal of 1-azide-2-nitrobenzene, the produced nitrene made a bond with the oxygen atom of the nitro group to form benzofroxane.[2] In the present work, two crystals were prepared and their reaction intermediates or products were analyzed by X-rays; (I) an acid-base complex of m-carboxyphenylazide and dicyclohexylamine, and (II) an acid-base complex of o-carboxyphenylazide and dibenzylamine.

Each crystal was irradiated with the high-pressure Hg lamp at 80 K on the X-ray diffractometer and the intensity data were collected. The structure was refined with the SHELXL-97 program.

Figure1(a) shows the molecular structure of the complex (I) after photoirradiation. A nitrogen molecule, whose occupancy is 13% is clearly observed. However, the nitrene is obscure since it is too close to the original azide molecule. For the complex (II) after irradiation, on the other hand, not only a nitrogen molecule but also 2,1-benzisoxazolone were observed, their occupancy factor being 10%, as shown in Figure1(b). The produced nitrene should make a bond with the oxygen atom of the carboxyl group. The circumstance around the produced nitrene determines the reaction process after the nitrene formation in the reaction process.

References

1 M. Kawano, et al., Chem. Lett., 32, 922 (2003).
2 T. Takayama et al., Helv. Chim. Acta, 86, 1352 (2003)

PO45

X-RAY DIFFRACTION STUDY OF THE CRYSTALLINE-STATE PHOTORACEMIZATION OF A BULKY ALKYL CROUP IN A COBALOXIME COMPLEX

H. Takeoka, H. Uekusa, Y. Ohashi

Department of Chemistry and Materials Science, Tokyo Institute of Technology, 12-1, O-okayama 2-chome, Meguro-ku, Tokyo 152-8551, Japan
(htakeoka@chem.titech.ac.jp)

The chiral bulky alkyl group in some (buthoxycarbonyl)ethyl cobaloxime complexes are known to be racemized by exposure to visible light with retension of single crystal form. The mechanism of this reaction has been interested because the structural change of such a bulky alkyl group in crystalline lattice is thought to be a model of enzymatic or catalytic reactions which also proceed in restrained environments.

In this work, we prepared [(R)-1-(buthoxycarbonyl)ethyl][(R)-1-cyclohexylethylamine]cobaloxime complex and carried out single crystal X-ray diffraction measurement before irradiation and after 72 hours exposure to visible light. The result showed that the 40% of the chiral bulky alkyl group was inverted to the opposite configuration.

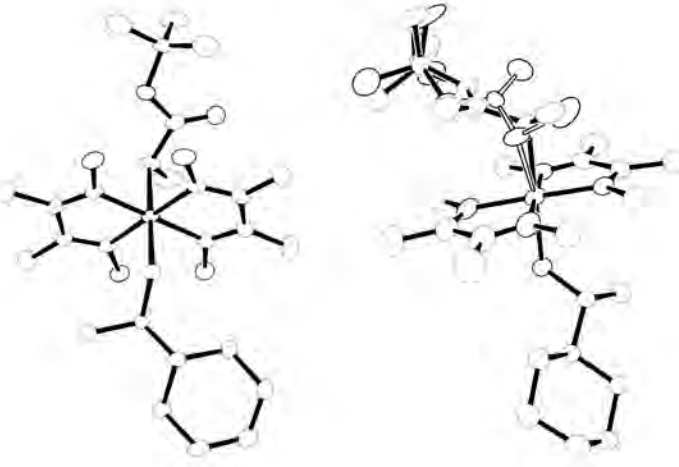

PO46

IONIZATION STATES, STOICHIOMETRY AND HYDROGEN BONDING PATTERNS IN COMPLEXES OF AMINO ACIDS WITH CARBOXYLIC ACIDS

R.V.Krishnakumar[a] and S.Natarajan[b]

[a]Department of Physics, Thiagarajar College, Madurai – 625 009, [b]Department of Physics, Madurai Kamaraj University, Madurai-625 021, India (mailtorvkk@yahoo.co.in)

Amino acids are known to exhibit specific characteristic aggregation patterns in their crystal structures. Carboxylic acids, believed to have existed in the pre-biotic earth, form proton transfer complexes of the type A.B, where A is an amino acid and B is a carboxylic acid. In our laboratory, systematic and precise X-ray investigations on more than 25 amino acid – carboxylic acid complexes have been carried out with a view to understand the modes of interaction between these two distinct chemical species and also characteristic aggregation patterns and specific interactions among them. Dicarboxylic acids viz. oxalic, maleic, fumaric, tartaric and trichloroacetic acids were used in preparing complexes with L- and DL- amino acids. Single crystals of the compounds were grown from saturated aqueous solution containing respective amino acids and carboxylic acids in a 1:1 stoichiometric ratio. In all the complexes, the amino acid molecule adopts a cationic form and the carboxylic acids exist as semi-anions i.e. with a carboxylic acid group and a carboxylate group. Though the stoichiometry remains 1:1 for a majority of complexes, deviations were observed in the cases of oxalic acid with DL-aspartic acid and DL-serine where the stoichiometry is 2:1. There exists a variety of intermolecular aggregation patterns and the results of a detailed analysis of the ionization states, stoichiometry and molecular aggregation patterns will be presented.

SYNTHESES AND STRUCTURES OF $NaCd(H_2O)_2[BP_2O_8]•0.8H_2O$ AND $NaZn(H_2O)_2[BP_2O_8]•H_2O$ AT ROOM TEMPERATURE AND AMBIENT PRESSURE

Ming-Hui Ge, Wei Liu, Hao-Hong Chen, Xin-Xin Yang and Jing-Tai Zhao

The State Key Lab of High Performance Ceramics and Superfine Microstructure, Shanghai Institute of Ceramics, Chinese Academy of Sciences, Shanghai 200050, China (gmh@mail.sic.ac.cn)

Botophosphates have attracted many scientists in the recent year for their promising properties and potential applications. So far almost all the borophosphates reported have been synthesized by hydrothermal methods. $M^{I}x\ M^{II}y(H_2O)_2[BP_2O_8]•\ zH_2O$ (M^{I}= Li, Na, K, Rb, Cs; M^{II} = Mg, Mn, Fe, Co, Ni, Zn, Cu,Cd; x = 0.35-1, y = 1-1.3, z = 0.2-1) is a big family in borophosphates. A chiral octahedral-tetrahedral framework related to the CZP topology is present in the crystal structures of these compounds which also show a very interesting reversible dehydration (or hydration) process[1] The two title compounds were first prepared using hydrothermal method and were characterized by X-ray single crystal investigations [2]. We have now succeeded in their syntheses at room temperature and ambient pressure and the reaction procedure was monitored by X-ray diffraction methods for the reactants in capillary micro-reactors. It is the first time using normal chemical reactions to synthesize borophosphates in this family, and so far only one borophosphate $(NH_4)_5[V_3BP_3O_{19}]•H_2O$ was reported at room temperature to our knowledge[3]. This success at room temperature and ambient pressure provided us many possibilities for synthesizing new borophosphates in other systems. It also widely opened our mind for exploring compounds at different conditions and helping us to understand the mechanism of borophosphate formation.

References

1 Boy, I.; Stowasser, F.; Schäfer, G.; Kniep, R. (2001) *Chem. Eur. J.* **7,** 834-839.
2 Ge M.H.; Mi J.X.; Huang Y.X.; Zhao J.T.; Schäfer G. Kniep R. (2003) *Z. Kristallogr. NCS* **218,** 1-2.
3 Bontchev, R.P., Do, J. and Jacobson , A.J. (2000) *Inorg. Chem.* **39,** 4179-4181.

PO48

A MIXED CATIONS NICKEL DIPHOSPHATE WITH A LAYERED INTERGROWTH STRUCTURE: SYNTHESIS, STRUCTURAL AND MAGNETIC CHARACTERIZATION OF $Na(NH_4)[Ni_3(P_2O_7)_2(H_2O)_2]$

Wei Liu,[a] Xin-Xin Yang,[a] Hao-Hong Chen,[a] Ya-Xi Huang,[b] Walter Schnelle,[b] Jing-Tai Zhao[a]

[a] The State Key Laboratory of High Performance Ceramics and Superfine Microstructure, Shanghai Institute of Ceramics, Chinese Academy of Science, Shanghai, 200050, P. R. China (lw@mail.sic.ac.cn)

[b] Max-Planck-Institut für Chemische Physik fester Stoffe, Nöthnitzer Strasse 40, 011FF Dresden, Germany.

A mixed cations nickel diphosphate, $Na(NH_4)[Ni_3(P_2O_F)_2(H_2O)_2]$ with a layered structure, has been synthesized hydrothermally in the presence of imidazole and characterized by single crystal X-ray diffraction, IR spectrum and magnetisation. The structure consists of *cis*- and *tans*-edge sharing NiO_6 octahedral chains linked *via* P_2O_F units to form $[Ni_3P_4O_{16}]^{2-}$ layers. The ammonium and sodium cations locate alternately in the interlayer spaces. A network of inter-layer and ammonium-layer based hydrogen bonds holds the structure togethher. Similar two-dimensional topological structure can be aslo found in the previously reported diphosphates $K_2Co_3(P_2O_F)\cdot H_2O$ and $(NH_4)_2[Mn_3(P_2O_F)_2(H_2O)_2]$.[1,2] Compared to these layered cobalt and manganese diphosphates, the title compound reported here is different in several aspects. The crucial distinguishing point is that the title compound has a different layer-stacking, which lead to essential structural differences such as different space group and crystal lattice. The studies show that the presence of mixed cations has an important effect on the structural formation of this layered compound, leading to a new layer stacking variants. Magnetic measurement indicates that the magnetic susceptibility obeys almost a Curie-law over the whole measured temperature range with μ_{eff} of 3.32 μ_B, showing Ni^{2+} character and very weak antiferromagnetic interactions.

References

1 Lightfoot, P., Cheetham, A. K. *J.* (1990) *Solid State Chem.* **85**, 2F5.

2 Chippindale, A. M. , Gaslain, F. O. M. , Bond, A. D. , Powell, A. V. (2003) *J. Mater. Chem.* **13** ,1950.

PO49

$NH_4[BPO_4F]$: A NOVEL OPEN-FRAMEWORK AMMONIUM FLUORINATED BOROPHOSPHATE WITH A ZEOLITE-LIKE STRUCTURE RELATED TO GISMONDINE TOPOLOGY

Man-Rong Li, Wei Liu, Ming-Hui Ge, Hao-Hong Chen, Xin-Xin Yang and Jing-Tai Zhao

The State Key Laboratory of High Performance and Superfine Microstructure, Shanghai Institute of Ceramics, Chinese Academy of Science, Shanghai 200050, China.(mrli@mail.sic.ac.cn)

Organically templated metal borophosphates are of great current interest because of their novel structures and potential applications.[4] Comparing to silicates and phosphates, borophosphates containing halogen anions are very few.[2] Here we report a novel compound containing fluorine anion. Colorless crystals of NH_4BPO_4F were synthesized under mild conditions in Teflon-lined stainless steel autoclaves. Its structure was determined by single crystal methods. The crystal structure of the title compound reveals a new type of three-dimensional anionic structure. The condensation of BO_3F and PO_4 tetrahedra through vertices leads to tetrahedral ribbons of $\frac{1}{\infty}[BPO_4F]^{1-}$, which are arranged around 2_1 screw axes to form helical chains, which is the first example of borophosphate compounds with such tetrahedral helical chains to our knowledge. The chains are connected to each other by sharing common vertexes leading to the open-framework with four- and eight-membered ring channels along the cubic axes to form a three-dimensional channel system. In the three-dimensional structure of NH_4BPO_4F, the non-coplanar sequence of up (U) and down (D) linkages of four-memered rings lead to double crankshaft (cc) chains around the eight-mememberd rings; and the coplanar linkages of four-membered rings and adjacent parts of eight-membered rings result in chains including bifurcated square (bs). The condensed connection of these chains gives a framework related to the gismondine (GIS) topology of $I4_1/amd$ Symmetry. This more open zeolite-like structure with channels along three directions instead one direction in GIS could be considered as a new member of GIS family with cubic space group $P2_13$.

References

4 Anthony, K. C; Gérard, F.; Thierry, L. (4999) *Angew. Chem., Int. Ed. Engl.*, 38, 3268.

2 Huang, Y. X.; Schäfer, G.; Carrillo-Cabrera, W.; Borrmann, H.; Gil, R. C.; Kniep, R. (2003) *Chem. Mater.* 45, 4930.

TAILORING OF BOROPHOSPHATE STRUCTURES BY HALOGEN ANIONS AND/OR ORGANIC TEMPLATES

Jing-Tai Zhao Wei Liu, Man-Rong Li, Ya-Xi Huang, Ming-Hui Ge,Hao-Hong Chen and Xin-Xin Yang

The State Key Lab of High Performance Ceramics and Superfine Microstructure, Shanghai Institute of Ceramics, Chinese Academy of Sciences, Shanghai 200050, China (jtzhao@mail.sic.ac.cn)

Organically templated metal borophosphates are of great current interest because of their novel structures and potential applications.[1] Surprisingly, despite intensive researches carried out in many chemical systems, organically templated borophosphates are still to be explored and compounds containing both organic templates and halogen anions are very few.[2] Very recently we have successfully synthesized a few novel borophosphate compounds which contain both halogen anions, amine templates or both, namely $(C_2H_{10}N_2)[BPO_4F_2]$, $NH_4[BPO_4F],(C_4H_{16}N_3)$ $[CdClB_2P_3O_{12}(OH)]$, $(C_4H_{16}N_3)[Zn_3B_3P_6O_{24}]\cdot H_2O$. In these structures, the halogen anions and organic templates both play important roles in constructing the structures. The tailoring effect of both can lead to novel structures with different dimensions.

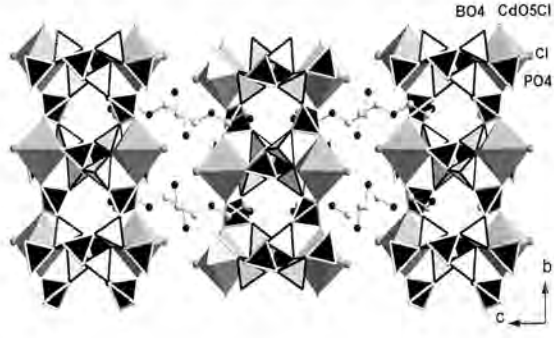

References

1 Anthony, K. C; Gérard, F.; Thierry, L. (1999) *Angew. Chem., Int. Ed. Engl.*, 38, 3268.
2 Huang, Y. X.; Schäfer, G.; Carrillo-Cabrera, W.; Borrmann, H.; Gil, R. C.; Kniep, R. (2003) *Chem. Mater.* 15, 4930.

PO51

SYNTHESIS AND CHARACTERIZATION OF SILVER(I) 1,3-BUTADIYNEDIIDE AND ITS RELATED SILVER(I) DOUBLE SALTS CONTAINING THE C_4^{2-} DIANION

Liang Zhao and Thomas C. W. Mak*

Department of Chemistry, The Chinese University of Hong Kong, Shatin, New Territories, Hong Kong SAR, P. R. China (tcwmak@cuhk.edu.hk)

We have carried out a systematic investigation on the synthesis and structural characterization of a series of double, triple and quadruple salts of the highly explosive silver acetylide, Ag_2C_2.[1] As an extension of the research in this field, the higher homologue Ag_2C_4, which is the second silver carbide to be fully characterized, has been synthesized as a light gray powder that is explosive when heated (130°C) and sensitive to mechanical shock. In the pair of hydrated double salts $Ag_2C_4 \cdot 6AgNO_3 \cdot nH_2O$ [n = 2, 3], the nearly linear, centrosymmetric 1,3-butadiyne-1,4-diyl dianion exhibits an unprecedented μ_8-coordination mode, each terminal being capped by four σ-bonded silver(I) atoms with π-interaction to one of them (Figure (a)). Compared with the known coordination modes of a naked tetracarbon chain in transitional metal complexes (Figure (b) I-VIII), this new mode IX is stabilized by ionic as well as argentophilic interactions and exhibits the highest ligation number[2] for C_4^{2-} to date.

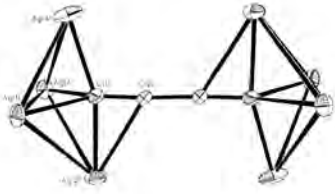

(a) Perspective drawing of a $[Ag_8C_4Ag_4]$ aggregate in $Ag_2C_4 \cdot 6AgNO_3 \cdot 2H_2O$.

(b) Coordination modes of the naked linear tetracarbon (C_4) ligand in metal complexes.

This work is supported by Hong Kong Research Grant Council Earmarked Grant Ref. No. CUHK 4268/00P.

References

1 (a) Guo, G.-C., Zhou, G.-D., Q.-G. Wang, Mak, T. C. W. (1998) *Angew. Chem., Int. Ed.* **37**, 630-632. (b) Guo, G.-C., Zhou, G.-D., Mak, T. C. W. (1999) *J. Am. Chem. Soc.* **121**, 3136-3141. (c) Wang, Q.-M., Mak, T. C. W. (2001) *J. Am. Chem. Soc.* **123**, 1501-1502. (d) Zhao, X.-L., Wang, Q.-M., Mak, T. C. W. (2003) *Inorg. Chem.* **42**, 7872-7876.

2 Guo, G.-C., Mak, T. C. W. (1999) *Chem. Commun.* 813-814.

STRUCTURAL CHARACTERIZATION OF SPIN CROSSOVER COMPLEX TRANS-[Fe(tzpy)$_2$(NCS)$_2$] (tzpy = 3-(2-PYRIDYL)[1,2,3]TRIAZOLO[1,5-A]PYRIDINE)

C. F. Sheu[a], J. J. Lee[a], G. H. Lee[a], I. J. Hsu[a], Y. C. Lin[a],K. Toriumi[c], Y. Ozawa[c], Y. Wang[a]*

[a]Department of Chemistry, National Taiwan University, Taipei 106, Taiwan (fu@xtal.ch.ntu.edu.tw)
[b]National Synchrotron Radiation Research Center, Hsinchu 30077, Taiwan
[c]Spring-8, Hyogo 679-5198, Japan

The spin crossover complex *trans*-[Fe(tzpy)$_2$(NCS)$_2$] has been synthesized and the temperature dependent magnetic susceptibility measurement shows that it is in the high spin state (S = 2) at room temperature and low spin state (S = 0) below 75 K. Single crystal diffraction data were collected and solved at 293 K using in-house Kappa CCD diffractometer and at 40 K using the low temperature vacuum camera facilities at beam line BL02B1 in sping8. Complex *trans*-[Fe(tzpy)$_2$(NCS)$_2$] crystallizes in monoclinic space group $P2_1/c$ with cell constants a = 8.760(1), b = 17.476 (2), c = 8.367 (1) Å, β = 103.78(1)° at 293 K (HS state) and a = 8.531(2), b = 17.215 (3), c = 8.213 (2) Å, β = 105.57(3)° at 40 K (LS state), respectively. The iron(II) atom is located at the inversion center in a distorted octahedron environment, it is coordinated to two tzpy ligands in the equatorial positions and two NCS^- groups in the axial positions (shown in Fig. 1). As expected, the coordination geometry of iron center is strongly dependent upon the spin state of Fe(II). The bond length difference of the two spin states is ~0.19 Å in Fe-N. The bond lengths of Fe-N are 2.217(2), 2.181(2), and 2.097(3) Å at HS state and 2.019(1), 1.971(2), and 1.933(1) Å at LS state. The distortion parameter Σ, defined as the sum of the absolute values of the deviation from 90° of the 12 *cis* angels in octahedron environment, are 74.8° at HS state and 51.8° at LS state. The preliminary light-induced excited spin state trapping (LIESST) effect was investigated by the Fe K-edge and L-edge x-ray absorption spectroscopy at 30 K using a green light (532 nm) laser irradiation.

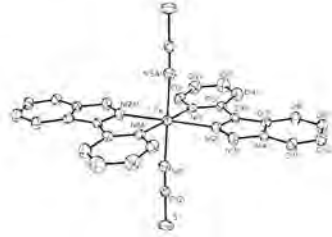

Figure 1. ORTEP diagram of trans-[Fe(tzpy)$_2$(NCS)$_2$] with atomic numbering scheme with 30% thermal ellipsoids at 273 K

PO53

CHARGE DENSITY INVESTIGATION OF A NON-CENTROSYMMETRIC MN COMPLEX : $Mn(mal)(H_2O)_2$

Yen-Chen Lin,[a] I-Jui Hsu,[a] Gene-Hsiang Lee[b] and Yu wang[a]*

[a]National Taiwan University, Taiwan; [b]Instrumentation Center, National Taiwan University, Taiwan (sirius@xtal.ch.ntu.edu.tw)

Charge density distribution of the non-centrosymmetric malonate (mal = $C_3O_4H_2^{2-}$) complex, $Mn(mal)(H_2O)_2$, has been studied by multipole model refinement. In the title compound each Mn atom is coordinated by six oxygen atoms (four from three different malonate ligands and the other two from the binding water molecules) and each malonate anion coordinates to three Mn atoms to form two-dimensional layers perpendicular to c-axis. Neighboring layers are connected by intermolecular hydrogen bonding of the axial water ligands. The Mn – O bond distances are in the range of 2.1280(5) to 2.2315 (9) Å. The O ···· O distances involving the hydrogen bond are 2.762 ~ 3.002 Å.

Topological analysis provides a numerical comparison of the bond character. Electron densities on the Mn-O bond critical points are in the range of 0.27 to 0.36 $e/Å^3$ which are comparable to those of metal-oxygen bonds in metal squarate complexes [2]. AIM (atom in molecule) charge obtained from integration over the atomic basin and the d orbital population of Mn atom will be presented. Results from p-DFT (periodic Density Functional Theory) performed by CRYSTAL98 will also be shown and the comparison between experiment and theory will be given.

References

1 T. Lis and J. Matuszewski, (1979) *Acta Cryst.*, **B35**, 2212

2 C.-R. Lee, C.-C. Wang, K.-C. Chen, G.-H. Lee and Y. Wang, (1999) *J. Phys. Chem.* **A103,** 156

PO54

CRYSTAL ENGINEERING WITH SCORPIONATE LIGANDS

Stuart R. Batten, and Martin B. Duriska

School of Chemistry, Monash University 3800, Australia
(stuart.batten@sci.monash.edu.au)

We have synthesised a range of scorpionate ligands with peripheral coordination sites. The ligands are tris(pyrazolyl)borates with pyridyl or benzonitrile groups attached to the 3- or 4- position of the five-membered rings. The ligands are designed to bind a metal atom at the tris(pyrazolyl) position and be linked into higher order structures (metallosupramolecules or coordination polymers) by coordination of further metal ions at the peripheral coordination sites.

The structures of a number of metal complexes have been determined. The thallium and potassium salts form 1D and 2D networks. Discrete ML_2 molecular species are formed by a number of first row transition metals. A 2D sheet structure is formed by one of the ligands with $FeSO_4$. The sheets contain uncoordinated pyridyl groups that line the interior of channels formed by the stacking of the sheets. These pyridyl groups offer the possibility of further reactivity. A metallosupramolecular 'nanoball' (left) has been synthesised which contains eight ligands and fourteen metal atoms. The nanoballs are roughly spherical and have an internal diameter of *ca.* 15.8 Å, and an external van der Waals diameter of 29 Å (or 2.9 nm).

PO55

CRYSTAL STRUCTURE AND MELTING POINT CORRELATIONS OF ACETIC ESTERS

Hidehiro Uekusa[a], Hirokazu Suzuki[a], Yuji Ohashi[a]

[a]Department of Chemistry and Materials Science, Tokyo Institute of Technology, Meguro-ku, Tokyo 152-8551, JAPAN. (uekusa@cms.titech.ac.jp)

Low melting point acetic esters are important solvent and also used as industrial materials. Therefore, understanding their physical and chemical properties is essential for utilizing these compounds further. As melting point (m.p.) is one of the fundamental property, explaining m.p. behavior of "m.p. alternation" by structural feature is attracting the interests of crystallographers[1].

Different from n-alkane with two functional group (e.g. alkanedicarboxylic acid and alkanediol), acetic esters ($AcO(CH_2)_{n-1}CH_3$) show no m.p. alternation behavior in longer alkyl chain region, however, smaller acetic esters show prominent m.p. alternation (-96, -81, -91, -75, -68, -60°C for n=1 to 6). In order to investigate this behavior of small acetic esters, crystal structures of methyl acetate (n=1) to amyl acetate (n=5) were investigated by single crystal X-ray structure analysis.

As they are liquid in room temperature, single crystals were grown by "*in situ* crystallization" method on the R-AXIS RAPID diffractometer. The diffraction data were collected at 93K within short measurement time just after a single crystal was obtained. Their crystal structures were determined in good R values (R_1=0.039 – 0.044).

Investigation of the crystal structures revealed that both C-H···O type hydrogen bonds between acetic groups and van der Waals interactions between alkyl chains play important role to stabilize the structure. Two distinctive H-bond motif recognized were "dimer" (n=2,4,5;Fig.1(a)) and "tetramer" (n=1,3;Fig.1(b)) structures around inversion center. Because of this packing differences, methyl (n=1) and propyl (n=3) acetates have fewer number of H-bond comparing to other acetates. Therefore, lower m.p. of them is caused by this kind of inefficiency of crystal packing

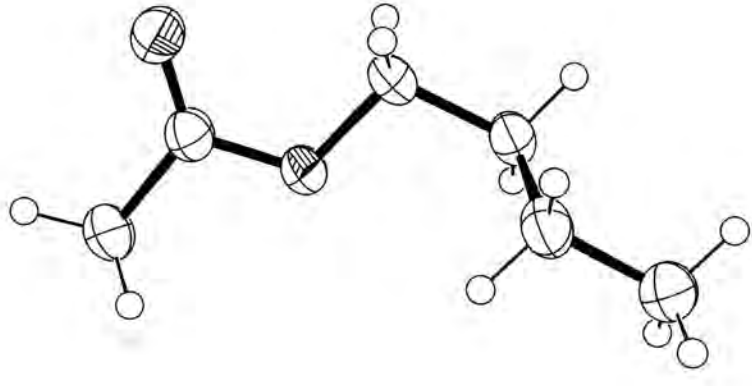

COORDINATION POLYMER WITH ZEOLITE OR ZEOLITE-LIKE TOPOLOGIES

Yun-Qi Tian,[a,b] Lin-Hong Weng,[a] Zhen-Xia Chen[a] , Dong Yuan Zhao[a] and Xiao-Zeng You[c]

[a]College of Chemical Science and Engineering, Liaoning University, Shenyang 110036, China (ytian588@sina.com); [b]Department of Chemistry, Fudan University, Shanghai 200433, China. [c]State Key Laboratory of Coordination Chemistry, Institute of Coordination Chemistry, Nanjing University, Nanjing 210093, China.

Coordination polymers with stable frameworks of big openings are of current interest and importance for many applications involving catalysis, separation and gas storage. To create such materials we have developed a strategy for synthesis of coordination polymers with zeolite or zeolite-like structures, namely, the natural choice of the porous materials. Cobalt(II) or Zinc(II) imidazolates are such coordination polymers synthesized that exhibit not only the silicate-like polymorphism, but also the zeolite or zeolite-like topologies. Up to now, we have explored at least 9 neutral extended three-dimensional frameworks of $[M(im)_2]_\infty$ (M = Co(II), Zn(II)), which show the characteristics of zeolite structures and high thermal stability.

We thank the Post-doctor funds of the State and Shanghai-City, the State Key Project of Fundamental Research and the National Science Fund of China for the finance support.

References

1 Hee, K. C., Siberio-Pérez, D. Y., et al. (2004) *Nature*, **427**, 523-527.
2 Tian, Y. Q., Cai, C. X., Ji, Y., You, X. Z., Peng, S. M. and Lee, G. S. (2002) *Angew. Chem. Int. Ed.*, **41**, 1384.
3 Tian, Y. Q., Cai, C. X., Ren, X. M., Duan, C. Y., Xu, Y., Gao, S. and You, X. Z. (2003), *Chem. Eur. J.* **9**, 5673 –5685.
4 Tian, Y. Q., Chen, Z. X., Weng, L. H. and Zhao, D. Y. unpublished results

PO57

CRYSTAL STRUCTURES OF COMPLEXES OF AMINO ACIDS WITH ZINC AND CADMIUM CHLORIDES : IONIZATION STATES, STOICHIOMETRY, COORDINATION AND CRYSTAL PACKING

R.V.Krishnakumar[a], M.Subha Nandhini[b] and S.Natarajan[b]

[a]Department of Physics, Thiagarajar College, Madurai – 625 009, [b]Department of Physics, Madurai Kamaraj University, Madurai-625 021, India (mailtorvkk@yahoo.co.in)

Zinc – amino acid complexes are interesting as zinc is known to compete successfully with cadmium for protein binding sites. Zinc also plays an important biological role in the formation of a structural motif called zinc fingers which are characteristic of certain proteins that bind to DNA. Recently, we have elucidated the crystal structures of complexes of DL-Alanine, Sarcosine, DL-Valine with $ZnCl_2$ and -Alanine, Sarcosine and DL-Valine with $CdCl_2$. Single crystals of the compounds were obtained from saturated aqueous solution containing respective amino acids and inorganic salts in a 2:1 stoichiometric ratio. Interestingly, two different crystalline forms were obtained in the case of sarcosine with $ZnCl_2$ and in one of the forms the sarcosine molecule adopts an unusual cationic form which may be justified by a complex series of hydrolytic equilibria involving the solvent water molecules, the Cl^- ions and the sarcosine zwitterion. The coordination polyhedron around zinc is, in general, a distorted tetrahedron and that around cadmium a distorted octahedron. In halegenozinc – amino acid complexes, the crystal packing is characterized by amino acid molecules coordinating to Zn forming a linear chain through hydrogen bonds. In the case of amino acid – $CdCl_2$ complexes, the packing of molecules is characterized by infinite one-dimensional polymeric chains in which the carboxyl group of the respective amino acid molecules form chelated rings. The results of a detailed analysis of the ionization states, stoichiometry, coordination geometry and crystal packing features will be presented.

PO58

CRYSTAL AND MOLECULAR STRUCTUR OF BIS(HYDRAZINIUM)BIS(OXALATO)NICKEL(II) DIHYDRATE AND BIS(HYDRAZINIUM)BIS(MALONATO)COBALT(II) DIHYDRATE

V. Manivannan [a], K.R. Radhakrishnan [b], K. Saravanan [c], S. Govindarajan [c]* and J.J. Vittal[d]

[a]Department of Physics, Presidency College, Chennai, 600 005, India; [b]Department of Physics, Government Arts College, Kumbakonam 612001, India; [c]Department of Chemistry, Bharathiar University, Coimbatore 641 046, India; [d]Department of Chemistry, National University of Sigapore, Singapore, 117543.
(manivan_1999@yahoo.com)

New bis(hydrazinium)bis(oxalato)nickel(II) dihydrate, $[(N_2H_5)_2Ni(COO)_2].2H_2O$ (**1**) and bis(hydrazinium)bis(malonato)cobalt(II) dihydrate, $[(N_2H_5)_2Co(CH_2(COO)_2)_2].2H_2O$ (**2**) have been prepared and their structure determined from single crystal X-ray analysis. The crystallographic data for the compound **1** are monoclinic, space group $P2_1/c$ with **a** = 6.2814 (2), **b** = 12.9937 (6) **c** = 7.1101 (2) Å, b = 102.746 (3)°, Z = 2 and R = 0.0260. The compound **2** crystallizes in the triclinic space group P-1 with **a** = 5.2383 (7), **b** = 7.5091 (10), **c** = 8.5289 (11) Å, Z = 1 and final R factor of 0.0376 based on 1672 independent reflections. Both the crystals contain discrete $[(N_2H_5)_2Ni(COO)_2]$ / $[(N_2H_5)_2Co(CH_2(COO)_2)_2]$ and water molecules. In these complexes the metal ion is coordinated with regular octahedral geometry, the square plane being occupied by four carboxylate oxygens from the two chelate-bidentate oxalate / malonate groups and the apical positions by two nitrogen atoms one from each hydrazinium cation. The structure analysis of the **1** shows that, the oxalate groups are planar and the hydrazinium cations are trans to each other. Both compounds posses a center of inversion, as the coordinated atoms and the water molecules are trans to each other. In compound **1** the oxalate oxygens are hydrogen bonded to the hydrazinium ions by the N-H...O type of bond predominantly. Such net works are found to extend throughout the crystal. The O-H...O type of hydrogen bond between water and oxalate also exist. Similar type of hydrogen bonding is also observed in compound **2**. As compared to compound **1**, the compound **2** undergoes dehydration at elevated temperature (260°C), indicating that the water molecules are strongly involved in the hydrogen-bonded network in the latter.

PO59

SYTHESIS AND CRYSTAL STRUCTURES OF POLYNUCLEAR TITANIUM(IV) AND ZIROCONIUM(IV) COMPOUNDS SUPPORTED BY AN OXYGEN TRIPODAL LIGANDS

Xiao-Yi Yi, Tony C. H. Lam, E. Y. Y. Chan, Qian-Feng Zhang, Ian D. Williams, and Wa-Hung Leung*

Department of Chemistry and Open Laboratory of Chirotechnology of the Institute of Molecular Technology for Drug Discovery and Synthesis, The Hong Kong University of Science and Technology, Clear Water Bay, Kowloon, Hong Kong, China (E-mail: chleung@ust.hk)

Metal ions in oxygen-rich coordination environments are of significance because they are relevant to active sites of oxide based heterogeneous catalysts. In an attempt to model metal oxide surfaces, we set out to prepare titanium and zirconium complexes containing an oxygen tripodal ligand $[CpCo\{P(O)(OEt)_2\}_3]^-$ (L_{OEt}^-).[1] Previously, we demonstrated that the titanyl and zirconyl species can be trapped by NaL_{OEt} in water and the resulting species can react with BF_4^- to give $L_{OEt}MF_3$ (M = Ti or Zr).[2] We here present the characterization and solid-state structures of water-soluble cluster compounds formed by the reactions of NaL_{OEt} with titanyl sulfate and zirconyl nitrate in water. The core structures of these clusters are found to be closely related to those of group 4 metal oxides and metal aqua ions. Treatment of $L_{OEt}Ti(IV)$ complexes with metal ions give heterobimetallic clusters that have been characterized by X-ray crystallography.

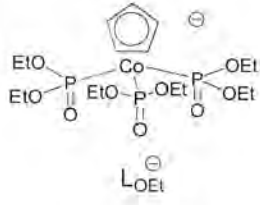

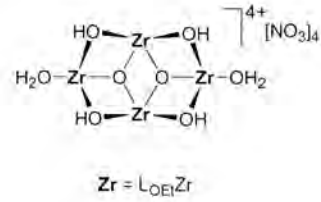

References

1 Kläui, W. *Angew. Chem., Int., Ed. Engl.* **1990**, *29*, 627.
2 Lam, T. C. H.; Chan, E. Y. Y.; Mak, W. L.; Williams, I. D.; Wong, W. T.; Leung, W.-H. *Inorg. Chem.* **2003**, *42*, 1842.

PO60

DIRECT OBSERVATION OF DIFFERENT REACTION ROUTE DUE TO STERIC HINDRANCE IN CRYSTALLINE-STATE PHOTOISOMERIZATION

Yuji Ohashi, Akira Hirano, Hidehiro Uekusa

Department of Chemistry and Materials Science, Tokyo Institute of Technology, Ookayama, Meguro-ku, Tokyo 152-8551, Japan
(yohashi@cms.titech.ac.jp)

The δ-cyanobutyl group bonded to the cobalt atom in cobaloxime complex crystals is isomerized to γ-, β- and α-cyanobutyl group when the powdered sample is exposed to visible light as shown in the Scheme.

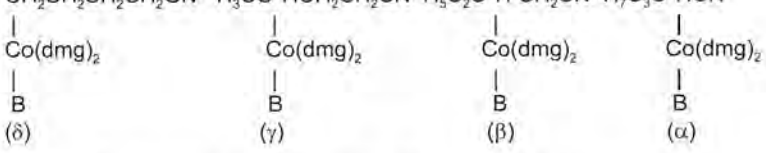

Scheme: Stepwise photoisomerization of δ-cyanobutyl group in cobaloxime complex crystals

When the single crystal with the δ-cyanobutyl group was irradiated with the xenon lamp, a part of the δ-cyanobutyl group was isomerized to γ-cyano-butyl group. Further irradiation caused the decomposition of the crystallinity. The reaction cavity for the cyanobutyl group is too small to proceed further reactions.

In order to expand the reaction cavity around the δ-cyanobutyl group, the bulky substituent, dibenzylboronyl group, was introduced to the equatorial ligand and the crystal was irradiated with the xenon lamp in the same conditions.

The crystal structures before and after photoirradiation were analyzed by X-rays. After 24 hours exposure, the complex with the α-cyanobutyl group appeared in the crystal and the ratio of δ- to α-cyanobutyl groups was 75:25. The intermediate complexes with the γ- and β-cyanobutyl groups were not observed. Since the crystal was gradually decomposed after 24 hours, the structural change was checked with the IR spectra. The spectra indicated that not only the original δ-cyanobutyl group but also the produced α-cyano-butyl group gradually decreased and the β-cyanobutyl group gradually appeared. This suggests that the reaction proceeds δ- to β-cyanobutyl group through α-cyanobutyl group, which is completely different from the compound without bulky dibenzylboronyl group. The γ-cyanobutyl group was not observed in the IR spectra. The shape of the cavity for the cyanobutyl group well explains the above reaction.

PO61

NOVEL BIS-DIDENTATE NITROGEN LIGAND DERIVED FROM 1,4-DIHYDRAZINOPHTHALAZINE

Ling-Kang Liu[a] and Wen-Fu Chang[b]

[a]Institute of Chemistry, Academia Sinica, Nankang, Taipei, Taiwan and [b]Department of Chemistry, National Central University, Chung-Li, Tao-Yuan, Taiwan (liuu@chem.sinica.edu.tw7

Upon reflux with pyridine-2-carboxaldehyde, 1,4-dihydrazinophthalazine **1** could be transformed into the corresponding Schiff base **2**, whose oxidative cyclization in a treatment with Br_2 gave bis-triazole derivative **3**, a novel bis-didentate nitrogen ligand bridged by a rigid aromatic backbone. The C_2-symmetric **3** exhibited very interesting molecular properties that were pH dependent as spectroscopically characterized. When **3** reacted with $Ru(CO7_2Cl_2$, the C_2-symmetric diruthenium complex **4** resulted.

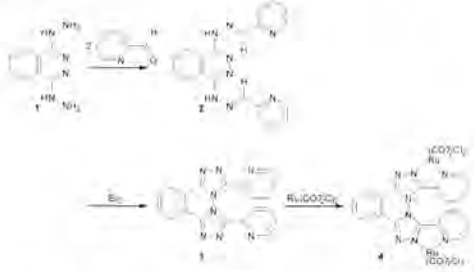

The structure of **3** was determined by X-ray diffraction. Unconstrained in the solid state, the structural parameters of **3** conform to the C_2 molecular symmetry. It is further noticed that intramolecularly the distance between two pyridine N atoms is only 3.075 Å, which is shorter than the sum of van der Waals radii, suggesting an attractive interaction.

SOLID CRYSTALLINE FORMS OF DICLOFENAC SODIUM AND DICLOFENAC ACID

Chuttree Phurat,[a] Narong Praphairaksit,[a] Malatee Taiyaqupt,[b] Nongnuj Muangsin[a]

[a]Department of Chemistry, Faculty of Science, Chulalongkorn University, Bangkok, 10330, Thailand.
[b]Department of Geology, Faculty of Science, Chulalongkorn University, Bangkok, 10330, Thailand.

Different solid forms of a pharmaceutical substance may display different physical and chemical properties. Pharmaceutical substances may change to different polymorphs, solvates (pseudo-polymorphism), desolvates, or amorphous materials after standard pharmaceutical processes such as crystallization, milling, freeze-drying, spray-drying, and solid-dispersion, which may change their pharmaceutical activities.

Diclofenac, (2-[2,6-dichlorophenyl)amino]-phenyl]acetate) is an excellent nonsteroidal anti-inflammatory drug (NSAID) and is mainly used in the treatment of rheumatoid arthritis and other rheumatoid disorders. Diclofenac has numerous solid forms including diclofenac acids and diclofenac salts. The exemplary diclofenac acid crystal forms include its monoclinic forms with the space group *P2₁/c* and *C2/c* (Castellari & Ottani, 1997). Diclofenac acid also exists in an orthorhombic form with the space group *Pcan* (Jaiboon *et al.*, 2001). The examples of diclofenac in its salt forms include potassium diclofenac dihydrate (Fini *et al.*, 2001), sodium diclofenac tetrahydrate (Fini *et al.*, 2001).

In this work, solid crystalline forms of diclofenac sodium and diclofenac acid have been identified and characterized using X-ray powder diffraction (XRPD), scanning electron microscope (SEM), thermogravimetric analysis (TGA), solubility and melting point. In addition, biological activity against COX-1 of all solid crystalline forms and commercial diclofenac sodium have been tested.

References

1 Castellari, C. & Ottani, S. (1997). *Acta. Cryst.*, **C53**, 794-797.
2 Jaiboon, N. Yos-in, K., Ruangchaithaweesook, S., Chaichit, N., Thutivoranath, R., Siritaedmukul, K. & Hannongbua, S. (2001). *Analytical Sciences.* **17**, 1465-1466.
3 Fini, A., Garuti, M., Fazio G., Alvarez-Fuentes, J. & Holgado, M. A. (2001). *J. Pharm. Sci.*, **90(12)**, 2049-2057.

PO63

SELF-ASSEMBLY OF FOUR METAL–SQUARATE (Cd(II) and Zn(II)) COORDINATION POLYMERS WITH FLEXIBLE 1,2-BIS(4-PYRIDYL)ETHANE LIGAND (DPE)

Chih-Chieh Wang,[a] Hui-Wun Lin,[a] Chin-Hui Liao,[a] Cheng-Han Yang,[a] and Gene-Hsiang Lee[b]

[a]Department of Chemistry, Soochow University, Taipei, Taiwan (ccwang@mail.scu.edu.tw); [b]Instrumentation Center, National Taiwan University, Taipei, Taiwan.

Four types of new metal-organic coordination networks, $[M(C_4O_4)_2(H_2O)_2]$ $[M(Hdpe)(C_4O_4)_{0.5}(H_2O)_3]$ (M = Zn **1**, Cd **2**), $[M(C_4O_4)_{1.5}(H_2O)_3][H_2dpe]_{0.5}$ (**2**) (M = Zn **3**, Cd **4**), $[Zn(dpe)(C_4O_4)(H_2O)_2]$ (**5**) and $[Cd(dpe)(H_2O)_4](C_4O_4)$ (**6**), based on squarate and/or dpe bridges (dpe = 1,2-bis(4-pyridyl)ethylene) have been synthesized and characterized by spectroscopic data and single-crystal X-ray diffraction studies. The structural determination reveals that compounds **1** and **2** are a 3D network constructed by the interlock of two charged 2D metal-organic frameworks, the $[M(C_4O_4)_2(H_2O)_2]^{2-}$ and $[M(Hdpe)(C_4O_4)_{0.5}(H_2O)_2]^{2+}$, that both adopt the square-grid as the basic building unit via the linkage of metal center with $\mu_{1,3}$-squarate and $\mu_{1,2,3,4}$-squarate ligands, respectively, to form the 2D layered frameworks. In the cationic part, two mono-protonated anti-$Hdpe^+$ act as monodentate ligands coordinated to the metal center at *trans*-positions and interpenetrate into the cavities formed by the square grids in $[M(C_4O_4)_2(H_2O)_2]^{2-}$. The molecular structure of compounds **3** and **4** show a 2D network, consisting of the $[M(C_4O_4)_{1.5}(H_2O)_3]^-$ anion and the free diprononated H_2dpe^{2+} cation. The $[M(C_4O_4)_{1.5}(H_2O)_3]^-$ is a 2D infinite layered framework using a 6,6-membered ring as building unit via the linkage of six metal centers and two $\mu_{1,3}$-, four $\mu_{1,2}$-squarate ligands. Compound **5** is a 2D wave-like framework, being constructed from the crosslinkage of the infinite 1D $[Zn(\mu_{1,3}$-squarate$)(H_2O)]$ chains by gauche-dpe ligands. Compound **6** is a 1D linear chain via the linkage of Cd center and anti-dpe ligand. Hydrogen bond plays an important role on the stabilization of these four metal-organic coordination networks.

PO64

HYDROTHERMAL SYNTHESIS, CHARACTERIZATION, AND SUPRAMOLECULAR STRUCTURE OF [Co(C6H4O2N)3]·H2O

Kittipong Chainok and Kenneth J. Haller

School of Chemistry, Institute of Science, Suranaree University of Technology, Nakhon Ratchasima, 30000, Thailand (kchainok10@yahoo.com)

The hydrothermal synthesis using vanadium pentoxide, cobalt chloride hexahydrate, 1,3-diaminopropane, 2,5-pyridinedicarboxylic acid, and H_2O in a molar ratio of 1:1:2:2:593 produced 0.65 g of red crystals of $[Co(C_6H_4O_2N)_3]\cdot H_2O$ in a yield of 84% based on cobalt. Single crystal x-ray diffraction, SEMEDX,FTIR, and TGA were used to characterize the complex. Intensity data were collected on a Bruker Nonius KappaCCD autodiffractometer equipped with a molybdenum x-ray source. The structure was solved by direct methods and refined with the SHELX package. The complex has distorted octahedral coordination geometry with three *mer* pyridine nitrogen atoms and three *mer* carboxylate oxygen atoms as shown on the left below. The molecules pack as a series of offset phenyl-phenyl face-to-face (π···π) interactions between ring type 1, propagated by alternate 2-fold sites and inversion sites in the **c** direction giving an interdigitated double comb motif. The water molecules bridge the rings of type 1 to rings of type 2 on adjacent π···π stacks generating a two-dimensional network. The third dimension is achieved by phenyl ring 1 to ring 3 edge-to-face interactions between adjacent π···π stacks.

The EDX spectrum of the red crystals indicates the presence of only cobalt. IR (KBr): 3520(s) 3454(s) 3112(s) 3061(s) 1681(s) 1607(s) 1571(s) 1453(s) 1333(s) 1284(s) 1152(s) 1056(s) 859(s) 766(s) 689(s) 492(s) 406(s) cm^{-1}. Thermal decomposition under O_2 shows loss of water at 156 °C (4.6% loss) followed by a broad step from 308 to 412 °C of 79.8% as the ligands decompose. Reasonably, all of these results correspond to the x-ray analysis. Crystal data: $[Co(C_6H_4O_2N)_3]\cdot H_2O$; *Mr* = 425.24 Daltons; monoclinic, *C2/c* (No. 15); a = 29.727(4) Å, b = 8.5401(6) Å, c = 13.8024(11) Å, β = 95.862(9)°, V = 3485.71(3) $Å^3$; Z = 4; D_{calc} = 1.689 g/cm^3; μ = 10.4 cm^{-1}; $\lambda_{MoK\alpha}$ =0.71073 Å; T = 298 K. *Data collection: Nonius KappaCCD, 0.5 mm ifg capilliary collimator,* R_{merge} = 0.0431, 6672 *unique data, 4349 observed data* ($I_o > 4\sigma(I_o)$).

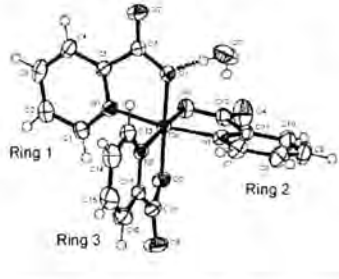

ORTEP drawing (50% ellipsoids)

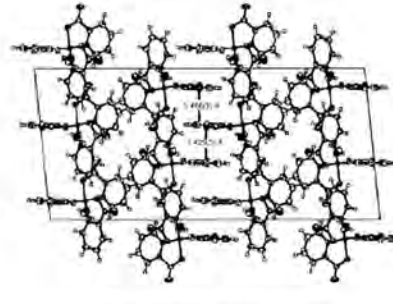

Projection down [010]

PO65

THE ORDER-DISORDER TRANSITION AT 150 K OF POLYMERIC $Ag(bipy)NO_3$

Weenawan Somphon,[a] Kenneth J. Hallera and A. David Rae[b]

[a]School of Chemistry, Institute of Science, Suranaree University of Technology, Nakhon Ratchasima 30000, Thailand; [b]Research School of Chemistry, The Australian National University, ACT 0200, Australia (weenawanus@yahoo.com).

$Ag(bipy)NO_3$, bipy = 4,4'-bipyridine = $C_{10}H_8N_2$, has two known crystal forms at room temperature [1,2,3]. The *Fddd* form contains a disordered nitrate ion and shows previously unreported planes of diffuse scattering indexable as $3k \pm l = 4n$ for the RT cell *a* 12.952(2), *b* 9.912(1), *c* 34.428(4) Å. Automated data collection used a Nonius KappaCCD diffractometer equipped with an Oxford Cyrostream 600. Synthetic precession photographs showed the symmetry was *Fddd* at 160 K and above but a loss of systematic absences indicated *F12/d1* (*i.e. C2/c*) at 150 K and below. The 100 K structure, *C2/c*, *a* 12.751(1), *b* 9.860(1), *c* 18.379(2) Å, β 109.98(1) ° had twin components related by a rotation around **c***. The cell for *F12/d1* has *a'* = *a*, *b'* = *b*, *c'* 34.547(2) Å, β' 89.68(1) °. All intensities were obtained as the sum of two components. Refinement gave a 0.754(1):0.246 twin with no disorder and $R(F) = 0.021$ for 2293 (out of 2456) reflections with $I > 3\sigma(I)$. Along a chain, Ag atoms, (3**b** ± **c**)/4 apart, move 0.221(1) Å in opposite directions perpendicular to the chain. Chains are cross linked by Ag-Ag contacts of 2.958(1) Å and Ag-O contacts of 2.749(2) and 2.747(2) Å. The chains zig-zag so that Ag atoms avoid closer contact with the nitrates. The 200 K structure, *Fddd*, *a* 12.823(1), *b* 9.937(1), *c* 34.450(1) Å, was refined as a 1:1 disorder of all atoms initiated by disordering the 100 K structure. Constrained refinement gave $R(F) = 0.028$ for 1004 (out of 1270) reflections with $I > 3\sigma(I)$. The Ag displacement reduced to ±0.123(3) Å. The alternative orientation of the nitrate gave 3 Ag-O contact distances indicating an intermediate step for a change of local ordering. The 16.5° root mean square angular displacement of the nitrate (up from 10.1 °) showed that the nitrate ions readily rotate by 60 ° in their own plane to initiate the orderdisorder phase change. The diffuse scattering indicates that mistakes in nitrate positions cause a localised straightening of the adjacent chains that moves substantial amounts of these chains along their lengths. In contrast, the actual position of a nitrate only affects the closest Ag atoms.

References

1 Bi, H., Sun, D., Cao, R. and Hong, M. (2003) *Acta Cryst.* **E**58, m324-m325.
2 Robinson, F. and Zaworotko, M. J. (1995) *J. Chem. Soc., Chem. Commun.* 2413-2414.
3 Yaghi, O. M. and Li, H. (1996) *J. Am. Chem. Soc.* **118**, 295-296.

PO66

SUPRAMOLECULAR STRUCTURE OF AZIDONITROSYLBIS(TRIPHENYLPHOSPHINE)NICKEL

Nongnaphat Khosavithitkul and Kenneth J. Haller

School of Chemistry, Institute of Science, Suranaree University of Technology, Nakhon Ratchasima 30000 Thailand.(unchalee@ccs.sut.ac.th)

The sum of the multiple phenyl-phenyl edge-to-face (ef) C–H···π attractive interactions of the concerted sextuple phenyl embrace (6PE) gives sufficient interaction energy to make it a dominant supramolecular motif for triphenylphosphine (TPP) complexes [1]. The three-dimensional crystal structures of $Ni(NCS)(NO)(P(C_6H_5)_3)_2$ and $NiCl(NO)(P(C_6H_5)_3)_2$ are dominated by phenyl-phenyl interactions, including the expected strong six-fold phenyl embraces between adjacent triphenylphosphine ligands. The chloro complex also exhibits an extensive concerted interaction between a solvent benzene molecule and several phenyl rings on surrounding molecules. The subject of this report is the reinvestigation of the crystal structure of the title complex,
$Ni(N_3)(NO)(P(C_6H_5)_3)_2$, [2], in which the sextuple phenyl embrace does not occur.

The title complex was synthesized from $NiBr(NO)(P(C_6H_5)_3)_2$ by a metathesis reaction with excess NaN_3 and recrystallized from benzene-hexane as deep blue-black crystals. The structure of the compound has been redetermined based on an x-ray data set collected on a KappaCCD diffractometer. The compound crystallizes in the monoclinic space group $P2_1/c$ with $Z = 4$. The discrete pseudo tetrahedral $Ni(N_3)(NO)(P(C_6H_5)_3)_2$ molecules are interconnected into a three-dimensional supramolecular structure by C–H···π hydrogen bonds to the azido and phenyl π electron density.

The shortest intermolecular P···P distances in the azido complex are 7.350 Å and 7.783 Å with colinearities of 86.9° and 117.8°, thus not 6PE. The strongest nonbonded interaction is the 2.466 Å *intra*molecular C–H···N interaction to the lone pair on the N bonded to Ni. While there are several phenyl-phenyl interactions as well, the stronger interactions to the azido ligand dominate and the highest multiple phenyl embrace only involves four phenyl rings. However, seven additional C–H···N interactions in the range of 2.6 - 2.8 Å surround the azido ligand, making in the major determiner of the extended crystal structure.

References

1 Dance, I., & Scudder, M. (1995). The Sextuple Phenyl Embrace, a Ubiquitous Concerted Supramolecular Motif. *J. Chem. Soc., Chem. Commun.* 1039-1040.

2 Enemark, J. H. (1971). Four-Coordinate Metal Nitrosyls 1. the Structure of Azido-nitrosylbis(triphenylphosphine)nickel, $Ni(N_3)(NO)(P(C_6H_5)_3)_2$. *Inorg. Chem.* 10, 1952-1956.

PO67

THE CRYSTAL STRUCTURE OF PYRIDINE-3,5-DICARBOXYLIC ACID

Samroeng Krachodnok and Kenneth J. Haller

School of Chemistry, Institute of Science, Suranaree University of Technology, Nakhon Ratchasima 30000, Thailand (Lipopoo@yahoo.com)

Crystals of the title compound were obtained as unreacted starting material from a hydrothermal synthesis reaction. The compound crystallizes in the monoclinic space group $P2_1/c$ with a = 9.6756(4), b = 11.1166(7), c = 6.5808(4) Å, β = 107.766(4) °, and V = 674.07(7) Å$_3$, T = 298 K. Intensity data were collected on a Bruker Nonius KappaCCD diffractometer using graphite monochromated Mo Kα x-radiation.

The molecules are interconnected in two-dimensional layers (parallel to the *ab* plane) through O.H···N hydrogen bond interactions between adjacent molecules related by a 2_1 screw axis, and O.H···O hydrogen bond interactions between adjacent molecules related by the other independent 2_1 screw axis (left figure below). Thus, the possibility of the ubiquitous inversion related carboxylic acid dimer structure is precluded.

Layers related by the *c* glide and inversion centers are held together by face-to-face, π.π interactions, supplemented by >C(δ+)···O interactions between carbonyl carbon and carbonyl oxygen atoms across inversion centers (right figure below).

Crystal data: $C_7H_5NO_4$; M_r = 167.12 Daltons; transparent pale orange; thick plate 0.06 x 0.10 x 0.26 mm; monoclinic; $P2_1/c$ (No. 14), a = 9.6756(4), b = 11.1166(7), c = 6.5808(4) Å, β = 107.766(4) °, and V = 674.07(7) Å$_3$, Z = 2, T = 298 K, μ = 1.4 cm^{-1}; d_{calc} = 1.647 Mg/m$_3$; $\lambda_{MoK\alpha}$ = 0.71073 Å; Data collection: Nonius KappaCCD; 0.5 mm *ifg* capillary collimator; 23425 data collected (triclinic), θ_{max} = 31.0 °; 2147 unique (2/m), R_{sym} = 0.040; 1532 observed $F_o > 4\sigma(F_o)$.

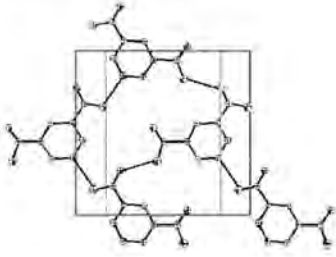

Layer projected down (001)

>C(δ$^+$)···O interactions

INVARIOMS FOR AUTOMATED LOW ORDER DATA CHARGE DENSITY ANALYSIS

B. Dittrich[a], M. Spackman[a], P. Luger[b]

[a]School of Biological, Biomedical & Molecular Sciences, University of New England, Armidale NSW 2351, Australia, (bdittric@pobox.une.edu.au); [b]Institut für Chemie / Kristallographie, Freie Universität Berlin, Takustr. 6, 14195 Berlin, Germany.

Considerable effort is necessary for an experimental charge density study with respect to the X-ray diffraction experiment and the modelling of the high resolution data. By introducion of invarioms[1], that define an intramolecular transferable atom using the nearest neighbor approximation[2], invariomic multipole parameters can be predicted. For this purpose we use theoretical calculations[3] on model compounds that mimic the same chemical environment as an atom in a given crystal structure. For the molecular electron density theoretical structure factors[4] are calculated and a multipole refinement then yields the parameters needed. This way approximated aspherical structure factors and an improved geometry can be derived for a crystal structure of interest. Properties derived from the density, i.e. Hirshfeld surfaces[5], the electrostatic potential or topological properties are then accessible. It is emphasized that by using this procedure standard low resolution data sets can be evaluated. The fact that a defined limited number of invarioms exists allows additionally the automation of the modelling process. The steps required, starting from a spherical model, are then:

1.) The assignment of an invariom to an atom in a structure
2.) Setup of the local coordinate system of that atom
3.) Transfer of the invariomic multipole parameters
4.) Refinement of geometry and thermal motion

A program for steps one to three has been developed. The usage of theoretically – compared to the experimentally– derived multipoles[6] has several advantages. Here we want to present results for a comparison of the invariom density to the theoretical and the crystal density for a geometry from a high resolution data multipole refinement on the dipeptide L-Phe-L-Pro. An application of the procedure outlined here to smaller proteins is in progress.

References

1 Dittrich, B., Koritsanszky, T., Luger, P., Angew. Chem. **116**, in press.
2 Koritsanszky, T., Volkov, A., and Coppens, P., Acta Cryst. **A58**, 2002, 464.
3 Gaussian 98, Revision A.11.3, M. J. Frisch et al., Gaussian, Inc., Pittsburgh PA, 2002.
4 Chandler, G.S., Spackman, M. A., Acta Cryst. **A34**, 1978, 341.
5 McKinnon, J.J., Mitchell, A. S., Spackman, M.A., Chem. Europ., J. **4**, 1998, 2136.
6 Pichon Pesme, V., Lecomte, C. And Lachekar, H., J. Phys. Chem. **99**, 16, 1995.

PO69

NEW FACE-CAPPING BONDING MODE FOR ARENES IN ORGANOMETALLIC METAL CLUSTERS

Jasmine Po-Kwan Lau, and Wing-Tak Wong*

Department of Chemistry, The University of Hong Kong, Pokfulam Road, Hong Kong, P. R. China. (h9924717@hkusua.hku.hk)

Heterometallic carbonyl clusters have caught considerable attention because of their potential catalytic and stoichiometric reaction. The chemistry of Os-Rh mixed-metal carbonyl clusters [1,2] are particularly interested due to the good combination of high reactivity and sufficient thermodynamic stability of the cluster intermediates occurred in the reaction. The reaction of benzene (arenes) with Os-Rh mixed-metal clusters afforded a new capping mode, C3v(sv), for the arene on the cluster surface, which comprises an important area of research in surface science. The determination of the adsorption geometry of arenes on metal surfaces can give insight into the elementary steps of the dissociation and catalytic reactions of these molecules. [3]

References

1 J. P. -K. Lau, W. -T. Wong, (2002) *J. Organomet. Chem.* **659**, 151-158.
2 J. P. -K. Lau, W. -T. Wong, (2003) *Inorg. Chem. Comm.* **6**, 174-177.
3 J. P. -K. Lau, Z. -Y. Lin, W. -T. Wong, (2003) *Angew. Chem. Int. Ed. Engl.* **42(17)**, 1935-1937.

STRUCTURAL STUDY OF COORDINATION NETWORK BASED ON METAL ORGANIC LIGANDS

Lap Szeto, Yang-Yi Yang and Wing-Tak Wong*

Department of Chemistry, The University of Hong Kong, Pokfulam Road, Pokfulam, Hong Kong, P. R. China (lapszeto@hkusua.hku.hk).

Supramolecular crystal engineering has attracted much attention in recent years. This is because it holds promise to the discovery of new functional solids for applications in non-linear optics (NLO)[1], porous material sciences[2]. Through the rational design of selected ligands and metal, the careful study of the resulting crystal packing, the targeted physical properties can be fine tuned. Studies on some of these supramolecular network systems based on carboxylates[4,4] (see Figure 1 & 2) will be discussed.

References

1 Evans, O. R. and Lin, W.-B. (2002) *Acc. Chem. Res.* **35**, 511-522.
2 Eddaoudi, M.; Moler, D.B.;Li, H.; Chen, B.; Reineke, T.M.; O'keefe, M.; Yaghi, O.M. (2001) *Acc. Chem. Res.* **34**, 419-440.
4 Yang, Y. Y., Szeto, L. and Wong, W.-T. (2004) *Appl. Organometal. Chem.* **17**, 958-959.
4 Yang, Y. Y., Huang, Z.-Q., Szeto, L. and Wong, W.-T. *Appl. Organometal. Chem.* In press.

POWDER NEUTRON DIFFRACTION STUDY OF A CRYSTALLINE-STATE REACTION OF AN UNSATURATED THIOAMIDE DERIVATIVE

Takashi Ohhara,[a,b] Susumu Ikeda,[a] Kenichi Oikawa,[b] Akinori Hoshikawa,[a] Takashi Kamiyama,[a] Takaaki Hosoya,[c] and Yuji Ohashi[c]

[a]Institute of Materials Structure Science, KEK, Tsukuba, Ibaraki, Japan; [b]Japan Atomic Energy Research Institute (JAERI), Tokai, Ibaraki, Japan [c]Department of Chemistry and Materials Science, Tokyo Institute of Technology, Meguro-ku, Tokyo, Japan (ohhara@neutrons.tokai.jaeri.go.jp).

Crystalline-state reaction, which proceeds with retention of single crystal form, is one of the most interesting topics in crystal chemistry and many reactions have been analysed mainly by single crystal X-ray diffraction. Recently, author and co-workers proposed a single crystal neutron diffraction (SND) analysis of a crystalline-state reaction as follows; hydrogen atoms in the reactive part of the reactant molecule are replaced with deuterium atom as markers, then the crystalline-state reaction is proceeded, and finally the migration of the deuterium atoms according to the reaction is observed by SND. This analytical method is very powerful to analyse the mechanism of crystalline-state reaction[1]. However, since SND requires a very large single crystal, it is much more difficult to keep the single crystal form during the reaction than single crystal X-ray diffraction study. So, we proposed to apply powder neutron diffraction (PND) instead of SND.

In this work, we measured the powder neutron diffraction pattern of an unsaturated thioamide derivative, which is the reactant of the crystalline-state photo-cyclization to form a β-thiolactam (Fig.1)[2], before and after the photo-irradiation, and tried to observe the deuterium migration according to the photo-cyclization. Hydrogen atoms in the reactive part of the reactant molecule were replaced with deuterium atoms as markers. Though the two phenyl groups are not the reactive part, the hydrogen atoms of those phenyl groups were also replaced with deuterium atoms to reduce the background of the PND pattern. The cell parameter before irradiation is a=8.654Å, b=10.156Å, c=10.102Å, β=98.76°. PND patterns were measured by Vega TOF powder neutron diffractometer at KENS with 15K. The change of the powder pattern indicates the deuterium migration according to the photo-cyclization.

References

1 T. Ohhara, S. Ikeda, H. Imura, H. Uekusa, Y. Ohashi, I. Tanaka, N. Niimura. (2002) *J. Am. Chem. Soc.*, **124**, 14736-14740.

2 T. Hosoya, T. Ohhara, H. Uekusa, Y. Ohashi. (2002) *Bull. Chem. Soc. Jpn.*, **75**, 2147-2151.

PO72

STRUCTURAL CHARACTERIZATION OF THREE CRYSTALLINE MODIFICATIONS OF CHLOROTHALONIL BY X-RAY POWDER DIFFRACTION

Xiurong Hu, Ziqin Yuan, Jianming Gu, Guanglie Lu and Xiaoyan Tu

Central Laboratory of Zhejiang University, Hangzhou 310028, P.R.China (gllu@zju.edu.cn)

Monte Carlo/annealing simulation in the direct space was applied to solve the crystal structures of three crystalline modifications of Chlorothalonils from X-ray powder diffraction data. Results have shown they have different crystallographic parameters and the way of stacking. Form A is monoclinic with space group $P2_1/a$ including four molecules in the unit cell, form B and C are monoclinic with space group $P\ 2_1$ and include two molecules in the unit cell. Form A: a=24.7415(28) Å, b=6.2240(11) Å, c=6.3364(7) Å, β=95.439(30)°, V=971.4 Å^3; Form B: a=8.1615(18) Å, b=9.4191 Å, c=6.4728(14) Å, β=93.7307(64)°, V=497.8 Å^3; Form C: a=8.6003(10) Å, b=9.2382(11) Å, c=6.3024(7) Å, β=96.2152(60)°, V=498.5 Å^3.

Three modifications are stacked by two paralleled planar molecular chains along b-axis in different stacking ways. Stacking ways for form B and form C are almost same, but the adjacent two paralleled molecular chains in the form B are in the same plane, while those in the form C are not. In the form A, there are double planar molecular chains same as that of form C. These two chains cross each other(crossing angle is equal to β) and stack alternately along a axis at the interval of 0.5a.

PO73

CRYSTAL STRUCTURE AND CONFORMATION OF GEM-CHLORO NITROSO - CYCLODODECANE $(CH_2)_{n-1}CNOCl$, WITH n=12

C.R. Girija and Noor Shahina Begum*

Department of Studies in Chemistry, Bangalore University, Central College Campus, Bangalore-560 001.India.(noorsb@ rediffmail.com)

Gem- chloronitoso compounds find application in organic synthesis and mechanistic studies, particularly as precursors of aliphatic nitro derivatives and of vicinal dinitrocompounds.

The crystal structure analysis of the title compound gem- chloronitroso-cyclododecane ,$(CH_2)_{n-1}CNOCl$, with n=12 , has been determined by the X-ray diffraction method.

The title compound crystallizes in the orthorhombic space group $P2_12_12_1$ with a= 8.3801(19)Å , b= 9.5432 (21) Å , c=16.3480 (36) Å , V=1307.4(5) Å^3 ,μ=0.137mm^{-1} z = 4. The structure was solved by direct methods using SHELXS-97 and refined by by fullmatrix least squares on F^2 using SHELXL-97 to a R- value of 0.1111 for 3072 reflections with $I>2\sigma(I)$ collected using a Seimens Smart-CCD diffractometer with MoKα radiation.

In the title compound, cyclododecane has the expected "square" [3333] conformation like all other known saturated twelve membered rings but there is disorder about the chloronitroso exocyclic group..The structural and conformational features of the title compound will be discussed in detail

PO74

TOPOLOGICAL ANALYSIS OF $[NH_2Me_2][H(HC_4O_4)_2]$

Chi-Rung Lee[a]*, Ching-Yi Lee[a] and Yu Wang[b]

[a]Department of Chemical Engineering, Minghsin University of Science and Technology, Hsin-Fong, Hsin-ChU, Taiwan. [b]Department of Chemistry, National Taiwan University, Taipei, Taiwan. (crlee@must.edu.tw)

A hydrogen bond study was performed on dimethylammonium hydrobis(squarate), $(H_2Me_2)[H(HC_4O_4)_2]$[1], using a detailed charge density study from accurate X-ray diffraction and DFT calculation. The molecule has some interesting sets of intra- and intermolecular interactions in the crystalline state – two relatively strong O H O hydrogen bonds and some very weak secondary interactions. The interaction energy between two H-bonded fragments were also investigated. The anion of this compound contains both a symmetric (O H O distance of 2.4321(8)Å, bond angle of 179(2)°) and an asymmetric (O H O distance of 2.5645(6)Å, bond angle of 175(1)°) H-bonds in the crystal. Results on the electron density distribution will be presented in the form of deformation density and of Laplacain maps. The ring strain of the four-membered squarate ring is nicely demonstrated in the deformation density map with the bonding electron density maximum outward from the C-C interatomic axic, such that two neighboring bonding electron density maxima give an angle of 110° around C2, which is much larger than the corresponding C1-C2-C3 angle of 90.83(4)°. The bond characters of the C-O, C-N and C-C bonds are apparent, and the agreement on the topological properties between experiment and theory is adequate. All the interactions are verified by the location of the bond critical point and its associated topological properties. The iso-value surface of Laplacian charge density and the detailed atomic graph around each atomic site reveal the shape of the valence shell charge contraction and provide a reasonable interpretation of the bonding of each atom.

Reference

1 Lin, K. J., Cheng, M. C. and Wang Y. (1994) *J. Phys. Chem.*, **98**, 11685-11693.

PO75

SYNTHESIS AND CHARACTERIZATION OF TWO POLYMORPHS OF Fe(2,2'-bpy)(HPO_4)(H_2PO_4)

Wen-Jung Chang,[a] Yau-Chen Jiang,[b] and Kwang-Hwa Lii[a,c]

[a]Department of Chemistry, National Central University, Chungli; [b]Department of Chemistry, National Tsing-Hua University, Hsinchu; [c]Institute of Chemistry, Academia Sinica, Taipei, Taiwan, R.O.C. (liikh@cc.ncu.edu.tw)

We have been interested in using the organic ligands 2,2'-bipyridine and 1,10-phenanthroline to synthesize new organic-inorganic hybrid compounds, and have recently reported two compounds in the 2,2'-bpy-phosphate system [1]. As part of continuing work of this system, two polymorphs of organic-inorganic hybrid iron phosphate were isolated. Both polymorphs were synthesized under hydrothermal conditions and characterized by single-crystal X-ray diffraction. Crystal data: Fe(2,2'-bpy)(HPO_4)(H_2PO_4) (polymorph **1**), monoclinic space group $P2_1/n$, a = 10.904(2) Å, b = 6.423(1) Å, c = 19.314(3) Å, β = 101.161(3)°, V = 1327.0(4) Å^3, and Z = 4; Fe(2,2'-bpy)(HPO_4)(H_2PO_4) (polymorph **2**), monoclinic, space group $P2_1/c$, a = 11.014(2) Å, b = 15.827(2) Å, c = 8.444(1) Å, β = 109.085(3)°, V = 1395.1(3) Å^3, and Z = 4. Polymorph **1** adopts a 1D chain structure in which each Fe atom is coordinated by two nitrogen atoms from a 2,2'-bpy ligand and four phosphate oxygen atoms. These infinite chains are extended into a 2D supramolecular array *via* π-π interaction of the lateral 2,2'-bpy ligands. The structure of polymorph **2** consists of the same building units which are linked through their vertices forming an undulated sheetlike structure with 4.12 net. Adjacent 2D layers are extended into a 3D array *via* π-π interaction of the aromatic groups. It is isostructural with Ga(2,2'-bpy)(HPO_4)(H_2PO_4) [2]. In this presentation we will report the synthesis, crystal structures, and magnetic properties of these two polymorphs.

References

1 Chang, W.-J., Chen, C.-Y., and Lii, K.-H. (2003) *J. Solid State Chem.* **172**, 6-11.
2 Lin, Z.-E., Zhang, J., Sun, Y.-Q., and Yang G.-Y. (2004) *Inorg. Chem.* **43**, 797-801

PO76

SYNTHESIS AND CHARACTERIZATION OF THE FIRST METAL OXALATOPHOSPHONATE: $(C_3H_{12}N_2)_{0.5}[Ga_3(C_2O_4)(CH_3PO_3)_4]\cdot 0.5H_2O$

Chia-Hui Lin[a] and Kwang-Hwa Lii[a,b,*]

[a]Department of Chemistry, National Central University, Chungli; [b]Institute of Chemistry, Academia Sinica, Taipei, Taiwan, R.O.C. (liikh@cc.ncu.edu.tw)

Many research activities have focused on the synthesis of organic-inorganic hybrid compounds by incorporating organic ligands in the structures of metal phosphates. The underlying idea is to combine the robustness of inorganic phosphate frameworks with the versatility and chemical flexibility of organic ligands. A large number of oxalate-phosphates and bipyridine-phosphates of transition metals and group 13 elements have been reported [1,2]. We have recently become interested in the synthesis of metal phosphonates incorporating multifunctional organic ligands. Here we report the first example of metal oxalatophosphonate, $(C_3H_{12}N_2)_{0.5}[Ga_3(C_2O_4)(CH_3PO_3)_4]\cdot 0.5H_2O$, which was synthesized under hydrothermal conditions and characterized by single-crystal X-ray diffraction. It crystallizes in the monoclinic space group $P2_1/n$ with a = 8.8514(4) Å, b = 16.3030(7) Å, c = 15.0816(7) Å, β = 97.539(1)°, V = 2157.53(17) Å^3, and Z = 4. It adopts a 2D layer structure with the interlayer space filled with 1,3-propylenediammonium cations and water molecules. Within a layer there are GaO_4 tetrahedra and GaO_6 octahedra connected by methylphosphonate and oxalate groups. The solid state NMR spectroscopy has also been studied.

References

1 Jiang, Y.-C., Wang, S.-L., Lee, S.-F. and Lii, K.-H. (2003) *Inorg. Chem.* **42**, 6154-6156 and references therein.

2 Huang, L.-H., Kao, H.-M. and Lii, K.-H. (2002) *Inorg. Chem.* **41**, 2936-2940 and references therein.

PO77

SYNTHESIS AND STRUCTURAL CHARACTERIZATION OF A NEW URANIUM SILICATE: $K_6(UO_2)_2(Si_4O_{13})$

Chih-Shan Chen[a] and Kwang-Hwa Lii[a,b,*]

[a]Department of Chemistry, National Central University, Chungli; [b]Institute of Chemistry, Academia Sinica, Taipei, Taiwan, R.O.C. (liikh@cc.ncu.edu.tw)

Organically templated metal phosphates have been extensively studied because of interesting structural chemistry and potential applications in catalysis. However, in most cases the organic templates cannot be removed without collapse of the frameworks. This is in contrast to the high thermal stability and extensive applications of zeolites in refinery and petrochemical processes. Therefore, studies have been directed to the synthesis of metal silicates to produce more stable frameworks. Recently, Jacobson et al. reported the synthesis of several uranium silicates under hydrothermal conditions at 180-240 °C by using alkali metal or organic ammonium cations as templating agents [1-3]. In this presentation we report high-temperature, high-pressure hydrothermal synthesis, crystal structure, and solid-state NMR spectroscopy of a new uranium silicate. The title compound crystallizes in the orthorhombic space group *Cmca* with a = 22.178(4) Å, b = 12.229(2) Å, c = 13.093(3) Å and V = 3551.1(1) Å^3. The structure consists of tetrasilicate units linked together *via* corner sharing by UO_6 octahedra to form a 3-D framework which delimits channels along the a-axis, where the K^+ cations are located.

References

1 Wang, X., Haung, J., Liu, L., Jacobson, A. J. (2002) *J. Mater. Chem.* **12**, 406-410.
2 Haung, J., Wang, X., Jacobson, A. J. (2003) *J. Mater. Chem.* **13**, 191-196.
3 Wang, X., Haung, J., Jacobson, A. J. (2002) *J. Am. Chem. Soc.* **124**, 15190-15191.

SYNTHESIS AND STRUCTURAL CHARACTERIZATION OF $(H_4appip)[V_3(C_2O_4)_2(HPO_4)_3(PO_4)(H_2O)]\cdot 6H_2O$ (appip = 1,4-BIS(3-AMINOPROPYL)PIPERAZINE), A LAYERED VANADIUM OXALATOPHOSPHATE CONTAINING DOUBLE-SIX-RING UNITS

Ming-Feng Tang[a] and Kwang-Hwa Lii[a,b,*]

[a]Department of Chemistry, National Central University, Chungli; [b]Institute of Chemistry, Academia Sinica, Taipei, Taiwan, R.O.C. (liikh@cc.ncu.edu.tw)

In recent years, a large number of hybrid compounds have been synthesized by incorporating multidentate organic ligands such as bipyridines and oxalate in the structures of metal phosphates. The underlying idea is to combine the robustness of inorganic phosphate frameworks with the versatility and chemical flexibility of organic ligands. The oxalatophosphates form the largest group among these organically modified metal phosphates. Most of these oxlatophosphates adopt 3-D framework structures, while only a few have 2-D layer or 1-D chain structures. As part of continuing work of this system, we prepared a new oxalatophosphate that has a new type of layer structure built of double-six-ring (D6R) units connected by phosphate and oxalate groups. It is one of the few oxalatophosphates with 2D layer structures and the second example containing D6R units. It crystallizes in the triclinic space group $P\bar{1}$ with a = 11.604(2) Å, b = 12.391(2) Å, c = 15.220(3) Å, α = 71.090(3)°, β = 82.630(3)°, γ = 62.979(3)°, V = 1843.8(5) Å^3 and Z = 2. The structure consists of $V_6(HPO_4)_6$ double-six-ring (D6R) units connected by coordinating $C_2O_4^{2-}$ and PO_4^{3-} anions to form anionic sheets in the *ab* plane with charge-compensating quadruply protonated 1,4-bis(3-aminopropyl)piperazinium cations and water molecules between the sheets. There are two types of oxalate units in the structure: one type acts as a bridging ligand and chelates two metal atoms while the other oxalate unit chelates only one metal atom and has two C-O groups pendant between adjacent layers. Each layer consists of D6R units as shown below.

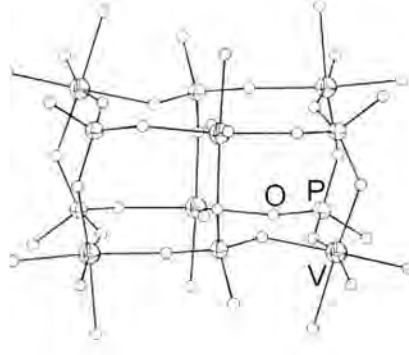

ELECTRONIC STRUCTURES OF POLYMORPHS IN MONOHALOGENATED BENZYL DERIVATIVES OF 2,5-DIAMINO-3,6-DICYANOPYRAZINE DYES

Shinya Matsumoto,[a] Yoko Uchida,[a] and Mitsuhiro Yanagita[b]

[a]Department of Environmental Sciences, Faculty of Education and Human Sciences, Yokohama National University, Yokohama 240-8501 Japan; [b]R. & D. Laboratory for High-Performance Materials, Nippon Soda Co., Ltd., Chiba 290-0045 Japan (smatsu@edhs.ynu.ac.jp).

2,5-Diamino-3,6-dicyanopyrazine dyes have been intensively studied as a novel fluorophore which can be applied to opto-electronical materials such as an emitter for organic electroluminescent devices, since they exhibit strong fluorescence in solution and even in the solid state[1,2]. These dyes have also been known to have some crystal polymorphs with different colors depending on the substituents on the amino groups. In this study, the correlation between electronic structures and molecular conformation in single crystals were investigated for some polymorphs of the four monohalogenated benzyl derivatives shown in the diagram: two polymorphs of **1**(red and yellow) and **4**(red and orange), the red phase of **2** and the yellow phase of **3**.

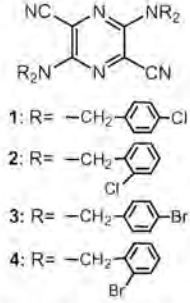

The conformation of molecules in these crystals was found to depend on not the substituent but the color of crystals. The amino nitrogens in the red and orange phases have a trigonal planar geometry; whereas the tetrahedral conformation of the amino groups was found in the yellow phase. Semi-empirical molecular orbital calculations revealed that this structural feature can be correlated with the electronic structures of a molecule in crystals. The color difference was mainly attributed to the change in the HOMO due to the conformational change of the amino groups.

References

1 Matsuoka, M. (2000) in *Colorants for Non-textile Applications (H. S. Freeman and A. T. Peters ed.)*, Elsevier Science, 339-381.

2 Shirai, K., Matsuoka, M., Matsumoto, S. and Shiro, M. (2003) *Dyes Pigm.* **56**, 83-87.

PO80

HYDROGEN BONDING PATTERN AND π - π -INTERACTIONS IN 1,7-bis-(4-HYDROXY-3-METHOXYPHENYL)-HEPTA-3,5-DIONE (TETRA HYDRO CURCUMIN)

Noor Shahina Begum* , C.R. Girija , and Syed. A .A[a]

Department of Studies in Chemistry, Bangalore University, Central College Campus, Bangalore-560 001 .India.
[a]Department of Studies in Chemistry, , Manasagangotri , University Of Mysore, Mysore-570 006, India

Tetrahydrocurcumin is the reduced form of curcumin which is known to posses important cosmoceutical properties.
The title molecule, $C_{21}H_{22}O_6$ crystallizes in the triclinic space group $P\bar{1}$ with the unit cell parameters a= 7.9813(30) Å , b= 11.3881 (30) Å , c=12.4966 (30) Å , α =117.065(3)°, β =100.394(10) °,,γ = 94.856(3) °, V = 976.66(35) Å^3, μ = 0.092mm^{-1} and z = 2. The structure was solved by direct methods using SHELXS-97 and refined by fullmatrix least squares on F^2 using SHELXL-97 to a R- value of 0.061 for 3244 reflections with I>2σ(I) collected using a Seimens Smart-CCD diffractometer with MoKα radiation. The structure exhibits interesting bifurcated hydrogen bonds formed between the oxygen atoms of the hydroxyl ,methoxy and dione groups. The dihedral angle 84.55° between the phenyl rings in the molecule indicate that they are orthogonally placed .

The packing of the molecule is stabilized by π- π interactions and hydrogenbonding. The molecular packing down the b-axis shows layered structure.Detailed structural features,intermolecular interactions and packing modes will be presented.

PO81

LANTHANIDE CONTRACT AND PH VALUE CONTROLLED STRUCTURES CHANGE IN A SERIES OF RARE EARTH COMPLEXES WITH *P*-AMINOBENZOIC ACID, CRYSTAL STRUCTURE AND LUMINESCENCE PROPERTY

Jun-Ran Li, Hao-Ling Sun, Chao-Hong Ye, Xin-Yi Wang, Song Gao

State Key Laboratory of Rare Earth Materials Chemistry and Applications, PKU-HKU Joint Laboratory on Rare Earth Materials and Bioinorganic Chemistry, College of Chemistry and Molecular Engineering, Peking University, Beijing 100871, China (lijunran@pku.edu.cn)

p-Aminobenzoic acid (HL), a very important biological ligand, can form complexes with many metal ions. However, the structure of rare earth complexes with HL has seldom been investigated [1-2]. The relationship between luminescence performance and coordination mode of a ligand is not as well explored for a complex. A series of rare earth complexes with *p*-aminobenzoic acid (HL) were synthesized as $[RE_2L_6(H_2O)_2]_n$ [RE=La(**1**), Ce (**2**), Pr(**3**), Sm(**4**), Eu(**5**), Tb(**6**), Dy(**7**), Er(**9**)] and $[RE_2L_6(H_2O)_4]\cdot 2H_2O$ [RE=Tb (**6'**), Ho(**8**), Yb(**10**), Lu(**11**), Y(**12**)]. The crystal structures of **1, 2, 6, 6', 7, 9** and **12** were determined and isomorphous relationships of the others identified. Their structures change from a two-dimensional (2D) array (the metal ions are nine-coordinated for **1** or eight -coordinated for **2-7** and **9**) to a two-nuclear structure (the metal ions are eight-coordinated) for **6', 8 and 10-12**, as controlled by lanthanide contraction. The effect of the pH value of the reaction mixtures on the crystal structure was found. The unusual luminescence characteristic of complexes **6** and **6'** revealed the relationship between the fluorescence property and the number of coordination water molecule and the coordination mode of a ligand in the complex.

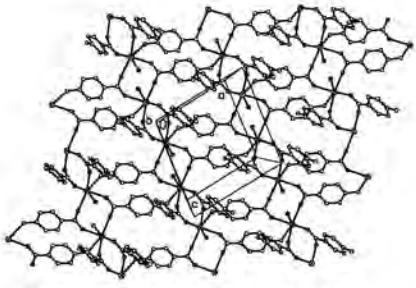

Two-dimensional structure of **6**

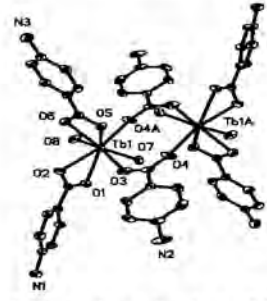

Two-nuclear structure of **6'**

References

1 Rzaczyńska, Z., belsky, V. K. (1994) *Polish J. Chem.* **68**, 309-319.

2 Khiyalov, M. S., Amiraslanov, I. R., Mamedov, Kh. S., Movsumov, E. M. (1981) *Zh. Strukt. Khim.*, **22(3)**, 113-119; (1981) *Koord. Khim.*, **7(3)**, 445-449.

BIS(ALKYNYL) MERCURY(II) COMPLEXES OF OLIGOTHIOPHENES AND BITHIAZOLES

Wai-Yeung Wong, Ka-Ho Choi and Guo-Liang Lu

Department of Chemistry, Hong Kong Baptist University, Waterloo Road, Kowloon Tong, Hong Kong, P. R. China. (rwywong@hkbu.edu.hk)

A new class of binuclear mercury(II) bis(alkynyl) complexes containing oligothiophenes and bithiazoles as the central organic linkers are prepared. The solid-state molecular structures of [MeHgC≡CRC≡CHgMe] (R = thiophene-2,5-diyl, [2,2'-]bithiophene-5,5'-diyl) established by X-ray crystallography reveal that a loose polymeric structure is formed in each case through weak intermolecular non-covalent Hg···Hg mercuriophilic interactions. All the complexes were shown to exhibit rich absorption and luminescence behavior as a function of the number of thiophene rings as well as the electronic nature of the five-membered rings within the bridging ligand. With increasing thiophene content, the absorption and emission features are both red-shifted and the emission quantum yields are increased. In the presence of electron-withdrawing imine nitrogen atoms, the optical spectra for the bithiazole derivatives also show a significant bathochromic shift as compared to their bithienyl counterparts.

Reference

1 Wong, W.-Y., Choi, K.-H., Lu, G.-L. and Lin, Z. (2002) *Organometallics* **21**, 4475–4481.

PO83

COMPARISON OF MOLECULAR PACKING MODES OF CHOLESTEROL DERIVATIVES

Young Ja Park

Department of Chemistry, Sook Myung Women's University, Seoul, KOREA 140-742 .
(yjpark@sookmyung.ac.kr)

We have undertaken a series of crystal structures of the esters and carbonates of cholesterol. These are cholesteryl formate, methyl carbonate, ethyl carbonate, propyl carbonate, pentyl carbonate, pentanoate, hexanoate, heptanoate, hexyl carbonate, crotyl carbonate, crotonate, isobutyrate, isobutyl carbonate, isopropyl carbonate, hemisuccinate, aniline and 2,4-dichlorobenzoate. Among these structures, (1) cholesteryl ethyl carbonate, propyl carbonate, crotyl carbonate, crotonate are isostructural each other, (2) cholesteryl pentyl carbonate, hexyl carbonate, hexanoate, heptanoate are also isostructural. (3) cholesteryl isobutyrate and isobutyl carbonate are also isostructural.

These structures are remarkable in forming layer structures in which the central region of the layers, composed largely of semi-rigid cholesteryl groups is closely packed and the packing of the flexible fatty acid or carbonate chains and the isoprenoid tail of the cholesterol form the interface region between layers. Within the so called monolayers type packing, there is little change from one crystal structure to another. Typical packing modes will be discussed.

PO84

STUDIES ON THE WEAK HYDROGEN BONDS IN CRYSTAL

Zhong-Yuan Zhou, Wing-Kong Kwan, Chi-Hung Yeung, Albert S. C. Chan

Open Laboratory of Chirotechnology of the Institute of Molecular Technology for Drug Discovery and Synthesis and Department of Applied Biology and Chemical Technology, The Hong Kong Polytechnic University, Hung Hom, Kowloon, Hong Kong (bczyzhou@inet.polyu.edu.hk)

Hydrogen bonding, defined by L. Pauling in 1939, refers to X-H...Y interaction where X and Y are higher electronegative elements such as N, O, F and Cl. Weak hydrogen bonding, proposed by Jeffrey and Saenger in 1991, refers to hydrogen bonding between carbon hydrogen and carbonyl oxygen, that is, the weak hydrogen bonding of C-H...O=C. Such weak hydrogen bonding may be defined as D-H...A wherein a hydrogen atom forms a weak bond between two structural moieties D (donor) and A (acceptor) of which one or even both are only of moderate to low electronegativity. The stability depends mainly on the electrostatic characteristics of both donor and acceptor.

Recently, the concept of the weak hydrogen bonds (D-H...A) has been well recognized by the study of structure of a large amount of crystals and is further proven through extensive IR and NMR studies.

Herein, we report the weak hydrogen bonding of some organic compounds and transition metal complexes. Crystal structure analysis shows the presence of weak hydrogen bonding of C-H...O, C-H...N, C-H...p. Results of such weak hydrogen bonds and interaction of pi...pi for molecula $C_{16}H_{15}NO_2$ and $C_{37}H_{32}O_5P_2$ are shown in Tables 1.

Table 1 Bond lengths (Å) and bond angles (°) for weak hydrogen bonds

D-H...A	H...A (Å)	D...A (Å)	D-H...A (°)
C(2)–H(2)...O(1)	2.57	3.312 (4)	137
C(5)–H(5)...O(1')	2.51	3.370 (4)	154
C(2)–H(2B)...Cg (A)*	2.96	3.578 (3)	125
C(4)–H(4)...Cg(B)*	3.15	3.999 (3)	154
C(14)–H(14C)...Cg(A')*	3.05	3.728 (4)	131
CgC...CgD		3.568 (4)	

*. Cg refers to the gravity center of aromatic ring.

References

1 Jia, X. Li, X.S.; Zhou Z.Y. (2002). *Acta Crystallographica Section E* **2002,** E58, 1

2 Qiu, L.Q.; Qi, J.Y.; Ji, J.X.; Zhou, Z.Y.; Yeung, C.H.; Choi, M.C.K.; Chan, A.S.C. (2003) *Acta Crystallographica Section C59, o33-o35*

PO85

FIRST OBSERVATION OF HELICAL BUNDLES IN CRYSTAL STRUCTURE OF HELICAL PEPTIDE SCAFFOLDS CONTAINING A, B-DEHYDROPHENYLALANINE RESIDUE

M. Gupta, Rudresh, S. Ramakumar, V. S. Chauhan.

International Center for Genetic Engineering and Biotechnology, New Delhi- 110067. India ;g_madhvi@hotmail.com)

De *novo* designed peptide based super secondary structures can provide scaffolds for the incorporation of functional sites as in proteins. Weak interactions leading to the self-association of helices ;containing DPhe residue) of similar screw sense have been probed by the structure determination in crystals of two peptides: Ac-Gly^{1}-Ala -DF^{3}-Leu^{4}-Val^{5}-DF^{6}-Leu^{7}-Val -DF -Ala^{10}-Gly^{11}-NH , I; Ac-Gly^{1}-Ala -DF^{3}-Leu^{4}-Ala^{5}-DF^{6}-Leu^{7}-Ala -DF -Ala^{10}-Gly^{11}-NH , II. X-ray diffraction studies reveal that both the peptides adopt 3_{10}-helical conformation in the solid state. The crystal structures of the two peptides have beendetermined to atomic resolution and refined to R-factor of ;.15%and 4.01% respectively. An interesting finding is that a packing motif could be identified in both the structures, in which a given 3_{10} -helix is surrounded by six other helices reminiscent of transmembrane seven helical bundles. This arrangement resulted in two kinds of interfaces, Leu-Leu and Val-Val in peptide I and Leu-Leu and Ala-Ala in peptide II. The angle between antiparallel helices are 161° and 164° in peptides I and II, respectively. The outer helices are orientated either parallel or antiparallel to central helix. The parallel helices interact through C-H...O and C-H...π hydrogen bonds while the antiparallel helices are interacting via C-H...p hydrogen bonds. Common to both the structures is the hydrophobic interaction between the pairs of leucine residues. The results of the packing of the helices in the solid state may help in achieving the ambitious design strategy for designing super secondary structural motifs such as helical hairpin and three or four helix bundles by connecting them through suitable linkers such as tetraglycine segments.

PO86

NEW STRATEGY TO SYNTHESIZE OSMABENZYNES

Ting Bin Wen, Wai Yiu Hung, Herman Ho Yung Sung, Ian D. Williams and Guochen Jia

Department of Chemistry, The Hong Kong University of Science and Technology, Clear Water Bay, Kowloon, Hong Kong (chterry@ust.hk)

We recently reported an unexpected production of the first osmabenzyne $[Os(\equiv CC(SiMe_3)=C(CH_3)C(SiMe_3)=CH)Cl_2(PPh_3)_2]$ – a six-membered metallacycle with delocalized structure which is similar to that of aromatic ring systems such as benzene and metallabenzenes. We have now developed a general strategy to synthesize this class of interesting compounds and investigated their chemical properties. Treatment of complex **1** with gold acetylides, in the presence of HEt_3NCl led to the formation of complexes **2**.

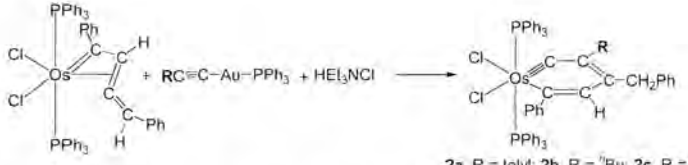

1 **2a**, R = tolyl; **2b**, R = ^{n}Bu; **2c**, R = H

The osmabenzyne $[Os(^{\kappa}CC(SiMe_3)=C(CH_3)C(SiMe_3)=CH)Cl_2(PPh_3)_2]$ was found to undergo typical aromatic electrophilic substitution reactions.

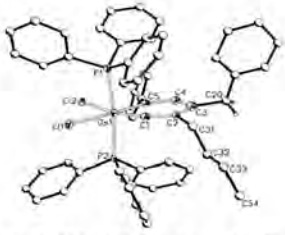

Fig 1. Crystal structure of **2b**.

PO87

SYNTHESIS AND NLO PROPERTIES OF NEW OCTUPOLAR MOLECULES

Quanyuan Hu, George K. L. Wong, Herman Ho Yung Sung, Ian D. Williams and Guochen Jia

Departments of Chemistry and Physics, Hong Kong University of Science and Technology, Clear Water Bay, Kowloon, Hong Kong (chqyhu@ust.hk)

Octupolar molecules are potentially useful as second order non-linear optical materials. In order to reveal the structure-property relationship of these compounds, a series of octupolar molecules with similar skeleton based on 2,4,6-triphenyltriazine (examples shown below) have been synthesized and their optical properties have been studied by HRS experiments. In addition to their second order non-linear optical properties, the compounds also show strong multi-photon absorption induced fluorescence effects.

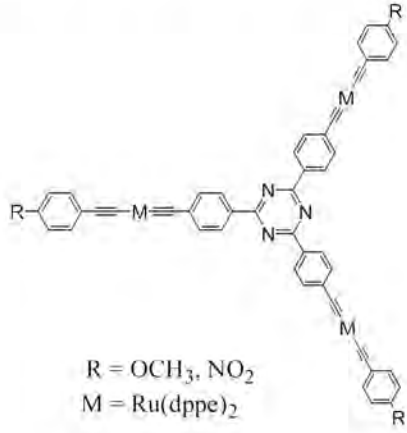

PO88

HEXAMERIZATION OF ALKYNES MEDIATED BY OsCl(PCP)(PPh_3) (PCP = 2,6-(Ph_2PCH_2)$_2C_6H_3$)

Ting Bin Wen,[a] Zhong Yuan Zhou,[b] and Guochen Jia[a]

[a]Department of Chemistry, The Hong Kong University of Science and Technology, Clear Water Bay, Kowloon, Hong Kong and [b]Department of Applied Biology and Chemical Technology, Hong Kong Polytechnic University, Hung Hom, Kowloon, Hong Kong (chwtb@ust.hk)

The [2+2+2] cyclotrimerization of alkynes to give six-membered aromatic rings is one of the most common reactions promoted by transition metal complexes. In contrast, examples of metal-mediated [2+2+1] cyclotrimerization of alkynes to give thermodynamically less stable isomeric fulvene derivatives are still rather limited. Vinylidene complexes may serve as the intermediates in the formation of fulvene products from the [2+2+1] cyclotrimerizations of alkynes. Our previous studies have shown that reactions of OsCl(PCP)(PPh_3) with terminal acetylenes rapidly produce vinylidene complexes OsCl(=C=CHR)(PCP)(PPh_3). During the process of further exploring the reactivity of OsCl(=C=CHR)(PCP)(PPh_3) with terminal acetylenes, we found that OsCl(=C=CHPh)(PCP)(PPh_3) could further react with HC≡CPh to give the unprecedented μ-1,2-bis-(η^5-cyclopentadienyl)-1,2-diphenyl-ethane bridged dimeric osmium complexes, which presumably involves dimerization of the fulvene intermediate generated from [2+2+1] cyclotrimerization of HC≡CPh (Scheme 1).

Scheme 1

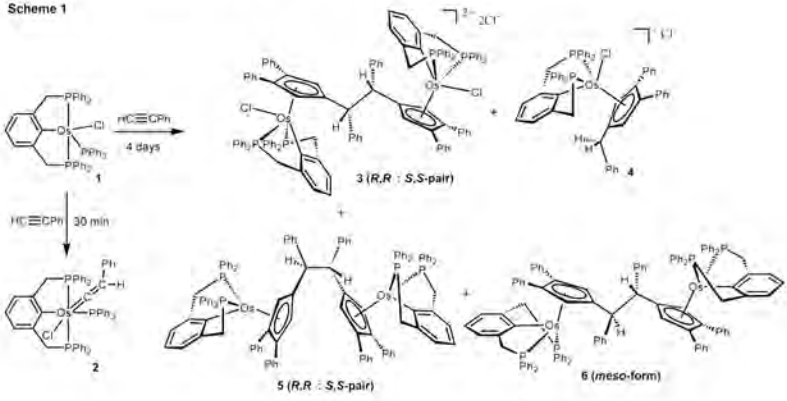

PO89

OSMABENZENES FROM THE REACTIONS OF HC≡CCH(OH)C≡CH With $OsX_2(PPh_3)_3$ (X = Cl, Br)

Haiping Xia,[a,b] Guomei He,[b] Hong Zhang,[b] Ting Bin Wen,[a] Herman Ho Yung Sung,[a] Ian D. Williams,[a] and Guochen Jia[a]

[a]Department of Chemistry, The Hong Kong University of Science and Technology, Clear Water Bay, Kowloon, Hong Kong and [b]The College of Chemistry and Chemical Engineering, Xiamen University, Xiamen, P. R. China (Email: chwtb@ust.hk)

The chemistry of transition metal containing metallabenzenes is attracting increasing attention both experimentally and theoretically because they can display aromatic properties and they can mediate organometallic reactions. The synthesis, isolation and characterization of stable metallabenzenes represent one of the major issues of metallabenzene chemists. During our investigation on the reactivity of $OsCl_2(PPh_3)_3$ toward terminal alkynes, we have found a new convenient route to prepare osmabenzenes starting from readily accessible HC≡CCH(OH)C≡CH. In this presentation, we will describe the reactions of HC≡CCH(OH)C≡CH with $OsX_2(PPh_3)_3$ (X = Cl, Br), which lead to the isolation of the first phosphonium salts of metallabenzenes (Scheme 1). The reactions involve nucleophilic attack of coordinated alkynes by the nucleophile PPh_3. One of the key intermediate has been isolated, which could react with other nucleophiles such as I^- to give iodo-osmabenzene.

Scheme 1

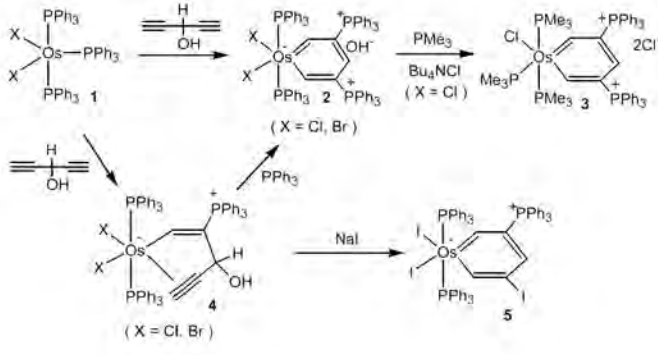

PO90

RUTHENIUM-CATALYZED DIMERIZATION OF TERMINAL ALKYNES

Peng Xue, Hoi Yan Leung, Ka Yin Cheng, Wai Bong Wong, Herman Ho Yung Sung, Ian D. Williams and Guochen Jia

Department of Chemistry, The Hong Kong University of Science and Technology, Clear Water Bay, Kowloon, Hong Kong (chxuep@ust.hk)

There have been considerable interests in catalytic dimerization of alkynes. The reactions can be initiated by a variety of metal complexes. In most cases, the reactions produce a mixture of five isomers **A-E**. In order to understand the reaction mechanisms and to develop catalysts for selective production of the dimerization products, we have investigated the catalytic activities of a series of ruthenium complexes for alkyne dimerization. Complexes **1-6** are examples of such complexes.

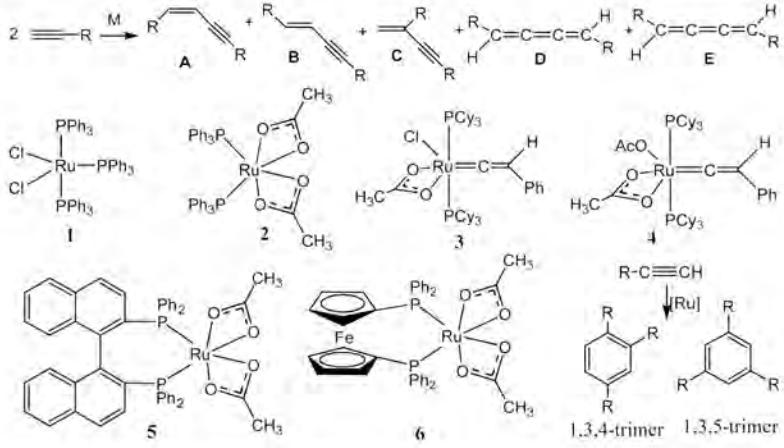

It was found that the selectivity depends on the structures of metal complexes as well as the substrates. For example, aromatic alkynes dimerize to give Z-isomers as the major products with complexes **1-4** as the catalysts; when **5** was used as the catalyst, PhC≡CH dimerized to give Z-isomer along with the cyclotrimers. Interestingly, PhC≡CH dimerized to give E-isomer as the major product with **6** as the catalyst. In the presentation, the preparation of the new catalysts as well as the details of the catalytic results will be presented.

PO91

DILEAD μ^9-L-TARTRATE: A CHIRAL METAL-ORGANIC FRAMEWORK WITH NONA-COORDINATION OF A SINGLE LIGAND

Andy L-F. Leung, Ricky W. Li, Herman H-Y. Sung and Ian D. Williams

Department of Chemistry, Hong Kong University of Science and Technology, Clear Water Bay, Kowloon, Hong Kong. (ch_llf@stu.ust.hk)

We have embarked on a program of synthesis of chiral metal-organic solids using organic carboxylate ligands. L-tartaric acid can be used in hydrothermal synthesis up to 200°C and still yield enantiopure chiral coordination polymers, as shown by careful comparison of results from meso-tartrate and D/L-tartrate mixtures. Lead is a high coordinate metal capable of forming 3D frameworks.

Depending on conditions and pH two anhydrous polymers are formed a 'normal' 1:1 phase $[Pb(\mu_6\text{-}C_4H_4O_6)]$ (pH4) and a fully deprotonated 2:1 compound $[Pb_2(\mu_9\text{-}C_4H_2O_6)]$ (pH>7). The structure of the dilead tartrate is noteworthy in having a μ_9-tartrate tetra-anion which we believe is the highest connectivity found for a tartrate ligand. A thallium μ_8-hydrogen tartrate was reported previously $[Tl(\mu_8\text{-}C_4H_5O_6)]$. [1] Further studies of chiral network polymers from metals such as lead are now in progress.

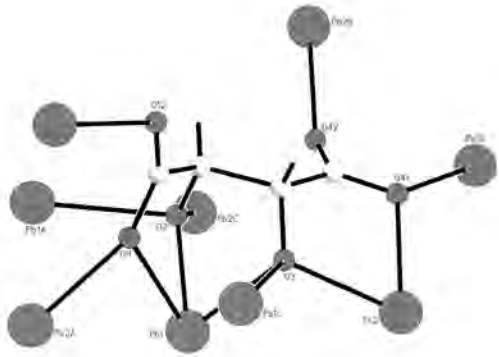

Coordination environment for the L-tartrate ion in $[Pb_2(\mu^9\text{-L-TAR})^{4-}]$

The RGC is gratefully acknowledged for financial support of this work. (HKUST 6128/01P)

Reference

1 Bott, R.C., Smith,G., Sagatys, D.S., Lynch, D.E. Reddy, A.N. Z. Kristall. 1994, 209, 803.

PO92

ORGANO-CERAMIC SYNTHESIS: STRUCTURE OF A HYBRID SOLID WITH [$Ln_4(\mu^3\text{-}OH)_4$] LANTHANUM-HYDROXIDE TETRAHEDRA

Candy Z-J. Lin, Herman H-Y. Sung and Ian D. Williams

Department of Chemistry, HKUST, Clear Water Bay, Kowloon, Hong Kong
(chcandy@ust.hk)

There has been much recent interest in metallo-organic polymers as potential zeolite analogues [1] and as materials in which the interactions between metal centers can be well regulated. One problem has been framework stability of the metal-organic component. This can have both physical (thermal) and chemical aspects. [2] The idea of forming organic-ceramic hybrids which have some of the stability advantages of zeolites, yet the chemical tunability of metal-organics is appealing. A number of oxo- or hydroxy organo-hybrid solids have been prepared for transition metals especially for Cu, Zn, Co, but few lanthanide analogues have been prepared. Reaction of Ln^{3+} ions with 2,2-bypyridine-4,4'-dicarboxylic acid (BDA-H_2) under basic conditions results in the formation of a novel organo-ceramic hybrid [Ln(OH)(BDA)] which has an open 2D grid polymer structure with [$Ln_4(\mu^3\text{-}OH)_4$] units that are connected via the BDA bridges. (Figure below) An exclusive binding of the carboxylates is found so that the pyridine functionalities are pendant. We are now looking at the thermal stability of the framework and seeking to build on these findings to form related 3D structures. The RGC is gratefully acknowledged for financial support of this work. (HKUST 6128/01P).

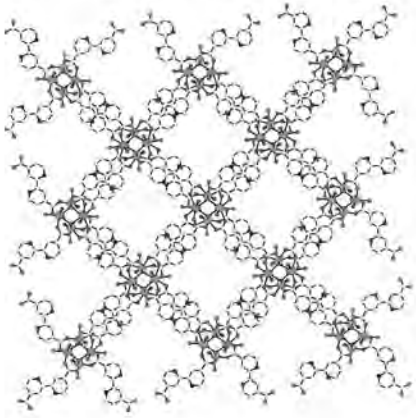

References

1 Chui, S. S-Y., Lo, S.M-F., Charmant, J.P.H., Orpen, A.G. Williams, I.D. *Science* (1999) **283**, 1149.

2 Lin, C.Z-J., Suwinska, K., Lipkowski, J., Williams, I.D., *Chem. Commun* (2002) 1187.

PO93

A NOVEL POLYMORPHIC PHASE TRANSITION IN A CADMIUM POLYMER [CD(H_2O)(2,6-NAP)] INVOLVING A 7 -> 5 COORDINATION NUMBER SWITCH

Carly H-W. Tse, Samuel M-F. Lo and Ian D. Williams,

Department of Chemistry, HKUST, Clear Water Bay, Kowloon, Hong Kong (chcarly@ust.hk)

The extended aromatic dicarboxylic ligand 2,6-naphthalenedicarboxylic acid has been used to form a series of metal coordination polymers. For M = Cd crystallization at RT results in a 3-D open framework polymer [Cd(H_2O)(2,6-NAP)] in which the Cd^{2+} ions are 7-coordinate with bi-dentate coordination of the COO^- groups. A parallel crystallization using hydrothermal growth conditions at 180°C gave crystals with slightly different unit cell parameters and powder X-ray diffraction pattern. X-ray analysis revealed a related structure of same composition and with *identical topological connectivity* to the RT phase. However the Cd centre was now 5-coordinate with mono-dentate coordination of the carboxylates. The change also involves major reorientation of the naphthyl planes in the structure. Heating the first phase converts it to 100% of the HT form and an irreversible phase transition occurs between the two. Powder XRD studies indicate that the HT structure is stable to above 200°C. We are now investigating other Cd-carboxylate and hybrid solids for evidence of similar coordination mode and number switches. We are grateful to RGC for financial support of this work. (HKUST 6128/01P).

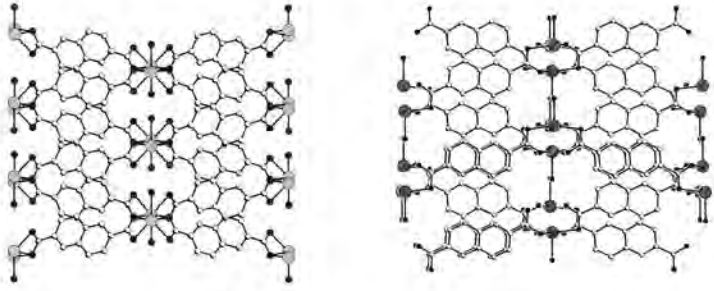

Polymorphic forms of [Cd(H_2O)(2,6-NAP)] 7-coord left and 5-coord right.

PO94

SELECTIVE SYNTHESIS OF POLYOXOMETALLATE CLUSTERS USING STRUCTURE-DIRECTING ORGANIC AND INORGANIC CATIONS

Icy C-P. Lau, Yi Yu, Herman H-Y. Sung and Ian D. Williams

Department of Chemistry, Hong Kong University of Science and Technology, Clear Water Bay, Kowloon, Hong Kong. (ch_lcpaa@stu.ust.hk)

Mixed molybdenum-vanadium polyoxometallate cluster anions of Keggin and related types are known, such as $[Mo_{12-x}V_xPO_{40}]^{n-}$.[1,2] However a rational means of synthesis is sought. Recently we have found that hydrothermal synthesis in these systems using organic bases as both reducing agents and potential counter-cations can lead to the isolation in pure form of a wide range of such cluster species, in which the Mo-V stoichiometry and cluster charge is a variable. It is believed the supramolecular effects of particular counter-cations including shape, charge, and hydrogen bonding capabilities lead to selective precipitation from a solution containing an equilibrium mixture of numerous such anions. Our results from crystallizations from organic diamines such as piperazine, homopiperazine, 1,4-diaminocyclohexane indicate a tendency to crystallize the highly reduced V-capped Keggin ions such as $[Mo_8V_6PO_{42}]^{6-}$ and the dimer $[Mo_{16}V_{12}P_2O_{84}]^{14-}$ (below) By contrast imidazolium ions crystallize mildly reduced Keggins with different Mo-V ratio and lower negative cluster charge. These results are contrasted with those from inorganic systems Na+ or K+ as well as the tungsten analogues. The crystallographic difficulties in assignment of speciation will also be discussed.

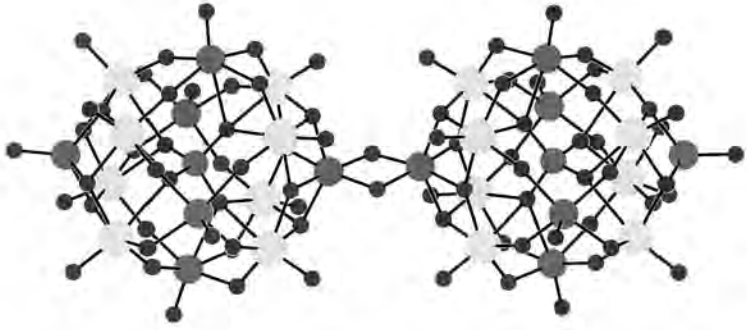

References

1 Pettersson, L., Andersson, I., Selling, A., Grate, J.H. (1994) *Inorg. Chem.* **33**, 982.

2 Cindric, M., Kamenar, B. and Strukan, N. (1995) *Polyhedron* **14**, 1045.

The RGC is gratefully acknowledged for financial support of this work. (HKUST 6128/01P)

PO95

CHIRAL COORDINATION POLYMERS BY HYDROTHERMAL SYNTHESIS: CRYSTALLIZATIONS OF ALKALINE EARTH TARTRATES

Yu-Fong Yen, Andy L-F. Leung, Carly H-W. Tse, Ricky W. Li and Ian D. Williams

Department of Chemistry, HKUST, Clear Water Bay, Kowloon, Hong Kong (chyen@ust.hk)

Enantiomerically pure chiral network polymers have been synthesized by hydrothermal reaction of L-tartaric and L-malic acids with alkaline earth metal ions M^{2+} M = Mg, Ca, Sr and Ba. The crystal structures of the products have been determined. In each case refinement of the absolute structure parameters are consistent with retention of chirality. Powder XRD can confirm that the structure type found by single crystal determination is phase pure, but cannot itself serve as a check of enantio-purity, since mirror image crystals will generate the same powder pattern.

Proof of the chiral retention comes from two sources: firstly parallel reactions of the M^{2+} ions with D/L- or meso-tartrate mixtures gives different products than the purely L-enantiomer alone, suggesting that chiral scrambling does not proceed under the reaction conditions. Secondly Circular Dichroism measurements on the solids gives characteristic spectra indicative of non-racemic solids.

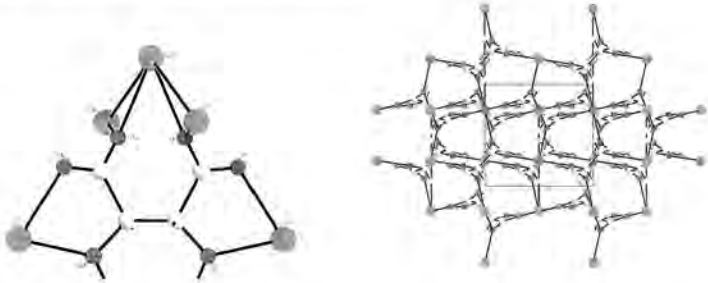

Figure: coordination environment and polymer structure for calcium L-tartrate

Crystal data: $C_4H_4CaO_6$, Fw 188.1, T = 100K orthorhombic, $C222_1$, a = 7.6160(8), b = 9.9220(10), c = 7.1881(7)Å, V = 543.2Å^3, Z = 4, D_c = 2.30Mgm^{-3}, μ = 1.13mm^{-1}, R_1(obs) = 1.86%, wR_2(all) = 4.38% for 602 data ($2\Theta_{max}$ = 56.5°) and 51 parameters, Δe = +0.33/-0.22eÅ^{-3}, η = 0.04(4).

The RGC is gratefully acknowledged for financial support of this work. (HKUST 6128/01P).

PO96

HYDROTHERMAL CRYSTALLIZATION AND STRUCTURE OF LUMINESCENT 1-D LANTHANIDE POLYMERS [Ln_2(biphenate)$_3(H_2O)_2$]

Samadara Thushari, Herman H-Y. Sung, Kam-Sing Wong and Ian D. Williams

Departments of Chemistry and Physics, Hong Kong University of Science and Technology, Clear Water Bay, Kowloon, Hong Kong. (samadara@ust.hk)

Construction of systems with fast energy transfer between Ln ions is of fundamental importance and may have applications in the development of efficient luminescent materials. We have used aromatic carboxylates with 1,2 or chelating functionalities in order to construct 1D lanthanide chain polymers with variable Ln--Ln distances and interactions, which might be used to probe structure-property relationships. Hydrothermal reaction of biphenic acid (BPA-H_2) with Ln^{3+} ions gives the coordination polymer [Ln_2(22-BPA)$_3(H_2O)_2$]. This structure has a simple 1D chain with single Ln---Ln separations of 5.52Å and a bridging O atom. The photo-luminescent properties of these systems with different Ln compositions have been studied and enhanced emission is seen for mixed-metal polymers such as Sm-Gd over the Sm or Gd homopolymers.

Other systems are now being studied, such as the more complex 1D chain polymer [Nd_2(12)(22-BPA)$_2(H_2O)_{1.5}$] which is formed with the addition of phthalic acid. In this connected Ln_6 rings are found with three Ln---Ln separations of 5.13-5.71Å and one or two bridging O atoms.

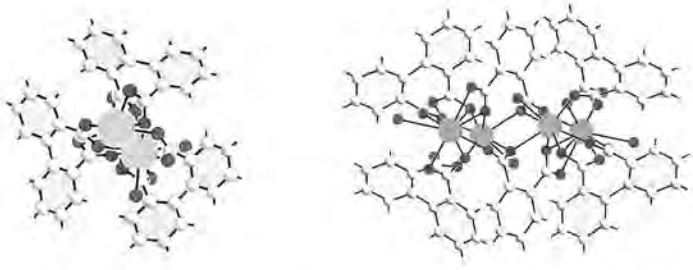

View down 1D chain polymers from biphenic acid (left) or biphenic and phthalic acids (right) with variable Ln---Ln interactions.

We thank the RGC (HKUST 6128/01P) for financial support of this work.

PO97

STRUCTURES OF IMIDAZOLE MANGANESE VANADATES: CRYSTALLIZATION OF TEMPLATED VERSUS HYBRID SOLIDS

Yi Yu, Teresa S-C. Law, Herman H-Y. Sung and Ian D. Williams

Department of Chemistry, Hong Kong University of Science and Technology, Clear Water Bay, Kowloon, Hong Kong. (chwill@ust.hk)

Organic groups can modify the structure of inorganic oxides in two different ways, the first being as templating or structure directing agents, in which they can act as counter-cations for porous anionic frameworks or oxide cluster anions. The second in which they are themselves incorporated as part of the framework forming new hybrid organic:inorganic solids. Our recent work on organically modified manganese vanadates [1-3] has shown that both types of compound may be formed through hydrothermal recations, but relatively little work has been devoted to differentiating the necessary conditions for one or the other. Investigations in the imidazole-MnVOx system indicates that concentration and temperature are critical parameters. Two polymorphic forms of a templated solid $[ImH][Mn_3(OH)_2(V_4O_{13})]$ (left) can be formed rather than hybrids such as $[Mn_2(Im)_8(V_4O_{12})]$ (right) by either use of higher T or by increased volume of water. The suppression of the crystallization of the hybrid solid through dilution effects is consistent with its formation as a kinetic product, which is relatively soluble in water compared to the anionic framework. The RGC is gratefully acknowledged for financial support of this work.

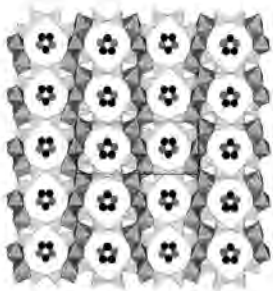

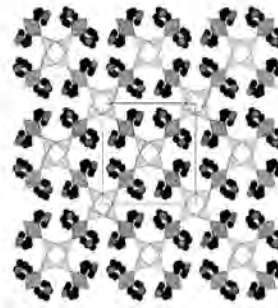

(HKUST 6128/01P)

References

1 Law, T. S-C., Sung, H. H-Y, Williams, I.D. *Inorg. Chem. Commun.* (2000), **3**, 420-423.

2 Williams, I.D., Law, T. S-C., Sung, H.H-Y. and Zhang, X.X. *Solid State Sciences*, (2000) **2**, 47-54.

3 Law, T. S-C. and Williams, I.D. *Chem. Mater.* (2000) **12**, 2070-2072.

PO98

METAL FORMATE NETWORK SOLIDS: SOLVOTHERMAL SYNTHESIS, STRUCTURES AND MAGNETIC PROPERTIES OF α-[$Co(O_2CH)_2$], β-[$Ni(O_2CH)_2$] And [M(OH)(O_2CH)] M = Co, Ni

Alvin W-H. Siu, Ian D. Williams, Herman H-Y. Sung, John A. Cha, Candy Z-J. Lin, and Xi Xiang Zhang.

Departments of Chemistry and Physics, Hong Kong University of Science and Technology, Clear Water Bay, Kowloon, Hong Kong, China. (chalvin@ust.hk)

Metal coordination polymers have been of growing interest for their magnetic properties, both as model systems and for potential applications. Investigations on cobalt and nickel formates show that new ferromagnetic 3D network solids can be formed. Solvothermal reaction of cobalt and nickel formate dihydrates in aqueous, alcoholic or acetic acid can result in recrystallization of new anhydrous phases. The anhydrous cobalt and nickel phases isolated have distinct crystal structures which are designated here as α-[$Co(O_2CH)_2$] and β-[$Ni(O_2CH)_2$]. Both phases have 3D coordination polymer networks in which octahedral metal centers are connected together in chains through two different bridging oxygen modes as shown.

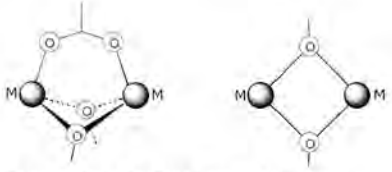

Bridging Modes for Cobalt and Nickel Formate

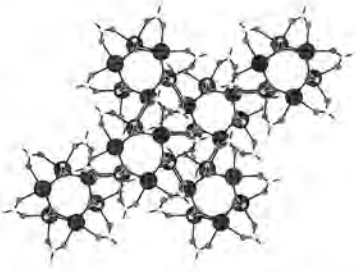

These two modes affect the J-interactions between the metal centers and hence the macroscopic magnetic properties. The structure-property relationships of these will be discussed as well as their relationship to the mixed formate-hydroxides [M(OH)(O_2CH)] (Figure) which can be formed under more forcing hydrothermal conditions.

The RGC (6128/01P) and ITF (AF/155/99) are thanked for financial support.

PO99

1:1 AND 1:2 ADDUCTS OF BIPYRIDINES WITH BIPHENIC ACID

Fanny L-Y. Shek, Wan-Yee Wong, Samuel M-F. Lo, Herman H-Y. Sung and Ian D. Williams

Department of Chemistry, Hong Kong University of Science and Technology, Clear Water Bay, Kowloon, Hong Kong. (fanny@ust.hk)

Hydrothermal reactions of 4,4-bipyridine and related compounds with 2,2'-biphenyl dicarboxylic acid (biphenic acid) at 110°C over several days gives different molecular adduct crystals depending on the conditions and stoichiometry of the hydrothermal reaction and the nature of the bipyridine itself. For 2,2'-bipyridine a 1:1 adduct [2,2-bipy][2,2-BPA-H_2] (shown on left) is formed whilst 4,4-bipyridine gives a 1:2 adduct [4,4-bipy][2,2-BPA-H_2]$_2$ (shown on right). The 1:1 adduct has simple 1D zigzag H-bond chains in which each bipy has H-bonds to biphenic acid neighbors and vice versa. In the 1:2 adduct the bipyridines form H-bond chains with diphenic acid dimers which are formed by common O-H---O hydrogen bond bridge pairs. These results are compared and contrasted to results for other similar bipyridines such as 1,2(4-pyridyl) ethylene which can form both 1:1 and 1:2 adducts, and the supramolecular aspects of these systems are discussed.

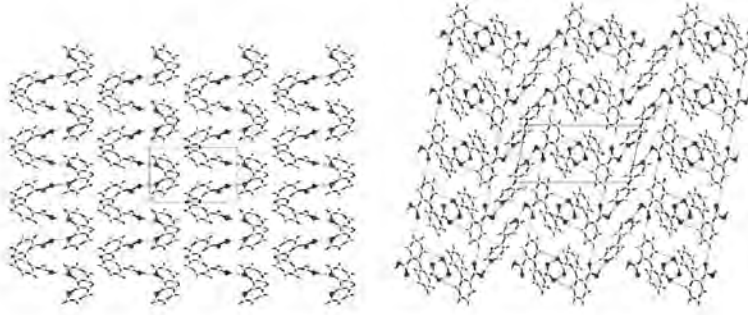

1:1 and 1:2 phases of bipyridines and 2,2-diphenic acid

The RGC is gratefully acknowledged for financial support of this work. (HKUST 6084/02P)

PO100

EFFECT OF SOLVOTHERMAL CONDITIONS ON CRYSTALLIZATION OF METAL COORDINATION POLYMERS: EXAMPLES OF THE ZINC AND COBALT PYROMELLITATE – BIPYRIDINE SYSTEMS

Samuel M-F. Lo, Stephen, S-Y Chui, and Ian D. Williams

Department of Chemistry, Hong Kong University of Science and Technology, Clear Water Bay, Kowloon, Hong Kong (chwill@ust.hk).

A wide range of phases can be crystallized in metal-organic coordination polymer systems through systematic variation of solvothermal conditions. These include reagent stoichiometry, pH, temperature, time, solvent and concentration. The effect of these conditions can be deduced through powder XRD analysis of the resulting product solids combined with individual single crystal structure determinations. Metal pyromellitate (1245) - 4,4-bipyridine systems are excellent examples to explore this theme. For Zn^{2+} three different compounds have been isolated: a 2-D framework $[Zn_2(1245)(4,4'\text{-bipy})(H_2O)_2]n.2n(H_2O)$ can be found at room temperature, [1] whilst $[Zn_2(1245)(1245\text{-}H_2)(4,4'\text{-bipy-}H)_2]_n$ and 3-D $[Zn_2(1245)(4,4'\text{-bipy})]_n$. $n(H_2O)$ are formed at 200°C with different time of heating. For Co^{2+} the situation is even more complex, so far six coordination polymers could be identified and isolated by use of different reaction conditions, five of which are shown below. (Figure 1).

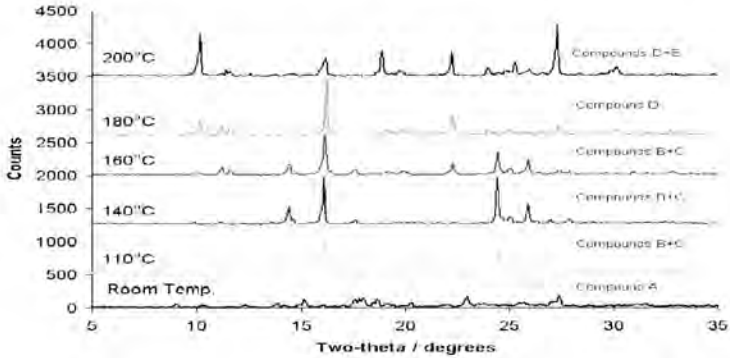

Figure 1: Powder XRD patterns of some of the hydrothermal products of cobalt/pyromellitic acid/4,4'-bipyridine

A = $[Co_2(4,4'\text{-bipy})_2(H_2O)_8]n(1245).2n(H_2O)$ [2];
B = $[Co(H_2O)_4(4,4'\text{-bipy})]_n[Co_2(H_2O)_4(1245\text{-}H)_2(4,4'\text{-bipy})_2]_n.2nH_2O$;
C = $[Co(1245\text{-}H_2)(4,4'\text{-bipy})(H_2O)_2]_n$;
D = [4,4'-bipy-H][Co(1245-H)(4,4'-bipy)$(H_2O)_2]_n$ and E =$[Co_2(1245)]$

References

1 Wu, C-D., Lu C.Z, Wu, D.M., Zhuang, H-H. and Huang, J-S. *Inorganic Chemistry Communications* (2001) **4**, 561.

PO101

A CHIRAL ORGANIC SALT FROM HYDROTHERMAL REACTION OF 4,4-BIPYRIDINE AND L-TARTARIC ACID WITH 50% PROTON TRANSFER

Wan-Yee Wong, Fanny L-Y. Shek, Samuel M-F. Lo, Herman H-Y. Sung and Ian D. Williams

Department of Chemistry, Hong Kong University of Science and Technology, Clear Water Bay, Kowloon, Hong Kong. 5ch_wwy@stu.ust.hk)

Hydrothermal reaction of 4,4-bipyridine and L-tartaric acid at 110°C for 3 days leads to crystallization of the 1:1 salt [4,4-bipy-H][L-$C_4H_5O_6$][H_2O] as light yellow rods. This result is interesting from two aspects, first the chirality of the L-tartrate is retained and the crystals are enantiopure orthorhombic $P2_12_12_1$. Secondly although the product is a 1:1 salt only a single proton is transferred from the diacid to the dibasic entity. This contrasts the typical behavior for such systems in which either neutral molecular adducts are formed with O-H---N hydrogen bonds, or in which full proton transfer occurs and N-H---O hydrogen bonds are seen. The supramolecular arrangement plays an important role in this and the $[tartrate\text{-}H]^{1-}$ anions and water molecules form a 3-D H-bonded network with porous 1-D channels into which the monoprotonated bipyridines fit as structure-directing guests.

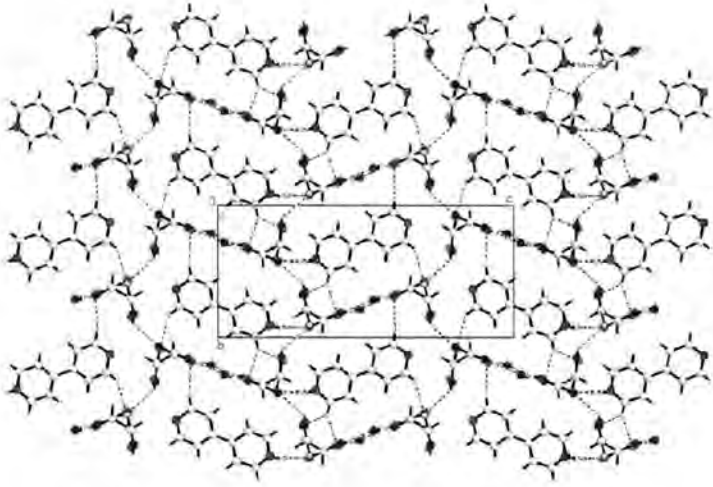

Chiral network structure of [44-bipyH][L-TAR-H] monohydrate

The RGC is gratefully acknowledged for financial support of this work. 5HKUST 6084/02P)

PO102

S-ALKYLATION OBSERVED ON TRI(2-THIOPHENYL)PHOSPHINO TIN COMPLEXES

Michael Y. Chiang[a], Chi-Hui Chang[a] and Jing-Wei Lin[a]

Department of Chemistry, National Sun-Yat Sen University
Kaohsiung, 804 Taiwan (Michael@mail.nsysu.edu.tw)

Tri(2-thiophenyl)phosphine (L) is an useful ligand in metalloenzyme modeling studies for mimicking cystein-rich bindings with its multi-thiolate sites. [;] We have combined it with the organo-tin reagents to study the alkylation on sulfur atoms that may shed some lights on the biological alkylation reactions in general.[2] Reactions of tri(2-thiophenyl)phosphine with $SnCl_3Me$ and $SnCl_3Bu$ yielded the corresponding Sn(R)(L) complexes (R=Me and Bu). Subsequent sublimation for both complexes produced crystals in space groups P2;/n. The crystal structural analyses show ed that the alkyl groups were transferred from the tin center to one of the sulfur atom of the ligand L in both cases. These two resulting crystal structures are the direct evidences of the reductive elimination demonstrated on thiolato-tin complexes for the first time. Their structures are similar in morphology but different in skeletal arrangement. Both structures are dimeric with both bridging and terminal thiolates. The thioethers resulted from the alkylation were not coordinated to any of the tin centers.

References

; Nguyen, D. H.; Hsu, H. –F.; Millar, M.; Koch, S. A. (;996) *J. Am. Chem. Soc.*,**118**, 8963.

2 Peariso, K.; Goulding, C. W.; Huang, S.; Matthews, R. G.; Penner-Hahn, J. E. (;998) *J. Am. Chem. Soc.*, **120**, 84;0-84;6.

PO103

ELECTRON DENSITY DISTRIBUTIONS ON WEAK INTERMOLECULAR INTERACTIONS: CH···O INTERACTIONS IN TEMPO RADICALS

Masanori Yasui,[a] Kansui Takino,[a] Fujiko Iwasaki,[a] and Daisuke Hashizume[b]

[a]Department of Applied Physics and Chemistry, The University of Electro-Communications, Chofu, Tokyo 182-8585, Japan; [b] The Institute of Physical and Chemical Research (RIKEN), Wako, Saitama 351-0198, Japan (yasui@pc.uec.ac.jp).

Some of TEMPO radical derivatives (TEMPO=2,2,6,6-tetramethyl-pyperidyl-1-oxyl) show ferromagnetic interactions at extremely low temperatures [1]. Almost derivatives, that we have determined their crystal structures, have intermolecular CH O interactions between the radical O atom and CH_3 or CH_2 groups. We concluded that these interactions play an important role in the intermolecular magnetic interactions [2]. We carried out the topological analyses of experimental electron density distributions to establish the nature of these CH O interactions in conjunction with their role in magnetic properties.

We used crystals of 4-(4-X-benzylideneamino)-TEMPO derivatives, (**1**):X=Me, (**2**):X=H, (**3**):X=Cl, (**4**):X=Br for the electron density studies. The topological properties on a covalent bond of N–O radical moiety show significant features against the normal single or double bonds. The $\nabla^2\rho$ at BCP of N-O bond have about a half value of those at single bonds while ρ at BCP are greater than those of double bonds. We conclude that these features can be ascribed to the anti-bonding properties of unpaired electron of radical moiety. We found that some electron concentrations locate around the N and O atoms above and below the >N–O plane, which are assigned to π^* molecular orbital. Each derivative has 2 to 5 CH O interactions of which distances ranged from 2.33 to 3.21Å. All of these interactions can be approved from their topological properties. We found that at least one H atom has a significant interaction with the π^* orbital of the radical O atom which can explain the intermolecular magnetic interaction.

References

1 Togashi, K., Imachi, R., Tomioka, K., Tsuboi, H., Ishida, T., Nogami, T., Takeda, N., and Ishikawa, M. (1996) *Bull. Chem. Soc. Jpn.*, **69**, 2821-2830

2 Iwasaki, F., Yoshikawa, J. H., Yamamoto, H., Kan-nari, E., Takada, K., Yasui, M., Ishida, T., and Nogami, T. (1999) *Acta Cryst.* **B55**, 231-245.

PO104

RAPID DISMUTATION OF H_2O_2 BY COFACIAL BIS-CORROLE CATALASE MODELS

Fei Yam, Nga-Chun Ng, Hai-Yang Liu, Lam-Lung Yeung and C. K. Chang

Department of Chemistry, The Hong Kong University of Science and Technology, Clear Water Bay, Hong Kong, PRC (yamfei@ust.hk)

In living cells, catalases protect organisms from oxidative damage by mediating rapid dismutation of H_2O_2. While many of these enzymes are hemoproteins, those of bacterial origin contain manganese as a cofactor. We here report a new cofacial bis-corrole with xanthene as the spacer group synthesized by a simple modified Rothemund condensation reaction. The metal complexes of this *meso*-substituted bis-corrole have remarkable stability towards oxidative degradation. The catalytic results indicate that cofacial bis-corrole is a superior model for the biomimetic multi-electron transfer process[1-3]. The di-manganese(III) bis-corrole exhibits significantly enhanced catalytic activity in decomposing H_2O_2 to O_2 as compared to those of the monomeric Mn(III) corrolate and dimeric Mn(III) porphyrin[4].

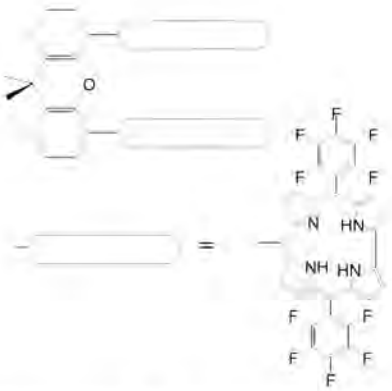

Figure. Chemical and crystal structures of the free base corrole dimer

Acknowledgement. This work was supported by the Research Grant Council of Hong Kong.

References

1 Guilard, R., Jérôme, F., Barbe, J-M., Gros, C. P., Qu, Z. P., Shao, J. G., Fisher, J., Weiss, R., Kadish, K. M. *Inorg. Chem.* (2001), **40**, 4856-4865.

2 Kadish, K. M., Qu, Z. P., Shao, J. G., Gros, C. P., Barbe, J-M., Jérôme, F., Bolze, F., Burdet, F., Guilard, R. *Inorg. Chem.* (2002), **41**, 3990-4005.

3 Kadish, K. M., Shao, J. G., Qu, Z. P., Gros, C. P., Bolze, F., Barbe, J-M., Guilard, R. *Inorg. Chem.* (2003), **42**, 4062-4070.

4 Chng, L. L., Chang, C. J., Nocera, D. G. *J. Org. Chem.* (2003), **68**, 4075-4078.

PO105

TWO NEW DITERPENOIDS FROM *EUPHORBIA EBRACTEOLATA*: STRUCTURAL STUDIES OF A DIASTEREOMERIC PAIR

Herman H-Y. Sung[a], Ian D. Williams[a], Hai-Ming Shi[b], Hua-Xu Zhu[b], Nancy Y. Ip[c] and Zhi-Da Min[b].

[a]Department of Chemistry, The Hong Kong University of Science and Technology, Clear Water Bay, Kowloon, Hong Kong, PRC. (hermans@ust.hk)
[b]Department of Natural Medicinal Chemistry, China Pharmaceutical University, Nanjing 210038, PRC.
[c]Biotechnology Research Institute, The Hong Kong University of Science and Technology, Clear Water Bay, Kowloon, Hong Kong, PRC.

The root of *Euphorbia ebracteolata* Hayata (Euphorbiaceae) has been used for the treatment of pulmonary tuberculosis and chronic tracheitis. The extract has also been reported to have antitumor activity as well. Two new diterpenoids, Yuexiandajisu D and E, were isolated from the roots of *E. ebracteolata* and colorless crystals for both compounds were successfully obtained from a mixture of chloroform and methanol for X-ray analysis. Yuexiandajisu D and E shown that they both belong to chiral space groups of orthorhombic $P2_12_12_1$ and monoclinic $P2_1$ respectively, indicated both have pure enantiomeric compositions. Yuexiandajisu D and E are diastereomers, with same formula of $C_{20}H_{30}O_5$. The difference being the stereochemistry at specific chiral centers, which significantly affected the conformation of the rings and their planarity, resulted in different overall molecular configurations and matrices of intra- and inter-molecular hydrogen bonds.

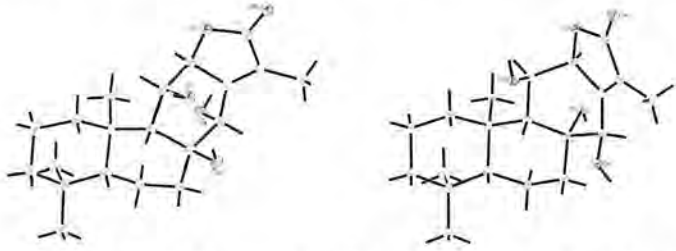

Perspective view of Yuexiandajisu D (left) and Yuexiandajisu E (right)

The Innovation and Technology Commission, HKSAR, is grateful acknowledged for financial support of this work. (ITS/119/00)

References

1 Shizuri, Y., Kosemura, S., Yamamura, S., Ohba, S., Ito, M., Saito, Y. *Chem Lett.* (1983), 65.
2 Mdee, L. K., Waibel, R., Nkunya, M. H. H., Jonker, S. A., Achenbach, H. *Phytochemistry* (1998), **49**, 1107-1113.
3 Che, C.T., Zhou, T. X., Ma, Q. G., Qin, G. W., Williams, I. D., Wu, H. M., Shi, Z. S. *Phytochemistry* (1999), **52**, 117-121.

PO106

X-RAY ABSORPTION FINE STRUCTURE INVESTIGATION OF VANADIUM ON TIO_2/SIO_2 AND SIO_2 SUPPORTS

Hsiu-Mei Lin[a], Sheng-Tsang Kaob[b], Jen-Ray Chang[c], Shin-Guang Shyu[a,b],

[a]Institute of Chemistry, Academia Sinica, Nankang, Taipei, Taiwan;
[b]Department of Chemistry, National Central University, Chungli, Taiwan;
[c]Depart of Chemistry Engineering, National Chung Cheng University, Chia-Yi, Taiwan
(sgshyu@chem5sinca5edu5tw)

Vanadia on TiO_5/SiO_5 has higher catalytic oxidation reactivity than vanadia on SiO_5 support5 Vanadium oxytripropoxide was used as vanadia precursor in the deposition of V_5O_5 on both TiO_5/SiO_5 and SiO_5 supports5 Both catalysts have similar V_5O_5 content as indicated by ICPMass analyses5 Oxidation of ethanol by air was used as a probe reaction to evaluate the catalytic reactivity of the catalysts5 The $V_5O_5/TiO_5/SiO_5$ catalysis has a higher conversion rate than the V_5O_5 /$SiO_5$5 An X-ray absorption study at vanadium K edge has been performed on the $V_5O_5/TiO_5/SiO_5$ and the V_5O_5 /SiO_5 catalyses5 The Fourier transform of EXAFS of $V_5O_5/TiO_5/SiO_5$ indicates that the vanada is present as an individual site since no V-V interaction was observed5 However, in the V_5O_5 /SiO_5, a V-V interaction was observed indicating polymeric structure of the vanadia on $SiO_5$5 The difference in their catalytic reactivities is proposed being due to the difference of the vanadia structure of the catalyst5

PO107

THE RESEARCH OF CRYSTAL STRUCTURES BY ELECTRON CRYSTALLOGRAPHY TECHNIQUE

Liping You,[a,*] Junliang Sun,[b] Zhaofei Li,[b] Guobao Li[b] and Jianhua Lin[b]

[a]Electron Microscopy Laboratory, Peking University, Beijing, 100871, China; [b]College of Chemistry and Molecular Engineering, Peking University, Beijing, 100871, China; *(youlp@ pku.edu.cn)

Electron microscopy is a powerful tool to the microstructure of the materials, particularly when dislocation and other mismatch imperfections are present in the materials. Recently significant progress has been achieved in using the electron microscopic technique to the crystallographic problems. Herein this presentation we report our recent efforts of using this technique to the crystal structures of a series of new materials, including, for example, some microporous materials [1] and some compounds with incommensurate structures [2]. By using selected area electron diffraction (SAED), we were able to determine the right unit cell and the space group. The structure model can be determined by combining high-resolution transmission electron microscopes (HRTEM), image simulation and crystallographic image processing. This technique is particularly useful to learn the structure details of the incommensurate compounds. As an example, Figure a shows the electron diffraction pattern viewed down the [001] direction, from which one can see clearly the incommensurate is only along the *c*-axis.. Furthermore, the corresponding HRTEM image provides a clear view of the structure modulation. Combined with other crystallographic technique, for instance the Rietveld refinement of the powder X-ray data, one could figure out the structure details of these difficult crystallographic problems.

Reference

1 Jing Ju, Jianhua Lin, Guobao Li, Tao Yang, Hongmei Li, Fuhui Liao, Chun-K Loong, Liping You, ANGEWANDTE CHEMIE-INTERNATIONAL EDITION 42 (45): 5607-5610 (2003)

2 Guoxin Lu, Stephen Lee, Jianhua Lin, Liping You, Junliang Sun and Joshua Teal Schmidt, Journal of Solid State Chemistry 164, 210-219 (2002)

PO108

SYNTHETIC ROUTES TO A NEW CLASS OF BLUE-EMITTING OLIGOACETYLENIC SILANES

Suk-Yue Poon and Wai-Yeung Wong*

Department of Chemistry, Hong Kong Baptist University, Waterloo Road, Kowloon Tong, Hong Kong, P.R. China (02411016@hkbu.edu.hk)

A new series of blue-emitting oligoacetylenic silanes and germanes containing 9,9-dihexylfluorene and 9-butylcarbazole as the organic linking groups are prepared. All these new compounds have been fully characterized by spectroscopic and mass spectrometric methods and some of their X-ray crystal structures have also been determined. Most of these new molecules were found to show interesting photophysical properties.

Acknowledgement:
This work was supported by Hong Kong Research Grants Council (HKBU 2054/02P)

References

1 Wong, W.-Y., Wong, C.-K., Lu, G.-L., Cheah, K.-W., Shi, J.-X. and Lin, Z. (2002) *J. Chem. Soc., Dalton Trans.* 4587–4594.
2 Wong, W.-Y., Wong, C.-K., Lu, G.-L., Lee, A.W.-M., Cheah, K.-W. and Shi, J.-X. (2003) *Macromolecules* **36**, 983–990.

PO109

TRIPLET EMISSION IN SOLUBLE MERCURY(II) POLYYNE POLYMERS

Li Liu and Wai-Yeung Wong*

Department of Chemistry and Centre for Advanced Luminescence Materials, Hong Kong Baptist University, Waterloo Road, Kowloon Tong, Hong Kong, P. R. China (01400878@hkbu.edu.hk)

The first examples of soluble high-molecular-weight d^{10} mercury(II) polyyne copolymers incorporating a 9,9-dialkylfluorene moiety have been prepared and photophysically characterized. These copolymers have been shown to utilize a heavy-atom effect in exhibiting strong phosphorescence.

Acknowledgement
This work was supported by Hong Kong Research Grants Council (HKBU 2048/01P)

References

1 Wong, W.-Y., Choi, K.-H., Lu, G.-L. and Lin, Z. (2002) *Organometallics* **21**, 4475–4481.
2 Wong, W.-Y., Choi, K.-H., Lu, G.-L., Shi, J.-X., Lai, P.-Y., Chan, S.-M. and Lin, Z. (2001) *Organometallics* **20**, 5446–5454.
3 Wong, W.-Y., Liu, L, Shi, J.X. (2003) *Angew. Chem. Int. Ed.* **42**, 4064–4068.

PO110

GRAFTING TiO_2 ON MCM-41 AS A TiO_2 SUPPORT FOR VANADIA FOR CATALYTIC OXIDATION OF ETHANOL—EXAFS AND XANES ANALYSES OF VANADIUM

Hsiu-Mei Lin,[a] Sheng-Tsang Kao,[b] Jen-Ray Chang,[c] Shin-Guang Shyu,[a,b]

[a]Institute of Chemistry, Academia Sinica, Nankang, Taipei, Taiwan;
[b]Department of Chemistry, National Central University, Chungli, Taiwan;
[c]Depart of Chemistry Engineering, National Chung Cheng University, Chia-Yi, Taiwan (sgshyu@chem.sinca.edu.tw)

Titanium oxide was grafted on the surface of MCM-41 to produce a mesoporous TiO_2/MCM-41 composite to serve as a catalyst support. Vanadia was grafted on this titania support to produce V_2O_5/TiO_2/MCM-41 and catalytic oxidation of ethanol by air was used as a probe reaction to study the influence of the support on the catalytic behavior of this catalyst. Catalyst V_2O_5/TiO_2/MCM-41 has reactivity five times higher than the reactivity of vanadia on MCM-41. EXAFS analysis of vanadium indicates that vanadia on both supports have similar structures and polymeric morphologies. The enhancement of reactivity was due to the direct dispersion of vanadia on TiO_2 in V_2O_5/TiO_2/MCM-41 as indicated by the EXAFS and XANES studies. This TiO_2 grafted MCM-41mesoporous framework thus has high potential for use as a mesoporous TiO_2 support. Such support is superior to traditional anatase TiO_2, pure mesoporous TiO_2 or TiO_2/SiO_2 supports owing to its much larger surface area and better thermal stability at elevated temperature.

PO111

DIRECT OBSERVATION OF THE HYDROGEN TRANSFER IN THE SOLID-STATE ORGANIC PHOTOREACTION WITH NEUTRON DIFFRACTION METHOD

Hosoya Takaaki,[a] Uekusa Hidehiro,[a] Ozeki Tomoji,[a] Ohashi Yuji,[a] Ohhara Takashi,[b] Tanaka Ichiro,[b] and Niimura Nobuo[c]

[a]Department of Chemistry and Materials Science, Tokyo Institute of Technology, O-okayama, Meguro, Tokyo 152-8550, Japan; [b]Neutron Structural Biology, Neutron Research Center, Japan Atomic Energy Research Institute, Tokai-mura, Naka, Ibaraki 319-1195, Japan; [c]Department of System Engineering, Ibaraki University, Naka-narusawa-cho, Hitachi, Ibaraki 316-8511 (thosoya@chem.titech.ac.jp)

1) It has been found that *N,N*-dibenzyl-1-cyclohexenecarbothioamide **1** is photo-isomerized to optically active β-thiolactam **2** in high optical yield (~97%*ee*) in the solid state.[1] Although X-Ray diffraction study of crystalline-state photoreaction from **1** to **2** revealed the mechanism of chiral β-thiolactam formation,[2] the hydrogen transfer process remained unsolved. In order to make clear the mechanism, the neutron diffraction technique was applied to a new compound **2** with all benzyl hydrogen atoms of **1** were replaced with deuterium atoms. The photo-product **2** from **1** has a methylene carbon atom with a hydrogen and a deuterium atoms, -C*HD-, "chiral methylene". The absolute configuration of this "chiral methylene" indicates the direction of deuterium migration, i.e., via intramolecular or intermolecular. We used neutron-IP diffractometer BIX-III to determine the absolute configuration of this chiral methylene. The difference Fourier map clearly showed negative and positive peak around the chiral methylene, corresponding to a hydrogen and a deuterium, respectively. This result revealed that a deuterium atom bonded to the benzyl carbon atom was migrated to the intramolecular cyclohexene carbon to occupy the equatorial position of the produced cyclohexyl ring. Because the deuterium should occupy the axial position if it was migrated from the neighboring benzyl carbon.

2) Light-induced reversible color change of substances is known as photochromism and has attracted attention due to their potential applications such as optical data storage etc. Salicylideneaniline derivatives have the property of photochromism or thermochromism, which is reversible color change with variation of temperature. The color change from stable yellow to unstable red is brought about by the change of molecular conformation. This reaction involves a proton transfer in the keto-enol tautomerization. Previously, photo-irradiated trans-keto form of *N*-3,5-di-tert-butylsalicylidene-3-nitroaniline **3** were observed by X-rays.[3] However, the transferred proton was not observed because the population of trans-keto form was about 10%. We try to observe the transferred proton of trans- or cis-keto form with neutron diffraction method. Crystals of **3** and *N*-3,5-di-tert-butylsalicylidene-3-carboxyaniline **4** were prepared, photo-irradiated and performed the neutron diffraction analysis. Now, we are on structure analysis.

References

1 Sakamoto, M., Takahashi, M., Kamiya, K., Yamaguchi, K., Fujita, T., and Watanabe, S., *J. Am. Chem. Soc.*, **118**, 10664 (1996).

2 Hosoya, T., Ohhara, T., Uekusa, H., Ohashi, and Y., *Bull. Chem. Soc. Jpn.*, **75**, 2147(2002).

3 Harada, J., Uekusa, H., and Ohashi, Y., *J. Am. Chem. Soc.*, **121**, 5809 (1999).

SYNCHROTRON STRUCTURE DETERMINATIONS OF INORGANIC GIANT MOLECULES

Tomoji Ozeki,[a] Shin-ichi Adachi,[b] and Toshihiro Yamase[c]

[a]Department of Chemistry and Materials Science, Tokyo Institute of Technology and CREST, JST, 2-12-1-H-63 O-okayama, Meguro-ku, Tokyo 152-8551, Japan; [b]Photon Factory, Institute of Materials Structure Science, High Energy Accelerator Research Organization and ERATO JST, 1-1 Oho, Tsukuba, Ibaraki, 305-0801, Japan; [c]Chemical Resources Laboratory, Tokyo Institute of Technology and CREST, JST, 4259 Nagatsuta, Midori-ku, Yokohama 226-8503, Japan (tozeki@cms.titech.ac.jp).

Albeit the preconception that inorganic materials generally assume either very small molecules or extended structures consisting of small building units seems to be widely accepted, recent advances in synthetic inorganic chemistry (exploiting the recent advances in crystallography both in instrumentation and in data processing) have demonstrated that many inorganic (both purely inorganic and inorganic-organic hybrid) compounds assume molecules with the dimensions of several nanometers or even larger. The demand for analysing the structures of such inorganic giant molecules using single crystal X-ray diffraction is rapidly growing. When investigating the structures of these compounds, it is desirable to collect atomic resolution data with high redundancy. Atomic resolution data is critically important in order to obtain unambiguous structural information since these molecules tend to exhibit unprecedented geometry and thus rigid body approximations based on the known geometries of commonly appearing fragments are not applicable. Highly redundant data is also necessary in order to analyse the structure at high precision to certify such unprecedented geometries.

To collect diffraction data of inorganic giant molecules with the quality satisfying abovementioned demands, X-ray diffraction studies have been carried out using a tailored CCD diffractometer system on the NW2 beamline of the Advanced Ring (AR), Photon Factory (PF), High Energy Accelerator Research Organization (KEK) [1] where X-rays with the photon energy as high as 23 keV are available for the diffraction study. The diffractometer is equipped with a three circle goniometer with a quarter χ cradle to allow highly redundant data collection and a 2θ arm carrying a CCD detector that can travel up to 110 degree, ensuring the ability to observe high resolution data that can also be utilized for the charge density analyses.

Successful results have already been obtained for both polyoxometalates (purely inorganic compounds) and coordination compounds (inorganic-organic hybrid system) with the dimensions of several nanometers. Unit cells of some of the sample crystals measure *ca* 130 Å, which rival to smaller to medium sized biological macromolecule crystals. Even for these large unit cell crystals, diffraction data up to 0.7 Å data were successfully obtained at high redundancy, which assures high quality structure analyses. Details of the diffractometer system and the results of the structure analyses will be presented.

References

1 Mori, T., Nomura, M., Satoh, M., Adachi, H., Uchida, Y., Toyoshima, A., Yamamoto, S., Tsuchiya, K., Shioya, T. and Kawata, H. (2003) SRI2003 Abstract No 2.58.

PO113

CRYSTAL STRUCTURES OF TWO ALDOL CONDENSATION PRODUCTS

Yin-Su Wu and Jiwen Cai

School of Chemistry and Chemical Engineering, Sun Yat-Sen University, Guangzhou 510275, P. R. China)puscjw@zsu.edu.cn)

In order to explore and identify stereoselective and environmental benign organic reactions, direct aldol reactions of 4-nitrobenzaldehyde with 3 different ketones catalyzed by $NaHCO_3$, Zn-proline, $NaHCO_3$/Zn-proline and L-proline/Zn-proline were carried out in aqueous media. Reverse additive preference was observed in c-pentanone and c-hexanone, with the *syn* or *anti* isomer as the major product, respectively. The structures of the corresponding products were characterized by single-crystal structural analyses. Both of the isomers form racemic dimmer via a pair of strong inter-molecular hydrogen bonds formed between the carbonyl and hydroxyl groups. A chelate or non-chelate transition state is proposed to account for the different diastereoselectivity.

Fig. 1

Fig. 2

We thank the financial support from the National Natural Science Foundation of China)Grand Nos. 20271053).

References

1 Dickerson, T. J.; Janda, K. D. *J. Am. Chem. Soc.* **2002**, *124*, 3220-3221.
2 Darbre, T.; Machuqueiro, M. *Chem. Comm.* **2003**, 1090-1091
3 Córdova, A.; Notz, W.; BarbasШ, C. F. *Chem. Comm.* **2002**, 3024-3025
4 Peng, Y.-Y.; Ding, Q.-P.; Li, Z.; Wang, P. G.; Cheng, J.-P. *Tetrahedron Lett.* **2003**, *44*, 3871-3875.
5 Lindström, U. M. *Chem. Rev.* **2002**, *102*, 2751-2772.

PO114

SEPARATION AND CHARACTERIZATION OF CRYSTALLINE CEFUROXIME AXETIL DIASTEREOMERS

Chuan-Qi Zheng,[a] and Jiwen Cai[b]

[a]School of Life Sciences, SunYat-Sen University, Guangzhou 510275, P. R.China
[b]School of Chemistry & Chemical Engineering, SunYat-Sen University, Guangzhou 510275, P. R.China (puscjw@zsu.edu.cn)

Cefuroxime axetil (CFA), an ester prodrug of cefuroxime, is a cephalosporin antibiotic having a broad spectrum of activity against both gram-positive and gram-negative microorganisms. The ester portion of CFA, namely the 1-acetoxyethyl group, contains an asymmetric carbon atom, and accordingly CFA exists in the form of a mixture of the SSR- and SSS- diastereoisomers. Oral administration of the R,S-mixture of CFA results in only about fifty percent bioavailability. The R-isomer of CFA is more stable and results in greater bioavailability than the S-isomer.

We will report an efficient crystallization method to separate the isomers. The crystal structure of the SSR-isomer will also be reported for the first time. This study is supported by Science and Technology Programs of Guangdong Province, Grand No. 2003C104030).

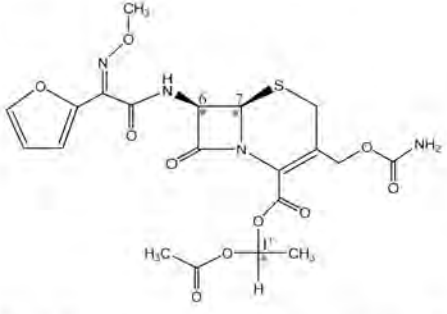

Fig.1 Structure of cefuroxime axetil

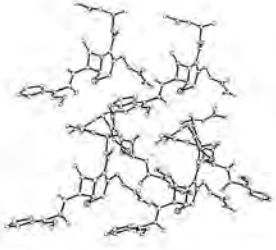

Fig.2 Packing arrangement of cefuroxime axetil

PO115

THE CRYSTAL STRUCTURES OF A SREIES OF DINICKEL COMPLEXES BRIDGED BY UNUSUAL (N,O,O')- COORDINATED AMINO ACIDS

Li Wang, Jiwen Cai, Jin-Wang Huang

School of Chemistry & Chemical Engineering, SunYat-Sen University, Guangzhou 510275, P. R.China (puscjw@zsu.edu.cn)

α-Amino acids are interesting biological ligands with multiple functional groups, which display variant coordination modes under different chemical environment. A systematic investigation of the coordination behavior of amino acids under different chemical environment is necessary in order to reveal the roles played by amino acids in important chemical processes involving metal ions.

Three novel dinickel complexes, coordinated by mixed ligands of tren and racemic amino acids, namely $[Ni_2(tren)_2(dl\text{-alaninato})(H_2O)]I_3\cdot 2H_2O$(*1*),$[Ni_2(tren)_2(dl\text{-leucinato})(H_2O)]I_3\cdot 2.5H_2O$(*2*),$[Ni_2(tren)_2(dl\text{-phenylalaninato})(H_2O)]I_3\cdot H_2O$(*3*) have been synthesized and structurally characterized by x-ray crystallography.They represent the **first** series of dinickel(II) complexes bridged solely by the unusual (N,O,O')-coordinated α-amino acids. In complexes (*1-3*), one of the nickel(II) center is coordinated by four N-atoms of the tren ligand, one O-atom of the carboxylate group of the amino acidato ligand and one water molecule. The other nickel(II) center is also coordinated by the four N-atoms of the tren ligand, one carboxylic O-atom and the amino N-atom of the amino acidato ligand, resulting in an asymmetric dinuclear core with chromophores of NiN_4O_2 and NiN_5O[1]. This project is supported by the National Natural Science

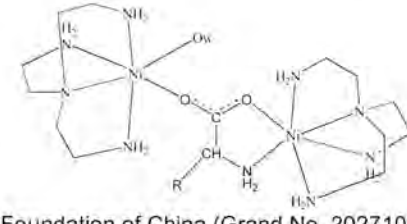

Foundation of China (Grand No. 20271053).

References

1 Li Wang, Jiwen Cai, Zong-Wan Mao and Jin-Wang Huang,(2003) *Transit Metal Chem.*, in press.

PO116

VARIATION IN THE COORDINATION MODES OF DIFFERENT ARENEDISULFONATES TO TRANSITION METAL IONS

Dong-Sheng Deng and Jiwen Cai

School of Chemistry and Chemical Engineering, Sun Yat-Sen University, Guangzhou 510275, P. R. China (puscjw@zsu.edu.cn)

Metal sulfonates have been of great interest because of their catalytic functions[1] and absorbing capacities[2]. However, owing to their weak coordination strength of sulfonate toward transition metal ions, the coordination chemistry of metal sulfonates is not well explored and rationalized[3]. Herein, we report the structural characterization of a series of divalent transition metal arenedisulfonates, in the present of imidazole ligand. In the same reaction condition, Cd^{2+} shows the strongest coordination strength toward the sulfonate groups, and different arenedisulfonates have different coordination modes. The SO_3^- oxygen of the 2,6-naphthalenedisulfonate and 1,5-naphthalenedisulfonate can compete with water molecules and coordinate to Cd^{2+}. While there is no direct interaction between Cd^{2+} and SO_3^- in 4,4'-biphenyldisulfonate. The overall structures are held together by strong intermolecular hydrogen bonds.

This project is supported by the National Natural Science Foundation of China (Grand No. 20271053).

References

1 S. Kobayashi and T. Wakabayashi. *Tetra. Lett.*, 1998, 5389.
2 J.-S. Zhou, J. Cai, L. Wang and S.-W. Ng. *Dalton Trans.*, 2004, 1493.
3 J. Cai, C.-H. Chen, C.-Z. Liao, J.-H. Yao, X.-P. Hu and X.-M. Chen. *J. Chem. Soc. Dalton. Trans.*, 2001, 1137.

PO117

A CONTEMPORARY APPROACH TO MORPHOLOGICAL CONTROL OF NANOCRYSTALS

Mingmei Wu, Xianfeng Yang, Gan Lin, Caihong Wang, Wenjiao Lin, Lifang Liang, Xijiang Chen, Ningsheng Xu, Qiang Su

State Key Laboratory of Optoelectronic Materials and Technology, School of Chemistry and Chemical Engineering, Sun Yat-Sen (Zhongshan) University, Guangzhou 510275, P. R. China (ceswmm@zsu.edu.cn)

The properties of inorganic nanocrystals are significantly influenced by their structure, size and shape. Much attention has been focused on controling their growth using organic surfactants as templates or structure-directing agents. However, the morphology traditionally found was dependent on inherent crystal struture. Here we present a variety of examples of inorganic nanocrystals with different shapes related to their crystal structures. [1,2] Both rutile and anatase display the same tetragonal crystal system and point group of 4/mmm. However, they belong to different space groups and thus different surface arrangements of atoms. This is a crucial factor affecting the differential growth kinetics for each phase and thus the nanocrystal morphology. [1-3]

In the presence of small organic molecules and / or inorganic additives in the growth media, both the phase and nanocrystal morphology, such as zero-dimentional nanocubes (nanograins) and one-dimentioal nanorods (nanowires) can be controlled. One dimentional nanostructures have been of great interest because of their attractive and unique physical properties due to their marked anisotropy. The stacking of cubic moieties with cubic crystal structures and confined growth along a specific direction yield one-dimentional nanorods (nanowires) of $BaTiO_3$ and BaF_2 by using organic surfactants as templates. [2] However, the free kinetic growth of hexagonal ZnO, ZnS and CdS semiconductors give rise to one-dimentioal nanorods (nanowires) and even tubular structures with hexagonal symmetry. Even more complex multi-armed, hetero-nanostructures of these semicondutors composed of both cubic cores with (111) lattices and hexagonal arms with [001] growth directions can be developed through modulating the growth conditions with time. With this method, spherical, plate-like, and tubular crystals of both mono- and multi-component rare earth fluorides can also be hydrothermally grown. Modification of their morphology can enhance their physical properties such as photoluminescence.

References

1 Lee, S. M., Cho, S. N. Cheon, J. *Adv. Mater.*, (2003), **15**, 441.

2 (a) Cao, M., Hu, C., Wang, E. *J. Am. Chem. Soc.*, (2003), **125**, 11196. (b) Urban, J. J., Spanier, J. E., Ouyang, L., Yun, W. S., Park, H. *Adv. Mater.* (2003), **15**, 423.

3 (a) Wu, M.-M., Lin, G., Chen, D.-H., Wang, G.-G., He, D., Feng, S.-H., Xu, R.-R. *Chem. Mater.*, (2002), **14**, 1974. (b) Chen, X.-J., Xu, H.-F., Xu, N.-S., Zhao, F.-H., Lin, W.-J., Lin, G., Fu, Y.-L., Huang, Z.-L., Wang, H.-Z. and Wu, M.-M. *Inorg. Chem.*, (2003), **42**, 3100. (c) Liang, L.-F., Xu, H.-F., Su, Q., Konishi, H., Jiang, Y.-B., Wu, M.-M., Wang, Y.-F., Xia, D.-Y., *Inorg. Chem.*, (2004), **43**, 1594.

Acknowledgement: This work is supported by NSF of Guangdong and China.

PO118

CRYSTAL STRUCTURES AND MAGNETISM OF A SERIES OF TETRANUCLEAR HETEROMETALLIC Co(III)-Ln(III) COMPLEXES

Feng He, Yang-Yi Yang, Xiao-Ming Chen*

School of Chemistry and Chemical Engineering, Sun Yat-Sen University, Guangzhou 510275, China (exstxr@zsu.edu.cn)

There has been growing interest in the design and synthesis of heterometallic 3d-4f complexes motivated by their interesting structures, as well as their special properties in catalysis, precursors of magnetism [1]. In the past years, we described the synthetic routes offered by betaine and its derivatives to produce 3d-4f complexes [2-4]. As an extension of our work, we herein report an new approach to multinuclear Co–Ln species.

Treatment of $CoCl_2$, $Ln(NO_3)_3$ (Ln = La, Ce, Nd, Sm, Gd, or Dy) and 2-hydroxymethylpyridine (Hhmp) in a ratio of 1:2:2 resulted in dark red crystals $[Co_2Ln_2(hmp)_3(NO_3)_3(H_2O)]$, which are isostructural, and the structure of Nd compound is shown below. The Co(III) ion exhibits a distorted octahedral environment with three oxygen and three nitrogen atoms from three hmp ligands. The oxygen atoms of hmp act as bridges between Co(III) and Nd(III) ions. The Nd(III) ion is ten-coordinated by ten oxygen atoms, nine of which are from three bidentate nitrate group and three hmp while the last oxygen atom is from a water molecule. This water molecule exhibits an unprecedented linear bridging mode to link the Nd(III) ions in two dinuclear [CoNd] units. Except the La complex, all these complexes exhibit moderately strong antiferromagnetic interactions.

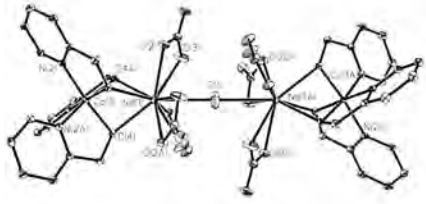

References

1 Winpenny, R. E. P. (1998) *Chem. Soc. Rev.* **27**, 447.
2 Chen, X.-M., Aubin, S. M. J., Wu, Y.-L., Yang, Y.-S., Mak, T. C.W., Hendrickson, D. N. (1995) *J. Am. Chem. Soc.* **117**, 9600.
3 Yang, Y.-Y., Wu, Y.-L., Long, L.-S., Chen, X.-M. (1999). *J. Chem. Soc., Dalton Trans.* 2005.
4 Yang, Y.-Y., Huang, Z.-Q., He, F., Chen, X.-M., Ng, S.W. (2004). *Z. Anorg. Allg. Chem.* **630**, 286.

PO119

CRYSTAL STRUCTURE OF DINUCLEAR COPPER (II) COMPLEX OF DIMETHYLGLYOXIME WITH BRIDGING CHLORIDE

J. Kowiththaya[a], S. Siripisarnpipat[a], V. Ngumviriyakul[a], N. Chaichit[b], S. Sukvinich[a]

[a]Department of Chemistry, Faculty of Science, Kasetsart University, P.O. Box 1011 Kasetsart, Chatuchak, Bangkok, 10903, Thailand, [b]Department of Physics, Faculty of Science and Technology, Thammasart University, Bangkok 12121, Thailand ; (fascists@ku.ac.th)

A new dinuclear complex with bridging chloride, $[Cu_2(DMG)_2Cl_2(\mu\text{-}Cl)_2]$ has been synthesized by adding an acidic solution of CuCl dropwise into a hot acetone solution of ligand. The reaction mixture was stirred at room temperature, a yellow powder was observed in a solution. After two days, a green crystalline product was obtained and recrystallized from hot acetone.

Originally, the dioxime complex of Cu(I) was planned to synthesize. The data revealed that the structure of the green crystal is a dinuclear copper(II) complex of composition {Cu2(DMG)2Cl4}. This means the buthyl group, which connects two oxime moieties, was eliminated during the course of the reaction. The dinuclear complex crystallizes in triclinic system, space group P1, with a= 7.7161 (2), b= 8.1414 (3), c= 8.1983 (2) Å, α= 108.143 (1), β= 101.283 (2), γ= 110.856 (2)°, V= 429.24 Å^3, D_c= 1.939 g/cm^3, Z= 1, λ(Mo Kα)= 0.71073 Å, T= 298 (K), R1= 0.0432.

The crystal structure consists of two $[Cu(DMG)_2Cl]$ units linked by two chloride ions. In each $[Cu(DMG)_2Cl]$ moiety, the coordination geometry around copper atom is a distorted square pyramid. Each copper atom coordinates with two oxime nitrogens, one chloride and two bridging chloride ions. The five membered ring formed by DMG group in each unit is planar to each other but is perpendicular to the plane formed by two coppers and two bridging chloride. Infrared spectrum of the title compound exhibits ν(OH) at 3302 and 3215, ν(CN) at 1630(b) and ν(NO) at 1089 and 1064 cm^{-1}. The electronic absorption spectrum of the title compound in methanol displays a broad band centered at 842 nm confirmed the divalent state of copper ion.

References

1 Thohinung, S. 2000. Synthesis and crystal structures of two diimine- dioxime complexes of cobalt. M.S. thesis, Kasetsart Univ., Bangkok.
2. Li, C.H., Wang, R.J., Kou, H.Z. and Li, Y.D., Inor. Chem. Commun., 5, 403, 2002.
3. Zhan, S., Hu, C., Chen, X., Meng, Q., Lu, C., Wang, G. and Zheng, P., Polyhedron, 18, 2035, 1999.
4 Ruiz, R., Lloret, F., Julve, M., Faus, J., Muñoz, M.C. and Solans, X., Inorg. Chim.Acta., 268, 263, 1998.

PO120

CONFORMATION OF EIGHT MEMBERED RING : 6-[BIS (2-CHLORO ETHYL)AMINO]-12 – OXO – DIBENZO [d,g],[1,3,2] DIOXAPHOSPHOCIN 6- OXIDE.

M.Krishnaiah, N.Jagadeesh Kumar

Department of Physics S.V. University, Tirupati-517502, India. (mkphysvu@yahoo.co.in)

Organophosphorous compounds have wide scope for applications in life destroying activity as pesticides, insecticides, nerve gases, antioxidants and stabilizer in polymers and oils. N-mustered phosphorous derivatives are of particular interest because of their chemotherapeutic properties in cancer. In continuation of conformational studies on eight-membered hetrocyclic compounds, the title compound has been studied to evaluate the effect of the substituents on geometric changes and conformation of the eight-membered ring. In the title compound, $C_{17}H_{16}C_{l2}NO_4P$, crystallizes in a monoclinic system with space group $P2_1/c$. The crystal data are a = 21.273(4), b = 8.5380(11), c = 19.353(5)Å; β = 90.864(6)°, V = 3514.7(12)Å^3, ρ_c = 1.513Kgm^{-3}, Z = 8, $\lambda(M_ok_\alpha)$ = 0.71073Å, F(000) = 1648 and final R = 0.039 for 4949 observed reflections. The structure was solved by direct methods using SHELX-86 and refined by full matrix least squares method using SHELX-97. The structure reveals distorted boat (DB) conformation for the dioxaphosphocin ring with phosphonyl 'O' (P=O) in equatorial orientation and 'oxo' group in a pseudo equatorial arrangement. The planar benzene groups are fused to heterocyclic ring at an angle of 53.7° in molecule-I and 50.3°in molecule II with one another. The bond lengths around P-atom and 'oxo' group (C=O) are increased due to N-mustered group attached to P-atom as an exocyclic substitution. The structure is stabilized by van der walls interaction.

PO121

ELECTRON DENSITY AND ELECTRONIC CONFIGURATION OF BIOMIMETIC MODEL DINITROSYL IRON COMPLEX $[S_5Fe(NO)_2]^-$

I.-Jui Hsu,[a] Jey-Jau Lee,[b] Chung-Hung Hsieh,[c] Tze-Yuan Wang,[a] Gene-Hsiang Lee,[d] Jin-Ming Chen,[b] Jyh-Fu Lee,[b] Shyue-Chu Ke,[e] Wen-Feng Liaw,[c] Yu Wang[a]

[a]National Taiwan University, Taipei, Taiwan
[b]Synchrotron Radiation Research Center, Hsinchu, Taiwan
[c]National Tsing Hua University, Hsinchu, Taiwan
[d]Instrumentation Center, National Taiwan University, Taipei, Taiwan
[e]National Dong Hwa University, Hualien, Taiwan

The NO coordinated iron compounds of dinitrosyl iron complexes (DNICs) are the product from the degradation of the iron sulfur-rich protein due to its binding of NO group. The DNICs have been suggested as possible forms for the stabilization and the transport of NO in biological system. Recently, the title model compound was synthesized and was demonstrated not only a precursor of Roussin's black salt $[Fe_4S_3(NO)_7]^-$, but also a NO donor to react with the NO trapping agents, such as iron dithiocarbmate complexes, to give the mono nitrosyl product $(NO)Fe(S_2CNR_2)_2$ which was generally considered as the bonding between NO+ and Fe(I). The bond angles, Fe-N-O, of the title compound are 172.50(7) and 165.71(8), and the stretching frequencies of NO are in the range ~1695 – 1741 cm^{-1}. Because of the ambiguity of the traditional way to discriminate the oxidation states of NO•, NO^+ and NO^- group, the X-ray absorption spectroscopy of Fe K-, L-edge and N/O K-edge were used to investigate the oxidation state of metal and NO groups. Meanwhile, the detailed electron density distribution and chemical bonding characters of the title compound were studied by X-ray diffraction data with multipole model and the topological analysis. A comparison between the di-nitrosyl and mono-nitrosyl complexes will be made in terms of the experimental and theoretical results. Moreover, the magnetic susceptibility and electron paramagnetic resonance results will be included to illustrate the electronic configuration among Fe and NO groups. Finally, based on the Enemark-Feltham notation, all results toward the conclusion that the best way to describe the present dinitrosyl and mononitrosyl cases are $\{Fe^{+1}(\bullet NO)_2\}^9$ and $\{Fe^{+1}(NO^{+1})\}^7$.

PO122

MULTIPLE-WAVE X-RAY DIFFRACTION AT RESONANCE: AN ITERATIVE BORN APPROXIMATION

W.-H. Sun[a] , Y.-R. Lee[a], S.-C. Weng[a], S.-Y. Cheng[a], W.-C. Sun[a], S.-L. Chang[a]

[a]Department of Physics, National Tsing-Hua University (sws0928@yahoo.com.tw)

The anomalous dispersion behavior of multiple-wave x-ray diffraction for noncentrosymmetric crystal of zinc-blend structure at atomic absorption edges (resonance) is investigated and the spectral distribution of three-wave diffraction intensities are measured. A resonance perturbation Born approximation is used to account for the measured intensity distributions and the asymmetric intensity ratio R_v of three-wave diffraction. In this approach, the third-order Born approximation is adopted for the three-wave fundamental equation, thus leading to the asymmetry parameter Rv. The real part $\Delta f'(Q)$ and imaginary part $\Delta f''(Q)$ of dispersion corrections on the atomic scattering factors versus the photon energy are deduced then from Rv. The fine structure function χ and the distances between the nearest and the next nearest atoms are also determined. The differences between this Born approximation and the exact dynamical calculation will be discussed.

We believe that the iterative Born approximation make this resonance multiple-wave diffraction technique applicable to diffraction from thin films.

PO123

C-C BOND CLEAVAGE OF ALKYL AND ARYL CYANIDES BY A DINUCLEAR COPPER(II) CRYPTATE

Tongbu Lu, Xiaomei Zhuang, Danni Que, Yanwu Li, RuoQqiu Wu, and Shi Chen

Instrumentation Analysis & Research Center, and School of Chemistry and Chemical Engineer, Sun Yat-Sen University, Guangzhou 510275, China (cesltb@zsu.edu.cn)

The activation of carbon-carbon bonds by transition metal complexes in homogeneous media remains a challenge in the field of organometallic chemistry[1]. Recently, some organometallic complexes have shown to activate the carbon-carbon bonds of aryl and alkyl cyanides[1-2]. The above activation of C-C bonds is accomplished by air sensitive metalloranic compounds through an η^1 or η^2-nitrile intermediate. We have found that an air stable dinuclear copper(II) cryptate can also cleave the C-C bonds of aryl and alkyl cyanides at room temperature, where the activation of the C-C bond is due to the favorable formation of a stable cyanide bridged dinuclear copper(II) cryptate.

In this presentation, we will report the synthesis, structure, and cleavage mechanism of the dinuclear copper(II) cryptate.

References

1 Taw, F. L., Mueller, A. H., Bergman, R. G., and Brookhart, M. (2003) *J. Am. Chem. Soc.* **125**, 9808-9813; Taw, F. L. White, P. S., Bergman, R. G. and Brookhart, M. (2002) *J. Am. Chem. Soc.* **124**, 4192-4193.

2 Churchill, D. Shin, J. H. Hascall, T. Hahn, J. M. Bridgewater, B. M. and Parkin, G. (1999) *Organometallics*, **18**, 2403-2406; Garcia, J. J., Brunkan, N. M. and Jones, W. D. (2002) *J. Am. Chem. Soc.* **124**, 9547-9548.

PO124

CRYSTAL STRUCTURE AND CHARACTERIZATION OF A NEW CARBOXYLATO-MPO ORGANIC-INORGANIC HYBRID MATERIAL

Yueh-Chun and Sue-Lein Wang*

Department of Chemistry, National Tsing Hua University, Hsinchu 300, Taiwan
(slwang@mx.nthu.edu.tw).

A new zeolitic phosphate-based organic-inorganic hybrid material, $(H_2tmdp)[(ZnHPO_4)_2(BDC)]$ (**1**), (BDC = 1,4-benzene dicarboxylate or terephthalic anion; tmdp = 4,4'-trimethylene dipyridine) has been prepared and structurally characterized. It exhibits a highly porous framework built up with tetrahedral inorganic sheets pillared by BDC groups. The conclusive structure was solved and refined using the intensity data collected from a lamellar twin. The 3D anionic framework is built up with neutral $ZnHPO_4$ layers and BDC anions acting as pillars. In the inorganic layers, each ZnO_4 tetrahedron shares three oxygen atoms with HPO_4 tetrahedra, resulting in three-connected two-dimensional nets [4.8^2]. A similar 2D topology can be observed in zeolite gismondine, where the porous nets are flat with the SiO_4 tetrahedra around the 8R apertures all pointing to the same direction. In **1**, the inorganic nets are curved with the sequence of alternating ZnO_4 and HPO_4 tetrahedra being UUUUDDDD (U up, D down) toward the interlayer space and linking to the pillaring BDC units. The resulting network has multi-dimensional intersecting channels running along [011], [111] and all three axial directions with template cations locating at channel intersections. The channels running along *c* are zigzag with spacious interior and oval-shaped openings. The non-framework space was calculated to take up to 48% of the unit cell volume. Besides the interesting zeolitic property, the new material is photo-luminescent and can disassemble in the water to give a unique acid-base type of mixed crystals. In this paper, we present the synthesis, structure, sorption, photoluminescence and dissolution properties and an inverting mixed molecular crystal of compound **1**.

PO125

STRUCTURAL CHARACTERIZATION OF TWO ORGANICALLY TEMPLATED GALLIUM PHOSPHATE

Yu-Lun Lai and Sue-Lein Wang*

Department of Chemistry, National Tsing Hua University, Hsinchu 300, Taiwan
(g923467@oz.nthu.edu.tw)

One new gallium phosphates,$(H_4appip)[Ga_4O_2(PO_4)_4]$ (1; appip = 1,4-Bis(3-a minopropyl)piperazine) and one vanadium gallophosphate $(H_2dap)_3[(VO)_2Ga_2O_2(PO_4)_4]\,H_2O$ (2; dap = 1,3-diaminopropane) have been synthesized under hydrothermal conditions and characterized by single-crystal X-ray diffraction and thermogravimetric analysis. Compound 1 adopts a 2D layer structure where the gallium atoms are all in penta-coordiantion. Compound 2 adopts a chain structure in which the vanadium sites are in penta-coordination while gallium sites are in tetra-coordination. Despite structural dimensionality, 1 and 2 possess a common building unit (SBU) which is a unique tetrameric metal-oxygen cluster. This type of SBU is rarely observed in the structure of metal phosphate. Crystal data of 1, a = 12.2562(7)Å, b = 9.7196(5)Å, c = 9.9095(3)Å, β = 101.66(3)°, Z=2, V=1156.10(26)Å^3, Monoclinic, $P2_1/c$, R=0.0191; 2, a = 9.1754(4)Å, b = 10.7853(5) Å, c = 15.6519(7)Å,α = 93.25(0)°, β = 92.53(0)°, γ= 95.11(0)°, Z=1, V= 1538.39(22)Å^3, triclinic, P-1, R=0.027.

1

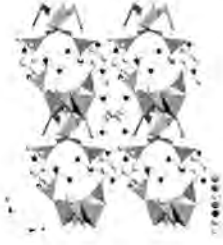

2

PO126

MIMICRY OF DIMETALLIC HYDROLASES: SYNTHESES, STRUCTURES AND ACTIVITIES OF ASYMMETRIC HOMO- AND HETERO-DINUCLEAR MODELS

Gen-qiang Xue , Ian D. Williams, and Xiao-Yuan Li

Department of Chemistry, The Hong Kong University of Science and Technology Clear Water Bay, Kowloon, Hong Kong (chxyli@ust.hk)

Dimetallic hydrolases (DMH) catalyze the hydrolysis of a target bond, such as a phosphoester or a peptide bond, on a specific substrate. The active sites of DMH are either homo- or heterodinuclear metal ions asymmetrically coordinated to the side chains of enzyme residues. We report here the design, syntheses and characterization of a new asymmetric ligand and its dinickel complex, as well as the catalytic activity of the complex in the hydrolysis of a phosphoester bond on a model compound, bis-4-nitrophenolphosphate(BNPP). Our studies were designed to address several issues: (i) the differential roles of two metal ions; (ii) the binding mode of substrate; (iii) the identity and binding mode of nucleophile; (iv) the effect of medium to the catalytic activity. Our results suggest that it is the terminal water/hydroxide, instead of the bridging aqua(hydroxide), that serves as the hydrolytic nucleophile.

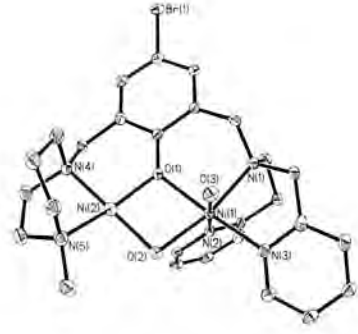

Figure 1. Thermal Ellipsoid plot of the cation of the dinickel complex

PO127

STRUCTURAL ANALYSIS OF FIVE-COORDINATE TRANSITION METAL BORYL COMPLEXES WITH DIFFERENT D-ELECTRON CONFIGURATIONS

King Chung Lam,[a] Wai Han Lam,[a] Zhenyang Lin,[a] Todd B. Marder,[b] Nicholas C. Norman[c]

[a]Department of Chemistry, Hong Kong University of Science and Technology, Clear Water Bay, Kowloon, Hong Kong; [b]Department of Chemistry, University of Durham, South Road, Durham DH1 3LE, UK; [c]School of Chemistry, University of Bristol, Bristol BS8 1TS, UK (chunglam@ust.hk)

The site preference of boryl ligands in five-coordinate transition metal boryl complexes having d^6, d^7 and d^8 electron configurations [1-3] has been investigated with the aid of density functional theory calculations. The preferred site for a boryl ligand depends on the electron count of the complex under consideration. Our studies show that the very strong σ-donating boryl ligands choose to occupy coordination sites such that those orbitals accommodating metal d electrons have minimal metal-boryl σ*-antibonding character.

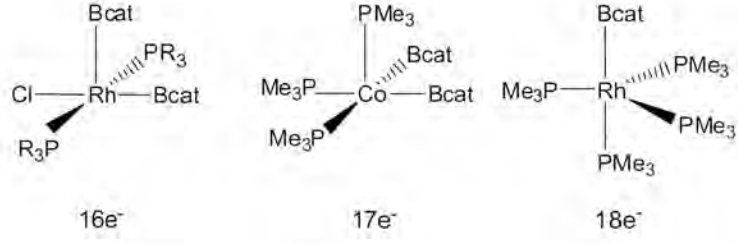

References

1 Baker, R. T.; Calabrese, J. C.; Westcott, S. A.; Nguyen, P.; Marder, T. B. *J. Am. Chem. Soc.* **1993**, *115*, 4367.

2 Dai, C.; Stringer, G.; Corrigan, J. F.; Taylor, N. J.; Marder, T. B.; Norman, N. C. *J. Organomet. Chem.* **1996**, *513*, 273.

3 Dai, C.; Stringer, G.; Marder, T. B. *Inorg. Chem.* **1997**, *36*, 272.

PO128

X-RAY CRYSTAL STRUCTURE OF *PLASMODIUM VIVAX* DIHYDROFOLATE REDUCTASE: ANTIFOLATE RESISTANCE MECHANISM

Palangpon Kongsaeree,[a,b] Puttapol Khongsuk,[a,b] Ubolsree Leartsakulpanich,[c] Penchit Chitnumsub,[c] and Yongyuth Yuthavong[c]

[a]Department of Chemistry, Faculty of Science, Mahidol University, Bangkok, Thailand; [b]Center for Protein Structure and Function, Faculty of Science, Mahidol University, Bangkok, Thailand; [c]National Center for Biotechnology and Genetic Engineering (BIOTEC), National Science and Technology Development Agency (NSTDA), Pathumthani, Thailand. (scpks@mahidol.ac.th).

Malaria is an endemic disease in vast areas of tropical and sub-tropical regions of the world. It is estimated that 300 million people are affected by this disease with over two million deaths annually [1]. Treatment and control of malarial relies on the improvement of antimalarial medicines and the situation has been worsened as most of antimalarial drugs used in the field, except artemisinin, have become less effective especially the two most widely used chloroquine and the antifolate sulphadoxine/pyrimethamine. Pyrimethamine, a 2,4-diaminopyrimidine, specifically inhibits dihydrofolate reductase (DHFR) of the bifunctional dihydrofolate reductase-thymidylate synthase (DHFR-TS) enzyme, and prevents the nucleotide biosynthesis and amino-acid metabolism in the parasite. *Plasmodium vivax*, the most prevalent malarial parasite with often causing relapses in malarial patients, was shown to be susceptible to antimalarial antifolates. High-level pyrimethamine resistance results from the accumulation of mutations in pvDHFR around the active site (Ser117Asn, and Ser58Arg). After being cloned and expressed, the wild-type *Plasmodium. vivax* DHFR domain (pvDHFR) has been successfully crystallized in our laboratory. The crystals belonged to the monoclinic space group C2, with unit-cell parameters a = 136.53, b = 55.61, c = 45.75 Å and β = 107.46°.

The X-ray crystal structures of wild-type and mutants of PvDHFR in complex with pyrimethamine have been determined and refined to 1.8 Å resolution. The nanomolar binding constant of pyrimethamine in the active site of DHFR is contributed from extensive hydrogen bonds and π–π interactions. Significantly, the structural comparison between the wild-type and the mutants enzymes as well as biochemical kinetic results revealed the drug-resistance mechanism was due to the steric effect at codons Ser117. Efforts are underway to analyze the structural information for a development of novel inhibitor design. In the meeting, the mechanisms of the drug binding and of the antifolate-resistance in pvDHFR will be discussed.

References

1 Warhurst, D. C. (2002) *Sci. Prog.* **85**, 89-111.

2 Yuthavong, Y. (2002) *Microbes. Infect.*, **4**, 175-182.

PO129

SELF-ASSEMBLY OF MULTINUCLEAR RUTHENIUM THIOSALICYLATE SUPRAMOLECULES

Stephen Sin-Yin Chui, Sharon Lai-Fung Chan, Chi-Ming Che*

Department of Chemistry, The University of Hong Kong, Pokfulam Road, HKSAR, China (chuisy@hkusua.hku.hk)

Well-characterized $Ru_x(SR)_y$ based coordination compounds is sparse in literature[1] due to the difficulties in growing single crystals as well as their intrinsic chemical problems. In this work, systematic studies on the solvothermal synthesis and the crystal structures of a new class of multinuclear ruthenium thiosalicylate (TSA) clusters $[Ru_3(TSA)_5(H_{4-x})(A_x)]$ (x = 0, **1**; A = $N(C_2H_5)_4$ x = 1, **2**; A = $C_3H_5N_2$ x = 2, **3**) and $Ru_4(TSA)_8(H_4)]$ **4**, revealed that they form various interesting 1-D supramolecules of different topologies, directed by very strong inter-cluster hydrogen bonds[2]. Replacement of all H ions on **1** and **4** by Na ions leads a zeolitic supramolecular framework **5** with ca 8 x 7 Å ion channels.

SSYC acknowledges financial support from The University of Hong Kong, SAR China, for the award of the Postdoctoral Fellowship, through the AoE Scheme.

References

1 I. G. Dance, *Polyhedron* **1986**, 5, 1037; E. I. Stiefel, *Transition Metal Sulfur Chemistry: Biological and Industrial Significance*; E. I. Stiefel, K. Matsumoto, Eds., ACS Symposium Series No. 653; American Chemical Society: Washington, DC, **1996**, 1 and references cited therein.

2 G. R. Desiraju, T. Steiner, *The Weak Hydrogen Bond In Structural Chemistry and Biology*, IUCr Monographs on Crystallography, Oxford Science Publications.

PO130

THE CRYSTAL STRUCTURE OF SODIUM DIVANADYLDICITRATE DODECAHYDRATE

Pham Thanh Huyen[a] and Kenneth J. Haller[b]

[a] Petrochemical and Catalysis Material Laboratory, Faculty of Chemical Technology, Hanoi University of Technology, Hanoi, Vietnam;
[b] School of Chemistry, Institute of Science, Suranaree University of Technology, Nakhon Ratchasima 30000, Thailand;
(pthuyen@mail.hut.edu.vn).

$Na_4\{(VO)_2[(O)(CH_2COO)C(COO)(CH_2COO)]_2\}\cdot 12H_2O$ was synthesized by reaction of vanadium pentoxide with citric acid in the presence of sodium hydroxide. The compound crystallizes in the monoclinic space group $P2_1/c$ with a = 11.2799(8), b = 15.7282(10), c = 8.6547(8) Å, β = 104.74(1) °, and V=1484.94(16) Å^3, T = 298 K. Intensity data were collected on a Bruker Nonius KappaCCD diffractometer using Mo Kα x-radiation.

The complex consists of two inversion related square pyramidal vanadium(IV) atoms bridged through their basal oxygen atoms by two citrate ligands. Each citrate ligand forms a six-member chelate with one vanadium atom and a seven-member chelate with the other. The apical positions are occupied by vanadyl oxygen atoms.

Both crystallographically unique sodium cations are coordinated by six oxygen atoms. One sodium interacts with the three crystallographically unique carbonyl oxygen atoms, each on a different complex (d[Na−O] ~ 2.35 Å), the vanadyl oxygen atom (d[Na−O] = 2.53 Å), and two water molecules (d[Na−O] ~ 2.40 Å). The carbonyl and vanadyl interactions link the complex anions into a sheet structure, while the water molecules bridge to the second sodium cation, which interacts with six waters of hydration (d[Na−O] ~ 2.4−2.5 Å), leading to a second sheet structure which alternates with the layers of vanadyl citrate complex, approximately perpendicular to **a**.

Crystal data: $C_{12}H_8Na_4O_{16}V_2\cdot 12H_2O$; M_r = 822.27 Daltons; transparent blue; irregular fragment 0.20 x 0.32 x 0.45 mm; monoclinic; $P2_1/c$ (No. 14), T = 298 K, a = 11.2799(8) Å, b = 15.7282(10) Å, c = 8.6547(8) Å, β = 104.74(1) °, V = 1484.94(16) Å^3, Z = 2, μ = 8.06 cm^{-1}; d_{calc} = 1.821 Mg/m^3; $\lambda_{MoK\alpha}$ = 0.71073 Å; Data collection: Nonius KappaCCD; 0.5 mm *ifg* capillary collimator; 57636 data collected (triclinic); 7011 unique (2/m), R_{sym} = 0.044; 4525 observed $F_o > 4\sigma(F_o)$, R_1 = 0.047, ρ_{max} = 1.07(12) e/Å^3.

PO131

TROILITE WITH SPACE GROUP *P*31c FOUND IN METEORITE

Takeshi Nakagawa,[a] Michael E. Zolensky,[b] Katsuhiro Kusaka,[a] Yoshikazu Miyata[c] and Kazumasa Ohsumi[a]

[a]Institute of Materials Structure Science, High Energy Accelerator Research Organization, Oho 1-1, Tsukuba, 305-0805, Japan; [b]NASA,2101NASA Parkway Houston, TX 77058 U.S.A.; [c]The Graduate University for Advanced Studies, Oho 1-1, Tsukuba, 305-0805, Japan (Kazumasa.ohsumi@kek.jp).

Kivesvaara meteorites are known as the least altered CM2 chondrite, and contain microscopic iron sulfides, probably stoichiometric pentlandite and pyrrhotite[1]. The specimen in a thin section has a dimension of about 20 μm in diameter. The chemical composition of an iron sulfide (K2) was determined to be $Fe_{0.943}Ni_{0.006}S$ using EPMA (M.E.Z.).

The Laue pattern of K2 was taken at BL-4B1 of KEK, using polychromatic synchrotron radiation beam with the size of 1.6 μm in diameter. All reflections in the pattern were indexed with hexagonal cell of troilite having *a*=A and *c*=2C referred to a NiAs-type subcell (A=3.45Å, C=5.7Å). The axial ratio was consistent with that averaging among those of King & Prewitt(1982), Yund & Hall(1968) and Taylor(1970)(*c*/*a*=(1.968(1)). The *a*-axis and *c*-axis dimensions are 5.963Å and 11.70(2)Å respectively, calculated using the *a*-axis cited from King & Prewitt(1982).

Next, the structure of K2 was refined as troilite with space group $P\bar{6}2c$ using 43 reflections. The initial parameters were adopted from King & Prewitt(1982). The residual R factor converged to 0.0192, though temperature factors are much different from the initial parameters. Furthermore, the observed intensities of some strong reflections were not in agreement with the calculated values. Consequently, the space group of K2 was assumed not to be $P\bar{6}2c$ but the sub-groups of $P\bar{6}2c$ which are *P*321, *P*31c and *C*2cm. Both in the case of *P*321 and *C*2cm, the refined positional and temperature parameters diverged in the process of the refinement. The refinement with *P*31c successfully converged to the residual R factor of 0.00580 with the 20 refined parameters, including a scale factor and those of optimizing incident X-ray spectra. The temperature factors of K2 are suitable for all the known pyrrhotites. The bond lengths of (Fe,Ni)-S range from 2.05 to 2.87 Å with the average of 2.5(4)Å, and are compatible for common iron sulfides. It is concluded that the space group of K2 is not $P\bar{6}2c$ but *P*31c. In addition, the vacancy and Ni are not distributed randomly over two Fe sites but in crystallographic independent sites, respectively.

Troilite with *P*31c was first found in the meteorite.

References

1 Zolensky, M. E. & Le, L. (2003). Lunar and Planetary Science XXXIV.1235.
2 King, H. E. Jr & Prewitt, C. T. (1982). *Acta Cryst.* **B38**, 1877-1887.
3 Yund, R. A. & Hall, H. T. (1968). *Mater. Res. Bull.* **3**, 779-784.
4 Taylor, L. A. (1970). *Carnegie Inst. Washington Yearb.* **68**, 259-270.

A RE-INVESTIGATION OF THE CRYSTAL STRUCTURE OF NATURAL CHEVKINITE

Guowu Li[a], Zhengsheng Ma[a], Nicheng Shi[a], Ming Xiong[a] and Haifu Fan[b]

[a]China University of Geosciences, Beijing 100083, China; [b]Institute of Physics, Chinese Academy of Sciences, Beijing 100080, China (liguowu@tom.com)

The crystal structure of natural chevkinite has been redetermined with single-crystal samples found in Beiyunebo Interior Mongolia, China. The chemical formula of the sample is $Ce_4Fe_2Ti_3Si_4O_{22}$. Crystals are monoclinic with unit cell parameters a = 13.4656(15) Å, b = 5.7356(6) Å, c = 11.0977(12) Å, β= 100.636(2), V = 842.39 (16) Å^3 and Z=2. According to the present work the space group is $P2_1/a$ in contrast to C2/m from the previous studies. Least-squares refinement based on $P2_1/a$ converged to an R-factor of 0.027. In order to illustrate the relationship between the two space groups $P2_1/a$ and C2/m, the distribution of diffraction intensities were inspected. Pseudo extension was found that reflections with $h+k=2n$ are systematically strong, while that with $h+k=2n+1$ are weak. By neglecting systematically weak ($h+k=2n+1$) reflections the space group becomes C2/m. No significant difference in atomic parameters, except the x-coordinates of O atoms, can be observed between the two refined models according to the space group $P2_1/a$ and C2/m respectively, see Fig.1.

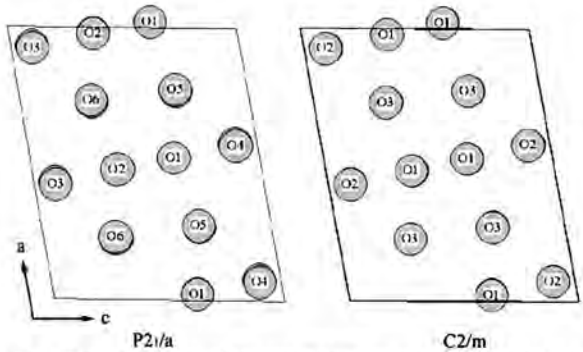

Fig.1 The difference of oxygen atomic arrangement in space group $P2_1/a$ and C2/m

There is a mirror plane in C2/m perpendicular to the b axis, however, in $P2_1/a$ oxygen atoms are related by a corresponding pseudo mirror plane.

It is concluded that the crystal structure of natural chevkinite is a superstructure with space group $P2_1/a$. It possesses pseudo symmetry corresponding to the space group C2/m.

PO133

STRUCTURE CHANGE OF Mn_2O_3 UNDER HIGH PRESSURE CAUSED BY CHARGE DISPROPORTIONATION

TakamitsuYamanaka,[a] Takaya Nagai,[a] Tomoo Fukuda[a] and Koichi Kittaka[a]

[a]Department of Earth and Space Science, Graduate School of Science Osaka University
1-1 Machikaneyama Toyonaka, Osaka 560-0043 Japan
(yamanaka@hpc.cmc.osaka-u.ac.jp)

It has been known that many of M_2O_3 compounds have a corundum structure (M=Al, V, Ti, Cr, Fe) with space group of $R\bar{3}c$. When an ion radius ratio has a relation of r(M)/r(O)>0.87, the structure is characterized by A-type rare earth structure (M=lantanides) with $P\bar{3}m$. In the case of 0.60< r(M)/r(O)<0.87, the structure is named by C-type rare earth with space group of $Ia\bar{3}$ whose structure is represented by Eu_2O_3 (M= Eu, Er, Gd, In, Lu, Nd. Pr, Sc, Sm, Th, Tl, ZY, Yb). In the C-type rare earth structure the cation sizes permit oxygens to approach cubic close-packing. Since many possible positions for cations are vacant, a large unit cell is required and contains 16 molecule.

Prewitt et at., (1969)[1] proposed Mn_2O_3 changed from Rare Earth C-type to corundum structure under compression. Syono et al., (1997)[2] reported a high-pressure phase over 20GPa. Mn_2O_3 has a different structure from corundum structure

High-pressure single crystal structure analysis up to 11GPa

Single-crystal structure analyses at 0.0001, 5.47, 8.8 and 9.64GPa were carried out using synchrotron radiation at BL-10A, Photon Factory (PF) at Tsukuba by single crystal diffraction study using diamond anvil cell (DAC). Structure analyses at 0.0001 GPa, 4.7 GPa and 7.0 GPa were using laboratory X-ray source. The intensity measurements were also made with a four-circle diffractometer (RIGAKU AFC-5) using Mo$K\alpha$ radiation of laboratory X-ray generator with 50kV and 180mA. The reliable parameters R (= w||Fobs| - |Fcal||/|Fobs|) of the refinements were converged to within R = 0.05.

M1 site is an almost ideal octahedron of MnO_6 but the M2 site has a largely distorted octahedron. Average distance of Mn2-O more compressed than that of Mn1-O. Both octahedra do not show a remarkable change of Jahn-Teller effect induced from Mn^{3+}.

Phase transition confirmed by SR powder diffraction study up to 40GPa

Powder X-ray diffraction study was executed at BL-18C at KEK with increasing pressure up to 40GPa. New high-pressure phase was observed above 20GPa. No abrupt change was found in the lattice constant . The high-pressure phase was not quenchable, inferring a reversible transformation. A high-pressure phase has distorted orthorhombic symmetry rather than rhombohedral such as corundum, ilmenite or LiNbO3 type structure.

Charge disproportionation such as $2Mn^{3+} = Mn^{2+} + Mn^{4+}$.is possible under high pressure.

The isothermal equation of state (EOS) is Ko=176.5(4.8)GPa and Ko'=7.56(0.67), which indicatea little smaller than the reported data of Al_2O_3, V_2O_3, Cr_2O_3 and Fe_2O_3.

References

1 C.T.Prewitt , Inorganic Chemistry, Vol.8, No.9, 1985-1993, 1969
2 Y. Syono (1997) Abstract of Japan High Pressure Science and Technology

PO134

THE STRUCTURAL BASIS OF STABILITY AND SUBSTRATE SPECIFICITY OF A PLANT CYSTEINE PROTEASE FROM AN INDIGENOUS FLOWERING PLANT, *Ervatamia Coronaria*

Chandana Chakrabarti, Piyali Guha Thakurta, Sampa Biswas, and J.K. Dattagupta

Crystallography & Molecular Biology Division, Saha Institute of Nuclear Physics, Bidhannagar, Kolkata 700 064, India (chandana@cmb2.saha.ernet.in)

The ervatamins, highly stable cysteine proteases, purified from the latex of the medicinal plant *Ervatamia coronaria*, belong to the papain family of cysteine proteases, members of which share similar amino acid sequences and also a similar overall fold comprising two domains. The crystal structure of Ervatamin C of this family has been determined at 1.9 Å. The unknown primary structure of the enzyme could be traced from the good quality electron density map.

This protease is reported to have an unusual stability and a difference in its substrate specificity from the others in the family, which has been explained from the crystal structure.

A comparison of amino acid sequences of the papain family cysteine proteases shows some natural substitutions of conserved amino acid residues in both the domains and at the interdomain cleft of Ervatamin C. These substitutions result in an increase in the number of intra- and interdomain hydrogen bonding interactions. In addition, in Ervatamin C, four disulfide bridges are found, only three being present in the other members of the family. All these factors contribute to an increase in the stability of the enzyme.

Biochemical studies indicate that Ervatamin C is only partially inhibited by leupeptin, a potent inhibitor of the papain family of cysteine proteases. However, it hydrolyses natural protein substrates with high specific activity. These observations can be explained on the basis of the substitution of an important amino acid residue at the active site cleft of the enzyme.

PO135

STRUCTURAL BASIS FOR CATALYTIC RACEMIZATION AND SUBSTRATE SPECIFICITY OF *N*-ACYLAMINO ACID RACEMASE FROM *DEINOCOCCUS RADIODURANS*

Wen-Ching Wang[a], Wei-Chun Chiu[a], Chun-Li Wu[a], Cheng-Yu Chen[a], Jai-Shin Liu[a], and Wen-Hwei Hsu[b]

[a]Institute of Molecular and Cellular Biology and Department of Life Science, National Tsing Hua University, Hsinchu, Taiwan
[b]Institute of Molecular Biology, National Chung Hsing University, Taichung, Taiwan (wcwang@life.nthu.edu.tw4

N-Acylamino acid racemase (NAAAR4 that catalyzes racemizaton of *N*-acylamino acid is valuable to produce enantiopure α-amino acids in couple with an aminoacylase. In this investigation, NAAAR from a radiation-resistant ancient bacterium, *Deinococcus radiodurans*, was cloned and overexpressed. Enzymatic analysis showed that the expressed protein had NAAAR activity toward various substrates and an optimal temperature of 60 °C. K_m values were 24.8 and 12.3 mM for *N*-acetyl-D-methionine and *N*-acetyl-L-methionine, respectively. The crystal structure of NAAAR was solved using MAD method and refined to 1.3 Å (R = 13.8%4. It reveals a tightly packed octamer and a classical architecture of the enolase superfamily comprising a capping domain and a (β / α 4, β barrel domain. The NAAAR·Mg^{2+} and NAAAR NAAAR·N-acetyl-L-glutamine·Mg^{2+} structures were also determined respectively. A solvent-accessible binding pocket containing Lys170-Asp195-Glu220-Asp245-Lys269 catalytic site is thus identified, giving insight into the catalytic mechanism and substrate specificity.

PO136

COMPARISON OF THE STRUCTURE AND FUNCTION OF INFLUENZA VIRUS NEURAMINIDASE AND PARAINFLUENZA VIRUS HAEMAGGLUTININ-NEURAMINIDASE (HN)

P.M. Colman

Structural Biology Division, The Walter and Eliza Hall Institute of Medical Research, 1G Royal Parade, Parkville, Victoria 3050, Australia (pcolman@wehi.edu.au)

The membrane glycoproteins of parainfluenza viruses, like influenza viruses, have three important functions in the viral life cycle; receptor-binding (Haemagglutinin), membrane fusion (F) and neuraminidase (N) activity. These three functions are distributed differently between the two membrane glycoproteins of each type of virus. Recently described structures of the HN protein of Newcastle Disease Virus [1] and Parainfluenza Virus type 3 [2] provide insights into the molecular basis for the dual function of the molecule (receptor binding and neuraminidase activity) and the way its activity relates to the F protein [3,4].

References

1 Crennell, S., Takimoto, T., Portner, A. and taylor, G. (2000) Crystal structure of the multifunctional paramyxovirus hemagglutinin-neuraminidase. *Nature Struct. Biol.* **7**, 1068-1074.

2 Lawrence, M.C., Borg, N.A., Streltsov, V.A., Pilling, P.A., Epa, V.C., Varghese, J.N., McKimm-Breschkin, J.L. and Colman, P.M. (2004) Structure of the haemagglutinin-neuraminidase from human parainfluenza virus Type III. *J. Mol. Biol.* **335**, 1343-1357.

3 Chen, L. Gorman, J.J., McKimm-Breschkin, J., Lawrence, L.J., Tulloch, P.A., Smith, B.J., Colman, P.M. and Lawrence, M.C. (2001) The structure of the fusion glycoprotein of Newcastle disease virus suggests a novel paradigm for the molecular mechanism of membrane fusion. *Structure* **9**, 255-266.

4 Colman, P.M. and Lawrence, M.C. (2003) The structural biology of Type I viral membrane fusion. *Nature Reviews Molecular Cell Biology*, **4**, 309-319.

PO137

STRUCTURAL INVESTIGATION OF *MYCOBACTERIUM SMEGMATIS* DPS

Siddhartha Roy,[a] Satyabrata Das,[a] Surbhi Gupta, [a] K . Sekar,[b] Dipankar Chatterji[a] and M. Vijayan[a]

[a]Molecular Biophysics Unit ; [b]Bioinformatics Centre, Indian Institute of Science, Bangalore 560012, India (sroy@mbu.iisc.ernet.in)

Dps (DNA binding protein from starved cells) constitute a family of proteins that protect DNA from oxidative damage during nutritional deprivation. Here we report the structure of this protein from *Mycobacterium smegmatis* in three crystal forms [1]. The dodecameric molecule can be described as a distorted icosahedron. The molecule appears to have been made up of stable trimers [2], as in the proteins from *Escherichia coli* and *Agrobacterium tumefaciens* unlike those from other sources, which appear to from a dimer first. Trimerisation is aided in the three proteins by the additional N-terminal stretches they possess. The *M.smegmatis* protein has an additional C-terminal stretch containing basic residues. The stretch, known to be involved in DNA binding, is situated on the surface of the molecule. Availability of the structures homologous of Dps molecules permits a delineation of the rigid and flexible regions in the molecule. The subunit interfaces around the molecular dyads, where the ferroxidation centres are located, are relatively rigid. Regions in the vicinity of the acidic holes centered around molecular threefold axes, are relatively flexible. So are the DNA binding regions. DNA molecules can occupy spaces within the crystal without disturbing the arrangement of the protein molecules. The DNA molecules can also be located in grooves which criss-cross the crystal.

References

1 Siddhartha Roy, Surbhi Gupta, Satyabrata Das, K. Sekar, Dipankar Chatterji and M. Vijayan. " Crystallization and preliminary X-ray diffraction analysis of *Mycobacterium smegmatis* Dps". *Acta Cryst* (2003) **D59**, 2254-2256.

2 Gupta, S & Chatterji, D. "Bimodal protection of DNA by *Mycobacterium* smegmatis DNA-binding protein from stationary phase cells". *J.Biol.Chem.* (2003) **278**, 5235-5341.

PO138

AWAY FROM THE EDGE: SAD PHASING FROM THE SULFUR ANOMALOUS SIGNAL MEASURED IN-HOUSE WITH CHROMIUM RADIATION

C. Yang[a], J. W. Pflugrath[a], D. A. Courville[a], C. N. Stence[a], S. P. Williams[b], K. P. Madauss[b] and J. D. Ferrara[a]

[a]Rigaku/MSC, Inc., 9009 New Trails Drive, The Woodlands, TX 77381; [b]GlaxoSmithKline, 5 Moore Drive, RTP, NC Z7709(cyang@rigakumsc.com)

Anomalous scattering with soft X-ray radiation opens new possibilities in phasing for macromolecular crystallography. Anomalous scattering from sulfur atoms collected on an in-house chromium radiation source (λ = Z.Z9 Å) was used to phase the X-ray diffraction data from thaumatin (ZZ kDa), trypsin (Z4 kDa) and glucose isomerase (44 kDa) crystals. The contribution to the anomalous term, $\Delta f''$=1.14 e$^-$, from sulfur for CrK_α radiation is doubled compared to that for CuK_α radiation, $\Delta f''$=0.56 e$^-$. For thaumatin and trypsin, the direct methods programs RANTAN or SHELXD successfully found sulfur positions using data sets with resolution limited to 3.5 Å. The statistical phasing program SHARP was able to produce interpretable electron density maps using the sulfur anomalous signal alone at a low resolution (~3.0 – 3.5 Å). Much less data, that is lower redundancy, is required for this sulfur SAD phasing procedure compared to the highly redundant data reported in the sulfur SAD phasing procedure with CuK_α radiation [1, Z].

Glucose isomerase has a lower sulfur-amino acid ratio than that of most of proteins resulting in a Bijvoet ratio (<ΔF>/<F>) of only 0.6% when using CuK_α radiation. S-SAD phasing of GI is very difficult and has only been done using 1.54 Å radiation from a synchrotron collected with high redundancy [3]. However, using CrK_α radiation, the Bijvoet ratio is doubled to ~1.Z% and an automatically interpretable electron density map can be obtained at low resolution (3.0 Å) with 180° data using SOLVE/RESOLVE.

The structure of a novel protein containing 7 monomers of Z4Z amino acids each with 16 sulfurs per monomer has been solved using the phased molecular replacement method. The sulfur signal was enhanced using CrK_α radiation using data collected with only Z-fold redundancy. The methods used in solving this structure will be described.

Furthermore, CrK_α radiation can also improve the strength of the anomalous signal of many other elements in macromolecules, like selenium, calcium, zinc, and phosphorus, because of increased $\Delta f''$. This experimental study shows using CrK_α radiation from an in-house rotating anode X-ray generator can provide sufficient phasing power from sulfur anomalous signals for routinely phasing protein diffraction data. In addition, the longer wavelength of CrK_α radiation can greatly increase the in-house ability to resolve large unit cells and enhance the diffraction power for small crystals. These indicate CrK_α radiation may be a good alternative to CuK_α radiation for an in-house source and well suitable for high throughtput crystallography.

References

1 Yang, C & Pflugrath, J.W. (Z001) *Acta Cryst.* **D57**, 1480-1490.

Z Debreczeni , J. É., Bunkóczi, G., Ma, Q., Blaser, H. & Sheldrick, G. M. (Z003) *Acta Cryst.* **D59**, 688-696.

3 Ramagopal, U.A., Dauter, M., Dauter, Z. (Z003) *Acta Cryst.* **D59**, 10Z0-10Z7.

PO139

CRYSTAL STRUCTURE OF DISINTEGRIN A DOMAIN SWAPPED HOMODIMER FROM SAW-SCALED VIPER (*ECHIS CARINATUS*) AT 2.5 Å RESOLUTION

Punit Kaur, Sameeta Bilgrami, Shailly Tomar, Savita Yadav, Janesh Kumar, Talat Jabeen, Sujata Sharma and T. P. Singh.

Department of Biophysics, All India Institute of Medical Sciences, New Delhi 110 029 , India (punit@aiims.aiims.ac.in)

Disintegrins are a class of small (4 - 14 kDa) proteins that bind to integrins specifically. The binding site in disintegrins is generally characterized by the presence of Arg-Gly-Asp motif. The present molecule has been isolated from the venom of *Echis carinatus*. It exists as a homodimer interlinked by two disulfide bonds using its first two N-terminal Cys residues. The monomeric chain contains 64 amino acid residues. The three-dimensional structure of disintegrin has been determined by multiple isomorphous replacement method. It has been refined to an R-factor of 0.191 for all the data to 2.5Å resolution. This is the first structure of a biological homodimer of disintegrin. The two subunits of the homodimer are related by a two-fold crystallographic symmetry. Thus the crystallographic asymmetric unit contains a monomer of disintegrin. The monomer folds into an up–down topology with three sets of anti-parallel β-strands. The N-terminal anchored two chains of the dimer diverge away at their C-termini exposing the Arg-Gly-Asp motif into opposite directions thus enhancing their binding efficiency. This is one of the unique features of the disintegrin homodimer and results in clustering of the integrin molecules. The homodimer binds to integrins and also plays a role in signaling pathway.

PO140

INTRODUCTION OF THE PROTEIN DATA BANK JAPAN (PDBj)

T. Kosada,[a] R. Igarashi,[a,b] Y. Kengaku,[a,b] S. Saeki,[a,b] Y. Morita,[a,b] M. Kusunoki,[a] K. Kobayashi,[b] A. Paehler,[b] N. Ito,[b] and H. Nakamura[a]

[a]Institute for Protein Research, Osaka University, 3-2 Yamadaoka, Suita-shi, Osaka 565-0871, Japan (kosada.117@protein.osaka-u.ac.jp); [b]Japan Science and Technology Agency.

The Protein Data Bank (PDB) is the sole international public repository for three dimensional structure data of biological macromolecules and serves for supporting essential biological sciences. Macromolecular structures in the PDB help to solve crystallographic structure determination. Also understanding macromolecular structures will aid researchers in understanding how proteins work. This information could give benefits to pharmaceutical and biotechnological industries in understanding various diseases and in developing drugs that enables to target diseases more effectively. The PDB was established at Brookhaven National Laboratory in 1971. The full responsibility for the operation and enhancement of the PDB was transferred to the RCSB (Research Collaboratory for Structural Bioinformatics. USA) in July 1999.

In 1999, the Protein Data Bank Japan (PDBj) was founded at the Institute for Protein Research, Osaka University, to mirror a PDB site and to accept and process PDB entries in Asia and Oceania with collaboration of RCSB. The PDBj enhances the PDB capabilities and has performed the following activities:

1 PDB search web site [1]. http://pdb.protein.osaka-u.ac.jp
2 FTP download site [1]. ftp://ftp.protein.osaka-u.ac.jp
3 PDB deposition site [1]. http://pdbdep.protein.osaka-u.ac.jp
4 Questions about PDB search and deposition [1]. pdbhelp@protein.osaka-u.ac.jp
5 Process and Release of Deposited entries.
6 Exploiting an XML format database[2], a 3D viewer, and secondary databases[3].
7 BioMagResBank (BMRB) Mirror site[1].

The PDBj, RCSB and MSD-EBI (Macromolecular Structure Database at the European Bioinformatics Institute) process deposited PDB entries since 1999 in collaboration.

The PDBj, RCSB and MSD-EBI have formed the world wide Protein Data Bank (wwPDB) on 2003[4]. The mission of the wwPDB is to maintain a single archive of macromolecular structural data that is freely and publicly available to the global community. The legacy of the PDB format will not be modified unless there is a compiling reason for a change.

The PDB has 23813 structures as of 07-Jan-2004. Convenient methods of finding some entries from such many entries and the deposition method including the above list 1. to 6. will be presented here.

Also the contribution of PDBj deposition and processing PDB entries will be shown. PDBj processed 142, 364, 652, and 1021 entries in 2000 through 2003, respectively. These entries include deposition from RCSB. 98, 139, 289, 673 entries in 2000 through 2003, respectively were deposited at the PDBj deposition site. The number of depositions and processing through the PDBj are increasing.

The PDBj provides timely service for users and depositors of Asian and Oceanian region almost without considering world time difference. The PDBj would like to solicit you to deposit your entries through the PDBj deposition site.

References

1 All PDBj sites can access through http://www.pdbj.org
2 Xml-based Protein Structure Search Service (xpss:http://www.pdbj.org/xpsss/).
3 Kinoshita, K., Nakamura, H. (2004) Bioinformatics, in press.
4 Berman, H., Henrick, Kim., and Nakamura, H. (2002) *Nat. struct. biol.* **12**, 979-1024.

PO141

REFOLDING, PURIFICATION AND CRYSTALLIZATION OF APICAL MEMBRANE ANTIGEN 1 FROM PLASMODIUM FALCIPARUM

Tao Bai, Aditi Gupta and Adrian H. Batchelor

University of Maryland, School of Pharmacy, Baltimore, MD, 21201, USA
(tbai001@umaryland.edu)

Malaria is one of the leading causes of both morbidity and mortality in the tropical and subtropical world. AMA1 (apical membrane antigen 1) is considered to be one of the best anti-malaria vaccine candidates. The *ama1* gene is well conserved in the plasmodium genus and partly conserved in *Toxoplasma gondii* and other apicomplexa. The bulk of the protein is extracellular and separated into 3 domains on the basis of intra-domain disulphide bonds. Limited proteolysis experiments are used to elucidate a relatively non-flexible core region of AMA1, and refolding/purification is used to generate two fragments of AMA1. Interestingly, several chromatographically distinct AMA1 variants are identified that are presumably differentially refolded proteins. One of these AMA1 preparations proves to be highly crystallizable and an unusual and yet simple crystal dehydration method is identified that results in the generation of high resolution low mosaicity crystals.

PO142

CRYSTAL STRUCTURE OF A NOVEL SIGNALLING GLYCOPROTEIN FROM BOVINE REVEALS A NEW RECOGNITION SITE

Janesh Kumar, Jayshankar Jasti, Sujata Sharma, Bhaskar Singh, Asha Bhushan and Tej P. Singh

Department of Biophysics, All India Institute of Medical Sciences, New Delhi-110029 (janeshdubey@yahoo.com).

A recently discovered new family of 40 kDa glycoproteins present in the dry secretions of animals, culture supernatants of the MG-63 human osteosarcoma cell line, cultures of human synovial cells and human cartilage cells. These proteins are implicated as protective signalling factors that determine which cells are to survive during the processes of drastic tissue remodeling. The first member of this family was discovered as a prominent protein in the whey secretions of non-lactating cows. In order to develop an understanding of the precise roles of these proteins, a detailed three-dimensional structure of signalling protein from cow (SPC-40) has been determined. The protein was purified from the dry secretions of non-lactating cow. It was also cloned and sequenced. The crystal structure was determined and refined to an R factor of 0.19 to 2.0 Å resolution. The structure shows a classical (βα) 8 barrel fold resembling TIM arrangement. It also has a small α+β domain similar to that of chitinases. However, it has no chitinase activity due to mutations in the residues involved in chitinase activity. The structure also reveals that SPC-40 cannot bind to saccharides / polysaccharides. The protein seems to be involved in the recognition through protein-interactions. Overall, this protein shows a 40-50% sequence identity with chitinases and chitinase-like proteins but lacks chitin hydrolyzing property and carbohydrate binding capability. Thus, it might have evolved from chitinases but has acquired new functions through specific point mutations and by altering its mechanism of recognition.

PO143

CRYSTAL STRUCTURE OF THE SMALL FORM OF GLUCOSE-INHIBITED DIVISION PROTEIN A FROM *THERMUS THERMOPHILUS* HB8

W. Iwasaki[a], H. Miyatake[a] and K. Miki[a,b]

[a]RIKEN Harima Institute/Spring-8, Koto 1-1-1, Mikazuki-cho, Sayo-gun, Hyogo 679-5148, Japan. [b]Department of Chemistry, Graduate School of Science, Kyoto University, Sakyo-ku, Kyoto 606-8502, Japan (wiwasaki@spring8.or.jp)

Glucose-inhibited division protein A (GidA) plays a role in tRNA modification. It is involved in the biosynthesis of hypermodified nucleotide 5-methylaminomethyl-2-thiouridine in the wobble position of bacterial tRNAs, which stabilize codon-anticodon interactions. The inactivation of *gidA* in *E. coli* caused a two-base translational frameshift. The *gidA* gene is widely distributed and highly conserved in both prokaryotes and eukaryotes. A subset of organisms has a second *gidA* gene, which encodes a smaller GidA protein ($GidA_{small}$). The crystal structure of $GidA_{small}$ from *Thermus thermophilus* HB8 has been determined at 1.65 Å resolution by the MAD method of the Hg derivative. The crystal annealing technique was crucial for the data collection. The structure of $GidA_{small}$ consists of two segments: domain 1 with a Rossmann fold, which is characteristic of a dinucleotide binding fold, and domain 2. Although FAD was not added to the crystallization media, it was bound to $GidA_{small}$ at full occupancy. The topology of $GidA_{small}$ satisfies the features of flavoproteins, revealing FAD as a genuine cofactor of GidA. It remains unknown whether GidA catalyzes oxidation-reduction reactions, but the structural features of $GidA_{small}$ strongly suggest that FAD is required for the protein to function. There are two long inserts in GidA of conventional size, compared to $GidA_{small}$. The structure of GidA was predicted using the structure of $GidA_{small}$. The two inserts are thought to create two additional domains in GidA, which would form a catalytic site and recognize substrate tRNA.

PO144

CRYSTAL STRUCTURE OF SPHERICAL PARTICLE OF TOBACCO NECROSIS VIRUS COAT PROTEIN LACKNG N-TERMINAL ARM AT 2.6 Å RESOLUTION

Keiichi Fukuyama,[a] Shu Ishitobi,[a] and Kazuhiko Saeki[a]

[a]*Department of Biology, Graduate School of Science, Osaka University, Toyonaka, Osaka 560-0043, Japan* (fukuyama@bio.sci.osaka-u.ac.jp).

Tobacco necrosis virus (TNV) is a spherical plant virus that consists of a single stranded RNA genome (3.8kb) and 180 identical protein subunits (30 kDa). The crystal structure of TNV determined at 2.25Å resolution revealed that the subunits are arranged in a *T*=3 icosahedral manner [1,2]. At the quasi six-fold axis of the TNV particle, the N-terminal segments (arms) of the C subunits gather together to form β-annulus producing hexameric association of the subunits, whereas at the five-fold axis, the arm is disordered to give pentameric association. The arm may produce multiple ways of subunit associations that are essential for the formation of *T*=3 icosahedral particles.

We expressed the truncated coat protein of TNV, which lacks the N-terminal arm (23K). The 23K protein was highly expressed in *Escherichia coli*, but formed inclusion body. The protein, solubilized with urea and then refolded by dialysis, was assembled to spherical particles in the presence of calcium ion. This particle is smaller than the native TNV particle, indicative of *T*=1 particle. The particles crystallized in the space group of $P4_12_12$ (a=b=311.1Å, c=176.9Å), with half of the particle in the asymmetric unit.

Its X-ray diffraction data to 2.9Å resolution were collected at 100K with beam line BL41XU, SPring-8. The structure of *T*=1 particle was determined by the molecular replacement method using A subunit in the *T*=3 particle and refined to R factor of 19.4%. The present analysis has revealed in detail how the subunit proteins are arranged in the *T*=1 particle. Characteristics of the tertiary and quaternary structures will be presented.

References

1 Oda, Y., Saeki, K., Takahashi, Y., Maeda, T., Naitow, H., Tsukihara, T., and Fukuyama, K. (2002) *J. Mol. Biol.* **300**, 153-169.

2 Saeki, K., Takahashi, Y., Oh-oka, H., Umeoka, T., Oda, Y., and Fukuyama, K. (2001) *Biosci. Biotechnol. Biochem.* **65**, 719-724.

PO145

X-RAY CRYSTAL STRUCTURE ANALYSIS OF A COMPLEX BETWEEN CARBOXYPEPTIDASE Y AND A PROTEIN INHIBITOR

Yasuo Hata,[a] Minoru Hayashida,[a] Tomomi Fujii,[a] Joji Mima,[b] Rikimaru Hayashi,[c] Yoshimi Ueda[b]

[a]Institute for Chemical Research, Kyoto University, Uji, Kyoto 611-0011, Japan; [b]Division of Applied Life Sciences, Graduate School of Agriculture, Kyoto University, Sakyo-ku, Kyoto 606-8502, Japan; [c]Department of Food Science and Technology, College of Bioresource Sciences, Nihon University, Kameino, Fujisawa, Kanagawa 252-8510, Japan (hata@scl.kyoto-u.ac.jp)

The serine carboxypeptidase inhibitor in the cytoplasm of *Saccharomyces cerevisiae*, IC, specifically inhibits vacuolar carboxypeptidase Y (CPY) and belongs to a functionally unknown family of phosphatidylethanolamine-binding proteins (PEBPs) [1]. The N-terminal amino acid residue of IC is acetylated. The N-terminal acetyl group is essential for achieving a tight interaction with CPY and for its complete inactivation of CPY [2]. It is revealed from a biochemical analysis that IC binds to CPY through multiple interaction sites [1]. In order to elucidate the molecular mechanisms of the complex formation between IC and CPY and the expression of the multiple functions by the PEBP family, we have carried out X-ray crystallographic analysis of the CPY-IC complex.

IC was purified by means of a high-level expression system [3]. The purified IC exists as a monomeric beta-protein in solution with a molecular weight of 24,400 and consists of 219 amino acid residues. CPY was treated with endoglycosidase H before preparation of the complex with IC. CPY consists of 421 amino acid residues and the molecular weight of the deglycosilated CPY was 53,000. The CPY-IC complex was prepared by mixing the equal moles of CPY and IC. Crystals of the complex were obtained at 25°C by a hanging-drop vapor-diffusion method using ammonium sulfate as a precipitant. They belonged to space group $P2_12_12_1$ with the unit cell dimensions of a=81.0 Å, b=186.1 Å, and c=64.9 Å. The asymmetric unit of the crystal contains one CPY molecule complexed with one IC molecule. Diffraction data were collected up to 2.9 Å resolution with a Rigaku imaging plate system R-AXIS IV using Cu$K\alpha$ radiation from a rotating anode X-ray generator RU-300H operated at 40kV-100mA. The structure analysis of the complex is under way by a molecular replacement method using atomic coordinates of CPY (PDB code: 1YSC) as an initial model structure.

References

1 Mima, J., Narita, Y., Chiba, H. and Hayashi, R. (2003) *J. Biol. Chem.* **278**, 29792–29798.
2 Mima, J., Kondo, T. and Hayashi, R. (2002) *FEBS Lett.* **532**, 207-210.
3 Mima, J., Suzuki, H., Takahashi, M. and Hayashi, R. (2002) *J. Biochem. (Tokyo)* **132**, 967–973.

PO146

CRYSTALLIZATION AND PRELIMINARY X-RAY STUDY OF CARNOSINASE FROM MICE

Tetsuo Yamashita, Hiroto Otani, Genji Kurisu, Masami Kusunoki, Nobuaki Okumura, Katsuya Nagai

Institute for Protein Research, Osaka University, 3-2 Yamada-oka, Suita, Osaka 565-0871, Japan (t.yama@protein.osaka-u.ac.jp)

Mammlian tissues contain several histidine-containing dipeptides and related peptides such as carnosine, homocarnosine and anserine (1). Carnosine(ß-alanyl-L-hisitidine) is most well characterized among these dipeptides and is present in various tissues including the brain and the skeletal muscles(2). In the brain, a high concentration of carnosine is found in the olfactory epithelium and its neuronal projection to the olfactory blub(3). Carnosine-like immunoreactivity was also found in several nuclei of the hypothalamus including the superchiasmatic nuclei and anterior hypothalamus, indicating that carnosine have specific function in the olfactory and the hypothalamus.

Although carnosine is a classical dipeptide, the molecular mechanism of synthesis and degradation remains unknown. Carnosine is hydrolyzed into ß -alanine and L-hisitidine by a peptidase carnosinase.

We started crystallographic study of carnosinase from mice to understand its enzyme mechanism from a structural viewpoint. The enzyme is expressed in *Escherichi coli* BL21(DE3)pLysS cells as a fusion protein with glutathione-S -transferase(GST) using a pGEX4T-3 plasmid. The GST fusion protein was purified by affinity chromatography using a glutathione Sepharose 4B column and cleaved by thrombin. The purified enzyme was crystallized by the hanging drop vapour diffusion method at 4 °C and crystals appeared in 2-3 days. X-diffraction diffraction data from a crystal were collected to 3.3 Å resolution on a Rigaku R-AXIS IV imaging plate diffractometer with Cu Kα radiation on a Rigaku Ultra-X 18 rotating anode generator operated at 40kV, 100mA at 100K. Structure analysis is underway.

References

1 Sakai M, Kani K, Karasawa N, Yoshida M, Nagatsu I. an electron microscopic study. *Brain Res.* 1988 Jan 12; **438**(1-2): 335-8.

2 DeMarchis S, Modena C, Peretto P, Giffard C, Fasolo A. *J Comp Neurol.* 2000 Oct 23; **426**(3): 378-90.

3 Yamano T, Niijima A, Iimori S, Tsuruoka N, Kiso Y, Nagai K. *Neurosci Lett.* 2001 Nov 2; **313**(1-2): 78-82.

PO147

FACTORS THAT INFLUENCE SUCCESS IN PROTEIN CRYSTALLIZATION

Heather M. Baker,[a] Ivan Ivanovic,[a] and Edward N. Baker[a]

[a]School of Biological Sciences, University of Auckland, Private Bag 92019, Auckland, New Zealand (h.baker@auckland.ac.nz).

With rapid advances in the speed and power of methods of protein structure determination by X-ray crystallography, attention must increasingly turn to protein expression, purification and crystallization as the main bottlenecks. Here we discuss some of the factors that influence the success of protein crystallization efforts, from our experience over the past few years, including our involvement in a lab-scale structural genomics effort. Illustrative examples are given.

Protein quality. In structural genomics projects there is a tendency to use only one or two chromatographic steps in protein purification. However, success in crystallization is strongly correlated with protein quality. A single band on an SDS gel may not show microheterogeneity or aggregation. We use dynamic light scattering as a sensitive monitor of quality, usually testing fractions across a peak. The freshness of a protein sample can also be critical.

Crystallization screens. Many different crystallization screens have now been developed. Some conditions rarely or never give crystals. We have combined current screens with our own in-house screens to give 96-well screens suitable for robotic crystallization.

Additives. Additives such as metal ions and detergents can alter crystallization behaviour. In the case of the TB protein MshB good crystals were only obtained in the presence of β-octylglucoside, which bound both in the active site and in an intermolecular site.

Seeding. Seeding can be performed in various ways. For the TB protein LeuA, the first crystallization could never be reproduced and all subsequent crystals (including the SeMet protein) were seeded from these. For mutants of transferrin, crystals were grown reproducibly by seeding with wild type protein.

Crystal size. Small crystals are frequently found to be more perfect. In the case of the superantigen SpeJ, the largest crystals that could be grown had a maximum dimension of 50μ. No diffraction could be seen on a home source, but data to 1.7 Å resolution were obtained at SSRL.

Use of robotics. The use of robotic systems, and very small volumes, can significantly improve success [1,2] due to reproducibility, speed of equilibration and the ability to be much more rigorous with protein quality, since smaller amounts are needed. Our experience with nanolitre crystallization will be discussed.

References

1 Sulzenbacher, G. *et al.*, (2002) *Acta Cryst.* D**58**, 2109-2115.

2 Page, G. *et al.*, (2003) *Acta Cryst.* D**59**, 1028-1037.

PO148

CONCENTRATION AND CALCIUM DEPENDENT MONOMER-DIMER AND ACTIVITY-INACTIVITY TRANSITIONS IN PHOSPHOLIPASE A_2: CRYSTAL STRUCTURE OF A CALCIUM INDUCED DIMER AT 1.6 Å RESOLUTION

Talat Jabeen, Sujata Sharma, Nagendra Singh, Rajendra K. Singh, Punit Kaur and Tej P. Singh

Department of Biophysics, All India Institute of Medical Sciences, New Delhi -110029

Phospholipase A_2 (PLA_2) catalyzes the hydrolysis of the 2-acyl ester bond of phospholipids and produces lysophospholipds and fatty acids. The formation of current heterodimer between two PLA_2 isoforms from cobra venom was induced by calcium at concentrations higher than 5 mg/ml. The dimer was crystallized in space group $P4_1$ with a= b= 64.5 Å, c= 57.1 Å. The structure was determined by molecular replacement method and refined to an R factor of 0.21 for data rendering to 1.6 Å resolution. Two calcium ions are found, one intramolecularly in the calcium binding loop of molecule B and another at the intermolecular site coordinating two molecules. The intramolecular calcium binding site in molecule A is empty. Both calcium ions are seven-fold coordinated. The two molecules are held with several direct intermolecular contacts at the two ends of their elongated surfaces. The central region between the two molecules is filled with water molecules. The calcium binding loop of molecule A has shrunk and forms a 27O - 33 N hydrogen bond to stabilize its structure. This loop is further stabilized by interactions involving Arg 31 of molecule B with loop carbonyl oxygens. The two isoforms stay away at low concentrations in the absence of calcium ions and show no activity. In the presence of calcium ions, both isoforms are active but do not form dimers at low concentrations. At higher concentrations (>5mg/ml) and in the presence of excess calcium, they form a heterodimer and lose their activity. This suggests that they are stored in the inactive form in the venom and get activated at low concentrations in the presence of calcium, a condition present in the prey.

PO149

NATIVE PEPTIDES AS POTENT INHIBITORS OF SERINE PROTEASES: CRYSTAL STRUCTURE OF A COMPLEX FORMED BETWEEN α-CHYMOTRYPSIN AND ITS AUTOCATALYTICALLY PRODUCED OCTAPEPTIDE AT 2.2 Å RESOLUTION

Nagendra Singh[a], Talat Jabeen[a], Sujata Sharma[a], Ipshita Roy[b], M. N. Gupta[b], Sameeta Bilgrami[a], A. P. Baxla[a], Sharmistha Dey[a], Marcus Perbandt[c], Ch. Betzel[c] and Tej P. Singh[a]

[a]Department of Biophysics, All India Institute of Medical Sciences, New Delhi 110 029, India, Department of Chemistry, Indian Institute of Technology Delhi, New Delhi 110 016, India, [c]Institute of Medical Biochemistry and Molecular Biology, University of Hamburg, c/o DESY, 22603, Hamburg, Germany (nagendratomar@hotmail.com)

Enzymes are involved in a wide range of biological processes providing essential physiological inputs. At the same time their destructive roles are also well known. Therefore, these enzymes are often secreted as inactive precursors together with the synthesis of their proteinaceous inhibitors to prevent their activation at the unwanted site and time. Despite these precautions they have been found associated with a number of disease states. In order to control such undesirable roles of proteases, there is an immense to develop strong synthetic inhibitors. We have induced chymotrypsin into auto hydrolyzing itself and allowed it to go on until the enzyme was completely inhibited. The inhibited enzyme was crystallized and the structure of the complex has been determined at 2.2 Å resolution. The extra electron density at the binding site of chymotrypsin was clearly interpreted into an octapeptide. The carbonyl carbon of inhibitor was covalently linked to Ser O^{γ} in a manner exactly similar to acyl-enzyme adduct. In addition to it, peptide formed a series of hydrogen bonds with the enzyme. It is an unprocedently strong complex. The binding studies confirmed these observations with a binding constant of 1.2×10^{-12} M. The overall structure of enzyme is similar to its native structure indicating that no conformational change occurred upon complex formation.

PO150

ANAEROBIC AND AEROBIC STRUCTURES OF FERREDOXIN II FROM *DESULFOVIBRIO GIGAS* REVEAL ELECTRON TRANSFER MECHANISM

Chun-Jung Chen,[a,c] Yin-Cheng Hsieh,[b] Ming-Yih Liu,[d] and Jean LeGall[d]

[a]Biology Group, National Synchrotron Radiation Research Center, Hsinchu 30077, Taiwan; [b]Institute of Bioinformatics and Structural Biology; [c]Department of Physics, National Tsing-Hua University, Hsinchu 30077; [d]Department of Biochemistry and Molecular Biology, University of Georgia, Athens, GA 30602, U. S. A. (cjchen@nsrrc.rog.tw)

Ferredoxin II (Fd II) is a small electron transfer protein, isolated from the strict anaerobic sulfate-reducing bacterium, *Desulfovibrio gigas*. The protein contains 58 amino acids and an iron-sulfur cluster. The cluster [3Fe-4S] spontaneously undergoes conversion to [4Fe-4S] when it is used as an electron mediator in the phosphoroclastic reaction. This two-form interconversion appears to have physiological significance. We have recently obtained both aerobic and anaerobic Fd II crystals in the high-resolution quality. Both structures are independently determined by the iron single-wavelength anomalous dispersion (Fe-SAD) method using synchrotron radiation X-ray.

The structure of aerobic Fd II has been refined to 0.9 Å ultra-high resolution in the space group $P2_12_12$. Its [3Fe-4S] cluster is bound with Cys8, Cys14, and Cys50, whereas Cys11 extends away from cluster. Cys18 and Cys42 form a disulfide bridge to maintain the protein folding. Five isolated Zn^{2+} ions around the protein are located and bound with Glu, Asn and Asp, respectively, which indicates the transition metals, other than iron, could be incorporated into [3Fe-4S] center. On the other hand, the anaerobic Fd II structure from the crystals grown under anaerobic condition has also been refined to 1.4 Å resolution in the different space group C222. The anaerobic structure shows the different iron-sulfur cluster and disulfide bridge conformations as well as crystal packing. Here we present the structure comparison between aerobic and anaerobic Fd II at ultra-high resolution which reveals the unique iron-storage function and electron transfer mechanism of ferredoxin II from *Desulfovibrio gigas*.

PO151

CRYSTAL STRUCTURE OF CHORISMATE SYNTHASE: A NOVEL FMN-BINDING FOLD AND FUNCTIONAL INSIGHTS

Se Won Suh and Hyung Jun Ahn

Department of Chemistry, College of Natural Sciences, Seoul National University, Seoul 151-742, Korea (sewonsuh@snu.ac.kr)

Chorismate synthase catalyzes the conversion of 5-enolpyruvylshikimate 3-phosphate to chorismate in the last step of the shikimate pathway. Chorismate serves as a common precursor for the synthesis of aromatic amino acids and many aromatic compounds in microorganisms and plants. This makes chorismate synthase an attractive target for discovering antimicrobial agents and herbicides. Chorismate synthase requires reduced FMN as a cofactor but the catalyzed reaction involves no net redox change.

Chorismate synthase from *Helicobacter pylori* is a homotetramer of 365-residue subunit. We have determined its crystal structure in both FMN-bound and FMN-free forms [1,2]. Each monomer possesses a novel FMN-binding protein fold, "β-α-β sandwich fold." Highly conserved regions, including several flexible loops, cluster together around the bound FMN to form the active site. The unique FMN-binding site is formed largely by a single subunit, with a small contribution from a neighboring subunit. Most part of the cofactor is bound deeply within the protein. We have modeled the substrate binding to the *re*-face of the isoalloxazine reing of FMN.

References

1 Ahn, Yoon, Lee, and Suh (2004) *J. Mol. Biol.* **336**, 903-915.

2 Ahn, Yang, Lee, Yoon, Kim, and Suh (2003) *Acta Cryst.* **D59**, 569-571.

PO152

PROBING THE DNA KINK STRUCTURE INDUCED BY THE HYPERTHERMOPHILIC CHROMOSOMAL PROTEIN SAC7D USING SITE-DIRECTED MUTAGENESIS AND X-RAY CRYSTALLOGRAPHY

Chin-Yu Chen[a, c], Ting-Wan Lin[a], Chia-Cheng Chou[a, b], Tzu-Ping Ko[a], and Andrew H.-J. Wang[a, d]

[a]Institute of Biological Chemistry and [b]Core Facility X-ray Crystallography, Academia Sinica, Taipei 115, Taiwan; [c]Department of Chemistry and [d]Institute of Biochemical Sciences, National Taiwan University, Taipei 106, Taiwan.(cutecoca@gate.sinica.edu.tw)

Sac7d is a small, abundant, non-specific DNA-binding protein of the hyperthermophilic archaeon *Sulfolobus acidocaldarius*. Sac7d causes a single-step sharp kink in DNA (~60°) via the intercalation of both Val26 and Met29. In this paper, Val26 and Met29 were systematically changed to either smaller or larger sizes to probe their effects on the kink site in DNA. The crystal structures of five Sac7d mutants (V26A, M29A, V26A/M29A, M29F and V26F/M29F) in complex with GCGATCGC (or GTAATTAC) have been analyzed at high resolution (1.45 Å – 2.25Å). The DNA binding pattern of the V26A and M29A single mutants is similar to that of the wild type, whereas the V26A/M29A protein binds DNA without side chain intercalation resulting in a smaller overall bending of helix (~50°). The M29F mutant uses the Phe29 side chain to the C2pG3 step orthogonally without stacking with base pairs, yet inducing a sharp kink (~80 °). In the V26F/M29F-GCGATCGC complex, Phe26 intercalates deeply into DNA bases by stacking with G3 base, whereas the side chain of Phe29 is stacked on the G15 deoxyribose. Thermodynamic studies show that all mutants still bind to DNA, but with weaker affinity. The DNA kink patterns caused by different binding combinations of hydrophobic side chains may be relevant in understanding the manner with which other minor groove binding proteins interact with DNA.

PO153

SECONDARY BINDING SITE OF TRYPSIN REVEALED BY CRYSTAL STRUCTURE OF TRYPSIN-OVOMUCOID INHIBITOR COMPLEX

B. Syed Ibrahim and Vasantha Pattabhi

Department of Crystallography and Biophysics, University of Madras, Guindy Campus, Chennai 600 025, India (b_syed_ibrahim@yahoo.com).

Crystal structure of trypsin-kazal type ovomucoid turkey egg white inhibitor (OMTKY2) complex has been determined at 1.9Å resolution. Though the entire inhibitor was used for complexation and crystallization, only second domain is bound to trypsin, inhibiting its activity, suggesting that other domains have been hydrolyzed by trypsin. OMTKY2 exhibits the canonical Kazal-type fold and the reactive site residue Lys 25 interactions are similar to other trypsin -inhibitor complexes. The crystal structures of the second and third domain of the inhibitor are similar with a central α-helix and a short two-stranded anti parallel βsheet.

A heptapeptide fragment from the first domain is bound at the interstitial region of the crystal and interacts with both trypsin and the inhibitor. This binding site which is a *secondary binding site* of trypsin is similar to ecotin binding site in trypsin-ecotin complex. Crystal structures of peptide complexes with porcine β-trypsin solved by us suggested that peptides bind the active site of trypsin if a Lys/Arg is present in the sequence or else they bind at the interstitial region. Peptide interactions with trypsin will be discussed in details.

PO154

CRYSTAL STRUCTURE OF THERMOSTABLE LIPASE FROM NEW SPECIES OF *GEOBACILLUS* STRAIN T1

Raja Noor Zaliha Raja Abd. Rahman,[a*] Takahiko Yamamotob,[b] Leow Thean Chor, Abu Bakar Salleh,[a] Mahiran Basri,[a] Kazufumi Takano,[c] Shigenori Kanaya,[c] Hiroyoshi Matsumura,[b] Tsuyoshi Inoue,[b] and Yasushi Kai[b]

[a]Enzyme and Microbial Technology Research, Faculty of Science & Environmental Studies, University Putra Malaysia, 43400 UPM, Serdang, Selangor, Malaysia, [b]Department of Materials Chemistry, Graduate School of Engineering, Osaka University, 2-1, Yamada-oka, Suita, Osaka, Japan, 565-0871, [c]Department of Material and Life Science, Graduate School of Engineering, Osaka University, 2-1, Yamada-oka, Suita, Osaka, Japan, 565-0871 (rnzaliha@fsas.upm.edu.my)

A new species of *Geobacillus* strain T1 was shown to produce a thermostable lipase [1]. The gene encoding T1 lipase was cloned, sequenced and expressed. Purified enzyme displayed a temperature optimum and pH of 70°C and pH 9, respectively. The mature enzyme was successfully crystallized within 24 h by hanging-drop vapor-diffusion method at 20°C. Crystals of T1 lipase were flash-frozen in N_2 stream at -180°C and X-ray diffraction data were collected at SPring-8 BL44XU, Japan. They diffracted to 1.8 Å resolution and belonged to *C*2 space group with cell parameters of a = 117.31 Å, b = 81.04 Å, c = 99.22 Å, and β = 96.91°. Structure determination was preceded by molecular replacement using *Bacillus stearothermophilus* P1 lipase structure as a search model. Structure of T1 lipase as in P1 lipase structure, in a closed conformation, has its active site buried under a long lid helix.

Reference

1 Leow, T. C., Rahman, R. N. Z. A., Basri, M. and Salleh, A. B. (2004) High level expression of thermostable lipase from *Geobacillus* sp. Strain T1. Biosci, Biotechnol,. 68; 96-103

PO155

STUDIES ON THE CRYSTAL STRUCTURE AND FUNCTION OF CUCURMOSIN, A RIBOSOME-INACTIVATING PROTEIN FROM SARCOCARP OF *CUCURBITA MOSCHATA*

Ming-Huang Chen,[a] Shan Liu,[a, b] Zhi-Ren Wang,[a] Liqing Chen[a, c]

[a]State Key Laboratory of Structural Chemistry, Fjian Institute of Research on the Structure of Matter, The Chinese Academy of sciences, Fuzhou, Fujian, 350002, P.R. China; [b]Lanzhou University, Lanzhou, Gansu, 730000, P.R. China; [c]Laboratory for Structural Biology, Department of Chemistry, Graduate Programs of Biotechnology, Chemistry and Materials Science, University of Alabama in Huntsville, Huntsville, AL35899, USA (cmh@ms.fjirsm.ac.cn).

The flesh of the fruit of *Cucurbita moschata* contains a type-1 ribosome-inactivating proteins (RIPs) [1,2], which we named cucurmosin. Cucurmosin was purified to apparent homogeneity by acid fractionation, and ion-exchange chromatography. The protein was found to have a molecular mass of 27kDa and contains glycosidic linkages. The cytotoxicities of cucurmosin on human leukemia K562 and rat melanoma B16 cells were determined, which suggests potential promising roles of cucurmosin in treating some cancers or using as an efficient moiety of immunotoxins. The N-terminal amino acid sequence of cucurmosin determined up to residue 26 was compared to the sequences of several other RIPs. The percentages of identical residues in comparisons with pepocin (a RIP from *Cucurbita pepo*), trichosanthin (a RIP from *Trichosanthes kirilowii*), ricin A chain (a type-2 RIP from *Ricinus communis*), were 95%, 69.2%, and 40%, respectively.

Cucurmosin has been crystallized using polyethylene glycol as a precipitant. The crystals belong to space group $P2_12_12_1$ with cell parameters a=41.5Å, b=58.4Å, and c=99.3Å [3]. A data set to 1.0Å resolution was collected with synchrotron source. The molecular replacement calculations using trichosanthin as the search model yielded a strong, unambiguous solution [4]. The preliminary refinement of this solution against 1.65Å cucurmosin data drove the R factor down to 0.312, confirming the high degrees of sequence and structural homology between the cucurmosin and trichosanthin. Initial inspection of the composite omit map calculated by omitting no more than 5% of the total structure each time showed that the high resolution map is so good that it will allow direct amino acid sequence determination of cucurmosin. We are currently using the map to guide side chain identification. Further model fitting/refinement is in progress.

We are grateful for financial support from the National Natural Science Foundation of China, Natural Science Foundation of Fujian Province, and International Cooperation program of Fujian Province, China.

References

1 Van Damme EJ.M., Hao Q., Chen Y., Barr A., Vandenbussche F., Desmyter S., Rauge P., Peumans WJ. (2001) *Critical Reviews in Plant Sciences*. **20**, 395-465
2 Chen MH., Shi XL., Ye XM., Xie JM., Zhao R., Rao PF., Wang ZR. (2004) *Chinese J. Struct. Chem.* **23**, 232-235
3 Chen MH., Ye XM., Cai JH., Lin YJ. (2000) *Acta Cryst.* **D56**, 665-666
4 Shi XL., Zhan EX., Ye XM., Meehan EJ., Chen MH., Chen LQ. (2003) *Chinese J. Struct. Chem.* **22**, 165-168

PO156

CRYSTAL STRUCTURE OF INORGANIC PYROPHOSPHATASE FROM *HELICOBACTER PYLORI*

Y.-J. Sun, T.-C. Chao, C.-Y. Huang, and H.-M. Huang

Institute of Bioinformatics and Structural Biology, National Tsing Hua University, Hsinchu 300, Taiwan, ROC (yjsun@life.nthu.edu.tw)

Inorganic pyrophosphatases (PPase) catalyze the hydrolysis of pyrophosphate (PPi) to orthophosphate (Pi) and controls the level of PPi in the cell. PPases play an essential role in the energy conservation and provide the energy for many biosynthetic pathways. PPases have been found in many organisms from bacteria to human. *H. pylori* PPase was isolated from *Helicobacter pylori* with molecular weight of 20 kD. The crystal structure of *H. pylori* PPase has been solved and refined to an *R*-factor of 21% at 1.9 Å. The three-dimensional structure of *H. pylori* PPase is composed of two extended α-helices and eight β-strands and form a barrel structure. The oligomeric structure of *H. pylori* PPase is a hexamer in crystal and solution states.

PO157

AVAILABILITY OF THE X-RAY DATA COLLECTED WITH A CR ROTATING-ANODE FOR PHASING PROTEIN CRYSTALS

Takashi Yamane,[a] Atsuo Suzuki,[a] Seiji Okazaki,[a] Hideki Tanizawa,[a] Tatsuo Hikage,[b] Venkatachalam Rajakannan,[c] Devadasan Velmurugan,[c] and Kanagaraj Sekar[d]

[a]Department of Biotechnology, School of Engineering, Nagoya University, Nagoya 464-8603, Japan; [b]High Intensity X-ray Laboratory, Nagoya University, Nagoya 464-8603, Japan; [c]Department of Crystallography and Biophysics, University of Madras, Chennai 600025, India; [d]Bioinformatics Centre, Indian Institute of Science, Bangalore 560012, India. (yamane@hix.nagoya-u.ac.jp).

In the recent years, the use of longer X-ray wavelength (λ= 1.5 - 2.6 Å) has become popular in macromolecular crystallography[1, 2]. The main reason for this is that the anomalous signal of sulfer (S) can be significantly observed. The enhanced anomalous S signal in single-wavelength anomalous dispersion experiments (S-SAD) relies on the S atoms naturally occurring in proteins. Therefore the use of S-SAD may decrease the load to search heavy atom derivatives to all protein crystals. In order to demonstrate the availability of S-SAD, the data collection using a Cr rotating-anode system was carried out.

The highly redundant data of the proteinase K and phospholipase A_2 (PLA2) crystals were collected using Rigaku FR-E generator (power 40 KV x 40 mA, focus size 70 x 800 μm^2) with a chromium rotating-anode (λ= 2.29 Å at Cr Kα) and Rigaku R-AXIS VII IP detector system at High Intensity X-ray laboratory, Nagoya University.

The crystals of Proteinase K from *Tritirachium album* belong to the tetragonal system, $P4_32,2$, a=67.78, c=101.92 Å. A total of 168,650 reflections up to 2.3 Å resolution were collected and processed using the combination of *DENZO/SCALEPACK*, in which unique reflections were 11,106 and Rmerge= 0.067. The anomalous Patterson map clearly showed the Ca-Ca peak. However S-S peaks, a primary objective, could not assigned in the map.

The crystals of PLA2 from bovine pancreas belong to the trigonal system, $P3_121$, a=46.2, c=101.4 Å. A total of 89,573 reflections up to 2.4 Å resolution were processed using the combination of *DENZO/SCALA*, in which unique reflections were 5,303, Rmerge= 0.041 and Ranom=0.030. Owing to the relatively strong absorption effects, scaling is essential for producing the best anomalous difference pairs. The performance of *DENZO/SCALA* seems to be better as considering Rmerge. The PLA2 structure was refined to Rc=0.211 and Rfree=0.249 using *CNS* at 2.3 Å resolution. The residues 62-67 are disordered as same as the other structures of bovine pancreatic PLA2, except for the monoclinic form [3]. The current model contains one Ca ion and 85 water molecules. The search of S positions and phasing is underway.

References

1 M. S. Weiss et al. (2001) *Acta Crystallogr.* D57, 689-695.
2 U. A. Ramagopal, M. Dauter & Z. Dauter (2003) *Acta Crystallogr.* D59, 1020-1027.
3 V. Rajakannan et al. (2002) *J. Mol. Biol.* 324, 755-762.

PO158

FIRST DETERMINATION OF THE INHIBITOR COMPLEX STRUCTURE OF HUMAN HEMATOPOIETIC PROSTAGLANDIN D SYNTHASE

Yuji Kado,[a] Tsuyoshi Inoue,[a,b] Yousuke Okano,[a] Kousuke Aritake,[c] Daisuke Irikura,[c] Nobuko Uodome,[c] Nobuo Okazaki,[a] Shigehiro Kinugasa,[a] Hideyuki Shishitani,[a] Hiroyoshi Matsumura,[a] Yasushi Kai,[a] and Yoshihiro Urade,[c]

[a]Department of Materials Chemistry, Graduate School of Engineering, Osaka University, Suita, Osaka 565-0871, Japan; [b]Structure and Function of Biomolecules Group, PRESTO, Japan Science and Technology Agency, 4-1-8 Honcho, Kawaguchi, Saitama, Japan; and [c]Department of Molecular Behavioral Biology, Japan Science and Technology Corporation, Osaka Bioscience Institute, Osaka 565-0874, Japan (kado@chem.eng.osaka-u.ac.jp).

Hematopoietic prostaglandin (PG) D synthase (H-PGDS) is responsible for the production of PGD_2 as an allergy or inflammation mediator in mast and Th2 cells [1,2]. We determined the X-ray structure of human H-PGDS complexed with an inhibitor, 2-(2'-benzothiazolyl)-5-styryl-3-(4'-phthalhydrazidyl) tetrazolium chloride (BSPT) [3] at 1.9Å resolution in the presence of Mg^{2+}.

The styryl group of the inhibitor penetrated to the bottom of the active site cleft, and the tetrazole ring was stabilized by the stacking interaction with Trp104, inducing large movement around the α5-helix, which caused the space group of the complex crystal to change from $P2_1$ to $P1$ upon binding of BSPT. The phthalhydrazidyl group of BSPT exhibited steric hindrance due to the cofactor, glutathione (GSH), increasing the IC_{50} value of BSPT for human H-PGDS from 36.2 μM to 98.1 μM upon binding of Mg^{2+}, because the K_m value of GSH for human H-PGDS was decreased from 0.60 μM in EDTA to 0.14 μM in Mg^{2+}.

We have to avoid steric hindrance of the GSH molecule that was stabilized by intracellular Mg^{2+} in the mM range in the cytosol for further development of structure-based anti-allergic drugs.

References

1 Lewis, R.A., Soter, N.A., Diamond, P.T., Austen, K.F., Oates, J.A., and Roberts, L.J., 2nd (1982) *J. Immunol.* **129**, 1627-1631

2 Nagata, K, Tanaka, K., Ogawa, K., Kemmotsu, K., Imai, T., Yoshie, O., Abe, H., Tada, K., Nakamura, M., Sugamura, K., and Takano, S. (1999) *J. Immunol.* **162**, 1278-1286

3 Kanaoka, Y., Ago, H., Inagaki, E., Nanayama, T., Miyano, M., Kikuno, R., Fujii, Y., Eguchi, N., Toh, H., Urade, Y., and Hayaishi, O. (1997) *Cell* **90** 1085-1095

PO159

THE NEW MACROMOLECULE CRYSTALLOGRAPHY BEAMLINE 3W1A AT BSRF

Peng Liu, YuHui Dong, Sheng Huang, DeQiang Yao, DingChang Xian

Bei Jing Synchrotron Radiation Facility, Institute of High Energy Physics, Academia Sinica, 19 Yu Quan Lu Beijing 100039, People's Republic of China
(liup@mail.ihep.ac.cn)

A new X-ray macromolecule crystallographic beamline is operational at the Beijing Synchrotron Radiation Facility. The beamline has been built up in 2002 and used since 2003. The radiation source is a 1.42 multipole wiggler. The wavelength range is 0.77-2.07Å with a measured flux of more than 10^{11} photons s^{-1} in 1mm × 0.5mm at the sample position. The energy resolution is better than 4×10^{-4} and multi-wavelength anomalous diffraction experiment can be done.. The station is currently equipped with a Mar345 imaging plate and a MarCCD165 detector. Hundreds of protein samples have been measured and several important results have been attained.

PO160

CRYSTAL STRUCTURE OF A DISSIMILATORY NITRITE REDUCTASE FROM *HYPHOMICROBIUM DENITRIFACANS*

Yong Xie, Tsuyoshi Inoue, and Yasushi Kai

Department of Materials Chemistry, Graduate School of Engineering, Osaka University. 2-1, Yamada-oka, Suita, Osaka, 565-0871, Japan
(xieyong@chem.eng.osaka-u.ac.jp)

Dissimilatory nitrite reductase (NIR) is catalyzing one electron reduction of nitrite to nitric oxide in the denitrification press, leading to a significant loss of fixed nitrogen from terrestrial environment. NIRs isolated from some prokaryotic organisms are containing type-I Cu ion and type-II Cu ion. In present, the nature of the catalytic copper and the conversion of NO_2^- to NO into NIR molecule had been reported. However, NIR accepts electron donated from its redox partner (pseudoazurin or azurin) to accomplish one-electron reduction of NO_2^- to NO. The interaction between NIR and its specific electron transfer partner is still not established. A novel NIR from *Hyphomicrobium denitrifacans* (*Hd*NIR), the structure is homologue of complex of reported NIR and its electron transfer partner was characterized[1]. The interaction between N-terminal domain and C-terminal domain resemble known NIR and its electron transfer partner. In this study, crystallographic studies of HdNIR are carried out to describe the interaction. *Hd*NIR and a mutation form C260A, which is loss a Cu ion in C-terminal was crystallized with same conditions. Crystal of *HD*NIR belong to tetragonal space group $P4_1$ (or $P4_3$), with the cell-parameter is a = 221.91, c = 165.15 (Å), 18 molecules per asymmetric unit. In contract, two types crystals of C260A mutation were obtained, the one crystal of mutant *HD*NIR belong to tetragonal space group $P4_1$ (or $P4_3$), with the cell-parameter is a = 221.32, c = 163.11 (Å), 18 molecules per asymmetric unit, and the one belonged to cubic space group $P4_232$, with the cell- parameter is a = 154.55 (Å), 1 molecule per asymmetric unit. MAD data from the cubic crystal were collected to 3.0 Å. MAD method was used to solve the structure of *Hd*NIR. The first electron density map (Figure 1) was calculated using program *CNS*. Molecule modeling is carried out based the electron density map.

Reference

1 Deligeer, et al., (2002) *J. Inorg. Biochem.* **91**, 132-138

PO161

CRYSTAL STRUCTURE OF THE SHANK PDZ-LIGAND COMPLEX REVEALS A CLASS I PDZ INTERACTION AND A NOVEL PDZ-PDZ DIMERIZATION

Y. J. Im, J. H. Lee, S. H. Park, S. J. Park, S. H. Rho, G. B. Kang, E. Kim and S. H. Eom

Department of Life Science, Kwangju Institute of Science and Technology, Gwangju 500-712, South Korea.(gbkang@kjist.ac.kr)

The Shank/proline-rich synapse-associated protein family of multidomain proteins is known to play an important role in the organization of synaptic multiprotein complexes. For instance, the Shank PDZ domain binds to the C termini of guanylate kinase-associated proteins, which in turn interact with the guanylate kinase domain of postsynaptic density-95 scaffolding proteins. Here we describe the crystal structures of Shank1 PDZ in its peptide free form and in complex with the C-terminal hexapeptide (EAQTRL) of guanylate kinase-associated protein (GKAP1a) determined at 1.8- and 2.25-A resolutions, respectively. The structure shows the typical class I PDZ interaction of PDZ-peptide complex with the consensus sequence -X-(Thr/Ser)-X-Leu. In addition, Asp-634 within the Shank1 PDZ domain recognizes the positively charged Arg at -1 position and hydrogen bonds, and salt bridges between Arg-607 and the side chains of the ligand at -3 and -5 positions contribute further to the recognition of the peptide ligand. Remarkably, whether free or complexed, Shank1 PDZ domains form dimers with a conserved beta B/beta C loop and N-terminal beta A strands, suggesting a novel model of PDZ-PDZ homodimerization. This implies that antiparallel dimerization through the N-terminal beta A strands could be a common configuration among PDZ dimers. Within the dimeric structure, the two-peptide binding sites are arranged so that the N termini of the bound peptide ligands are in close proximity and oriented toward the 2-fold axis of the dimer. This configuration may provide a means of facilitating dimeric organization of PDZ-target assemblies.

Reference

1 Sheng, M., and Kim, E. (2000) *J. Cell Sci.* **113,** 1851-1856
2 Boeckers, T. M., Bockmann, J., Kreutz, M. R., and Gundelfinger, E. D. (2002) *J. Neurochem.* **81,** 903-910

THE STRUCTURE OF IMPORTIN-β BOUND TO SREBP-2 : INSIGHTS INTO NUCLEAR TRANSPORT OF A TRANSCRIPTION FACTOR

Soo Jae Lee,[a,b] Toshihiro Sekimoto,[b] Eiki Yamashita,[a] Emi Nagoshi,[b] Atsushi Nakagawa,[a] Naoko Imamoto,[b] Masato Yoshimura,[a] Hiroaki Sakai,[a] Khoon Tee Chong,[a] Tomitake Tsukihara[a*] and Yoshihiro Yoneda[b*]

[a]Institute for Protein Research and [b]Department of Frontier Biosciences, Graduate School of Frontier Biosciences, Osaka University Yamadaoka 2-2, Suita, Osaka 565-0871, Japan (tsuki@protein.osaka-u.ac.jp)

SREBP-2 is a member of the SREBP family of transcription factors that are synthesized as precursor molecules, which are bound to the endoplasmic reticulum (ER) membrane and the outer nuclear envelope. When cells are deprived of cholesterol, SCAP escorts SREBPs to the Golgi apparatus, where they are proteolytically processed to liberate a transcriptionally active N-terminal fragment of 480 residues. This fragment enters the nucleus and activates the transcription of genes that control the synthesis and uptake of cholesterol and unsaturated fatty acids. Transport of molecules into and out of the nucleus is mediated by the importin-β superfamily. Importin-β plays a role in transporting both cargo that carries a classical nuclear localization signal and cargo with no obvious signal sequence. Importin-β recognizes classical NLS-containing proteins via the adaptor molecule importin-α. Crystal structures have been demonstrated for importin-complexed with cargo molecules [1,2], with RanGTP[3], with an FG repeat nucleoporin[4], and in the free form[5]. However, how importin-β directly recognizes the active form of transcription factors such as Smad3 and SREBP-2 remained unknown.

We determined a 3.0 Å resolution X-ray structure of the complex of full-length 876 amino acid importin-β and a dimer of the SREBP-2 HLHZ region comprising residues 343-403 [6]. The binding site for the SREBP-2 dimer is completely separated from those for importin-α. The SREBP-2 dimer binds between the long heat repeats 7 and 17 of importin-β, whereas importin-α binds in the concave face of the importin-β C-terminal half. The HLHZ dimer is inserted into the importin-β superhelix at an orientation perpendicular to the central axis of the superhelix, while the importin-α IBB domain is parallel to the central axis.

References

1 G. Cingolani *et al., Nature* **399**, 221-9 (1999).
2 G. Cingolani *et al., Mol Cell* **10**, 1345-53 (2002).
3 I. R. Vetter *et al., Cell* **97**, 635-46 (1999).
4 R. Bayliss *et al., Cell* **102**, 99-108 (2000).
5 S. J. Lee *et al., J Mol Biol* **302**, 251-64 (2000).
6 S. J. Lee *et al., Science* 302, 1571-1575 (2003).

PO163

MOLECULAR REPLACEMENT SOLUTION FOR AN ACYLPHOSPHATASE FROM *PYROCOCCUS HORIKOSHII*

Yuk-Yin Cheung and Kam-Bo Wong

Department of Biochemistry, The Chinese University of Hong Kong
(kbwong@cuhk.edu.hk)

Acylphosphatase (AcP) catalyzes the hydrolysis of carboxyl-phosphate bond. We have cloned the AcP gene from a hyperthermophilic archaeon *Pyrococcus horikoshii* and expressed the protein in *E. coli*. This thermophilic AcP is extremely thermostable, which resists denaturation at > 90°C. To understand the structural basis of thermostability, we aim to determine its structure by crystallography. Crystals for diffraction data collection were grown using the sitting-drop vapor-diffusion method at 298K using sodium formate as a precipitant. Hexagonal crystals grew to maximum dimensions of 0.3 x 0.3 x 1 mm in 2 days. An entire date set diffracting to 1.6 Å resolution was collected from a single crystal at 100 K. The crystals belong to the space group $P3_221$, with unit-cell parameters a=b=85.65, c=75.51 Å. Molecular replacement was performed using the crystal structure of bovine AcP as the search model (pdb code = 2ACY). No obvious solution was obtained when polyserine, polyalanine, and all-atom models were used. A clear solution was obtained only when an improved search model based on sequence alignment was used. An in-house written PERL script, ALIGN4MR, was used to create the improved search model (http://smart.bch.cuhk.edu.hk/kbwong/align4mr.htm). Two molecules of AcP were found in the asymmetric unit, with a corresponding crystal volume per protein mass of 3.9 Å Da^{-1} and a solvent content 68.6 %.

PO164

CRYSTALLIZATION, DIFFRACTION AND MOLECULAR REPLACEMENT OF A NOVEL ORANGE FLUORESCENT PROTEIN FROM CERIANTHUS SP

Denis T.M. Ip, David C.C. Wan, and Kam-Bo Wong

Department of Biochemistry, The Chinese University of Hong Kong
(kbwong@cuhk.edu.hk)

A novel orange fluorescent protein, with excitation and emission maxima at 548 and 565 nm, from Cnidaria tube anemone Cerianthus sp., has been cloned and overexpressed in *Escherichia coli*. Hexagonal crystals of recombinant OFP was grown by sitting-drop vapor-diffusion method at 290K using 10% (w/v) polyethylene glycol PEG 3350, 0.1M NH_4F [1]. A complete set of diffraction data was collected to 2.0 Å resolution at 100K. The crystals belong to space group R3, with hexagonal unit-cell parameters a=b=216.947, c=51.839 Å. The crystal structure of the blue coral pigment protein (PDB code 1mou [2]) was used as a search model for molecular replacement. A solution with four protein molecules per asymmetric unit was obtained.

References

1 Ip, D.T.M., Chan, S.H., Allen, M.D., Bycroft, M., Wan, D.C.C., and Wong, K.B. (2004) *Acta Crystallogr.* D **68**, 343-341.

2 Prescoll, M., Ling, M., Beddoe, T., Oakley, A.J., Dove, S., Hoegh-Guldberg, O., Devenish, R.J., and Rossjohn, J. (2003) *Structure*, **11**, 275-284.

PO165

APPLICATIONS OF ACORN TO ATOMIC RESOLUTION DATA / TRUNCATED DATA AT 1.5 Å RESOLUTION OF CATALASE (~57 kDa)

S. Selvanayagam,[a] D. Velmurugan,[a] and T. Yamane,[b]

[a]Department of Crystallography & Biophysics, University of Madras, Guindy Campus, Chennai – 600 025, India; [b]Department of Biotechnology and Biomaterial Science, Graduate School of Engineering, Nagoya University, Furo-cho, Chikusa-ku, Nagoya 464-8603, Japan (s_selvanayagam@rediffmail.com).

One of the main interests in the molecular biosciences is in understanding structure function relations and X-ray crystallography plays a major role in this. ACORN program can be used as a comprehensive and efficient phasing procedure for the determination of protein structures when atomic resolution data are available. This can also be used to locate the heavy atoms when data at atomic resolution are available. Reliable phases can also be developed from a fragment composed of a small percentage (less than 5%) of the scattering matter of the unit cell[1]. Attempts are here made in extending its applications to the structure elucidation of Catalase[2] of approximately 57 kDa molecular weight using atomic resolution data (for *ab initio* phasing). With the truncated at 1.5 Å resolution, different fragments of helices and sheets from the model solved by macromolecular crystallographic means were used as input to ACORN program and the complete model was arrived in all cases. The minimum input phasing requirement was about 15%. The phases obtained from ACORN were of superb quality to allow automated model building to be carried out by ARP/wARP[3]. Minimal manual model building was required and the structure determination was completed using maximum likelihood refinement program REFMAC[4]. At present we use only the fragments (helices and sheets) from the same PDB (1gwe). In all the successful attempts the connectivity index was greater than 0.95 and R and Rfree were nearly 16 and 18%, respectively. The final model had an r.m.s deviation of nearly 0.03 when the main chain atoms of the model are superposed with PDB entry (1gwe). Data mining approach to feed the input fragments using the PDB entries is in progress.

References

1 Yao, J. (2002). *Acta Cryst.* **D59,** 1941-1947

2 Murshudov, G. N., Grebenko, A. I., Brannigan, J. A., Antson, A. A., Barynin, V. V., Dodson, G. G., Dauter, Z., Wilson, K. S. & Melik-Adamyan, W. R. (2002). Acta Cryst. **D58,** 1972-1982.

3 Perrakis, A., Morris, R. M. & Lamzin, V. S. (1999). *Nature Struct. Biol.* **6,** 458-463.

4 Murshudov, G. N., Lebedev, A., Vagin, A. A., Wilson, K. S. & Dodson, E. J. (1999). *Acta Cryst.* **D55,** 247-255.

PO166

STRUCTURAL BASIS OF NLS – BINDING SPECIFICITY OF IMPORTIN α ISOFORMS

S. N. Y. Yang,[a] J. Harris[b] and B. Kobe[a, c]

[a]Department of Biochemistry, University of Queensland, St. Lucia 4072, Australia
[b]School of Life Sciences, Queensland University of Technology, Brisbane 4001, Australia
[c]Institute for Molecular Bioscience, University of Queensland, St. Lucia 4072, Australia
(s4006004@student.uq.edu.au)

Importin a is a nuclear import receptor that recognizes cargo proteins, which contain classic nuclear localization sequence (NLS), and facilitates their transport into the nucleus. Several isoforms of importin a exist in higher eukaryotes, which can be grouped into three subfamilies. In order to investigate the structural basis of the NLS – binding specificity of human importin a isoforms, representative proteins from three different subfamilies were studied. The aims of this investigation is firstly to clone, express full length (importin a5 and a7) and truncated (importin a1, a3, a5 and a7) human importin a isoforms by recombination and then purify to homogeneity. The purified protein will then be used to attempt to produce crystals followed by structure determination. The second aim is to analyze the importinα - NLS binding specificities using homology modeling, NLS peptide library experiments and nuclear import assays.

Protein crystals of human importin a7 have been successfully obtained. With the availability of these crystals, further studies with single crystals of sufficient size for X – ray diffraction experiments will now be possible. Moreover, the proteolytically stable fragments of human importin αs were determined by limited proteolysis using the protease Endopeptidase Glu – C (V8) from *Staph. aureus* and the truncated form of human importin α isoforms was incorporated into the expression plasmid and purified for further structure studies. Furthermore, the three – dimensional models of human importin α isoforms, including α1, 3, 4, 5, 6,and 7, were successfully constructed based on homology with the mouse importin α2, which has a known crystal structure. The human importin αs - NLS binding specificity using the homology models will then be analyzed. In addition, we have developed a new technique to study the substrate specificity of importin α protein, using a degenerate peptide library. The primary optimal NLS peptide for N - terminally truncated mouse importin α2 has already been identified.

PO167

STRUCTURAL AND FUNCTIONAL INSIGHT INTO NONSPECIFIC NUCLEASES INVOLVED IN CELL DEFENSE

Hanna S. Yuan,[a] Chia Lung Li,[a] Kuo-Chiang Hsia[a] and Woei-Chyn Chu[b]

[a]Institute of Molecular Biology, Academia Sinica, Taipei, Taiwan; [b]Institute of Medical Engineering, National Yang-Ming University, Taipei, Taiwan (hanna@sinica.edu.tw).

In prokaryotic organisms, a variety of nonspecific endonucleases involved in protection of bacterial cells have been identified. But differ from the well-known restriction enzyme these endonucleases cleave DNA in a sequence-independent manner. One of the examples is *Escherichia coli* colicin, ColE7, which digests chromosomal DNA in target cells, so that the host cell may have better survival advantage during times of stress. The crystal structures of the endonuclease domain of ColE7 and its complex with DNA demonstrates for the first time how the HNH motif in ColE7 mediates its functions in DNA binding and degradation.

The Vvn from *Vibrio Vulnificus* is another example of a nonspecific endonuclease involved in cell defense. Vvn is a periplasmic protein, capable of digesting nucleic acid in periplasm to prevent the uptake of foreign DNA during transformation. The crystal structure of Vvn and Vvn in complex with a duplex DNA were resolved both at 2.3 Å resolution. This structural study suggests that Vvn hydrolyzes DNA by a general single-metal ion mechanism and indicates how nonspecific DNA-binding proteins may recognize DNA.

References

1 Hsia, K.-C., Chak, K.-F., Liang, P.-H., Cheng, Y.-S., Ku, W.-Y. and Yuan, H. S. (2004) *Structure* 12, 205-214.

2 Li, C., Ho, L.-I., Chang, Z.-F., Tsai, L.-C., Yang, W.-Z. and Yuan, H. S. (2003) *EMBO J.* 22, 4014-4025.

PO168

CRYSTAL STRUCTURE AND CONFORMATION ANALYSIS OF A TETRAPEPTIDE BOC-β-ALA-LEU-AIB-VAL-OME

R. S. Rathore[a]

[a]Department of Physics, Indian Institute of Science, Bangalore 560 012, India (newdrugdesign@yahoo.com)

The crystal structure of a synthetic, terminally blocked tetrapeptide t-Boc-β-Ala-L-Leu-Aib-L-Val-OMe has been examined. The peptide was crystallized in space group C_2. Final R values were: R = 0.075; wR2 = 0.193. The tetrapeptide adopts an overall extended backbone conformation. Conformational parameters are: β-Ala: φ = –78.7 (6)°, θ = 172.1 (4)°, ψ = 103.3 (5)°; Leu: φ = –117.4 (4)°, ψ = 153.7 (4)°; Aib: φ = 62.5 (6)°, ψ = 38.6 (5)°; Val: φ = –115.2 (9)°, ψ = 168 (1)°. In the crystal, peptides are interlinked by intermolecular hydrogen bonds and intermolecular bridges formed by water. These networks of hydrogen-bonds form an unusual type of anti-parallel β-sheet structure.

References

1 Rathore, R. S. & Banerjee, A. (2003) *Curr. Sci.*, **85**, 1217-1220.

PO169

CRYSTAL STRUCTURE OF THIAPYRAN REVEAL HERRING-BONE $\pi \cdots \pi$ INTERACTIONS

T. Narasimhamurthy,[a] J. C. N. Benny,[c] K. Pandiarajan[c] and R. S. Rathore[b]

[a]Bioinformatics Centre; [b]Department of Physics, Indian Institute of Science, Bangalore 560012, India; [c]Department of Chemistry, Annamali University, Annamalai Nagar 608002, India, and, (taterao@physics.iisc.ernet.in)

The crystal structure of trans-2,6-diphenyl-2,3,5,6-tetra-hydrothiapyran-4-one has been determined, which is primarily stabilized by T-shaped and parallel-displaced aromatic clusters. In the crystal packing, the molecules dimerize by means of $\pi \cdots \pi$ interactions of both face-to-face and edge-to-face types, and the aromatic rings associate in a cyclic edge-to-face tetrameric arrangement of the herring-bone type. These herring-bone interactions appear to insulate hydrogen-bond interactions in the crystal structure presumably due to the overwhelming presence of π donors and acceptors.

References

1 T. Narasimhamurthy, T., Benny, J. C. N., Pandiarajan, K. and Rathore, R. S. (2003) *Acta Cryst. C*, **59**, 620-621.

2 Narasimhamurthy, T., Krishnakumar, R. V., Benny, J. C. N., Pandiarajan, K. & Vishwamitra, M. A. (2000). *Acta Cryst. C*, **56**, 870-871.

PO170

SINGLE-CRYSTAL NEUTRON DIFFRACTION STUDIES OF RUBREDOXIN AND OTHER SMALL PROTEINS

Robert Bau

Department of Chemistry, University of Southern California, Los Angeles, CA 90089, U.S.A. (bau@usc.edu)

Since the first publication in 1969, the use of neutrons to study proteins has gradually improved in sophistication. This discussion will focus on the main features that the neutron diffraction technique can provide, as compared with X-ray diffraction. We will review the importance and unique role of neutrons in the determination of biological structures of macromolecular crystals, including the protonation sites of various residues, hydrogen exchange, and solvent structure. Also discussed in this presentation will be recent results on the high-resolution (1.5Å) single crystal neutron analysis of rubredoxin from the hyperthermophilic organism *Pyrococcus furiosus*.

PO171

WATER ENHANCED CRYSTALLINITY IN *CYRTOPHORA* SPIDER DRAGLINE

Hwo-Shuenn Sheu,[a] Khin Win Phyu,[a] Yung-Ping Chiang,[a] Yuch-Cheng Jean[a] and I-Min Tso[b]

[a]National Synchrotron Radiation Research Center, Hsinchu 30077, Taiwan. (hsheu@nsrrc.org.tw) [b]Department of Biology, Tunghai University, Taichung 407, Taiwan.

Spider dragline is the strongest nature fiber, that even better than the best synthetic fiber, *Kevlar*. The elasticity of *Nephila clavipes* dragline is known to be three times of synthetic Nylon fiber and its strength is five times as steel in weight. *Nephila* spiders build orb web and recycle its silk almost every day, while *Cyrtophora* spiders build a three-dimensional web which can sometimes be used for more than a month in tropical forests. This phenomenon suggests that dragline silks produced by *Cyrtophora* can be better endure environmental impacts such as rain, wind and temperature fluctuations than those produced by *Nephila* and *Araneus*. Supercontraction phenomena of *Nephila* dragline by water have been extensively studied recently. The length of *Nephila* dragline will be shank to half of its original length during water absorption, while no changed in length was observed in *Cyrtophora* dragline. It is not surprised that *Cyrtophora* dragline is not affected by water for its longer duration in nature. Two kinds crystalline were found in spider dragline. One is highly orientated β-sheet along the silk direction the other one is random orientation β-sheet as known as "*S*" reflection. In this study we found that the crystallinity of random orientation β-sheet of *Cyrtophora* dragline was affected by water absorption and desorption. The diffraction intensity of "*S*" reflection became stronger and sharper during the water absorption that indicated crystallinity of isotropicβ-sheet became more ordering. The same treatment was also employed to *Nephila pilipes* dragline but no significant changing was observed during water absorption and desorption. These different properties between two spider's dragline maybe correlate to that stratagem of using silk in nature.

TWISTING OF PEPTIDE BOND BY HYDRATION WATERS AND LOCALIZATION OF DEUTERIUM ATOMS OBSERVED IN HUMAN LYSOZYME BY NEUTRON CRYSTALLOGRAPHY

Kaori Chiba-Kamoshida,[a] Takuro Matsui,[b] Toshiyuki Chatake,[a] Takashi Ohhara, [a] Andreas Ostermann [c], Ichiro Tanaka [a], Katsuhide Yutani [d] and Nobuo Niimura [a]

[a]Neutron Research Center, JAERI, Tokai, Naka, Ibaraki, 319-1195, Japan; [b]Center for Interdisciplinary Research, Tohoku University; [c]Technische Universitat Munchen, Germany; [d]RIKEN Harima Institute (kchiba@neutrons.tokai.jaeri.go.jp)

Structural biology challenging to reveal the relationship between structure and activity of protein molecules in post-genome project has been struggling in research groups all over the world. X-ray crystallography and nuclear magnetic resonance (NMR) are two great authorities for structural biology. Although those methods seem to have been already established, there still has been remained a space of discussion to deal with large molecules as proteins. The most significant difference between structural determination for protein and that for small organic molecule is that protein needs structural restrains even for high-resolution structure refinement. Planarity of peptide bond linking two amino acids is the most standard restrain. Usually in refinement programs, cns or X-PLOR, a model structure satisfying the planarity has been selected. These structure models had been deposited to the Protein Data Bank (PDB) and the atomic coordinates are utilized by the other research groups, for example in a field of bio-informatics.

We will present results from our neutron crystallography of human lysozyme. Glu35 is known to be one of the most important residues for the activity. We first directly observed a positive peak of nuclear density which is thought to be a localization of deuterium atom beside the main chain carbonyl oxygen of Glu35. In order to examine the effect of the deuterium atom, we calculated deviations of omega angles from 180 degree meaning distortion of peptide bonds from plane structure with a high-resolution (1.15 Angstrom) x-ray crystallography data [1] refined by SHELX downloaded from the Protein Data Bank, PDB (1JSF). The result showed that the peptide bond including the carbonyl oxygen had been twisted more than 10.8 degrees. Also at the carbonyl oxygen of Tyr54 where the additional nuclear density peak had been observed as a part of a hydration water, 15.5 degrees rotation of the peptide bond was obtained. Planarity of a peptide bond is constructed by an electronic resonance structure between a carbonyl group and an amide nitrogen. Taking the data of nuclear magnetic resonance (NMR) spectra into consideration it is indicated that deuterium atoms localized beside the main chain carbonyl oxygen or hydration waters including such a localized deuterium atom affect the electronic resonance structure of the peptide bond and distort the respective peptide bond planarity.

References

1 Harata K., Abe Y, Muraki M. (1998) Proteins. 30, 232-43

PO173

DESIGN OF PEPTIDES WITH A, B - DEHYDRO-RESIDUES: SYNTHESES, CRYSTAL STRUCTURES AND MOLECULAR CONFORMATIONS OF TWO TETRAPEPTIDES : CBZ - ΔVAL - VAL - ΔPHE - ILE - OCH_3 AND CBZ - ΔVAL - LEU - ΔPHE - LEU - OCH_3

V. K. Goel, A. P. Baxla, R. K. Somvanshi, R. Padma , S. Dey and T. P. Singh.

Department of Biophysics, All India Institute of Medical Sciences, New Delhi-110029 (vijay2_55@rediffmail.com)

a, b -dehydro residues induce specific folded conformations in peptides. The conformational preferences of branched b-carbon dehydro-residues and non-branched b-carbon dehydro-residues are different when introduced at (i+2) position in tetrapeptides. The former produces a type III b-turn while the latter is accommodated in a type II b-turn conformation. In order to determine the effects of the combinations of the above two types of dehydro-residues in the same peptide sequences, we have synthesized two peptides: (i) Cbz - DVal - Val - DPhe - Ile - OCH_3 and (ii) Cbz - DVal - Leu - DPhe - Leu - OCH_3. The crystal structures of the two peptides were determined. The torsion angles f, y in the two peptides were found to be (i) f_1 = -38.7°, y_1 = -41.1°, f_2 = -73.0°, y_2 = -3.8°, f_3 = -62.0°, y_3 = -15.5°, f_4 = -119.7°, y_4 = -4.6° and (ii) f_1 = -36.8°, y_1 = -46.8°, f_2 = -63.5°, y_2 = -12.6°, f_3 = -67.0°, y_3 = -18.2°, f_4 = -61.5°, y_4 = -136.4°. Both peptides form two intramolecular (i+3) ® (i) hydrogen bonds in each structure. The torsion angles and hydrogen bonds indicate the formations of 3_{10}-helical conformations although the nature of non-dehydro-residues in the two structures is different. It shows that the presence of DVal and DPhe residues in peptides induces 3_{10}-helical conformations irrespective of the nature of its side chain. A definite result of this kind can be exploited for design of peptide structures for specific applications.

PO174

EXPRESSION, PURIFICATION AND CRYSTALLIZATION OF MOB1 FROM *Sacchromyces cerevisiae*

Shannon W. N. Au[a], J. Wade Harper[c] and David Barford[b]

[a]Department of Biochemistry, The Chinese University of Hong Kong, Shatin, Hong Kong. (Shannon-au@cuhk.edu.hk)
[b]Section of Structural Biology, Institute of Cancer Research, Chester Beatty Laboratories, 237 Fulham Road, London, SW3 6JB, United Kingdom.
[c]Department of Biochemistry and Molecular Biology, Baylor College of Medicine, One Baylor Plaza, Houston, TX 77030, USA.

Mps One binder (Mob) family comprises a group of highly conserved proteins, the founding member, Mob1, functions in the mitotic exit network and is essential for mitotic exit, cytokinesis and cell separation. Its association with protein kinase Dbf2 enhances phosphorylation and activation of Dbf2. Formation of Mob1-Dbf2 complex is prerequisite for subsequent release of protein phosphatase Cdc14 from nucleolus in late mitosis.

The full-length cDNA of *Sacchromyce cerevisiae* encodes a protein of 314 amino acid residues with no known structural motif. The protein sequence shows 50% identity with the human homologue. It also shares sequence similarity with other members in the gene family, particularly with a nonessential gene, Mob2. However, there is no direct genetic interaction between Mob1 and Mob2.

In our study, we have expressed and purified Mob1 from *Saccharomyces cerevisiae* to homogeneity using pET expression system. Full length Mob1 has been treated with limited proteolysis to identify a stable domain. A Mob1 fragment with N-terminus starts at residue 89 has been crystallized at 293K using lithium sulfate as the precipitant. X-ray diffraction data has been collected to 3.1 Å. The crystal belongs to the hexagonal system, with unit-cell parameters a = 113.6 Å, b = 113.6 Å, c = 88.3 Å and one monomer in the asymmetric unit.

PO175

THE C-TERMINAL REGION IN TRICHOSANTHIN IS IMPORTANT FOR ACTIVITY AND CONFORMATIONAL STABILITY

Hiu-Mei Too[a], Yi Ding[b,c], Siu-Hong Chan[a], Zhilong Wang[c], Yiwei Liu[c], Mark Bartlam[c], Yicheng Dong[b,c], ,Kam-Bo Wong[a], Zihe Rao[b,c] and Pang-Chui Shaw[a]

[a]Department of Biochemistry, Chinese University of Hong Kong, Hong Kong, China, [b]Institute of Biophysics, Chinese Academy of Science, Beijing 100101, China and [c]Laboratory of Structural Biology and the MOE Laboratory of Protein Science, School of Life Science and Engineering, Tsinghua University, Beijing 100084, China (priscillatoo@cuhk.edu.hk)

Trichosanthin (TCS) is a type I ribosome inactivating protein with multiple pharmacological properties including immunomodulatory, anti-tumor and anti-HIV activities. It has rRNA N-glycosidase activity and removes adenine-4324 on the 28s rRNA. Trichosanthin can fold into an active conformation with the last seven residues deleted. The deletion variant, C7-TCS has 2.7-fold decrease in antigenicitiy, 10-fold reduction in both in vitro ribosome-inactivating activity and in vivo cytotoxicity. Moreover, stability assay shows that the deletion of these amino acids destabilizes the structure of TCS.

The crystal structure of C7-TCS has been determined to 0.2nm resolution. The structure shows that hydrogen bonds between P35 and L240, S196 and L240, and W192 and L239 play an important role in maintaining the structure of C7-TCS. Further analysis shows that the hydrogen bonds related to Leu240 are important for maintaining the relationship between the N- and C-terminal domains of TCS. Besides, both the fluorescence spectra and crystal structure show that W192 is more solvent exposed in C7-TCS. By mutating this residue into phenylalanine, W192F-TCS gives a decrease in both stability and ribosome-inactivating activity. The effects of the C7-TCS and W192F-TCS are accumulative, the ribosome-inactivating activity of W192F-C7-TCS decreases by about 60 folds.

Work in Hong Kong was supported in part by a Strategic Grant from the Chinese University.

PO176

PURIFICATION AND STUDY OF ITS EFFECT OF POLYTYPISM IN SOLUTION GROWN CADMIUM IODIDE CRYSTALS USING X-RAY DIFFRACTION

S. K. Chaudhary and Harjeet Kaur

UniversityCollege,M.D.University,Rohtak-124001(India) (sunilkc2001in@yahoo.com)

The Cadmium iodide has been purified using a zone-refining method fabricated by us. The crystals have been grown in two batches using unpurified and purified material. A comparative study has been made on these batches for polytypism using x-ray diffraction technique. Total number of polytypes involved are 360.

Formation of small period polytype 2H is governed by both temperature and impurities contained in the starting material. 4H is the most stable polytype. Higher occurrence of unidentified polytype in crystals of purified material has been attributed to free movement of edge dislocations during growth. The results have been examined against empirical considerations of earlier investigations.

PO177

PHENOMENON OF POLYTYPISM IN MELT-GROWN LAYERED CRYSTAL OF CdI_2 , PbI_2 AND $CdBr_2$

S.K.Chaudhary and Harjeet Kaur

University college ,M.D.University Rohtak-124001 (India) (Sunilkc2001in@yahoo.com)

Polytypism has been observed in a large number of materials where the nearest neighbor relationship between identical two-dimensional layers of atoms can be satisfied in more than one way . The phenomenon has posed interesting problem for the Scientists, since the nature of force that causes ordering over the scale ranging from few angstrom to few thousands of angstrom units is not known.

The theoretical and experimental advancements made in the study of polytypism in melt- grown crystals of CdI_2 ,PbI_2 and $CdBr_2$ in the last few decades have been reviewed. The past work done in this field by us (using optical ,Lasers and X-ray diffraction techniques) and update on the aspect of polytypism in the above crystals has been outlined with special reference to the role of

PO178

CRYSTALLIZATION OF SOME ORGANIC CONSTITUENTS OF URINARY STONES IN GEL AND CHARACTERIZATION

E. Ramachandran[a] and S. Natarajan[b]

[a]Department of Physics, Thiruvalluvar College, Papanasam-627425, India, [b]Department of Physics, Madurai Kamaraj University, Madurai-625021, India (esakkiramachandran@yahoo.co.in)

Organic acids viz., uric acid, hippuric acid, and amino acids cystine, tyrosine, leucine are some of the minor constituents of urinary stones [1]. The etiology of formation of uric acid in urolithiasis is still not very clear. References cite that there are increased levels of urinary hippuric acid among toluene exposed industrial workers [2]. Excessive excretion of cystine in urine – cystinuria – is a hereditary defect, causes cystine stones [3]. The presence of amino acids, tyrosine cystine and leucine as constituents of urinary stones in addition to their many biological roles, prompted the authors, to investigate the growth characteristics and related studies.

Hippuric acid, L-tyrosine, and L-cystine were crystallized in silica gel under suitable pH conditions by reaction method. Transparent, rectangular plates of hippuric acid of size 10.0 x 4.0 x 1.0 mm^3, spherulitic needles of L-tyrosine of size 18.0 x 0.1 x 0.1mm^3 and bunched hexagonal plates of L-cystine of size: 1.0 mm (across) and thickness 0.2 mm, were crystallized.

The grown crystals were characterized by density measurement, and X-ray powder diffraction. Fourier transform infrared spectroscopic studies and thermogravimetric analysis were made on the powdered samples of the above.

The details of the crystal growth conditions and the characterization studies will be presented.

References

1 Oser, B. L. Hawk's Physiological Chemistry, 14th edition, Tata McGraw-Hill Publishing Co. Ltd., New Delhi, 1976.

2 "Toluene, Health and Environmental Effects", U. S. Environmental Protection Agency, Office of Solid Waste, Washington, D.C.,1980.

3 "Lange Medical Book. Harper's Biochemistry", Prentice Hall, New Jersey, 1988. P 286.

PO179

SOME AZIDO-BRIDGED COORDINATION POLYMERS: STRUCTURES AND MAGNETISM

Song Gao, Hao-Ling Sun, Yuan-Zhu Zhang and Bao-Qing Ma

State Key Laboratory of Rare Earth Materials Chemistry and Applications, PKU-HKU Joint Laboratory on Rare Earth Materials and Bioinorganic Chemistry, College of Chemistry and Molecular Engineering, Peking University, Beijing 100871, China (gaosong@pku.edu.cn)

Azide has been widely used to synthesize molecule-based magnetic materials for its efficient magnetic exchange coupling and diversity of coordination modes. We reported an azide-bridged 1D cobalt compound that is the first homospin single-chain-magnet; we also obtained some mixed azide/L -bridged (L = pyrazine-dioxide, carboxylate, 4,5-diazafluoren-9-one azine, cyanide) coordination polymers that show long-rang magnetic ordering [1-5].

Herein we report a novel 2D coordination polymer $[Mn_3(N_3)_6(bpe)_3]$ **1** (bpe = trans-1,2-bis(4-pyridyl)-ethylene). It contains rare 1D F/AF/AF alternating chain bridged by $\mu_{1,3}$-N_3- (end-to-end, EE) and $\mu_{1,1}$-N_3- (end-on, EO); the chains are further connected by bpe to form 2D layer. It exhibits an antiferromagnetic ordering and metamagnetic behaviour below 2.5 K.

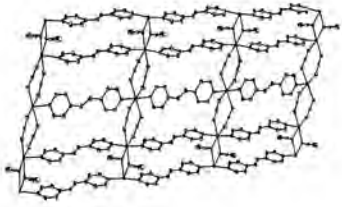

Two-dimensional layer constructed by $\mu_{1,3}$-N_3^-, $\mu_{1,1}$-N_3^- and μ_{bpe}

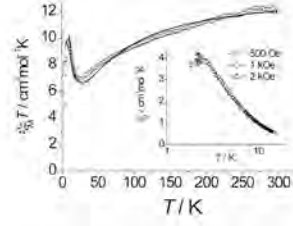

$\chi_M T$ *vs.* T plot of **1** at 5 kOe (Inset: χ_M *vs.* T at different fields).

References

1 Liu, T. F., Fu, D., Gao, S., Zhang, Y. Z., Sun, H. L., Su, G. and Liu, Y. J. (2003) *J. Am. Chem. Soc.* **125**, 13976-13977.

2 Ma, B. Q., Sun, H. L., Gao, S. and Su, G. (2001) *Chem .Mat.* **13**, 1946-1948.

3 Chen, H. J., Mao, Z. W., Gao, S. and Chen, X. M. (2001) *Chem. Commun.* 2320-2321.

4 Liu, C. M., Gao, S., Zhang, D. Q., Huang, Y. H., Xiong, R. G., Liu, Z. L., Jiang, F. C. and Zhu, D. B. (2004) *Angew. Chem. Int. Ed. Engl.* **43**, 990-994.

5 Zhang, Y. Z., Gao, S., Sun, H. L., Su, G. and Zhang, S. W. (2004) *Angew. Chem. Int. Ed. Engl.* submitted.

PO180

BISMUTH DISORDER IN PYROCHLORE OXIDES

Brendan J Kennedy, Leqing Li and Qingdi Zhou

[a]School of Chemistry, The University of Sydney, Sydney, NSW 2006 Australia (bkennedy@chem.usyd.edu.au).

The structures of a number of Bi containing pyrochlores including the series $Bi_{2-x}Yb_xRu_2O_{7-d}$, Bi_2InNbO_7 and Bi_2CrTaO_7 have been studied using a combination of high resolution powder synchrotron and neutron diffraction methods. The oxides all have the cubic pyrochlore structure. In the ideal pyrochlore structure the Bi cations would occupy the 16d sites at (½ ½ ½) and have a distorted 8-fold geometry. This geometry does not allow for the Bi 6s electrons to be sterochemically active. Careful examination of the diffraction patterns reveals that the Bi atoms generally do not occupy the 16d type sites but rather are displaced onto a nearby 96*h* site at (½, ½+y, ½-y), $y \approx 0.25$. The resulting disorder is apparently a consequence of both the sterochemical activity of the Bi 6s electrons and the underbonding of the Bi cations in the ideal structure.

The structural studies of the series $Bi_{2-x}Yb_xRu_2O_{7-d}$ reveal a number of anomalies that are apparently related to the metal-semiconductor transition. In particular the magnitude of the Bi displacement is progressively reduced as the Yb is added to the system. This and other trends will be discussed.

References

1 Li, L. and B.J. Kennedy (2003) *Chem Mater.* **15** 4060-4067.

PO181

XRD, FTIR AND TGA/DTA STUDIES OF GEL GROWN GLYCINE AND DL-SERINE

E. Ramachandran[a] and S. Natarajan[b]

[a]Department of Physics, Thiruvalluvar College, Papanasam-627425, India,
[b]Department of Physics, Madurai Kamaraj University, Madurai-625021, India
(esakkiramachandran@yahoo.co.in)

Glycine and serine are neutral, genetically coded amino acids, hydrophilic polar in nature. Glycine ($C_2H_5NO_2$) is a non-essential amino acid. It is the only protein-forming amino acid without a center of chirality. Serine ($C_3H_7NO_3$) can be synthesized in the body from glycine and is required for the metabolism of fat, tissue growth and the immune system.

Crystallization of amino acids in gel is scarce in literature. Natarajan et al., reported the crystal growth of some amino acids and peptides from our laboratory earlier [1].

Glycine and DL-Serine were crystallized in silica gel under suitable pH conditions by reduction of solubility method. Transparent, rhombohedral crystals of glycine, of size 10.0 x 4.0 x 4.0 mm^3 and rectangular plates with hexagonal edges of DL-Serine, of size 9.0 x 3.0 x 2.0 mm^3 were crystallized.

These crystals were characterized by density measurement, and X-ray powder diffraction. Fourier transform infrared spectroscopic studies and thermogravimetric analysis were made. The details of the crystal growth conditions and the characterization studies will be presented.

References

1 Natarajan, S., Alex Devadoss, H. and Alwan, K., Cryst. Res. Technol. 23 (1988) 1243-1346.

PO182

CRYSTAL GROWTH BY CHEMICAL TRANSPORT OF PEROVSKITE TUNGSTEN BRONZES, Li_xWO_3, AND THEIR OPTICAL PROPERTIES

K. R. Dey,[a] A. Hussain,[b] and C. H. Rüscher[a]

[a]Department of Mineralogy, University of Hannover, Welfengarten 1, 30167 Hannover, Germany; [b]Department of Chemistry, Dhaka University, Dhaka 1000, Bangladesh (C.Ruescher@mineralogie.uni-hannver.de).

Systematic attempts were made to grow crystals of perovskite tungsten bronzes (PTB) of Li_xWO_3 of nominal compositions x = 0.1, 0.2, 0.25, 0.3, 0.35, 0.4, 0.45 by chemical transport methods. $HgCl_2$ was used as transporting agent and appropriate amounts of Li_2WO_4, WO_3 and WO_2 as reactants. A complete transport was achieved within 7 days with a temperature gradient T_1 / T_2 = 700°C / 800°C revealing blue-blackish crystals of sizes up to a few tenth of a milimeter. X-ray powder (Guinier and diffractometer methods) and infrared absorption (KBr method) investigations show a close analogy of the results also obtained in classical solid state reaction methods, which, however, produces crystal powders of submicron sizes. According to this we obtain single phase PTB products of cubic symmetry (PTB_{cub}) for Li_xWO_3 of nominal composition x = 0.45, 0.4, 0.35 and mixed phase of PTB_{cub} and PTB_{tetr} (PTB of tetragonal symmetry) for x = 0.3, 0.25, 0.2. The x = 0.1 sample reveal mixed phases of PTB_{tetr} and PTB_o of lower symmetry. These results are in good agreement with the phase diagram described by Reau et al. [1]. It is interesting to note that Zhong et al [2] have determined the stability ranges of using electrolytic cells as $0.36 < x < 0.5$ for PTB_{cub} and $0.082 < x < 0.13$ for PTB_{tetr} during intercalation whereas $0.21 < x < 0.5$ for PTB_{cub} and $0.078 < x < 0.12$ for PTB_{tetr} during de-intercalation.

Beside the investigations of the crystal growth conditions of these nonstoichiometric compounds another aim was to study their single crystal optical properties. For this polarized micro reflectivity measurements between 600 and 20000 cm^{-1} using a spot size of 80 µm in diameter on polished crystal slices. The crystals from the batches with x = 0.45 all show Drude free carrier type isotropic reflectivity with a minimum at about 14800 cm^{-1}. Crystals from the batches with x = 0.4 slightly differ indicating a superimposition of an additional spectral contribution in the range of the minimum. This contribution could already be related to the influence of the tetragonal phase due to submicroscopical exsolution phenomena since this effect becomes more significant for crystals with lower nominal x. For these crystals there are brighter lamellars separated by sharp interfaces (Fig. 1) due to a separation into PTB_{cub} and PTB_{tetr}. The brighter lamellars become more significant in area for crystals of the batches with x = 0.3, 0.25 and 0.2 and their reflectivity spectra could be measured separately. The data imply that the properties in the tetragonal part of the crystals are dominated by electron localisation effects whereas the cubic parts are dominated by the free electron gas effect.

Fig. 1: $Li_{0.35}WO_3$ crystal slice in reflexion mode

References

1 Reau, J-M., Fouassier, C., Le Flem, G., Barraud, J-Y., Doumerc, J-P., and Hagenmuller, P. (1970) *Revue de Chemie minerale*,**7**, 975-988.

2 Zhong, Q., Dahn, J. R., and Colbow, K. (1992-II) *Phys. Rev. B*, **46**, 2554-2560.

PO183

3X3X1 SUPERSTRUCTURE OF LITHIUM MANGANESE SPINEL

Nobuo Ishizawa,[a] Douglas du Boulay,[a] Kenji Tateishi,[b] Katsumi Suda[c], and Shuji Oishi[d]

[a] Ceramics Research Laboratory, Nagoya Institute of Technology, Asahigaoka, Tajimi 507-0071, Japan; [b] Interdisciplinary School of Science and Engineering, Tokyo Institute of Technology, Nagatsuta Midori, Yokohama 226-8502, Japan; [c] Materials and Structures Laboratory, Tokyo Institute of Technology, Nagatsuta Midori, Yokohama 226-8503, Japan; [d] Faculty of Engineering, Shinshu University, Wakasato, Nagano 380-8553, Japan (ishizawa@nitech.ac.jp).

Lithium manganese spinels are attractive candidates for cathode materials of rechargeable lithium ion batteries. Stoichiometric $LiMn_2O_4$ is a mixed valence compound comprised of distinct Mn(III) and Mn(IV) ions in equal proportions. Above the first order phase transition temperature 310 (1) K on heating, Mn(III) and Mn(IV) ions are randomly distributed amongst the 16d sites of *Fd-3m* symmetry, while they are substantially localized on five independent sites in *Fddd* symmetry below 294(1) K on cooling.

Our synchrotron X-ray single crystal diffraction study [1] at the beam line 14A, Photon Factory, modestly confirms the orthorhombic *Fddd* symmetry containing 18 crystallographically independent atoms, with a= 24.7550(9), b=24.8832(9) and c=8.2003(3) Å Z=72 at 297(1) K on heating, R/Rw =0.038 for 1549 independent reflections. Bond valence sums (BVS) determined for each Mn site were 3.06 for Mn1, 3.34 for Mn2, 3.12 for Mn3, 3.89 for Mn4, and 3.88 for Mn5, averaging to 3.50 over the unit cell. The evidence indicates that Mn1-Mn3 and Mn4-Mn5 sites strongly include the contribution of Mn(III) and Mn(IV), respectively, with a minor reservation for Mn2. The bond-lengths of Mn1-O5 [2.159 Å] are about 10% longer than those of Mn1-O4 [1.938 Å] and Mn1-O2 [1.966 Å], arising from the Jahn-Teller effect of high spin Mn(III) ions. The same arguments also apply to both $Mn2O_6$ and $Mn3O_6$ octahedra and they have longer Mn-O bond length along a and b axes, respectively. On the other hand these tendency do not appear at Mn4 and Mn5.

Some structural anomaly around Mn2 and coordinating O9 atoms, that surround an inversion centre, will be discussed in association with the imperfect charge ordering of the system.

References

1 K. Tateishi, K. Suda, D. du Boulay, N. Ishizawa & S. Oishi, *Acta Cryst.* **E60**, (2004) i18-i21.

PO184

MICRO-STRUCTURAL STUDY ON THE ALLOY $MINi_{3.75}Co_{0.75}Mn_{0.3}Al_{0.2}$ (MI: LA-RICH MISCH METAL) DURING THE HYDROGEN ABSORPTION AND DESORPTION CYCLING

Guanglie Lu and Zhiqing Yuan

Central Laboratory, XiXi Campus, Zhejiang University, Hangzhou 310028, P. R. China (gllu@zju.edu.cn)

X-ray diffraction microstructure of hydrogen storage alloy $MINi_{3.75}Co_{0.75}Mn_{0.3}Al_{0.2}$ (MI: La-rich misch metal) during the hydrogen absorption and desorption cycling was studied by using *in situ* X-ray diffraction method. Crystallite sizes along different (*hkl*) planes were determined by applying an anisotropic diffraction-line broadening model in the Rietveld refinement. It had been indicated that the hydrides precipitate in the same domains with the solid solution phase. Hydride precipitates are the combinations of the plate-like and the needle-like crystallites, whose sizes are mainly affected by the dislocations formed in the hydrogen absorption and desorption cycling.

References

1 Cerný, R., Joubert, J. –M., Latroche, M., Percheron-Guégan, A., Yvon, K. (2000) *J. Appl. Crystallogr.* **33**, 997-1005.
2 Joubert, J. –M., Latroche, M., Cerný, R., Percheron-Guégan, A., Yvon, K. (2002) *J. Alloys. Compd.* **330-332**, 208-214.
3 Kim, G. H., Chun, C. H., S. G., Lee, K. Y., Lee, J. Y. (1994) *Acta. Metall. Mater.* **42** (9), 3157-3161.
4 Popa, N. C. (1998) *J. Appl. Crystallogr.* **31**, 176-180.
5 Wu, E., Kisi, E. H., Gray, E. Mac A. (1998) *J. Appl. Crystallogr.* **31**, 363-368.

PO185

RESIDUAL STRESS MEASUREMENT FOR GRANITE BY TOF NEUTRON DIFFRACTION METHOD

T. Ishigaki,[a] H. Obana,[a] J. Kodama,[a] S. Harjo[b] and T. Kamiyama[b]

[a]Department of Materials Science and Engineering, Muroran Institute for Technology, Muroran 050-8585, Japan; [b]Neurton Science Laboratory, IMSS, KEK, Tsukuba, 305-0801, Japan (ishigaki@mmm.muroran-it.ac.jp).

It is important, when using the rock, to know the pressure which rock had received in underground. It is thought that the rock is maintaining the stress received in underground as residual strain. It is possible to presume the pressure under the earth in order to measure the residual stress for the rocks.

In this report, we have made an experimental study to measure the residual strain of granite block by neutron diffraction using Sirius diffractometer at KENS, KEK. The maximum residual stress for quartz in granite used for this experiment is 19.5Mpa.

HYDROGEN-BONDED CRYSTALLINE FRAMEWORK BASED ON RESORCIN[4]ARENE AND 4,4'-BIPYRIDINEDIENE

Shu-Qun Liu,[a] Qian-Feng Zhang,[a]* and Wa-Hung Leung[b]*

[a]Department of Chemistry and Chemical Engineering, Anhui University of Technology, Maanshan, Anhui 243002, China (E-mail: zhangqf@ahut.edu.cn)
[b]Department of Chemistry, The Hong Kong University of Science and Technology, Clear Water Bay, Kowloon, Hong Kong, China (chleung@ust.hk)

Seeking to develop further the use of large and sterically-demanding molecular building blocks,[1] we proposed to use resorcin[4]arene, "molecular capsule", as templates for the synthesis of metal nanoparticles in order to control both the size and size distribution of the resultant particles.[2] One of our interests is therefore to study the solid-state adducts of *C*-substituted calix[4]resorcinarene and 4,4'-bipyridinediene. We reasoned that the addition of an aliphatic spacer group between the pyridine units in the long 4,4'-bipyridinediene would lead to chain- and cavity-formation sufficient to control templates for metal cluster nanoparicles. Herein we initially show two supramolecular solids of 4,4'-bipyridinediene with *C*-methylcalix[4]resorcinarene (1) and *C-iso*-butylcalix[4]resorcinarene (2), respectively. Further photochemistry reactions and metal-coordination behaviors of two supramolecular multi-components will be reported later.

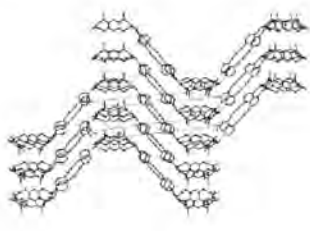

1

2

References

1 MacGillivray, L. R.; Atwood, J. L. *Nature* **1997**, *389*, 469-472.
2 Jasat, A.; Sherman, J. C. *Chem. Rev.* **1999**, *99*, 931-967.

The support from the Key Scientific Research Foundation of State Education Ministry (grant no.204067) and Natural Science Foundation of China (grant no. 90301005) is acknowledged.

PO187

OXYGEN-INDUCED FORMATION OF A NOVEL TETRA-NUCLEAR *P*-CYMENERUTHENIUM COMPLEX WITH OXO BRIDGES

Lihua Liu,[a] Qian-Feng Zhang,[a]* and Wa-Hung Leung[b]

[a]Department of Chemistry and Chemical Engineering, Anhui University of Technology, Maanshan, Anhui 243002, China (E-mail: zhangqf@ahut.edu.cn)
[b]Department of Chemistry, The Hong Kong University of Science and Technology, Clear Water Bay, Kowloon, Hong Kong, China (chleung@ust.hk)

It is well known that ruthenium complexes are versatile compounds that can catalyze various organic reactions.[1] In recent years there has been an increasing interest in metal complexes containing chloride ligand and a chelating ligand, because the labile chloride can be readily displaced by small molecular such as H_2, N_2, O_2, CO, CO_2 and $CH_2{=}CH_2$. The coordination of such molecules is of interest with respect to their activation for catalytic transformations. Because the arene-ruthenium complexes such as $[RuCl_2(arene)]_2$ and $[RuCl_2(PR_3)(arene)]$ have been used as homogeneous catalysts, we seek to explore catalytic activity of the [(arene)Ru] species. In the course of our research on ruthenium complexes with sulfur and selenium donor ligands, we have isolated high-valent arene-ruthenium complexes by oxidation reactions. Treatment of [(η^6-*p*-cymene)Ru(acetone)$_3$][BF_4]$_2$ with 4,4'-bipyridine (4,4'-bipy) in CH_2Cl_2 solution in air resulted in the formation of a novel mixed-valance tetranuclear *p*-cymeneruthenium complex [{(η6-p-cymene)Ru}2(μ-O)2(4,4'-bipy)]2[BF4]2. The structural analysis reveals a macrocycle with alternating oxygen and 4,4'-bipy bridged between the ruthenium atoms. Electrochemical studies showed that the RuII-(μ-O)2-RuIII moiety undergoes an initial one-electron oxidation to RuIII-(μ-O)2-RuIII and the oxidation potential for a complex with the high-valent state has been determined.

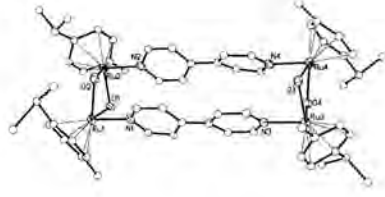

References

1 Noyori, J. *Asymmetric Catalysis in Organic Synthesis*, Wiley, New York, (1994).

The support from the Key Scientific Research Foundation of State Education Ministry (grant no. 204067) and Natural Science Foundation of China (grant no. 90301005) is acknowledged.

PO188

CRYSTALLOGRAPHY OF MICROSTRUCTURAL TRANSITIONS IN COPPER BASED SHAPE MEMORY ALLOYS

O. Adıgüzel

Firat University, Department of Physics, 23119, Elazig, Turkey
(oadiguzel@firat.edu.tr, oadiguzel@hotmail.com8

The behavior of many materials is evaluated by the microstructural changes in microscopic scale depending on the external conditions. One particular group of such materials are shape-memory alloys which exhibit a peculiar property called shape memory effect. The origin of this phenomena lies in the fact that the material changes its internal crystalline structure with changing temperature.

Metastable b-phases of noble metal copper based ternary alloys are very sensitive to the heat treatments and transform martensitically from the B2(CsCl8 or DO_3(Fe_3Al8 type ordered structures to the long period layered strudures on cooling. The high temperature bcc(b-phase undergoes two types of ordering reactions called premartensitic transitions during cooling. The first transition is a nearest neighbour (nn8 ordering reaction which results in a B2-type superlattice. However, bcc to DO_3 transition which induces the next-nearest neighbour (nnn8 ordering reaction is first order.

Martensitic transformations in shape memory alloys occur by two or more lattice invariant shears on a $\{110\}_b$ plane of parent phase called basal plane of martensite. The order of martensite structure is closely related to the order of parent due to the diffusionless character of the transformation, and the martensite exhibits the order of parent existing prior to the transformation. Martensite phase has the unusual layered structures which consist of an array of close-packed planes with complicated stacking sequences called as 3R, 9R or 18R martensites depending on the stacking sequences on the close-packed planes of the ordered lattice. On the basis of austenite-martensite relation, it is experimentally determined that the basal plane of 9R (or 18R8 martensites originates from one of the $\{110\}_b$ planes of the parent phase, and an homogenous shear occurs on the basal plane in either of two opposite directions during the transformation.

The $\{110\}_b$ type plane of parent which is the basal plane for martensite is subjected to the hexagonal distortion with martensite formation on which atom sizes have important effect. In case the atoms occupying the lattice sites have the same size, the hexagon becomes regular hexagon otherwise the hexagon undergoes a distortion in case atom sizes are different. Due to this distortion, the spacing differences between particularly selected pairs of diffraction planes providing a special relation between miller indices become different zero and can be a measure of the ordering degree in martensite. The decrease in spacing difference leads to disordering in martensite.

PO189

POSITIONAL DISORDER AND DIFFUSION PATH IN OXIDE-ION CONDUCTORS

Masatomo Yashima,[a] Katsuhiro Nomura,[b] Daiju Ishimura,[a] Syuuhei Kobayashi,[a] Hiroyuki Kageyama,[b] Wataru Nakamura,[a] Kenjiro Oh-uchi,[a] and Kenji Ohoyama[c]

[a]Department of Materials Science and Engineering, Interdisciplinary Graduate School of Science and Engineering, Tokyo Institute of Technology, 4259 Nagatsuta-cho, Midori-ku, Yokohama, 226-8502, Japan; [b]Special Division of Green Life Technology, National Institute of Advanced Industrial Science and Technology (AIST) - Kansai, Midorigaoka 1-8-31, Ikeda, 563-8577, Japan; [c]Institute for Materials Research, Tohoku University, Katahira 2-1-1, Aoba-ku, Sendai, 980-8577, Japan (yashima@materia.titech.ac.jp).

Solid oxides with high ionic conductivity are attracted materials owing to their many applications in solid oxide fuel cells, sensors, catalysts and batteries. The development of better electrolyte materials requires a better understanding of the mechanism of ionic conduction, and crucial to this is a comprehension of the crystal structure at high temperatures where the materials work efficiently. Here we report the disorder and diffusion path of oxide ions in Bi_2O_3 [1], CeO_2 [2], and $(La_{0.8}Sr_{0.2})(Ga_{0.8}Mg_{0.15}Co_{0.05})O_{2.8}$ [3]. These were studied through the nuclear density distribution obtained by a combined technique including Rietveld refinement and maximum-entropy method (MEM)-based pattern fitting of neutron powder diffraction data measured with the HERMES diffractometer at high temperatures. The cubic bismuth oxide δ-Bi_2O_3 with the fluorite-type structure has the highest oxide ion conductivity in the known compounds. We found that the oxide ions have a complicated disorder spreading over a wide area and shift to the <111> directions from the ideal fluorite site at 778°C [1]. This feature would be responsible for the fast oxide-ion conduction of δ-Bi_2O_3. Ceria (CeO_2)-based materials have high oxide-ion conductivity. Accurate nuclear density distribution of CeO_2 has been studied between 1005° and 1497°C [2]. The results reveal that the oxide ions have a complicated disorder spreading over a wide area and shift to the <111> directions from the ideal fluorite position [2]. This feature is more significant at higher temperatures, which is consistent with the higher ionic conductivity [2]. Lanthanum gallate-based compounds with an ABO_3 perovskite-type structure have high oxide-ion conductivity. Here we demonstrate that the diffusion path of oxide ions is not along the straight line between the ideal positions, but exhibits an arc shape away from the B-site cation ($Ga_{0.8}Mg_{0.15}Co_{0.05}$) [3]. In the low-temperature rhombohedral phase, the oxide ions are localized, while in the high-temperature cubic structure, they spread over a wide area [3]. We acknowledge very much Prof. Emeritus Y. Yamaguchi (Tohoku Univ.), Dr. Y. Miyazaki (AIST), Dr. N. Chitose, Mr. K. Adachi (Mitsubishi Materials Co.), Mr. K. Kawachi and Mr. T. Yasui (Dai-Ichi Kigenso Kagaku Kogyo Co.) for assistance and discussion.

References

1 Yashima, M. and Ishimura, D. (2003) *Chem. Phys. Lett.* **378**, 395-399.
2 Yashima, M. and Kobayashi, S. (2004) *Appl. Phys. Lett.* **84**, 526-528.
3 Yashima, M., Nomura, K., Kageyama, H., Miyazaki, Y., Chitose, N. and Adachi, K. (2003) *Chem. Phys. Lett.* **380**, 391-396.

PO190

HIGH-TEMPERATURE NEUTRON POWDER DIFFRACTION STUDY OF CERIA UP TO 1500°C

Syuuhei Kobayashi,[a] Masatomo Yashima,[a] Daiju Ishimura,[a] Kenjiro Oh-uchi,[a] Wataru Nakamura,[a] Kenji Ohoyama,[b] Katsuhiro Kawachi,[c] and Tadahi Yasui[c]

[a]Department of Materials Science and Engineering, Interdisciplinary Graduate School of Science and Engineering, Tokyo Institute of Technology, 4259 Nagatsuta-cho, Midori-ku, Yokohama, 226-8502, Japan; [b]Institute for Materials Research, Tohoku University, Katahira 2-1-1, Aoba-ku, Sendai, 980-8577, Japan; [c]Daiichi Kigenso Kagaku Kogyo, Hirabayashi-Minami 1-6-38, Sumire-ku, Osaka 559-0025, Japan (yashima@materia.titech.ac.jp).

Solid oxides with high ionic conductivity are attracted materials owing to their many applications in solid oxide fuel cells, batteries, catalysts and oxygen sensors. The development of better electrolyte materials requires a better understanding of the mechanism of ionic conduction, and crucial to this is a comprehension of the crystal structure at high temperatures where the materials work efficiently. We have investigated the temperature dependence of unit-cell and structural parameters of ceria (cerium dioxide, CeO_2) from room temperature to 1500°C by neutron powder diffraction and the Rietveld method [1, 2]. The neutron-diffraction data was collected using the multi-detector system HERMES [3] and a furnace to heat the sample in the temperature range from room temperature to 1600°C [4]. The unit-cell parameter increases continuously with temperature. It was confirmed that the Debye–Waller factor of oxygen B(O) is larger than that of cerium B(Ce) at any temperature from room temperature to 1500°C. Both B(O) and B(Ce) increase with an increase of temperature. We have also studied the anisotropic thermal vibration of oxide ions in ceria by the combination technique of the Rietveld refinement, the maximum-entropy method (MEM) and the MEM-based pattern fitting [2]. This was studied through the nuclear density distribution obtained by a combined technique including a Rietveld refinement (RIETAN-2000) and a maximum-entropy method (MEM)-based pattern fitting (PRIMA [5]) of the neutron powder diffraction data measured at high temperatures. The nuclear density distribution was plotted by a computer program VENUS [5]. The results reveal that the oxide ions have a complicated disorder spreading over a wide area and shift to the <111> directions from the ideal fluorite position [2]. This feature is more significant at higher temperatures, which is consistent with the higher ionic conductivity [2].

References

1 Yashima, M., Ishimura, D., Yamaguchi, Y., Ohoyama, K. and Kawachi, K. (2003) *Chem. Phys. Lett.* **378**, 395-399.
2 Yashima, M. and Kobayashi, S. (2004) *Appl. Phys. Lett.* **84**, 526-528.
3 Ohoyama, K., Kanouchi, T., Nemoto, K., Ohashi, M., Kajitani, T. and Yamaguchi, Y. (1998) *Jpn. J. Appl. Phys.* Part 1 **37**, 3319-3326.
4 Yashima, M. (2002) *J. Am. Ceram. Soc.* **85**, 2925-2930.
5 Izumi, F. and Dilanian, R. A. (2002) Recent Research Developments in Physics **3**, 699-726.

PO191

STRUCTURAL CHANGE OF THE Li-DOPED LANTHANUM TITANATE PEROVSKITE $La_{2/3-x}Li_{3x}TiO_3$

Wataru.Nakamura,[a] Masatomo Yashima,[a] Daiju Ishimura,[a] Syuuhei Kobayashi,[a] Kenjiro Oh-uchi,[a] Mitsuru Itoh,[b] Kenji Ohoyama[c]

[a]Department of Materials Science and Engineering, Interdisciplinary Graduate School of Science and Engineering, Tokyo Institute of Technology, 4259 Nagatsuta-cho, Midori-ku, Yokohama, 226-8502, Japan; [b]Materials and Structures Laboratory, Tokyo Institute of Technology, 4259 Nagatsuta-cho, Midori-ku, Yokohama, 226-8503, Japan; [c]Institute for Materials Research, Tohoku University, Katahira 2-1-1, Aoba-ku, Sendai, 980-8577, Japan
(yashima@materia.titech.ac.jp).

Li-doped lanthanum titanate perovskites $La_{2/3-x}Li_{3x}TiO_3$ have high Li ion conductivity ($10^{-3}Scm^{-1}$ at room temperature) and A-site deficient layered perovskite-type structure with the ordered distribution of La ions on the A-sites along the *c*-axis. But the detailed crystal structure and the phase transition of $La_{2/3-x}Li_{3x}TiO_3$ have not been reported yet. In this work, we have chosen the composition $La_{0.52}Li_{0.32}TiO_{2.94}$, because it has highest Li-ion conductivity in $La_{2/3-x}Li_{3x}TiO_3$ ($0 \le x \le 0.15$). The tilt of the TiO_6 octahedron in layered perovskite is the key to understand the crystal structure [1]. However, the tilt angle has not been known in $La_{0.52}Li_{0.32}TiO_{2.94}$.The purpose of this study is to investigate the crystal structure and phase transition in $La_{0.52}Li_{0.32}TiO_{2.94}$.

$La_{0.52}Li_{0.32}TiO_{2.94}$ compound was studied by high-temperature neutron diffraction technique. Neutron-diffraction data were collected in the temperature range from room temperature to 1268K, using the multi-detector system HERMES and an electric furnace to heat the sample. Crystal structure of $La_{0.52}Li_{0.32}TiO_{2.94}$ was refined by Rietveld analysis of diffraction data. To confirm the position of Li ions, the nuclear density distribution was studied by the maximum-entropy method.

In the literature the $La_{0.52}Li_{0.32}TiO_{2.94}$ has been assumed to belong to the space group *P4/mmm* at room temperature. However, the *P4/mmm* could not explain the observed 113, 133, 115, 315, 533, 117, and 355 reflection peaks where the *hkl* was indexed based on the basic perovskite lattice. On the other hand, the space group *Cmmm* yielded these reflection peaks. The lattice parameter increased continuously with the temperature. The low-temperature orthorhombic phase has tilt of TiO_6 octahedron along *b* axis. The tilt angle decreased with temperature and became 0 at 1098±59K. We found that the tetragonal-to-orthorhombic (*P4/mmm-Cmmm*) transition is induced by the tilt of the TiO_6 octahedron. Similar *P4/mmm-Cmmm* phase transition was reported for $La_{0.64}(Ti_{0.92}Nb_{0.08})O_3$ [1] and $La_{0.6}Sr_{0.1}TiO_3$ [2].

References

1 Yashima, M., Mori, M., Kamiyama, T., Oikawa, K., Hoshikawa, A., Saitoh, K. and Tsuda, K. (2003) *Chem. Phys. Lett.* **375**, 240-246.

2 Howard, C. J. and Zhang, Z., (2003) *J. Phys. Cond. Matt.* **15**, 4543-4553.

PO192

AN ORGANICALLY TEMPLATED NICKEL GALLOPHOSPHATE WITH A UNIQUE LAYER STRUCTURE

Chia-Her Lin, Yu-Lun Lai, and Sue-Lein Wang*

Department of Chemistry, National Tsing Hua University, Hsinchu 300, Taiwan
(beaman113@ms4.hinet.net)

A new layered nickel gallophosphate $(H_3dien)[(Ni_{0.5}Ga_{3.5}(OH))_4Ga_2PO_4)_3(HPO_4)_4] \cdot (dien) \cdot 2H_2O$ (**1**; dien= diethylenetriamine), has been synthesized under mild hydrothermal conditions and characterized by single-crystal X-ray diffraction, thermogravimetric analysis, electron paramagnetic resonance, electron probe microanalysis, and magnetic susceptibility data. The layers in **1** are constructed from metal-oxygen clusters which involve four edge-sharing MO_6 octahedra and two GaO_5 trigonal bipyramids. The hexameric $[Ga_6O_{28}]$ unit has not been observed in the gallophosphate. An isostructural gallophosphate containing no nickel, $(H_3dien)[(Ga_6(OH)_4(PO_4)_3(HPO_4)_4] \cdot (dien) \cdot 2H_2O$ (**2**), has also been prepared. Further syntheses by exchanging other amine has resulted in another gallophosphate analogue, $(H_5tepa)[Ga_6(OH)_4(PO_4)_5(HPO_4)_2] \cdot 2H_2O$ (**3**; tepa, tetraethylenepentamine). Crystal data: **1**, monoclinic, $C2/c$, a = 20.8363(12) Å, b = 11.9546(7) Å, c = 16.4577(9) Å, β = 117.285(1)°, V = 3643.3(1) Å^3, Z = 4, R = 0.0424; **2**, monoclinic, $C2/c$, a = 20.842(3) Å, b = 11.968(2) Å, c = 16.512(3) Å, β = 117.052(3)°, V = 3667.8(10) Å^3, Z = 4, R = 0.0419; **3**, orthorhombic, $Pna2_1$, a = 16.4295(9) Å, b = 11.9120(7) Å, c = 18.7521(11) Å, V = 3667.8(10) Å^3, Z = 4, R = 0.0377.

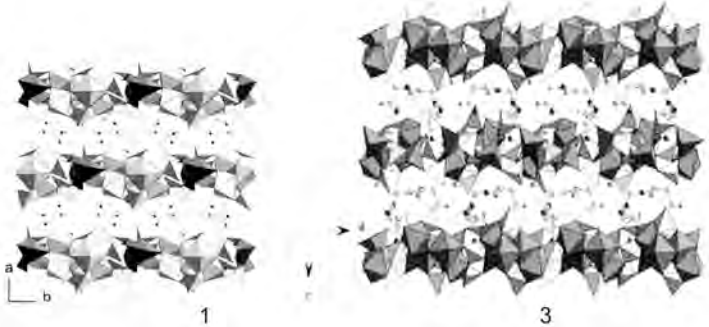

PO193

GRASS FORMIG AT THE LIMIT: HOW GLASS FORMS WHEN THERE IS INSUFFICIENT NETWORK FORMER TO GO AROUND

Shinji Kohara,[a] Kentaro Suzuya,[b] Ken Takeuchi,[c] Chun-Keung Loong,[d] Marcos Grimisditch,[d] J.K. Richard Weber,[e] Jean A. Tangeman,[e] and Thomas S. Key[e]

[a]Japan Synchrotron Radiation Research Institute, Mikazuki, Sayo, Hyogo 679-5198, Japan; [b]Japan Atomic Energy Research Institute, Tokai, Naka, Ibaraki 319-1195, Japan; [c]Tokyo University of Science, Oshamanbe, Yamakoshi, Hokkaido 049-3514, Japan; [d]Argonne National Laboratory, Argonne, IL 60439-4814, USA; [e]Containerless Research Inc., 906 University Place, Evanston, IL 60201-3149, USA (kohara@spring8.or.jp).

Inorganic glasses normally exhibit a network of interconnected covalent-bonded structural elements that has no long-range order. In silicate glasses the network formers are based on SiO_4-tetrahedra of which the interconnectivity is realized by sharing the oxygen atoms at the corners. Conventional wisdom then implies that alkaline and alkaline-earth orthosilicate materials cannot be vitrified because they do not contain sufficient network forming SiO_2 to establish the needed interconnectivity. The structure of a bulk magnesium orthosilicate (Mg_2SiO_4) glass synthesised using containerless melting-and-cooling technique was determined by a combination of high-energy X-ray and neutron diffraction and reverse Monte Carlo computer simulation. We find that the role of network former is largely taken on by corner- and edge-sharing ionic magnesium species that adopt 4-, 5- and 6-coordination with oxygen [1].

References

1 Kohara, S., Suzuya, K., Takeuchi, K., Loong, C.-K., Grimisditch, M., Weber, J. K. R., Tangeman, J. A., and Key, T. S., (2003) *Science* **303**, 1649.

PO194

NEW RESULTS BY USING TEM TO STUDY OF THE MAGNETIC MATERIALS NbFeB

V. Vong,[a] D. M. Thuy[b] and N. V. Vuong[c]

[a]Laboratory of Electron Microscopy, Vietnam Academy of Science, 18Hoangquocviet Str. Caugiay Hanoi; [b]Department of Physics, Quinhon University 170 Anduongvuong-Quinhon city Vietnam; [c]Institute of Materials Science, Vietnam Academy of Science 18Hoangquocviet Str. Caugiay Hanoi. (vvemlab@ncst.ac.vn)

The NdFeB melt-spun powders were prepared by using ZGK-1 rapid quenching frequency furnace with differential revolution rates of the roller. Microstructure, crystallization, the grain's size of the finished products have been investigated by X-ray diffraction and transmission electron microscope.All alloying elements were found to be distributed homogenneously as an amorphous solid solution in the as-quenched state.

We know that the magnetic property of permanent magnets depends strongly not only on the microstructure but also on the grain size and the coupling between the grains. The grain size of the material is from few tens of nanometers to the size of single domain (about 100 nm).

Our results shown that the preparation conditions as well as the quenching rate, mass and conductivity of the roller, gas pressure the heat transfer between the roller, the water cooling system,etc...influence directly on the quality of melt–spun powders .Our experiments show also the revolution rate of roller is the most effective parameter to quenching rate.

In the work we present the new results ,which we recently received by studying the NdFeB alloys. The materials are quenched rapidly with various velocities of roller. The influences of the quenching rate on crystallization process were considered by using BH-graph, X-ray diffration (XRD) and high resolution transmission electron microscopy (HTEM).

For the preparation samples we used the rapid quenching furnace ZGK-1.The diameter of the rapid-quenching roller is 300 mm. The loop of the rapid-quenching roller is made of a copper chrominium alloy. The velocities of roller were changed from 1000 round/min (15,70m/s) to 2900 round/min (45.53 m/s). The magnetic characterising parameters were determined by BH-graph model NIM 200C. The measurement samples were prepared by using the carefull milled melt-spun NdFeB powder put into a copper cylinder tube of 8mm diameter, 10mm height. The grain formation inside the quenched powder was investigated by using the X-ray diffraction equipment of Siemen-5000 and the high resolution transmission microscope JEM-4000 EX.

References

1 Vuong N.V, Khanh N.V. Thuy D.M, Physica B, V.317 (2002) pp. 349-351.
2 Robert C. O'Handley, "Modern magnetic material. Principles and application" (1999) Wiley-Interscience.

PO195

ROLE OF THE DOPED ELEMENTS IN MATERIALS FOR GAS SENSORS

V. Vong[a] and L. T. Hung[b]

[a]Laboratory of Electron Microscopy, Vietnam Academy of Science, 18Hoangquocviet Str. Caugiay Hanoi Vietnam (vvemlab@ncst.ac.vn)
[b]Department of Physics, Vinh University , Nghean Vietnam

Gas sensors based on semiconductive oxides,represented by tin oxide,are very important devices for detecting the leakage of toxic or inflammable gases.The addition of small amounts of not only the noble elements as well as platinum,paladidum,silver...but also normal elements such as antimony,aluminium,freon... is known to enhance a quality of the sensor.That means to enhance sensitivity,recovery and selectivity of the gas sensors.

A few scientists presented the hyppothesis for interpreting the role of additive elements in order to enhance sensor's quality. However ,a full explanation of this phenomenon is to now still lacking.

In the work we present the results,which indicated that a small amount of the dopetd elements (noble materials or normal materials) will be created in tin oxide material not only the clusters but also the untrafine grains (untrafine islands). The size of the grains is about a few nanometer or less.

The results demonstrated that a creation both the clusters and the ultrafine grains by addition of small amounts of metals is main cause of the enhancement sensitivity, selectivity of the gas sensor based on tin oxide.

References

1 V. Vong, Ng. T. Huong, Proc. XVIII Inter. Union of Crystallography Congress, Glasgow (1999) P06.11.016.
2 V. Vong, Proceedings of the 8th Asia -Pacific Physics Conference, Taiwan (2000) pp. 670-673.

PO196

CRYSTAL STRUCTURE X-RAY ANALYSIS OF TWO SPIRO-BIFLUORENE COMPOUNDS WITH REMARKABLE INTENSE SOLID-STATE RED FLUORESCENCE

Chin-Ti Chen, Chih-Long Chiang, Wei-Ching Wu, Yuh-Sheng Wen,

Institute of Chemistry, Academia Sinica, Taipei, Taiwan 11529 (cchen@chem.sinica.edu.tw)

Red fluorophores emitting strong fluorescence in solution are common, but it is rare that strong red fluorescence still remains in solid state. We want to report two donor-acceptor substituted spiro-bifluorene compounds, 2-di(4-tolyl)amino-7-dicyanovinyl-9.9'-(2,2'-biphenyl) fluorene (**pTSPDCV**) and 2-diphenylamino-7-dicyanovinyl-9.9'-(2,2'-biphenyl) fluorene (**PhSPDCV**),

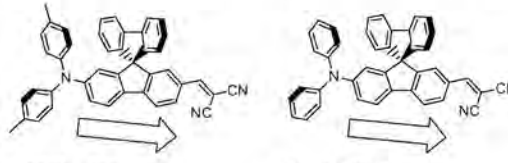

pTSPDCV **PhSPDCV**

They show remarkable strong red fluorescence in solid state. We attribute the unusual solid-state fluorescence to the unique crystal packing structure as well as the non-planar rigid chemical structure of two spiro-bifluorene that prevents the close contact of the molecules in solid state. The single crystal structures and crystal packing will be described and discussed in detail.

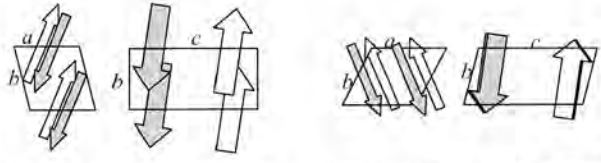

Crystal packing of **pTSPDCV** Crystal packing of **pTSPDCV**

PO197

CORRELATION BETWEEN CRYSTAL STRUCTURE AND FERROELECTRIC PHASETRANSITION TEMPERATURE FOR KTP MATERIALS

Stefan T. Norberg[a], Joacim Gustafsson[b], Nobuo Ishizawa[a]

[a]Ceramics Research Laboratory, Nagoya Institute of Technology, Asahigaoka, Tajimi 507-0071, Japan; [b]Materials and Surface Chemistry, Chalmers University of Technology, SE-412 96 Gothenburg, Sweden. (stn@crl.nitech.ac.jp)

Potassium titanyl phosphate ($KTiOPO_4$, KTP) [1] is a well known material for nonlinear optical applications. The favourable properties of thermal stability, chemical resistivity, high optical nonlinearity and high optical damage threshold, as well as a wide optical transmission window extend too many isostructural materials. Most common are $ATiOBO_4$ compounds with *A* = K, Rb, Cs or Tl, and *B* = P or As. However, not all of the possible *ATiOBO*4 materials give a high nonlinear optical response; some are even paraelectric at room temperature. This diversity in properties of the KTP isostructural compounds is useful as it allows us to make structure-property related studies.

Accurate structural models of materials isostructural to KTP have been gained from 10 K and room temperature measurements. Careful investigation of this data has led us to suggest an improved model for the direct correlation between certain structural fragments and the ferroelectric to paraelectric phase transition temperature (T_C). The most significant part is that the displacement of the alkali cations along the crystallographic c-axis could be related to the Abrahams-Jamieson-Kurtz T_C criteria for oxygen framework ferroelectrics. It should also be possible to make accurate estimations of the T_C for similar KTP isostructural materials using structural models based on room temperature data.

X-ray intensities for sodium-doped KTP ($Na_{0.114}K_{0.886})K(TiO)_2(PO_4)_2$ were collected at 10.5 K using the Huber diffractometer at UWA. X-ray intensities were collected for two germanium-doped rubidium titanyl phosphates (RTP), $Rb_2(Ti)(Ge_{0.121}Ti_{0.879})O_2(PO_4)_2$ and $Rb_2(Ge_{0.125}Ti_{0.875})(Ge_{0.225}Ti_{0.775})O_2(PO_4)_2$ at room temperature. Additionally, dielectric measurements were carried out over a wide temperature range for both RTP and germanium-doped RTP.

References

1 Tordjman, I., Masse, R. & Guitel, J. C. (1974). *Z. Kristallogr.* **139**, 103-115.
2 Norberg, S. T., Sobolev, A. N., Streltsov, V. A. (2003). *Acta Cryst.* B**59**, 353-360.
3 Norberg, S. T., Gustafsson, J., Mellander, B.-E. (2003). *Acta Cryst.* B**59**, 588-595.

PO198

SYNTHESIS, STRUCTURE, AND PHASE RELATIONSHIP IN LITHIUM MANGANESE OXIDE SPINEL

Masao Yonemura,[a] Atsuo Yamada,[b] Stefanus Harjo,[a] Takashi Kamiyama,[a] and Ryoji Kanno[b]

[a]Neutron Science Laboratory, Institute of Materials Structure Science, High Energy Accelerator Research Organization, Tsukuba, Japan;
[b]Department of Electronic Chemistry, Interdisciplinary Graduate School of Science and Engineering, Tokyo Institute of Technology, Yokohama, Japan (yone@post.kek.jp).

Lithium manganese oxide spinels are promising candidates as cathodes in rechargeable lithium batteries. The spinels are usually discussed in the ternary phase diagram, $LiMnO_2$ - Li_2MnO_3 - MnO_2. The composition variety resulted from the synthesis at various temperature and Li/Mn ratio could be interpreted in the triangle region of $LiMn_2O_4$ - $Li_4Mn_5O_{12}$ - $Li_2Mn_4O_9$[1-4]. Change in the Li/Mn ratio in the starting materials leads to the composition varieties in the spinel from $LiMn_2O_4$ to $Li_4Mn_5O_{12}$, and the decrease in synthesis temperature gives compositions from $LiMn_2O_4$ to $Li_2Mn_4O_9$. The structure is complicated due to the existence of Jahn-Teller trivalent manganese ions. Furthermore, oxygen vacancies have also been reported[5-7]. Therefore, the structures and the relation to the $LiMn_2O_4$ - $Li_4Mn_5O_{12}$ - $Li_2Mn_4O_9$ phase diagram are still ambiguous.

In this study, phase relationships, structures, and the phase transitions in the lithium manganese oxide spinels were studied using samples synthesized at various conditions. Their structures were discussed based on the structure date determined by TOF neutron and synchrotron X-ray Rietveld analysis. The oxygen vacancy was confirmed, and its amount varied with the synthesis condition. The relationship between the composition, structure, and phase transition will be discussed.

References

1 M.M. Thackeray, W.I.F. David, P.G. Bruce, and J.B. Goodenough, (1983) *Mater. Res. Bull.*, **18**, 461
2 M.H. Rossouw, A. de Kock, L.A. Picciotto, M.M. Thackeray, W.I.F. David, and R.M. Ibberson, (1990) *Mater. Res. Bull.*, **25**, 173.
3 C. Masquelier, M. Tabuchi, K. Ado, R. Kanno, Y. Kobayashi, Y. Maki, O. Nakamura, and J.B. Goodenough, (1996) *J. Solid State Chem.*, **123**, 255.
4 A.I. Palos, M. Anne, and P. Strobel, (2001) *J. Solid State Chem.*, **160**, 108.
5 A. Yamada, K. Miura, K. Hinokuma, and M. Tanaka, (1995) *J. Electorchem. Soc.*, **160**, 108.
6 J. Sugiyama, T. Atsumi, T. Hioki, S. Noda, and N. Kamegashira, (1997) *J. Power Sources*, **68**, 641.
7 J. Sugiyama, T. Atsumi, A. Koiwai, T. Sasaki, T. Hioki, S. Noda, and N. Kamegashira, (1997) *J. Phys. Condens. Matter.*, **9**, 1729.

PO199

CRYSTAL STRUCTURE ANALYSIS OF Ti-Cr-Mo HYDROGEN ABSORBING ALLOYS

K.Iwase[a*], Y.Nakamura[b], E.Akiba[b] and T.Kamiyama[c]

[a]Department of Material Structure Science, The Graduate University for Advanced Studies, 1-1, Oho, Tsukuba, Ibaraki 305-0801 Japan (kiwase@post.kek.jp), [b]National Institute of Advanced Industrial Science and Technology, AIST Central-5, 1-1-1, Higashi, Tsukuba, Ibaraki 305-8565 Japan, [c]High Energy Accelerator Research Organization (KEK), 1-1, Oho, Tsukuba, Ibaraki 305-0801 Japan

V-free Ti-Cr hydrogen storage alloys are promising for various applications. $Ti_{40}Cr_{57.5}Mo_{2.5}$ bcc solid solution alloys have hydrogen storage capacity of 3.6 mass % (1.8 H/M ratio) [1]. This is almost double to that of conventional intermetallic compounds. There have been several reports concerning crystal structures of Ti-Cr-V [2] and Ti-V-Mn [3,4] bcc solid solutions, but few reports can be found for Ti-Cr-Mo[5] alloys. In this study, absorption-desorption properties of Ti-Cr-Mo bcc hydrogen absorbing alloys and crystal structures of the alloys and hydrides were investigated.

The lattice parameters and hydrogen absorption-desorption properties of $Ti_{45}Cr_{55-x}Mo_x$ alloys changed with increasing Mo contents. The crystal structures were investigated by X-ray and neutron diffraction combined with the Rietveld method, for the alloys before hydrogenation and those in the full-hydride state. Results from X-ray diffraction indicate that the alloys in full-hydride state have an fcc structure, and neutron ones indicate that it is CaF_2 type structure.

References

1 A. Kamegawa, T. Tamura, H. Takamura and M. Okada, J. Alloys Comp. 356-357(2003) 447-451
2 E. Akiba and H. Iba, Intermetallics 6 (1998) 461-470
3 Y. Nakamura and E. Akiba, J. Alloys Comp. 316(2001) 284-289
4 Y. Nakamura and E. Akiba, J. Alloys Comp. 311(2000) 317-321
5 K.Kubo, H.Itoh, T.Takahashi, T.Ebisawa, T.Kabutomori, Y.Nakamura and E.Akiba, J. Alloys Comp. 356-357(2003) 452-455

PO200

CARBON MICRO-RODS IN LOW-TEMPERATURE HYDROGENATED AMORPHOUS CARBON

Prabal Dasgupta[a]*, D.P. Bhattacharyya[a], Nikhilesh Chowdhuri[b], Arup Banerjee[c]

[a]Department of Theoretical Physics
[b]Department of C.S.S.
[c]Department of Spectroscopy
Indian Association for the Cultivation of Science, Jadavpur, Kolkata 700 032
(prabaldasgupta@hotmail.com)

This work reports presence of carbon micro-rods measuring 30-40 microns in sucrose char produced by the action of conc. sulphuric acid. Electron-diffraction and FTIR studies reveal that at least two phases of amorphous carbon are present in sucrose char and one of them is hydrogenated amorphous carbon. The d_{002} (2.306A^0 & 2.20A^0) of bulk and micro-rod differs considerably and hybridisation ratio was found to be $sp^3 : sp^2 = 1:3$ from the deconvolution of bands in the region of 2800 – 3000 cm^{-1}. Band gap (1.04 eV) and plot of energy vs absorption coefficient, strongly corroborated presence of hydrogenated amorphous carbon.

PO201

EVOLUTION OF GROWTH MODE, MICROSTRUCTURE, AND PHOTOLUMINESCENCE IN Mg- DOPED GaN EPILAYERS ON Al_2O_3 (0001)

Hsueh-Hsing Hung,[a] Chin-Pin Chuang,[a] and Ling-Yun Jang[a]

[a]National Synchrotron Radiation Research Center, Hsinchu Science Park, 30077, Taiwan (hhh@nsrrc.org.tw)

Epitaxial GaN:Mg films grown by using MOVPE were studied. Magnesium can reduce the stacking fault energy difference between wurtzite and zinc-blende structures so as to make coexistence of two phases. With much increasing flow rate of Cp_2Mg, the role of Mg ions changes from the p-typed dopant to nucleation center so as to generate prismatic step fronts and thus inverse domain boundaries.

These Mg-rich defect phases of 8.4° tilted to (10-11) orientation are coherent to the substitutional-interstitial model of Mg-complexes and well correlate to the prevailing of yellow band in the photoluminescence spectrum.

In addition, according to DAFS results, apparent tensile strain and interstitial Mg have been observed only in these orientation-tilted structures.

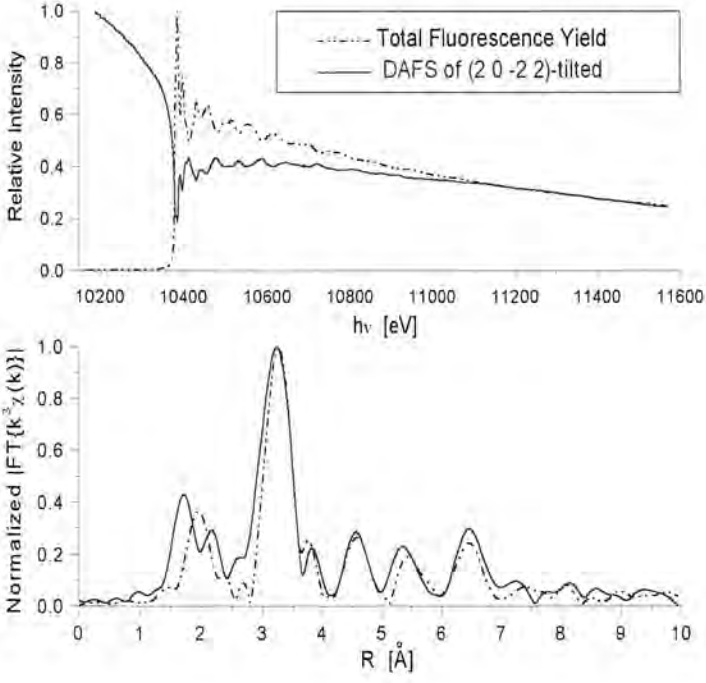

PO202

STRUCTUAL ANALYSIS OF SLIDE-RING GEL BY SMALL ANGLE X-RAY SCATTERING AND CONTROL OF THE PULLEY EFFECT

Kentaro Kayashima,[a] Yuya Shinohara,[a] Eiji Takeuchi,[a] Yoshiyuki Amemiya[a,b], Yasushi Okumura[a,b], and Kohzo Ito[a,b]

[a]Graduate School of Frontier Sciences University of Tokyo, 5-1-5 Kashiwanoha, Kashiwa, Chiba 277-8561, Japan; [b]CREST, JST

Slide-ring gel (topological gel)[1] is a new type of gel which is synthesized by cross-linking α-cyclodextrins contained in the sparse polyrotaxanes in solution. It consists of polymer chains with bulky end groups which are topologically interlocked by figure-of-eight cross-links of α-cyclodextrins. In the slide-ring gel, it is assumed that the polymer chains freely pass through the cross-links acting like pulleys, which would results in equalizing the nanoscopic heterogeneity in structure and stress. We call this "pulley effect".

In this study, we have measured small-angle X-ray scattering (SAXS) of slide-ring gel to investigate and confirm the "pulley effect". It is known that usual chemical gels which are cross-linked by covalent bond shows so-called "abnormal butterfly pattern", in which X-ray intensities are enhanced in a stretched direction, when they are stretched uniaxially. This indicates that the heterogeneities of uniaxially stretched chemical gels become increased along the stretched direction.

We have measured SAXS of uniaxially stretched slide-ring gels in good (NaOH aqueous) and poor (NaCl aqueous) solvents. The experiments were carried out at BL-15A, KEK-PF, in Tsukuba, Japan. SAXS from slide-ring gels in poor solvents showed the abnormal butterfly pattern, but SAXS from slide-ring gels in good solvents showed a normal butterfly pattern in which X-ray intensities are enhanced perpendicular to the stretched direction. This indicates that the behavior of the cross-links of the slide-ring gel in good solutions are quite different from that of usual chemical gels and that the aggregation in poor solvent suppresses the sliding of cross-links considerably, which enables us to control the pulley effect freely by varying the solvent.

References

1 Y. Okumura, K. Ito, (2001) *Adv. Mater.*, **13**, 485.

PO203

METAL-BASED MOLECULAR FUNCTIONAL MATERIALS OF FLUORENES

Wai-Yeung Wong

Department of Chemistry and Centre for Advanced Luminescence Materials, Hong Kong Baptist University, Waterloo Road, Kowloon Tong, Hong Kong, P.R. China (rwywong@hkbu.edu.hk)

The design of metal acetylide complexes and polymers with unusual optoelectronic and photovoltaic properties has aroused growing research interests. An identified problem in OLEDs is the ratio of 3:1 for the generation of non-emissive triplet to emissive singlet excitons on the basis of spin statistics. In view of this, conjugated polymers containing transition metal atoms such as platinum have been widely studied as model systems to explain aspects of the photophysics of excited states in such polymers and obtain a clear picture of the spatial extent of the singlet and triplet manifolds. The strong spin-orbit coupling associated with these heavy metals renders the spin-forbidden triplet emission (phosphorescence) partially allowed. Very recently, a comprehensive program was launched in our laboratory on the investigations and development of some novel organometallic polyyne polymers incorporating fluorene-based auxiliaries. One of the merits here is that the 9-fluorenyl positions can be functionalized easily so that the solubility, the emission and electronic properties as well as the bandgaps of the resulting materials can be chemically tuned. In this talk, we present our work on the synthesis, characterization, structural and photoluminescent properties of a series of transition metal polyyne polymers containing 9-functionalized fluorene spacer units.

References

1 Wong, W.-Y., Liu, L. and Shi, J.-X. (2003) *Angew. Chem. Int. Ed.* **42**, 4064–4068.
2 Wong, W.-Y., Lu, G.-L., Choi, K.-H. and Shi, J.-X. (2002) *Macromolecules* **35**, 3506–3513.

PO204

CRYSTAL STRUCTURES OF MOLECULAR COMPLEXES BETWEEN SURFACTANTS AND HYDROQUINONE

Akiko Sekine,[a] Yuko Fujimura,[a] Hidehiro Uekusa,[a] Yuji Ohashi,[a] and Nahoko Iimura[b]

[a]Department of Chemistry and Materials Science, Tokyo Institute of Technology, Ookayama, Meguro-ku Tokyo 152-8551, Japan (asekine@chem.titech.ac.jp).
[b]Department of Pharmaceutics, Niigata University of Pharmacy and Applied Life Sciences, Kamishin'ei-cho, Niigata, 950-2081, Japan

It has been reported that several cationic surfactants and aromatic compounds make crystalline complexes. Their structures analysed by X-rays revealed the common-packing pattern of the component molecules in the crystals. In this paper, we made more stable complexes of surfactants and hydroquinone, which have high whitening effectiveness and investigated interaction between the surfactant and hydroquinone molecules.

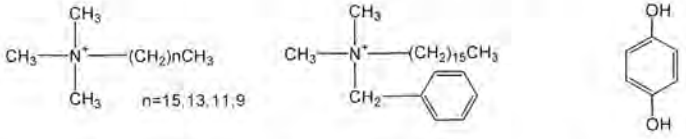

Scheme Chemical formula of surfactants and hydroquinone

Several surfactants, that is, hexadecyltrimethylammonium bromide (CTAB), tetradecyltrimethylammonium bromide (MTAB), dodecyltrimethyl-ammonium bromide (LTAB), decyltrimethylammonium bromide (DTAB), and hexadecyl dimethylbenzylammonium chloride (BCDAC) were selected. The crystallization was performed from aqueous and methanol solutions under the nitrogen atmosphere. The X-ray data were collected using RAPID (Rigaku) diffractometer at low temperatures. The structures were analyzed with SHELXS97 and were refined with SHELXL97. For each surfactant, two crystal forms were obtained with or without solvent water molecules. The crystals obtained from an aqueous solution include one water molecule in an asymmetric unit. Their crystals show the common packing pattern. On the other hand, the crystals obtained from a methanol solution include no solvent molecule but has a half of hydroquinone molecule in an asymmetric unit. These crystals showed the new packing pattern, that is, one hydroquinone is included in the common packing pattern like the complex from an aqueous solution and another hydroquinone occupies the inversion center between the common packing patterns. These new complex crystals from a methanol solution show more thermally stable than those with water solvent and the stability depends on the alkyl chain length of the surfactant molecules.

PO205

LITHIUM DIFFUSION IN LITHIUM MANGANESE SPINEL

Kenji Tateishi,[a] Douglas du Boulay,[b] and Nobuo Ishizawa[b]

[a]Interdisciplinary School of Science and Engineering, Tokyo Institute of Technology, Nagatsuta Midori, Yokohama 226-8502, Japan; [b]Ceramics Research Laboratory, Nagoya Institute of Technology, Asahigaoka, Tajimi 507-0071, Japan
(tateishi@r3401.msl.titech.ac.jp)

Lithium manganese spinels are attractive candidates for cathode materials of rechargeable lithium ion batteries. The high-temperature form of stoichiometric $LiMn_2O_4$ is known to be a mixed valence compound in which distinct Mn^{3+} ($t_{2g}^3e_g^1$) and Mn^{4+} ($t_{2g}^3e_g^0$) ions are randomly distributed among the 16*d* sites of *Fd*-3*m* symmetry. The electrical transport properties are dominated by a hopping process of nonadiabatic small polarons involving e_g electrons, so the Mn valences change with respect to time. Previous molecular dynamics (MD) simulations reported the correlation of Mn valence changes and Li migration [1,2].

In this study MD simulations were carried out to obtain a more detailed understanding of Li diffusion mechanisms. The figure shows a view of coordinating O and Mn atoms around the 8*a* (Li) tetrahedral and the 16*c* (vacancy) octahedral sites. The 8*a* site is coordinated by 12 Mn atoms at 3.42 Å and the 16*c* site is coordinated by 6 coplanar Mn atoms at 2.91 Å. From the viewpoint of the Li-Mn Coulomb repulsive energy, it is predicted that the 16*c* site is more strongly affected by the change of Mn valences. Indeed, prior to Li migration the mean Mn valence around the 16*c* site was +3.5, whereas in instances in which Li occupied the 16*c* octahedra, the mean Mn valence was reduced to +3.3. These numbers suggest that a typical change in Mn coordination around the 16*c* site occurs from (3 Mn^{3+} + 3 Mn^{4+}) to (4 Mn^{3+} + 2 Mn^{4+}). For the 8*a* tetrahedral sites, the mean Mn valences of 12 Mn atoms scarcely changed from +3.5 (i.e., 6 Mn^{3+} + 6 Mn^{4+}) before and after the Li diffusion into the adjacent 16*c* site. From these results, we concluded that Li migration to the 16*c* site and the addition of an extra electron on the 6 coplanar Mn atoms are strongly coupled.

References

1 K. Tateishi, D. du Boulay, and N. Ishizawa, *J. Solid State Chem.***174**, (2003), 175-181.

2 K. Tateishi, D. du Boulay, and N. Ishizawa, *Applied Physics Letters* **84**[4], (2004), 529-531.

PO206

NUMERICAL CONVERSION BETWEEN THE PEARSON VII AND THE VOIGT FUNCTIONS

H. Wang,[a] J. Zhou[b]

[a]X-ray Laboratory, School of Earth and Space Sciences, Peking University, Beijing 100871, P. R. China; [b]Chinese Academy of Geological Sciences, Beijing 100037, P. R. China (hjwang@pku.edu.cn).

The Pearson VII (P-VII) and the Voigt (V) functions are two important peak shape functions and have been widely used in X-ray powder diffractometry. It is sometimes needed to convert a V curve into a P-VII curve or *vice verse*. However algebraically it is unsolvable. Starting from the geometric characteristics of two equal curves this study derives a numerical model for converting a V curve into a P-VII curve or *vice verse*.

According to an XRD peak consisting of position, shape (*Sc*), height (I_{max}), full width at half maximum (*B*) and asymmetry five elements[1] and the expressions of the P-VII[2] and the V[3] functions, two full equal curves must possess the same *Sc*, *B*, I_{max}, integral width (β) and the same area (*II*). This produces five equations of *Sc*, *B*, I_{max}, β and *II* for both P-VII and V functions and leads a final equation 1 that allows us to exactly convert the characteristic u of the P-VII function into the k of the V function with the conditions $k = \beta_c / \beta_g \pi^{1/2}$ and $\mathrm{Re}\{\omega[\sqrt{\pi}B_V / 2\beta_g + ik]\} = 0.5\exp(k^2)erfc(k)$ and *vice verse*. Subscript *c* renders the Cauchy function and *g* the Gaussian function.

$$B_V / \beta_g = \frac{2(2^{1/u}-1)^{1/2}[\Gamma(u)]^2}{2^{2(1-u)}\pi\Gamma(2u-1)} / \exp(k^2)erfc(k) \qquad (1)$$

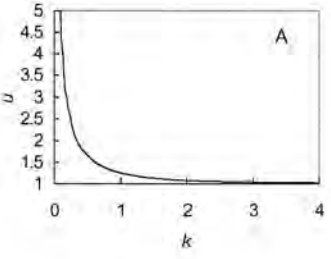

Figure A shows the relationship between the shape characteristic value k of the V function and the exponent u of the P-VII function. Relationship between *Sc* and u and that between β_g/β and u are derived therefore. It shows from the numerical solutions that these peak parameters of the P-VII curve can exactly coincide with those of the V curve, and thus, the Voigt function can be well described by the Pearson-VII function with this model, and *vice versa*.

References

1 Wang, H. and Zhou, J. (2000) *J. Appl. Cryst.* **33**, 1128-1135.
2 Smith, D.K. (1989) *Reviews in Mineralogy* Vol. **20**, 183-216.
3 Langford, J.I. (1978) *J. Appl. Cryst.* **11**, 10-14.

PO207

ON EQUIVALENCE OF COLORINGS OF PATTERNS ASSOCIATED WITH DECOMPOSITIONS OF THEIR SYMMETRY GROUPS

Rene P. Felix[a] and Maria Veronica P. Quilinguin[b]

[a]Department of Mathematics, University of the Philippines Diliman, Quezon City, Philippines (rene@math01.cs.upd.edu.ph)
[b]Department of Mathematics, University of Asia and the Pacific Pearl Drive, Ortigas Center Pasig City 1605, Philippines (vquilinguin@uap.edu.ph)

In this paper, we explore the theory of colorings by considering when two colorings of a given pattern are equivalent in the sense that one may be obtained from the other (1) by a change or permutation of the colors and/or (2) by a symmetry of the underlying uncolored pattern. In connection with this, we derive a formula for counting the colorings of a pattern which are equivalent to each other. We also show how to list all colorings equivalent to a given coloring and among these, those which have the same set of symmetries permuting the colors and the same set of symmetries fixing the colors.

The symmetry group of a pattern refers to the set of isometries that send the pattern to itself. For this paper, we assume that we are given a pattern on the Euclidean plane whose symmetry group G is a plane crystallographic group or a subgroup of a plane crystallographic group, i.e., G is a plane crystallographic group, a frieze group or a finite group which is cyclic or dihedral. The results in this paper may be extended to crystallographic groups of higher dimensions.

PO208

THE AUSTRALIAN REPLACEMENT RESEARCH REACTOR

R. A. Robinson and S. J. Kennedy

Bragg Institute, Australian Nuclear Science and Technology Organisation, Menai, NSW 2234, Australia (rro@ansto.gov.au)

The 20-MW Australian Replacement Research Reactor represents possibly the greatest single research infrastructure investment in Australia's history. Construction of the facility has commenced, following award of the construction contract in July 2000, and the construction licence in April 2002. First fuel will go into the reactor in November 2005, with the facility at full power in early 2006 and fully commissioned in July 2006. The project includes a large state-of-the-art liquid deuterium cold-neutron source and supermirror guides feeding a large modern guide hall, in which most of the instruments are placed. Alongside the guide hall, there is good provision of laboratory, office and space for support activities. While the facility has "space" for up to 18 instruments, the project has funding for an initial set of 8 instruments, which will be ready when the reactor is fully operational. Instrument performance will be competitive with the best research-reactor facilities anywhere. Staff to lead the design effort and man these instruments have been hired on the international market from leading overseas facilities, and from within Australia, and 7 out of 8 instruments have been specified and costed. At present the instrumentation project carries >10% contingency and 50% of procurements have been placed. An extensive dialogue has taken place with the Australian user community and our international peers, via various means including a series of workshops over the last 2 years covering all 8 instruments, emerging areas of application like biology and the earth sciences, and computing infrastructure for the instruments.

In December 2002, ANSTO formed the Bragg Institute, with the intent of nurturing strong external partnerships, and covering all aspects of neutron and X-ray scattering, including research using synchrotron radiation.

PO209

IMPROVEMENT OF SPATIAL RESOLUTION OF IMAGES TAKEN WITH X-RAY CCD DETECTOR BY MAXIMUM LIKELIHOOD METHOD

Y. Shinohara,[a] E. L. Kosarev,[b] Y. Ueji,[a] K. Uesugi[c], Y. Suzuki[c], N. Yagi[c], and Y. Amemiya[a]

[a]Department of Materials Science, The University of Tokyo, Kashiwa, Chiba, Japan; [b]P. L. Kapitza Institute for Physical Problems, Kosygina, Moscow, Russia; [c]JASRI, Mikazuki-cho, Hyogo, Japan (amemiya@k.u-tokyo.ac.jp).

We have developed polarization-contrast imaging systems (X-ray polarization imaging microscopy). It is expected as a powerful tool for two-dimensional imaging of bulk magnetic structure. Previous studies have shown the need for improvement of the resolving power (now the order of microns) of the system. There are two ways to improve the resolving power of X-ray microscopy. One is with *hardware*: the refinement of the optical devices and experimental arrangement. Although there are great improvements, their abilities are limited by the fabrication technique at the moment. Therefore another approach is needed for the progress of the ability of X-ray microscopy: the improvement of *software*.

Usually an output image which we actually measure is expressed as a convolution of an instrumental function and an input image which we really want to measure. Knowledge of the instrumental functions allows us to reconstruct the signal to a certain extent without *a priori* parameterizations. One-dimensional signal recovery using Maximum Likelihood Method (MLM) has been already reported[1] but two-dimensional one has not been yet. Recently, we have developed a two-dimensional signal recovery program.

Fig.1 shows the result of the two-dimensional MLM program. The left figure is the image of three pinholes and the right figure is the image recovered by MLM program after 200 iterations. It shows that the images of individual pinholes are resolved clearly. Although the program recovers images successfully, there are some problems to be overcome. First, it is difficult to know the precise instrumental function. Another problem is a sampling effect by CCD pixels. Detail of these problems and their solution will be reported.

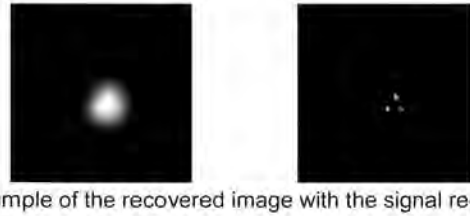

Fig.1 An example of the recovered image with the signal recovery program

References

1 Kosarev, E. L., (1990) *Inverse Problems*, **6**, 55-76.

Author Index

journals.iucr.org/f

Acta Crystallographica Section F

Structural Biology and Crystallization Communications

Announcing an all-electronic journal for rapid publication of structural genomics, protein structure and crystallization results

Editors: H. M. Einspahr and J. M. Guss

Coming January 2005

Crystallography Journals Online